REPORT DOCUMENTATION PAGE

Form Approved
OMB No. 074-0188

1. AGENCY USE ONLY (Leave blank)	2. REPORT DATE	3. REPORT TYPE AND DATES COVERED
	September 2000	Final (1 Sep 96 - 31 Aug 00)

4. TITLE AND SUBTITLE
Control of Breast Tumor Cell Growth by Dietary Indoles

5. FUNDING NUMBERS
DAMD17-96-1-6149

6. AUTHOR(S)
Leonard F. Bjeldanes, Ph.D.

7. PERFORMING ORGANIZATION NAME(S) AND ADDRESS(ES)
University of California
Berkeley, California 94720-5940

E-MAIL:
lfb@nature.berkeley.edu

8. PERFORMING ORGANIZATION REPORT NUMBER

9. SPONSORING / MONITORING AGENCY NAME(S) AND ADDRESS(ES)
U.S. Army Medical Research and Materiel Command
Fort Detrick, Maryland 21702-5012

10. SPONSORING / MONITORING AGENCY REPORT NUMBER

11. SUPPLEMENTARY NOTES
Report contains color photos

12a. DISTRIBUTION / AVAILABILITY STATEMENT
Approved for public release; distribution unlimited

12b. DISTRIBUTION CODE

13. ABSTRACT *(Maximum 200 Words)*

Indole-3-carbinol (I3C) is a naturally occurring component of dietary vegetables and a promising preventive agent against breast cancer. To further examine the properties of I3C and to establish the mechanism of action of this novel antiestrogen, we pursued the following specific aims: a) Identify I3C products that are responsible for I3C's growth inhibitory effects in breast tumor cells. b) Characterize effects of indoles on estrogen receptor- and Ah receptor-mediated cellular responses. c) Identify genes involved in the indole-mediated inhibition of growth of mammary tumor cells.

In summary, and contrary to our expectations, we found that high concentrations of I3C strongly and reversibly inhibited proliferation of cultured breast tumor cells accompanied by a specific arrest in the cell cycle. In contrast, however, the primary in vitro effects of the major in vivo products of I3C, i.e. DIM and CTr-1, were to activate estrogen receptor function and to promote proliferation of estrogen-dependent cells. Our results of gene expression analyses showed that the effects of DIM treatment on breast tumor cells were most pronounced in a group of genes important in late stage tumor growth and metastasis. Taken together, these results reveal distinct and promising cancer protective or chemotherapeutic activities of I3C and its in vivo products.

14. SUBJECT TERMS
Breast Cancer, dietary indoles, cancer protection

15. NUMBER OF PAGES
93

16. PRICE CODE

17. SECURITY CLASSIFICATION OF REPORT	18. SECURITY CLASSIFICATION OF THIS PAGE	19. SECURITY CLASSIFICATION OF ABSTRACT	20. LIMITATION OF ABSTRACT
Unclassified	Unclassified	Unclassified	Unlimited

NSN 7540-01-280-5500

Standard Form 298 (Rev. 2-89)
Prescribed by ANSI Std. Z39-18
298-102

AD_____

Award Number: DAMD17-96-1-6149

TITLE: Control of Breast Tumor Cell Growth by Dietary Indoles

PRINCIPAL INVESTIGATOR: Leonard F. Bjeldanes, Ph.D.

CONTRACTING ORGANIZATION: University of California
Berkeley, California 94720-5940

REPORT DATE: September 2000

TYPE OF REPORT: Final

PREPARED FOR: U.S. Army Medical Research and Materiel Command
Fort Detrick, Maryland 21702-5012

Table of Contents

Title: Control of breast tumor cell growth by dietary indoles.

4) Introduction:

There is growing public and scientific interest in the influence of dietary substances in the incidence of breast cancer (1-4). A potentially important dietary cancer protective agent is indole-3-carbinol (I3C), a modulator of carcinogenesis from *Brassica* vegetables such as cabbage, broccoli, and Brussels sprouts. In a screen of 90 potential chemopreventive agents in a series of short-term bioassays relevant to carcinogenesis I3C was found to be one of only 8 compounds that tested positive in all assays. Some of the most well established cancer protective effects of I3C have been observed in mammary tissue. In a long term feeding experiment, in which female mice consumed synthetic diets containing I3C, spontaneous mammary tumor incidence and multiplicity were decreased by 50%. Treatments with I3C or its major in vitro conversion product, 3,3'-diindoylmethane (DIM) were reported to reduce the mammary tumor yield in carcinogen treated rodents by as much as 95% in several different studies (5)(6)(7). A recent report of the results of a phase I clinical trial with recurrent respiratory papillomatosis indicate further the inhibitory effects of I3C on tumor development in humans (8). Although there are some concerns over the potential tumor promoting effects of I3C observed in some assays (9,10), both I3C and DIM are currently undergoing at least three additional phase I clinical trials as cancer chemotherapeutic and preventive agents. Our proposed research directed at defining the molecular mechanisms of tumor growth inhibition by the indoles, especially for DIM, were intended to facilitate both further clinical trials of the compounds and the development of analogs targeted at the regulation of specific tumor suppressive genes.

5) Body:

During the period of this grant, we have developed a solid understanding of the activities, primarily in cultured human breast cancer cells, of I3C, its gastric acid conversion products, as well as the activities of I3C's plant precursor (glucobrassicin) and product (ascorbigen).

In summary, and contrary to our expectations, we found that high concentrations of the parent indole, I3C, strongly and reversibly inhibited proliferation of cultured breast tumor cells accompanied by a specific arrest in the cell cycle, whereas the primary effect of the major in vivo products of I3C, i.e. DIM and CTr-1, was to activate ER function and to promote proliferation of estrogen-dependent cells. Our results show further that of the nearly 10,000 genes examined in a gene expression microarray experiment, the effects of DIM treatment of breast tumor cells were most pronounced in a group of genes important in tumor angiogenesis.

The accomplishments of this project to date are described in the following with reference to the tasks specified in the Statement of Work provided in the original proposal.

A. **Technical objective I**. Identify I3C products that are responsible for I3C's growth inhibitory effects in breast tumor cells.
B. **Technical objective II**. Characterize effects of indoles on estrogen receptor- and Ah receptor-mediated cellular responses.

1. **One of the major acid products, 2-(indol-3-ylmethyl)-3,3'-diindolylmethane (LTr-1) exhibits cytostatic and antiestrogenic activities in cultured human breast tumor cells (11).** Chromatographic separation of the crude acid mixture of I3C guided by cell proliferation assay in human MCF-7 cells resulted in the isolation of LTr-1 as a major antiproliferative component. LTr-1 inhibited the growth of both estrogen-dependent (MCF-7) and independent (MDA-MB-231) breast cancer cells by approximately 60% at a non-lethal concentration of 25 μM. LTr-1 also exhibited significant antiestrogenic activities. The IC50 determined by assay of competitive binding to the estrogen receptor was approximately 70 μM. As shown by gel mobility shift assay, LTr-1 efficiently inhibited the estrogen-induced binding of the estrogen receptor to its cognate DNA responsive element. LTr-1 showed weak agonist activity in this regard in the absence of estrogen. The antagonist effects of LTr-1 were also exhibited in transcriptional activation assays of endogenous pS2 gene expression and of CAT activity in cells transiently transfected with an estrogen-responsive reporter construct (pERE-vit-CAT). The IC50 for each assay was approximately 10 μM. A weak agonist effect was seen in the CAT reporter assay but not in the analysis of pS2 mRNA. Taken together, these results show that whereas LTr-1 can antagonize the transcriptional activation properties of estradiol, it can also inhibit the proliferation of both estrogen-dependent and estrogen-independent breast tumor cells.

2. **The major cyclic trimeric product of I3C is a strong agonist of the estrogen receptor signaling pathway (12).** We observed that 5,6,1,1,12,17,18-hexahydrocyclona[1,2-b:4,5-b':7,8-b"]triindole (CTr) stimulated the proliferation of estrogen-responsive MCF-7 cells in estradiol (E2-) depleted medium to a level similar to that produced by estradiol (E2), but did not affect the growth of the estrogen-independent cell line MDA-MD-231 in complete medium. CTr displaced E2 in competitive binding studies and activated ER binding to an estrogen-responsive DNA element in gel mobility shift assays with an EC50 of about 0.1 μM. CTr activated transcription of an E2-responsive endogenous gene and exogenous reporter genes in transfected MCF-7 cells, also with high potency. CTr (1 μM) failed to activate AhR-mediated pathways, consistent with the low binding affinity of CTr for the AhR reported previously. Comparisons of the conformational characteristics of CTr with other ER ligands indicated a remarkable similarity with tamoxifen. These studies have uncovered a new class of strong ER agonists that might be the source of the cancer-promoting activity of high oral doses of I3C seen in some experiments.

3. **Modulation of CYP1A1 activity by ascorbigen in murine hepatoma cells (13).** Ascorbigen (ASG) is the predominant indole formed during the degradation of glucobrassicin in plants. The major focus of this study was to examine the effects of ASG on CYP induction in a murine hepatoma-derived cell line (Hepa-1c1c7). ASG induced ethoxyresorufin O-deethylase (EROD) activity, a marker for CYP1A1, in a concentration dependent manner with maximum induction at 700 μM. Maximum ASG induction after 24 h treatment was 7% of maximal CYP1A1 activity induced indolo[3,2-b]carbazole (ICZ) (1 μM). Surprisingly, the CYP1A1 activity continuously increased up to 72 h when ASG had the same induction potency as 1 μM ICS after only 24 h. CYP1A1 protein level, measured by Western blot analysis, was maximally induced after 24-h incubation with ASG. ASG was a potent inhibitor of CYP1A1 enzyme activity above 50 μM. ASG increased the chloramphenicol

acetyl transferase (CAT) activity of a CAT reporter construct containing a dioxin responsive element (DRE) in transfected Hepa-1c1c7 cells, indicating activation of the Ah receptor.

4. **N-Methoxyindole-3-carbinol is a more efficient inducer of CYP1A1 in cultured cells than I3C (14).** The purpose of these experiments was to determine the effects of N-methoxyindole-3-carbinol (NI3C) on CYP1A1 induction in cultured cells and to compare the CYP-inducing potential of NI3C and I3C administered to rats. NI3C occurs in *Brassica* plants at about 25% of the levels at which I3C is present. NI3C induced EROD activity in Hepa-1c1c7 cells in a concentration-dependent manner with 10-fold higher efficiency than I3C. As NI3C induced binding of the AhR to the dioxin-responsive element and induced expression of both endogenous CYP1A1 mRNA and an AhR-responsive chloramphenicol acetyl transferase construct, we concluded that NI3C could activate the AhR. Besides the induction of CYP1A1, we observed an inhibition of EROD activity, with an IC50 of 6 μM. Oral administration of 570 μm of NI3C/kg b.w. to male Wistar rats increased the hepatic CYP1A1 and 1A2 protein levels, as well as the EROD and 7-methoxyresorufin O-demethylase activities at 8 and 24 h after administration, but the responses were less pronounced than after administration of 570 μmol I3C/kg b.w. Furthermore, NI3C did not induce hepatic 7-pentoxyresorufin O-depentylase activity whereas I3C did. Ascorbigen only weakly induced hepatic CYP1A1 and 1A2 but had no effect on CYP2B1/2. Compared to I3C, NI3C is a more efficient inducer of CYP1A1 in cultured cells but less active when administered to rodents.

5. **DIM induces apoptosis in both MCF-7 and MDA-MB-231 cells.** We observed that incubation of mammary tumor cell lines MCF-7 and MDA-MB-231 in complete medium with DIM at concentrations of greater than 10 μM produced cell death. We determined that DIM induced apoptosis in both cell lines. Apoptosis was characterized by cellular and nuclear shrinkage, chromatin condensation, DNA fragmentation, proteolytic cleavage of certain proteins and phosphatidylserine externalization. Annexin V assay indicated that after only 10 min of treatment with 100 μM DIM, the characteristic halo image of phosphatidylserine (PS) externalization could be observed by fluorescent microscopy, indicating early stage of apoptosis. By 3 hours of treatment with 50 μM DIM, we observed both early stage and late stage of apoptosis cells. Chromatin condensation, measured with propidium iodine and Hoechst 33342 staining, was apparent by 24 hours of incubation with 50 μM DIM. DNA fragmentation, as measured by the ApopAlert DNA Fragmentation assay was observed by fluorescence microscopy in cells treated with 50 μM DIM. Quantification with flow cytometry indicated that both DIM (100 μM) and TAM (25 μM) induced DNA fragmentation in about 60% of cells. Our continuing mechanistic studies indicate that DIM induced a rapid loss of Bcl-2 protein and an increased expression of TGF-ß. Taken together, these results indicate that pharmacological concentrations of DIM can induce apoptosis by a mechanism similar to tamoxifen and vitamin E succinate in terms of TGF-ß induction and to taxol in terms of drop in levels of Bcl-2.

6. **Ligand-independent activation of estrogen receptor function by 3,3'-diindolylmethane in human breast cancer cells (15).** We found that DIM was a promoter-specific activator of estrogen receptor (ER) function in the absence of estradiol (E2). DIM weakly inhibited the

E2-induced proliferation of estrogen receptor-containing MCF-7 cells and induced proliferation of these cells in the absence of steroid, by approximately 60% of the E2 response. DIM had little effect on proliferation of ER deficient MDA-MB-231 cells, suggesting that it is not generally toxic at these concentrations. Although DIM did not bind to the ER in this concentration range as shown by a competitive ER binding assay, it activated the ER to a DNA binding species. DIM increased the level of transcripts for the endogenous pS2 gene and activated the estrogen responsive pERE-vit-CAT and pS2-CAT reporter plasmids in transiently transfected MCF-7 cells. In contrast, DIM failed to activate transcription of the simple E2- and diethylstilbesterol - responsive reporter construct pATC2. The estrogen antagonist ICI-182780 was effective against DIM-induced transcriptional activity of the pERE-vit-CAT reporter, which supports further that DIM is acting through the ER. We demonstrated that ligand-independent activation of the ER in the MCF-7 cells could be produced following treatment with the D1 dopamine receptor agonist SKF 82958. We showed further that the agonist effects of SKF82958 and DIM, but not of E2, could be blocked by co-treatment with the PKA inhibitor H-89. These results have uncovered a promoter-specific ligand-independent activation of estrogen receptor signaling for DIM that may require activation by PKA, and suggest that this major I3C product may be a selective activator of the ER function.

7. **I3C and DIM as aryl hydrocarbon (Ah) receptor agonists and antagonists in T47D human breast cancer cells (16).** In aryl hydrocarbon receptor-responsive T47D human breast cancer cells, I3C and DIM did not induce significantly CYP1A1-dependent ethoxyresorufin O-deethylase (EROD) activity or CYP1A1 mRNA levels at concentrations as high as 125 or 31 μM, respectively. A 1 nM concentration of 2,3,7,8-tetrachlorodibenzo-p-dioxin (TCDD) induced EROD activity in these cells, and co-treatment with TCDD plus different concentrations of I3C (1-125 μM) or DIM (1-31 μM) resulted in a > 90% decrease in the induced response at the highest concentration of I3C or DIM. I3C or DIM also partially inhibited (< 50%) induction of CYP1A1 mRNA levels by TCDD and reporter gene activity, using an Ah-responsive plasmid construct in transient transfection assays. In T47D cells co-treated with 5 nM [^{3}H]TCDD alone or in combination with 250 μM I3C or 31 μM DIM, there was a 37 and 73% decrease, respectively, in formation of the nuclear Ah receptor. The more effective inhibition of induced EROD activity by I3C and DIM was due to in vitro inhibition of enzyme activity. Thus, both I3C and DIM are partial Ah receptor antagonists in the T47D human breast cancer cell line.

8. **NCI screen of antiproliferative effects of DIM in cancer cell lines.** DIM, LTr-1 and several other synthetic or natural products of I3C were submitted to the NCI for screening in 59 tumor cell lines. For these assays, cells are grown in serum-rich medium appropriate for each line. Although LTr-1 exhibited some selectivity for certain cell lines, especially with the melanoma group, pronounced antiproliferative activity in nearly all the lines required concentrations of greater than 1 μM. LTr-1 was clearly toxic to most lines at concentrations above 10 μM. With the exception of one of the non-small cell lung cancer lines, in which DIM produced a nearly 50% inhibition of proliferation at a concentration of only 0.1 μM, DIM was about an order of magnitude less active than LTr-1 in the assays. On the basis of

these results, neither of these substances was considered suitable for further testing by the NCI.

C. Technical objective III. Identify genes involved in the indole-mediated inhibition of growth of mammary tumor cells.

1. **Indole-3-carbinol inhibits the expression of cyclin-dependent kinase-6 and induces a G_1 cell cycle arrest of human breast cancer cells independent of estrogen receptor signaling (17).** Treatment of cultured human MCF-7 breast cancer cells with I3C reversibly suppressed the incorporation of [^{3}H]thymidine without affecting cell viability or estrogen receptor (ER) responsiveness. Flow cytometry of propidium iodide-stained cells revealed that I3C induced a G_1 cell cycle arrest. Concurrent with the I3C-induced growth inhibition, Northern blot and Western blot analyses demonstrated that I3C selectively abolished the expression of cyclin-dependent kinase 6 (CDK6) in a dose- and time-dependent manner. Furthermore, I3C inhibited the endogenous retinoblastoma protein phosphorylation and CDK6 phosphorylation of retinoblastoma *in vitro* to the same extent. After the MCF7 cells reached their maximal growth arrest, the levels of the p21 and p27 CDK inhibitors increased by 50%. The antiestrogen tamoxifen also suppressed MCF7 cell growth more stringently than did either agent alone. The I3C-mediated cell cycle arrest and repression of CDK6 production were also observed in estrogen receptor-deficient MDA-MB-231 human breast cancer cells, which demonstrates that this indole can suppress the growth of mammary tumor cells independent of estrogen receptor signaling. Thus, our observations have uncovered a previously undefined antiproliferative pathway for I3C that implicates CDK6 as a target for cell cycle control in human breast cancer cells. Moreover, our results establish for the first time that CDK6 gene expression can be inhibited in response to an extracellular antiproliferative signal.

2. **Combined antiproliferative effects of I3C and tamoxifen (18).** Combinations of I3C and the antiestrogen tamoxifen inhibited the growth of the estrogen-dependent human MCF-7 breast cancer cell line more effectively than either agent by itself. This more stringent growth arrest was demonstrated by a decrease in adherent and anchorage independent growth, reduced DNA synthesis, and a shift into the G1 phase of the cell cycle. A combination of I3C and tamoxifen also caused a more pronounced decrease in CDK2 specific enzymatic activity than either compound alone, but had no effect on CDK2 protein expression. Importantly, treatment with I3C and tamoxifen ablated expression of the phosphorylated retinoblastoma (Rb) protein, an endogenous substrate for the G1 CDKs, whereas, either agent alone only partially inhibited endogenous Rb phosphorylation. Several lines of evidence suggest that I3C works through a mechanism distinct from tamoxifen. I3C failed to compete with estrogen for estrogen receptor binding, induced a unique morphology, and specifically down regulated the expression of CDK6. These results demonstrate that I3C and tamoxifen work through different signal tranduction pathways to suppress the growth of human breast cancer cells and may therefore represent a potential combinatorial therapy for estrogen responsive breast cancer.

3. **Gene expression microarray analysis of DIM-treated breast tumor cells.** Gene expression microarray analysis of mRNA from MCF-7 cells treated with 50 μM DIM

compared to vehicle-treated controls indicated that after 24 hr., of the 9800 sequences examined, the expressions of 31 genes were induced by at least 2.0 fold and expressions of 39 genes were decreased by at least 2.0 fold. The up-regulated group includes two weakly induced AhR-responsive genes, consistent with the previous findings by us and others that DIM is a weak activator of Ah receptor functions (7). Of possible significance in this group of induced genes is the activation of several interferon-responsive genes, including a 3.3-fold increase in expression of 2'-5'oligoadenylate synthetase gene, the product of which is essential for the antiviral activity of the interferons (19). This result raises the intriguing possibility of a role of DIM in the regulation of pathways responsible for the antiproliferative and antiangiogenic activities of cytokines (20).

For the down-regulated group of genes, a much greater association with a significant cancer-protective process is apparent. For this group, all eight of the most strongly repressed genes are important cell growth-related transcription factors and/or are associated with angiogenic processes.

Down-regulated transcription factors.

The most strongly down-regulated gene, **NAK1/TR3** orphan receptor, is a member of the steroid/thyroid hormone receptor superfamily of transcription factors. Although the function of this gene product is poorly understood, NAK1/TR3 is the human homologue of the proteins encoded by the rat NGFI-B and mouse nur77 genes. These genes are induced rapidly by androgens and growth factors and may have functions related to cell proliferation, differentiation, and apoptosis. The nur77 protein product has many important functions related to cell proliferation including involvement in the signal transduction pathways mediated by retinoic acid, growth factors, and phorbol esters (21).

The immediate-early gene, **Egr-1**, produces a zinc finger protein involved in many cellular processes including the regulation of nur77 and of platelet-derived growth factor, the latter of established importance in the maintenance of normal vascular homeostasis (22). Hyaluronan-mediated activation of Egr-1 expression promotes angiogenesis in bovine aortic endothelial cells (23). Egr-1 is reported to be co-regulated with c-fos in several tumor lines, as we observed in DIM-treated MCF-7 cells. Although the function of **Egr-2** is poorly understood, one process in which this close relative of Egr-1 is implicated is the regulation of the expression of the pro-apoptotic Fas ligand (24). The nuclear oncogene, **c-fos**, has many important functions in the cell including activation of c-fos-induced growth factor/vascular endothelial growth factor D (Figf/Vegf-D) which mediates angiogenesis in several assay systems (25). **FosB/G0S3**, another component of the AP-1 family of transcription factors, is up regulated during apoptosis in breast tumor-derived cells (26).

Down-regulated cell adhesion and extracellular matrix proteins.

The **S1-5** gene product is a member of the fibulin family of extracellular matrix proteins, one member of which, fibulin-1, decreases migration of ovarian tumor cells (27). Human connective tissue growth factor (**CTGF**) and insulin-like growth factor binding protein 10/**Cyr61** belong to a family of secreted proteins involved in cell adhesion, migration and

mitogenesis in both fibroblasts and endothelial cells. Cyr61 was identified as an angiogenic inducer that can promote tumor growth and vascularization (28).

6) Key Research Accomplishments:

1) LTr-1, a major in vivo linear trimerization product of I3C, exhibits cytostatic and antiestrogenic activities in cultured human breast tumor cells and weakly activates the Ah receptor (11).
2) CTr-1, the major in vivo cyclic trimerization product of I3C, is a strong agonist of estrogen receptor function (12).
3) Ascorbigen, a major natural conjugate of I3C, is an inhibitor of CYP1A1, a weak direct inducer of Ah receptor function, and is converted in cell culture to a strong Ah agonist (13).
4) NI3C, a major I3C derivative in plants, is a more efficient inducer of CYP1A1 in cultured cells but less active when administered to rodents (14).
5) At pharmacologic concentrations, DIM, which is the major in vivo dimerization product of I3C, induces apoptosis in breast tumor cells that is accompanied by a loss of cytosolic Bcl-2 protein.
6) At physiologic concentrations, DIM is a weak estrogen and induces a ligand independent activation of estrogen receptor functions (15).
7) Whereas neither I3C nor DIM exhibits significant activity as activators of Ah receptor function, both indoles can inhibit Ah receptor-mediated gene expression and CYP1A1 activity in mammary tumor cells (16).
8) In the NCI tumor cell culture screen, pronounced antiproliferative effects required concentrations of DIM of greater than 10 μM and of LTr-1 of greater than 1 μM.
9) At high concentrations, I3C induces a reversible G1 cell cycle arrest in breast tumor cells that is accompanied by a down regulation of CDK6 gene expression (17).
10) Co-treatment of cells with I3C and tamoxifen produces a synergistic blockage of the cell cycle in breast tumor cells along with a pronounced decrease in CDK2 specific enzymatic activity (18).
11) Gene expression microarray analysis of mRNA from DIM-treated breast tumor cells indicates that all five of the most strongly down-regulated genes for which function is established are members of gene families important in processes involved in tumor angiogenesis. In addition, three other strongly down-regulated but poorly understood genes are thought to be transcription regulatory factors.

7) Reportable Outcomes:

a) Publications:

1. Chang, Y.C., Riby, J., Chang, G., Peng, B.C., Firestone, G., and Bjeldanes, L. (1999) Cytostatic and antiestrogenic effects of 2-(indol-3-ylmethyl)-3,3'-diindolylmethane, a major in vivo product of dietary indole-3-carbinol. J. Biochem. Pharm. **58**, 825-834.
2. Riby , J.E., Feng, C.-L., Chang , Y.C., Schaldach , C.M., Firestone , G.L., and Bjeldanes , L.F. (1999) The major cyclic trimeric product of indole-3-carbinol is a strong agonist of the estrogen receptor signaling pathway. Biochemistry **39**, 910-918.

3. Stephensen, P.U., Bonnesen, C., Bjeldanes, L.F., and Vang, O. (1999) Modulation of cytochrome P4501A1 activity by ascorbigen in murine hepatoma cells. J. Biochem. Pharm., **58**, 1145-1153.
4. Stephensen, P.U., Bonnesen, C., Schaldach, C.M., Bjeldanes, L.F., and Vang, O. (2000) N-Methoxyindol-3-carbinol is a more efficient inducer of cytochrome P-4501A1 in cultured cells than indol-3-carbinol. Nutrition and Cancer, **36**, 112-121.
5. Riby , J.E., Chang, G.H.F., Firestone , G.L., and Bjeldanes , L.F. (1999) Ligand-independent activation of estrogen receptor function by 3,3'-diindolylmethane in human breast-cancer cells. J. Biochem. Pharm **60**, 167-177.
6. Chen, I., Safe, S., and Bjeldanes, L. (1996) Indole-3-carbinol and diindolylmethane as aryl hydrocarbon (Ah) receptor agonists and antagonists in T47D human breast cancer cells. Biochem. Pharm. **51**, 1069-76.
7. Cover, C., Hsieh, S., Tran, S., Kim, G., Bjeldanes, L., and Firestone, G. (1998) Indole-3-carbinol inhibits the expression of cyclin dependent kinase-6 and induces a G1 cell cycle arrest of human breast cancer cells independent of estrogen receptor signaling. J. Biol. Chem. **273**, 3838-3847.
8. Cover, C.M., Hsieh, S.J., Cram, E.J., Hong, C., Riby, J.E., Bjeldanes, L.F., and Firestone, G.L.(1999) Indole-3-carbinol and tamoxifen cooperate to arrest the cell cycle of MCF-7 human breast cancer cells. Cancer Research **59**, 1244-1251.

b) Abstracts:

1) Era of Hope, Department of Defense, Breast Cancer Research Program Meeting
Atlanta, Georgia, June 8-12, 2000

Title: CONTROL OF BREAST TUMOR CELL GROWTH BY DIETARY INDOLES
Authors: Leonard F. Bjeldanes, Gary L. Firestone, Carolyn M. Cover, Erin J. Cram, Chibo Hong and Jacques E. Riby
Abstract: Indole-3-carbinol (I3C), a naturally occurring component of vegetables of the cabbage family has been shown to reduce the incidence of mammary tumors. Our studies of the molecular mechanisms and signal transduction pathways by which I3C mediates its antiproliferative effects have established that: **A)** I3C can induce a reversible G1 cell cycle arrest of cultured human breast cancer cells (MCF-7 cells) in the absence of estrogen receptor signaling. This cell cycle arrest is accompanied first by a rapid inhibition of expression of the cyclin dependent kinase-6 (CDK6) cell cycle component and later by a stimulation in production of both the p21 and the p27 CDK inhibitors. Importantly, these I3C-mediated effects functionally alter the ability of G1-acting CDK2 and CDK6 to phosphorylate the Rb tumor suppressor protein, which is a necessary event for cell cycle progression. **B)** I3C and tamoxifen work through different signal tranduction pathways to suppress the growth of human breast cancer cells. Most significantly, a combination of tamoxifen and I3C displayed a more effective growth suppression response, more stringent inhibition of CDK2 specific activity, and endogenous Rb phosphorylation compared to the effects of either compound alone. **C)** DIM, a major in vivo conversion product of I3C, exhibits primarily agonist activities against proliferation of MCF-7 cells and against transcriptional activation of endogenous and exogenous estrogen-responsive genes. These effects are independent of DIM binding to the estrogen receptor and do not appear

to involve Ah receptor binding. **D)** A second major product of I3C, the linear trimer (2-(indol-3-ylmethyl)-3,3´-diindolylmethane), is an antagonist of estrogen receptor function with little agonist activity. It is a strong inhibitor of proliferation of both estrogen dependent and independent cultured breast tumor cells. **E)** The major in vivo cyclic trimerization product of I3C, CTr, is a strong agonist of estrogen receptor function that binds with high affinity to the estrogen receptor.

Our results suggest the possibility of developing I3C and tamoxifen as a potential combinatorial therapy to control estrogen responsive breast cancers, and that contrary to our expectations, the primary effect of the major in vivo products of I3C, was to activate ER function and to promote proliferation of estrogen-dependent cells in culture.

2). American Institute for Cancer Research, 10th Annual Research Conference
"The Role of Nutrition in Preventing and Treating Breast and Prostate Cancer"
Washington D.C., August 31-September 1, 2000

Title: 3,3'-Diindolylmethane (DIM) Regulates Bcl-2/Bax Family, a Central Apoptotic Regulator, at Transcriptional and Posttranscriptional Level on Human Breast Cancer Cells (MCF-7 and MDA-231 Cells)

Authors: Chibo Hong, Gary L. Firestone and Leonard F. Bjeldanes

Abstract: The naturally occurring phytochemical indole-3-carbinol (I3C), found in vegetables of the Brassica genus, is a promising anticancer agent. 3,3'-Diindolylmethane (DIM) is a major active derivative of I3C formed both *in vivo* and *in vitro*. However, its exact intracellular target(s) and mechanism of anticancer effect remain unknown. In this study, human breast cancer cells, MCF-7 cells (estrogen receptor positive cells) and MDA-231 cells (estrogen receptor negative cells) were used to examine cell growth inhibition and apoptotic effect of DIM. It was found that DIM inhibited cell growth and DNA synthesis in both dose-dependent and time-dependent manners. When cells were exposed to 50 _M DIM, apoptosis was evidenced by the characteristic morphology of cell nuclei with fluorescent staining. DNA fragmentation was detected with TUNEL assay and phosphatidylserine (PS) externalization was observed with Annexin V assay. All these data from cell morphological and biochemical examinations suggested that DIM caused cell death through apoptosis. Western and coimmunoprecipitation assays were used to detect Bcl-2 and Bax protein level in MCF-7 and MDA-231 cells. It showed that DIM decreased total Bcl-2 protein level and Bax-bound Bcl-2 protein in dose and time-dependent manners. DIM 50 μM also increased Bax protein level along with treated time and different doses. These results have shown that DIM induces apoptosis in MCF-7 and MDA-231 cells by increasing the ratio of Bax/Bcl-2 and free Bax protein. When investigating the regulation at transcriptional level, Northern blot analysis revealed a decrease in the amount of Bcl-2 mRNA at dose-dependent and time-dependent manners in MCF-7 cells treated with DIM. Since Bcl-2 family is a central regulator in apoptosis pathway, these results demonstrate that DIM may represent a potential anticancer and apoptotic modulator in human breast cancer.

3). The American Society for Cell Biology, Fortieth Annual Meeting, December 9-13, 2000, San Francisco

Title: 3,3'-Diindolylmethane (DIM) Regulates Bcl-2/Bax Family, a Central Apoptotic Regulator, at Transcriptional and Posttranscriptional Level on Human Breast Cancer Cells (MCF-7 and MDA-231 Cells)

Authors: Chibo Hong, Gary L. Firestone and Leonard F. Bjeldanes

Lay Abstract: Your mother was right. Eating broccoli is good for you but until now we didn't know exactly why. Studies have shown that increased consumption of broccoli and other Brassica vegetables is linked to decreased cancer incidence. A mother's wisdom aside, how broccoli works its magic at the cellular level remained a mystery to biologists. They had clues. Indole-3-carbinol (I3C), a naturally occurring compound found in these vegetables, was considered a promising anti-cancer agent. I3C is rapidly converted in the stomach into its derivatives, including 3,3'-diindolylmethane (DIM), a major product active in fighting cancer. However, DIM's intracellular targets and mechanism of anticancer action were unknown.

Now the team of Chibo Hong, Gary Firestone, and Leonard Bjeldanes has come forward with details of how DIM works the broccoli effect. Using MCF-7 human breast cancer cells, Hong and company found that DIM has multiple effects on the pathways that control cell growth and apoptosis. Apoptosis, or programmed cell death, is a fundamental process to rid organisms of damaged or aged cells including tumors. In cancer, tumor cells grow uncontrollably.

They found that DIM inhibits cell growth and DNA synthesis, an essential step for cell division. DIM also promotes apoptosis, apparently by increasing the level of Bax, a protein that promotes cell death, and by decreasing the level of Bcl-2, a protein that counteracts Bax by binding to it. Tumor cells often express increased levels of Bcl-2.

Measuring the levels of Bcl-2 and Bax in tumor cells treated with DIM, they found decreased levels of Bcl-2 and Bax that was already bound by Bcl-2, along with increased levels of unbound Bax. In addition, the messenger RNAs that produce two other molecules known to mediate growth rates and apoptosis increased substantially in treated cells. Now it's back to the lab bench—and the vegetable aisle—to further explore the potential cancer therapeutic and protective effects of DIM.

c) Patents:

Title: Indole-3-carbinol (I3C) derivatives and methods

Gary L. Firestone, Leonard F. Bjeldanes, Carloyn M. Cover
Patent Number: 6,001,868
Date of Patent: 12/14/99
United States Patent Office

d) New grant funding:

Regulation of breast tumor angiogenesis by dietary indoles.

NIH/NCI	2RO1 CA69056-05	7/1/00-6/30/05	$1,522,800

The major goals of this continuation project are to examine the modes of protective action of indole-3-carbinol endogenous products on the post-initiation phases of breast cancer carcinogenesis.

8) Conclusions:

Results of our previous studies show clearly that neither I3C, the mixture of in vivo gastric acid products of I3C, nor any of the four major acid products tested individually (DIM,

CTr-1, LTr-1, ICZ), inhibits the proliferation of cultured breast tumor cells at concentrations that would be expected to occur in the blood following treatment of rodents with the strongly antitumorigenic doses of I3C or DIM. Thus, our results suggest that the antitumor effects of I3C do not result from the direct effects of this indole on the growth of tumor cells as they exist in the tumor. Instead, our results are consistent with an antitumorigenic mechanism that involves an effect of the indoles on the later stages of tumor development and metastasis, including angiogenesis. Consistent with this hypothesis, our preliminary results show further that a group of genes for transcription factors and metastasis regulators are the most strongly down-regulated of the nearly 10,000 genes assayed following incubation of breast tumor cells with DIM.

Taken together, the results of our initial studies lend considerable support to the exciting possibility that certain dietary indoles are novel antiangiogenic factors and that they function independently of activation of the Ah receptor. Thus, studies of these natural substances may reveal the regulatory mechanisms for this important group of genes and may provide valuable clues for the development of a new class of antitumor agents.

9) References:

1. Safe, S.H. (1994) Dietary and environmental estrogens and antiestrogens and their possible role in human disease. Environ. Sci. & Pollution Res. **1**, 29-33.
2. Raloff, J. (1993) EcoCancers: do environmental factors underlie a breast cancer epidemic? Science News **144**, 10-14.
3. El-Bayoumy, K. (1993) Environmental carcinogens that may be involved in human breast cancer etiology. Chem. Res. Toxicol. **5**, 585-590.
4. Sharpe, R.M. and Skakkebaek, N.F. (1993) Are oestrogens involved in the falling sperm counts and disorders of the male reproductive trait? Lancet **341**, 1392-1395.
5. Wattenberg, L.W. and Loub, W.D. (1978) Inhibition of polycyclic aromatic hydrocarbon-induced neoplasia by naturally occurring indoles. Cancer Res. **38**, 1410-1415.
6. Grubbs, C.J., Steele, V.E., Casebolt, T., Juliana, M.M., Eto, I., Whitaker, L.M., Dragnev, K.H., Kelloff, G.J., and Lubet, R.L. (1995) Chemoprevention of chemically-induced mammary carcinogenesis by indole-3-carbinol. Anticancer Research **15**, 709-716.
7. Chen, I., McDougal, A., Wang, F., and Safe, S. (1998) Aryl hydrocarbon receptor-mediated antiestrogenic and antitumorigenic activity of diindolylmethane. Carcinogenesis **19**, 1631-9.
8. Rosen, C.A., Woodson, G.E., Thompson, J.W., Hengesteg, A.P., and Bradlow, H.L. (1998) Preliminary results of the use of indole-3-carbinol for recurrent respiratory papillomatosis. Otolaryngology - Head and Neck Surgery **118**, 810-5.
9. Pence, B.C., Buddingh, F., and Yang, S.P. (1986) Multiple dietary factors in the enhancement of dimethylhydrazine carcinogenesis: main effect of indole-3-carbinol. Jour.Nat.Cancer.Inst. **77**, 269-76.
10. Srivastava, B. and Shukla, Y. (1998) Antitumour promoting activity of indole-3-carbinol in mouse skin carcinogenesis. Cancer Letters **134**, 91-5.
11. Chang, Y.C., Riby, J., Chang, G., Peng, B.C., Firestone, G., and Bjeldanes, L. (1999) Cytostatic and antiestrogenic effects of 2-(indol-3-ylmethyl)-3,3'-diindolylmethane, a major in vivo product of dietary indole-3-carbinol. J. Biochem. Pharm. **58**, 825-834.

12. Riby , J.E., Feng, C.-L., Chang , Y.C., Schaldach , C.M., Firestone , G.L., and Bjeldanes , L.F. (1999) The major cyclic trimeric product of indole-3-carbinol is a strong agonist of the estrogen receptor signaling pathway. Biochemistry **39**, 910-918.
13. Stephensen, P.U., Bonnesen, C., Bjeldanes, L.F., and Vang, O. (1999) Modulation of cytochrome P4501A1 activity by ascorbigen in murine hepatoma cells. J. Biochem. Pharm., **58**, 1145-1153.
14. Stephensen, P.U., Bonnesen, C., Schaldach, C.M., Bjeldanes, L.F., and Vang, O. (2000) N-Methoxyindol-3-carbinol is a more efficient inducer of cytochrome P-4501A1 in cultured cells than indol-3-carbinol. Nutrition and Cancer, **36**, 112-121.
15. Riby , J.E., Chang, G.H.F., Firestone , G.L., and Bjeldanes , L.F. (1999) Ligand-independent activation of estrogen receptor function by 3,3'-diindolylmethane in human breast-cancer cells. J. Biochem. Pharm **60**, 167-177.
16. Chen, I., Safe, S., and Bjeldanes, L. (1996) Indole-3-carbinol and diindolylmethane as aryl hydrocarbon (Ah) receptor agonists and antagonists in T47D human breast cancer cells. Biochem. Pharm. **51**, 1069-76.
17. Cover, C., Hsieh, S., Tran, S., Kim, G., Bjeldanes, L., and Firestone, G. (1998) Indole-3-carbinol inhibits the expression of cyclin dependent kinase-6 and induces a G1 cell cycle arrest of human breast cancer cells independent of estrogen receptor signaling. J. Biol. Chem. **273**, 3838-3847.
18. Cover, C.M., Hsieh, S.J., Cram, E.J., Hong, C., Riby, J.E., Bjeldanes, L.F., and Firestone, G.L.(1999) Indole-3-carbinol and tamoxifen cooperate to arrest the cell cycle of MCF-7 human breast cancer cells. Cancer Research **59**, 1244-1251.
19. Sarkar, S.N., Ghosh, A., Wang, H.W., Sung, S.S., and Sen, G.C. (1999) The nature of the catalytic domain of 2'-5'-oligoadenylate synthetases. Journal of Biological Chemistry **274**, 25535-42.
20. Yao, L., Sgadari, C., Furuke, K., Bloom, E.T., Teruya-Feldstein, J., and Tosato, G. Contribution of natural killer cells to inhibition of angiogenesis by interleukin-12. Blood **93**, 1612-21.
21. Chang C, Kokontis J, Liao SS, Chang Y (1989) Isolation and characterization of human TR3 receptor: a member of steroid receptor superfamily. J Steroid Biochem. **34**, 391-5.
22. Day, F.L., Rafty, L.A., Chesterman, C.N., and Khachigian, L.M. (1999) Angiotensin II (ATII)-inducible platelet-derived growth factor A-chain gene expression is p42/44 extracellular signal-regulated kinase-1/2 and Egr-1-dependent and mediated via the ATII type 1 but not type 2 receptor. Induction by ATII antagonized by nitric oxide. International Journal of Cancer **71**, 251-6.
23. Deed, R., Rooney, P., Kumar, P., Norton, J.D., Smith, J., Freemont, A.J., and Kumar, S. (1997) Early-response gene signaling is induced by angiogenic oligosaccharides of hyaluronan in endothelial cells. Inhibition by non-angiogenic, high-molecular-weight hyaluronan. Journal of Biological Chemistry **274**, 23726-33.
24. Mittelstadt, P.R. and Ashwell, J.D. (1999) Role of Egr-2 in up-regulation of Fas ligand in normal T cells and aberrant double-negative lpr and gld T cells. Journal of Biological Chemistry **274**, 3222-7.
25. Marconcini, L., Marchio, S., Morbidelli, L., Cartocci, E., Albini, A., Ziche, M., Bussolino, F., and Oliviero, S. (1999) c-fos-induced growth factor/vascular endothelial growth factor D induces angiogenesis in vivo and in vitro.

Proc. Natl. Acad. Sci. USA **96**, 9671-6.
26. Schaerli, P. and Jaggi, R. (1998) EGF-induced programmed cell death of human mammary carcinoma MDA-MB-468 cells is preceded by activation AP-1. Cellular and Molecular Life Sciences **54**, 129-38.
27. Tran, H., Mattei, M., Godyna, S., and Argraves, W.S. (1997) Human fibulin-1D: molecular cloning, expression and similarity with S1-5 protein, a new member of the fibulin gene family. Matrix Biology **15**, 479-93.
28. Jedsadayanmata, A., Chen, C.C., Kireeva, M.L., Lau, L.F., and Lam, S.C. (1999) Activation-dependent adhesion of human platelets to Cyr61 and Fisp12/mouse connective tissue growth factor is mediated through integrin alpha (IIb) beta (3). Journal of Biological Chemistry **274**, 24321-7.

10) Appendix -- Journal Articles

1. Chang, Y.C., Riby, J., Chang, G., Peng, B.C., Firestone, G., and Bjeldanes, L. (1999) Cytostatic and antiestrogenic effects of 2-(indol-3-ylmethyl)-3,3'-diindolylmethane, a major in vivo product of dietary indole-3-carbinol. J. Biochem. Pharm. **58**, 825-834.
2. Riby , J.E., Feng, C.-L., Chang , Y.C., Schaldach , C.M., Firestone , G.L., and Bjeldanes , L.F. (1999) The major cyclic trimeric product of indole-3-carbinol is a strong agonist of the estrogen receptor signaling pathway. Biochemistry **39**, 910-918.
3. Stephensen, P.U., Bonnesen, C., Bjeldanes, L.F., and Vang, O. (1999) Modulation of cytochrome P4501A1 activity by ascorbigen in murine hepatoma cells. J. Biochem. Pharm., **58**, 1145-1153.
4. Stephensen, P.U., Bonnesen, C., Schaldach, C.M., Bjeldanes, L.F., and Vang, O. (2000) N-Methoxyindol-3-carbinol is a more efficient inducer of cytochrome P-4501A1 in cultured cells than indol-3-carbinol. Nutrition and Cancer, **36**, 112-121.
5. Riby , J.E., Chang, G.H.F., Firestone , G.L., and Bjeldanes , L.F. (1999) Ligand-independent activation of estrogen receptor function by 3,3'-diindolylmethane in human breast-cancer cells. J. Biochem. Pharm **60**, 167-177.
6. Chen, I., Safe, S., and Bjeldanes, L. (1996) Indole-3-carbinol and diindolylmethane as aryl hydrocarbon (Ah) receptor agonists and antagonists in T47D human breast cancer cells. Biochem. Pharm. **51**, 1069-76.
7. Cover, C., Hsieh, S., Tran, S., Kim, G., Bjeldanes, L., and Firestone, G. (1998) Indole-3-carbinol inhibits the expression of cyclin dependent kinase-6 and induces a G1 cell cycle arrest of human breast cancer cells independent of estrogen receptor signaling. J. Biol. Chem. **273**, 3838-3847.
8. Cover, C.M., Hsieh, S.J., Cram, E.J., Hong, C., Riby, J.E., Bjeldanes, L.F., and Firestone, G.L.(1999) Indole-3-carbinol and tamoxifen cooperate to arrest the cell cycle of MCF-7 human breast cancer cells. Cancer Research **59**, 1244-1251.

Biochemical Pharmacology, Vol. 58, pp. 825–834, 1999.

ELSEVIER

ISSN 0006-2952/99/$–see front ma...
PII S0006-2952(99)00165-3

Cytostatic and Antiestrogenic Effects of 2-(Indol-3-ylmethyl)-3,3′-diindolylmethane, a Major *In Vivo* Product of Dietary Indole-3-carbinol

Yu-Chen Chang, Jacques Riby,* Grace H-F. Chang,* BaoCheng Peng,* Gary Firestone† and Leonard F. Bjeldanes*‡*

*Division of Nutritional Sciences and Toxicology, and †Department of Molecular and Cell Biology, University of California, Berkeley, CA 94720, U.S.A.

ABSTRACT. Under acidic conditions, indole-3-carbinol (I3C) is converted to a series of oligomeric products thought to be responsible for the biological effects of dietary I3C. Chromatographic separation of the crude acid mixture of I3C, guided by cell proliferation assay in human MCF-7 cells, resulted in the isolation of 2-(indol-3-ylmethyl)-3,3′-diindolylmethane (LTr-1) as a major antiproliferative component. LTr-1 inhibited the growth of both estrogen-dependent (MCF-7) and -independent (MDA-MB-231) breast cancer cells by approximately 60% at a non-lethal concentration of 25 μM. LTr-1 had no apparent effect on the proliferation of MCF-7 cells in the absence of estrogen. LTr-1 was a weak ligand for the estrogen receptor (ER) (IC_{50} 70 μM) and efficiently inhibited the estradiol (E_2)-induced binding of the ER to its cognate DNA responsive element. The antagonist effects of LTr-1 also were exhibited in assays of endogenous pS2 gene expression and in cells transiently transfected with an estrogen-responsive reporter construct (pERE-vit-CAT). LTr-1 activated both binding of the aryl hydrocarbon (Ah) receptor to its cognate DNA responsive element and expression of the Ah receptor-responsive gene *CYP1A1*. LTr-1 was a competitive inhibitor of CYP1A1-dependent ethoxyresorufin-O-deethylase (EROD) activity. In summary, these results demonstrated that LTr-1, a major *in vivo* product of I3C, could inhibit the proliferation of both estrogen-dependent and -independent breast tumor cells and that LTr-1 is an antagonist of estrogen receptor function and a weak agonist of Ah receptor function. BIOCHEM PHARMACOL 58;5:825–834, 1999. © 1999 Elsevier Science Inc.

KEY WORDS. indole-3-carbinol; 2-(indol-3-ylmethyl)-3; 3′-diindolylmethane; antiestrogenic; breast tumor cells; cytostatic; HPLC

I3C§ is a product of enzymatic hydrolysis of the indolylmethyl glucosinolate glucobrassicin, present in common vegetables of the *Brassica* genus, including cabbage, kale, rutabaga, cauliflower, turnips, broccoli, kohlrabi, mustard, collard, and Brussels sprouts, and is a promising cancer preventive agent (see structure in Fig. 1). Oral administration of I3C to rodents prior to treatment with a carcinogen reduces tumorigenesis in the stomach, liver, lung, and oral cavity by a mechanism that is thought to include induction of phase I and phase II xenobiotic metabolism and increased clearance of the carcinogen [1–5]. When administered at high doses following treatment with a carcinogen, I3C is reported to promote tumorigenesis in the thyroid gland, colon, pancreas, and liver [6–8]. Although the mechanism for these adverse effects of I3C is yet to be determined, one concern is that they might be associated with activation of the Ah receptor. Persistent activation of this receptor is thought to be responsible for the adverse effects of the potent environmental toxin TCDD [9].

The most pronounced and consistently protective effects of I3C have been reported against tumorigenesis in estrogen-responsive tissues. In one of the earliest studies of the protective effects of non-nutritive food components, I3C was shown to reduce by 75% the frequency of dimethylbenzanthracene-induced mammary tumors in rodents [1]. A recent extension of these studies found an even greater protective effect of I3C, i.e. 95% reduction in tumor multiplicity, when the indole was administered prior to and following treatment with the carcinogen [10]. I3C treatment also produced a dramatic decrease (65%) in mammary tumor multiplicity induced by the direct-acting carcinogen methylnitrosourea [10]. Furthermore, I3C is reported to inhibit spontaneous formation of mammary and endometrial tumors in rodents [11, 12]. The protective effects of

‡ Corresponding author: Dr. Leonard F. Bjeldanes, Division of Nutritional Sciences and Toxicology, 119 Morgan Hall, University of California at Berkeley, Berkeley, CA 94720. Tel. (510) 642-1601; FAX (510) 642-0535; E-mail: lfb@nature.berkeley.edu

§ *Abbreviations*: I3C, indole-3-carbinol; LTr-1, 2-(indol-3-ylmethyl)-3,3′-diindolylmethane; ER, estrogen receptor; E_2, 17β-estradiol; Ah, aryl hydrocarbon; EROD, ethoxyresorufin-O-deethylase; TCDD, 2,3,7,8-tetrachlorodibenzo-*p*-dioxine; ICZ, indolo[3,2-*b*]carbazole; DMEM, Dulbecco's modified Eagle's medium; DTT, dithiothreitol; FBS, fetal bovine serum; SSC, 0.15 M sodium chloride + 0.015 M sodium citrate; THF, tetrahydrofuran; DIM, 3,3′-diindolylmethane; RXM, acid reaction mixture; and ERE, estrogen responsive element.

Received 10 August 1998; accepted 7 January 1999.

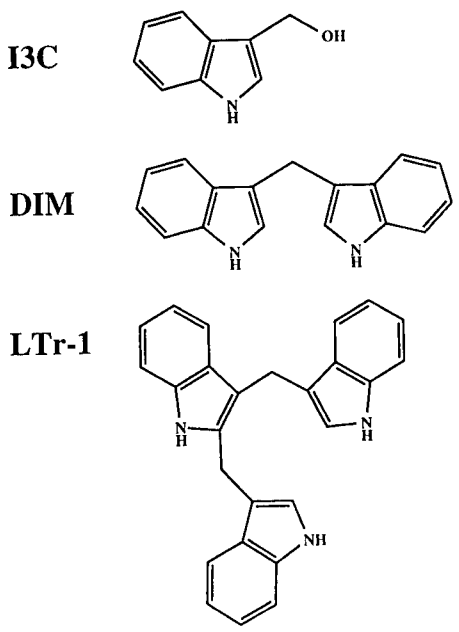

FIG. 1. Structures of I3C, DIM, and LTr-1.

I3C in these studies have been attributed to alterations in E_2 metabolism and/or modifications of ER function.

An important consideration in studies of the biological effects of I3C is its chemical instability. I3C, being a vinylogous hemiaminal, is dehydrated readily in acidic and basic solutions and is converted rapidly to a mixture of oligomeric products [13]. These products, which are produced readily in gastric acid following ingestion, are thought to be responsible for the biological effects of orally administered I3C [14]. We have shown previously that a minor product, ICZ, is a potent activator of Ah receptor pathways and exhibits antiestrogenic activities [15, 16]. DIM, a major product of I3C, is a weak ligand for the Ah receptor, inhibits CYP1A1 enzyme activity, and can act as an antagonist of E_2-mediated tumor cell growth and gene activation [17, 18].

As part of our continuing efforts to understand the mechanisms of action of I3C, we have begun to identify the components of the RXM of I3C that are responsible for the cancer protective effects of I3C and the antiproliferative activity of RXM in cultured breast tumor cells. We report here the effects in tumor cells of the linear trimeric product LTr-1, a second major component of RXM. We show that this novel compound can inhibit proliferation of both estrogen-dependent and -independent cultured breast tumor cells and that it is an antagonist of ER function with little agonist activity. We show further that LTr-1 is a weak agonist of Ah receptor function.

MATERIALS AND METHODS

Materials

DMEM, Opti-MEM, and Lipofectamine were supplied by Gibco/BRL. Phenol red-free DMEM, FBS, calf serum, tamoxifen, and E_2 were supplied by the Sigma Chemical Co. [γ-^{32}P]ATP and [^{3}H]acetyl-CoA were supplied by New England Nuclear. All other reagents were of the highest grade available.

Preparation of RXM

The procedure reported by Grose and Bjeldanes [13] was followed for the preparation of RXM. Briefly, I3C (100 mg, Aldrich Chemical Co.) was suspended in 1 M HCl (100 mL) at room temperature for 15 min. The acid suspension was neutralized with aqueous ammonia to pH 7.0, and the precipitate was filtered and dried under vacuum to give RXM as a reddish powder. LTr-1 is stable under the neutral aqueous conditions of the cell proliferation assay.

Fractionation of RXM

RXM (200 mg) was dissolved in THF (1 mL) and purified by silica gel vacuum liquid chromatography. Mixtures of hexane/THF with increasing polarity were used as the mobile phase. HPLC purification of bioactive components of the crude fractions was performed using a Shimadzu HPLC system (SCL-10A; Shimadzu Scientific Instruments, Inc.) equipped with a C_{18} bonded-phase semi-preparative column (Ultrasphere-ODS, 10 × 250 mm, 5 μm; Beckman) and UV/VIS detector (SPD-10AV; Shimadzu Scientific Instruments, Inc.). The peaks were monitored at 280 nm. For isocratic elution, we used a mixture of acetonitrile: water (60:40) at a flow rate of 2 mL/min. Crude RXM fractions were resuspended in THF before injection into HPLC. The electron impact mass spectrometry analyses of HPLC fractions of interest were obtained by the Mass Spectrometry Facility of the College of Chemistry, University of California at Berkeley.

Cell Culture

The human breast adenocarcinoma cell lines MCF-7 and MDA-MB-231 and the murine hepatoma cell line Hepa-1c1c-7, obtained from the American Type Culture Collection (ATCC), were grown as adherent monolayers in DMEM (Gibco, Life Science Technology), supplemented to 4.0 g/L of glucose and 3.7 g/L of sodium bicarbonate in a humidified incubator at 37° and 5% CO_2, and passaged at approximately 80% confluence. Cultures of human cells were used in subsequent experiments for fewer than 25 passages.

Cell Proliferation

Before the beginning of the treatments, cells were depleted of estrogen for 7–10 days in medium composed of DMEM base without phenol-red (Sigma), with 4 g/L of glucose, 3.7 g/L of sodium bicarbonate, and 5% calf serum twice stripped in dextran-coated charcoal and microfiltered, supplemented with non-essential amino acids (Gibco), 2 mM

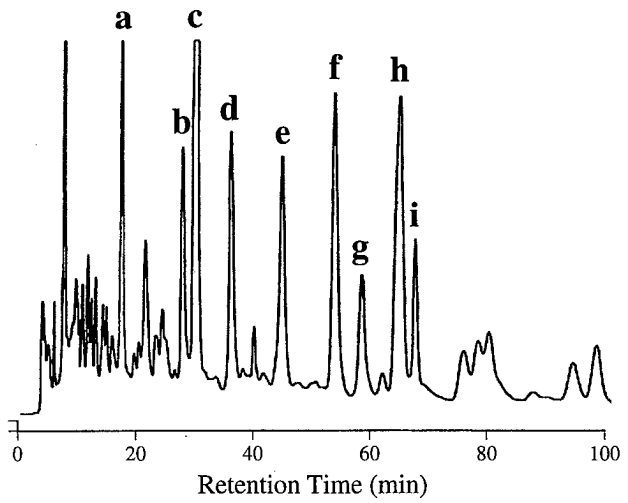

FIG. 2. HPLC chromatogram of fraction B under the conditions described in Materials and Methods. Major peaks were labeled and collected individually.

RNA Extraction and Northern Blot Analysis

Cells were lysed by addition of Tri-reagent (Molecular Research Center, Inc.), and chloroform was used for phase separation. After centrifugation, the water-soluble upper phase was collected, and total RNA was precipitated with isopropanol, washed with 75% ethanol, and dissolved in diethyl pyrocarbonate-treated water. Total RNA was electrophoresed on a 1.2% agarose gel containing 3% formaldehyde, using MOPS as the running buffer. The gel then was washed gently with 10x SSC and blotted with a Zeta nylon membrane (Bio-Rad) overnight. The RNA was fixed to the membrane by UV cross-linking. The hybridization probes were labeled with [^{32}P]CTP using random primers and the pS2-cDNA and GADPH-cDNA plasmids provided by ATCC as the template. Hybridization and quantitation of results were done as described previously [14]. Specific pS2 mRNA levels were normalized using GADPH as a standard.

Nuclear Extracts

Three near confluent (80–90%) cultures of MCF-7 cells in 100-mm Petri dishes were used for each treatment. LTr-1, E_2, and tamoxifen were added as 1 μL of a 1000x stock solution in DMSO per mL of medium. After 2 hr of incubation at 37°, the plates were placed on ice and washed twice with 5 mL of hypotonic buffer (10 mM HEPES, pH 7.5) and incubated with 2 mL of the same buffer for 15 min. Cells were harvested in 1 mL of MDH buffer (3 mM $MgCl_2$, 1 mM DTT, 25 mM HEPES, pH 7.5) with a rubber scraper, homogenized with a loose-fitting Teflon pestle, and centrifuged at 1000 *g* for 4 min at 4°. The pellets were washed twice with 3 mL of MDHK buffer (3 mM $MgCl_2$, 1 mM DTT, 0.1 M KCl, 25 mM HEPES, pH 7.5), resuspended in 1 mL of MDHK, and centrifuged at 600 *g* for 4 min at 4° in a microcentrifuge. The pellets were resuspended in 100 μL of HDK buffer (25 mM HEPES, pH 7.5, 1 mM DTT, 0.4 M KCl), incubated for 20 min on ice with mixing every 5 min, and centrifuged at 14,000 *g* for 4 min at 4°. Glycerol was

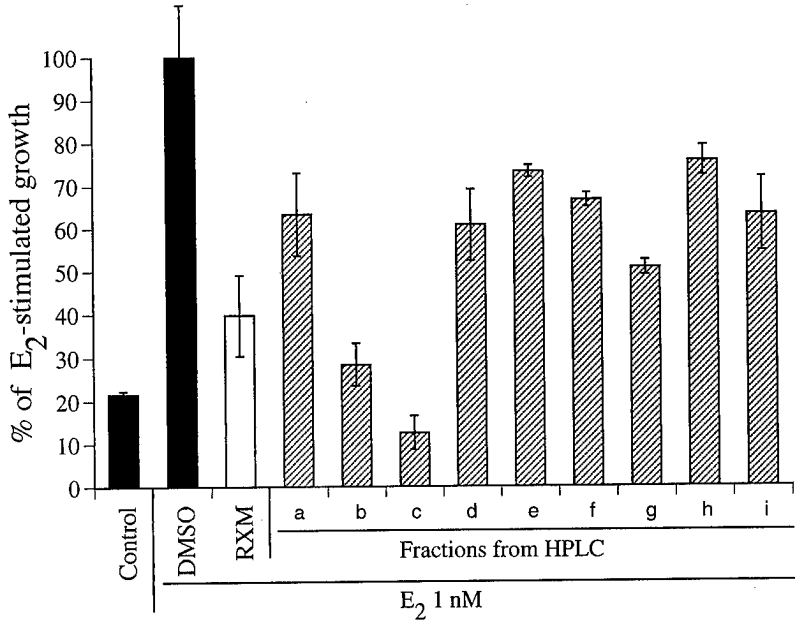

FIG. 3. Antiproliferative effect of subfractions Ba–Bi on MCF-7 cells. Estrogen-depleted MCF-7 cells were plated at a density of 4 × 10^4 cells per well in 24-well plates and treated as indicated with RXM and HPLC fractions at a concentration of 50 μM I3C equivalent. Duplicate aliquots of cells from individual wells were counted after 5 days. The results are shown as the average and SD from three identical wells. Growth was reduced significantly following treatment with RXM and all subfractions (a–i) as determined by Dunnett's test with a procedurewise error rate of < 0.05.

glutamine, and 10 ng/mL of insulin. During the depletion period, medium was changed every other day. Treatments were administered by the addition of 1 μL of 1000x stock solutions in DMSO per mL of medium. Once the treatment period started, medium was changed daily to counter possible loss of readily metabolized compounds. Cells were harvested by trypsinization and counted in a Coulter particle counter.

Estrogen Receptor Binding Assay

Rat uterine cytosol was prepared as described previously [19]. Briefly, 2.5 g of uterine tissue from five Sprague–Dawley rats (12 weeks old) was excised and placed on ice. The fresh tissue was homogenized with 30 mL of ice-cold TEDG buffer (10 mM Tris, pH 7.4, 1.5 mM EDTA, 1 mM DTT, 10% glycerol) using a Polytron at medium speed for 1 min on ice. The homogenate was centrifuged at 1000 *g* for 10 min at 4°. The supernatant solution was transferred to ultracentrifuge tubes and centrifuged at 100,000 *g* for 90 min at 4°. The supernatant solution was divided into 1.0-mL aliquots, quickly frozen in a dry-ice/ethanol bath, and stored at −80°. Protein concentration of the uterine cytosol was measured by the Bradford assay using bovine serum albumin as the standard. For each competitive binding assay, 5 μL of 20 nM [^{3}H]E_2 in 50% ethanol, 10 mM Tris, pH 7.5, 10% glycerol, 1 mg/mL of BSA, and 1 mM DTT was placed in a 1.5-mL microcentrifuge tube. Competitive ligands were added as 1.0 μL of 100x stock solutions in DMSO. After mixing, 95 μL of uterine cytosol was added, and the tubes were vortexed and incubated at room temperature for 2–3 hr. Proteins were precipitated by the addition of 100 μL of 50% hydroxylapatite slurry equilibrated in TE (50 mM Tris, pH 7.4, 1 mM EDTA) and incubated on ice for 15 min with vortexing every 5 min to resuspend hydroxylapatite. The pellet was washed with 1.0 mL of ice-cold wash buffer (40 mM Tris, pH 7.4, 100 mM KCl), and centrifuged for 5 min at 10,000 *g* at 4°. The supernatant was aspirated carefully, and the pellet was washed two more times with 1.0 mL of wash buffer. The final pellet was resuspended in 200 μL of ethanol and transferred to a scintillation vial. The tube was washed with another 200-μL portion of ethanol, which then was added to the same counting vial. A negative control contained no uterine cytosol. Non-specific binding was determined using 100-fold (0.1 μM) excess unlabeled E_2. Relative binding affinities were calculated using the concentration of competitor needed to reduce [^{3}H]E_2 binding by 50% as compared with the concentration of unlabeled E_2 needed to achieve the same result.

Reporter Plasmids and Expression Vectors

The ER responsive CAT reporter plasmid pERE-vit-CAT [20] was a gift from D. J. Shapiro (University of Illinois). pERE-vit-CAT contains the 5′-flanking and promoter region (−596 to +21) of the *Xenopus* vitellogenin-B1 gene, including two imperfect endogenous EREs (at −302 and −334) and one consensus exogenous ERE inserted at position −359. The transfection efficiency control vector pCMVβ constitutively expressing β-galactosidase was obtained from ATCC.

Transient Transfections with Reporters

Transfections were done by the lipofection method using Lipofectamine (Gibco BRL). Cells were grown in 10% FBS-DMEM until 80% confluent and transferred to 6.0-cm Petri plates 24 hr before transfection. The plates were seeded with the appropriate number of cells to be 50–60% confluent at the time of transfection. For each 6-cm plate, 8 μL of Lipofectamine was diluted with 92 μL of Opti-MEM serum-free medium (Gibco). Plasmid DNA (0.1 to 1.0 μg) was diluted in 100 μL of serum-free medium. Lipid and plasmid dilutions were combined, mixed gently, and incubated at room temperature for 30–45 min. Meanwhile, the plates were washed with 4 mL of serum-free medium, and 2 mL of serum-free medium was added to each plate. A 200-μL portion of the lipid/DNA suspension was added to each plate and mixed gently. The plates were returned to the incubator for 5–6 hr, and 2 mL of medium containing 10% calf serum was added. The next day, the plates were treated with fresh stripped medium without phenol red (5% DCC-FBS), and the 48-hr treatments were started by the addition of 1 μL of 1000x stock solutions in DMSO per mL of medium. The transfection efficiency determined with the constitutive galactosidase expression plasmid pCMVβ in duplicate sets of plates was unaffected by the treatments.

Chloramphenicol Acetyl Transferase (CAT) Assay

The CAT assay was done using a modification of the phase extraction assay described by Seed and Sheen [21]. At the end of the 48-hr treatment period, the transfected cells were harvested by scraping with a rubber policeman, transferred with the medium to a conical 15-mL tube, centrifuged at 600 *g* for 2 min, resuspended in 1 mL of cold PBS, transferred to Eppendorf tubes, centrifuged at 600 *g* for 2 min, and washed in PBS a second time. Cell pellets were resuspended in 200 μL of 0.1 M Tris, pH 8.0, and lysed by 3 cycles of freeze/thaw treatment (alternating 5 min in a dry-ice/alcohol bath and 5 min in a 37° bath). Cell lysates were incubated at 65° for 15 min to inactivate acylases and centrifuged at 14,000 *g* for 8 min. A 165-μL aliquot of the cytosol was transferred to a 7-mL scintillation vial, and a 20-μL aliquot was reserved for determination of protein concentration by the Bradford assay. The substrate mixture (85 μL) was added to the scintillation vial for final concentrations of 100 mM Tris–HCl, pH 8.0, 250 nmol chloramphenicol, and 1 μCi [^{3}H]acetyl-CoA (200 mCi/mmol) in a total volume of 250 μL and mixed thoroughly. The organic scintillation fluid (4 mL) was added slowly, and the vials were incubated at 37° for 1–2 hr or until sufficient counts were obtained.

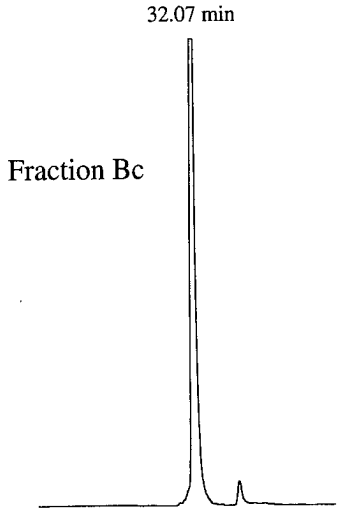

FIG. 4. HPLC analysis of subfraction Bc under the conditions described in Materials and Methods.

added to the supernatants to a concentration of 10%, and aliquots of the nuclear extracts were stored at −80°.

Gel Mobility Shift Assay

The following two sets of complementary oligonucleotides: 5′-GATCCCAGGTCACAGTGACCTGAGCTAAAAT-3′ and 5′-GATCATTTTAGCTCAGGTCACTGTGACC-TGG-3′ containing the palindromic consensus ERE motif (underlined), and 5′-GATCTGGCTCTTCTCACGCA-ACTCCG-3′ and 5′-GATCCGGAGTTGCGTGAGA-AGAGCCA-3′ containing the consensus DRE motif (underlined), were annealed and 5′-end-labeled with [γ-^{32}P]ATP using T4 nucleotide kinase. The resulting labeled double-stranded DNA probes were purified on a Sephadex G50 spin-column, precipitated in ethanol, dissolved in TE buffer, and diluted in 25 mM HEPES, 1 mM DTT, 10% glycerol, 1 mM EDTA to contain approximately 25,000 cpm of ^{32}P/μL. Nuclear extracts (7 μg of proteins) were mixed with 90 ng poly-dIdC, 25 mM HEPES, 1 mM DTT, 10% glycerol, 1 mM EDTA, 160 mM KCl in a total volume of 21 μL. For antibody supershift experiments, 0.5 μg of monoclonal mouse-IgG anti-human-ER (Santa Cruz Biotechnology) was added to the incubation mixture. After incubation for 15–20 min at room temperature, 4 μL (100,000 cpm) of end-labeled ^{32}P probe was added and incubated for another 15 min at room temperature. After the addition of 2.8 μL of 10x Ficoll loading buffer (0.25% bromophenol blue, 25% Ficoll type 400), 22-μL aliquots were loaded onto a pre-run, non-denaturing 4.0% polyacrylamide gel in TAE (67 mM Tris, 33 mM sodium acetate, 10 mM EDTA, pH 8.0) at 120 V for 2 hr. The gel then was dried and autoradiographed.

EROD Assay

Enzymatic activity associated primarily with cytochrome P4501A1 was measured by the EROD assay as described

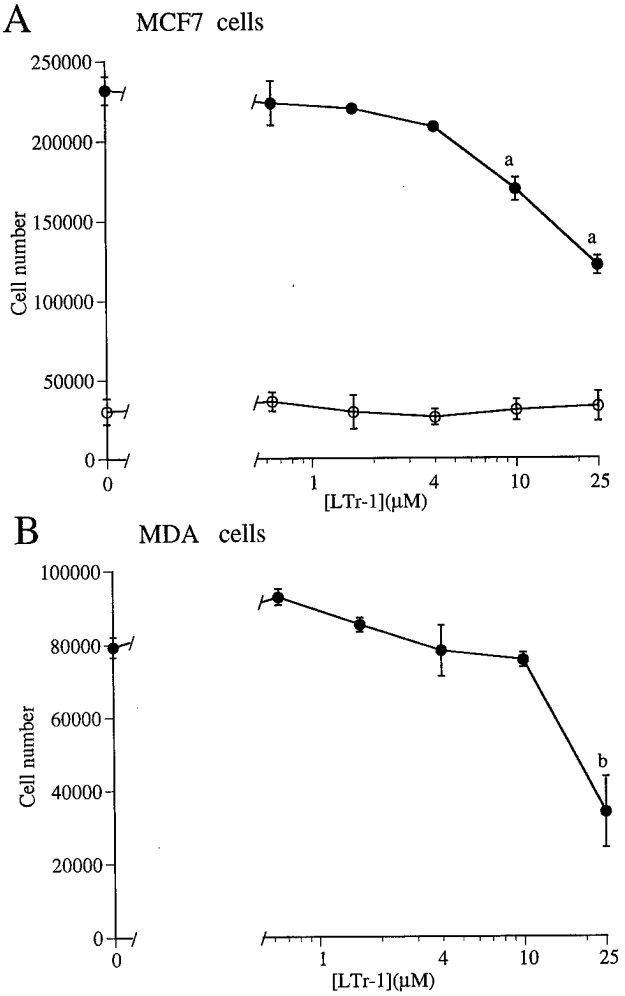

FIG. 5. Effect of LTr-1 on proliferation of breast cancer cells. Panel A: estrogen-depleted MCF-7 cells were plated at a density of 10^5 cells per well in 6-well plates and treated with LTr-1 at the concentrations indicated, in the presence (●) or absence (○) of E_2 (1 nM). Panel B: MDA-MB-231 cells were plated at the same density in complete medium and treated with LTr-1 at the concentrations indicated. Duplicate aliquots of cells from individual wells were counted after 5 days. Data from three identical wells were averaged. The statistical differences between groups were determined using ANOVA and Tukey's Studentized range test. The results are expressed as means ± SD for at least three replicate determinations for each experiment. Key: (a) significantly different ($P < 0.05$) from E_2 induced, and (b) significantly different ($P < 0.05$) from the DMSO control.

previously [22]. Briefly, after the 18- to 24-hr treatment, cells were trypsinized, and 5 mL of PBS was added to the cells. The reaction was done at room temperature, and the cells and the reaction solutions were incubated first at 37°. An aliquot of the cell suspension was counted to obtain the cell number, and 1.5 mL of the cell suspension was placed into a fluorometer cuvette, followed by the addition of 0.5 mL of 2.5 mM ethoxyresorufin (Sigma). The reaction mixture was mixed by inversion of the cuvette, and the linear fluorescence produced was measured at the excitation wavelength of 510 nm and the emission wavelength of 586 nm with a 20-nm slit width using a Perkin-Elmer

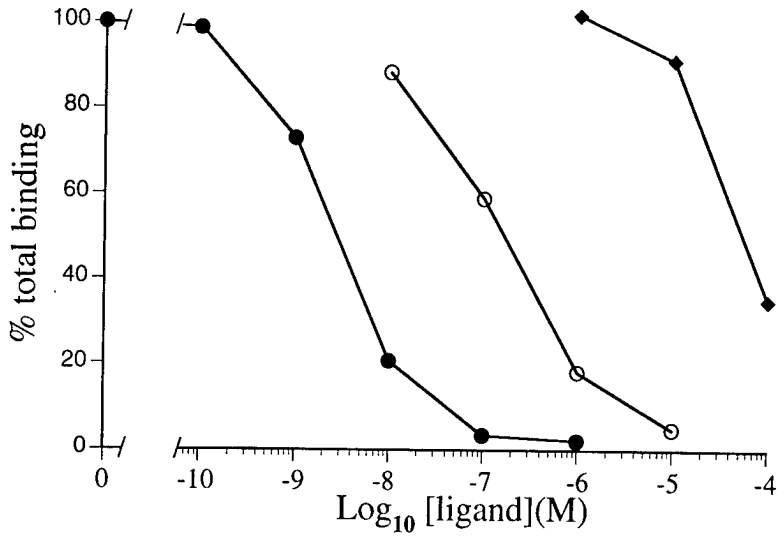

FIG. 6. Competitive binding to the ER. The binding of [^{3}H]E_2 (1 nM) to the ER from rat uterine cytosol was measured in the presence of the unlabeled competitors, E_2 (●), tamoxifen (○), and LTr-1 (◆), at the concentrations indicated and reported as the percentage of binding in the absence of competitors. Results are presented as the averages of two independent determinations. Relative binding affinities were calculated using the concentration of competitor needed to reduce [^{3}H]E_2 binding by 50% as compared with the concentration of unlabeled E_2 needed to achieve the same result.

650–10S spectrofluorometer. Chart speed was recorded for time determination, and a standard curve was obtained using resorufin (Sigma) added to the heated control cells. The enzyme activity was then presented as picomoles of resorufin produced per minute per million cells.

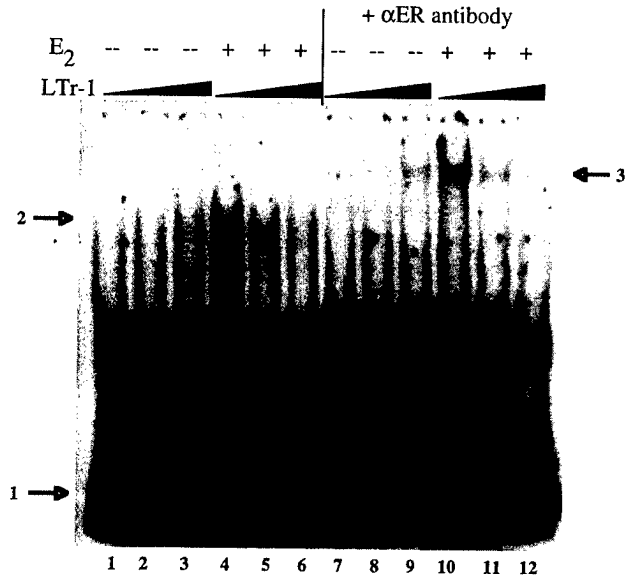

FIG. 7. Binding of nuclear proteins to the ERE. Gel mobility shift analysis of nuclear extracts from estrogen-depleted MCF-7 cells treated for 2 hr with DMSO (lanes 1, 4, 7, 10) or with LTr-1 (1.0 and 10.0 μM in lanes 2, 5, 8, 11 and 3, 6, 9, 12, respectively) and E_2 (1 nM) (lanes 4–6 and 10–12). A monoclonal antibody specific for the human ER also was added to the incubation mixture for lanes 7–12. Arrows indicate the locations of the free labeled probe (arrow #1), the ligand-responsive shifted band (arrow #2), and the antibody-supershifted band (arrow #3).

RESULTS

RXM Fractionation

Silica gel vacuum liquid chromatography was used for the initial crude fractionation of RXM. Five fractions were collected, 100% hexane (A), hexane:THF, 2:1 (B), hexane:THF, 1:1 (C), hexane:THF, 1:2 (D), and 100% THF (E), with gradually increasing mobile phase polarity. At a concentration of 50 μM (I3C equivalent) based on weight of residual material after evaporation of solvent, RXM and all five fractions inhibited MCF-7 cell proliferation in the presence of 1 nM estrogen. Fraction B, the most active fraction, was purified further on a reverse-phase semi-preparative HPLC column using the conditions described in Materials and Methods. The chromatogram shown in Fig. 2 contained a predominant peak and many minor peaks. Of the nine major fractions collected (from Ba to Bi), fraction Bc exhibited the strongest toxic and antiproliferative activities against MCF-7 cells (Fig. 3). In several experiments, crude RXM inhibited cell proliferation by about 70% at the highest non-lethal concentrations (Fig. 3).

HPLC analysis of fraction Bc (Fig. 4) indicated that it contained a compound with the retention time of LTr-1, identified previously as a major component of RXM [23, 24]. Mass spectrometric analysis confirmed this structural assignment.

Cell Proliferation Studies of LTr-1

Results of tumor cell growth experiments showed that both the estrogen-induced proliferation of MCF-7 cells and the estrogen-independent proliferation of the MDA-MB-231 breast tumor cell line were inhibited by LTr-1 by up to 60% in a concentration-dependent manner (Fig. 5). The de-

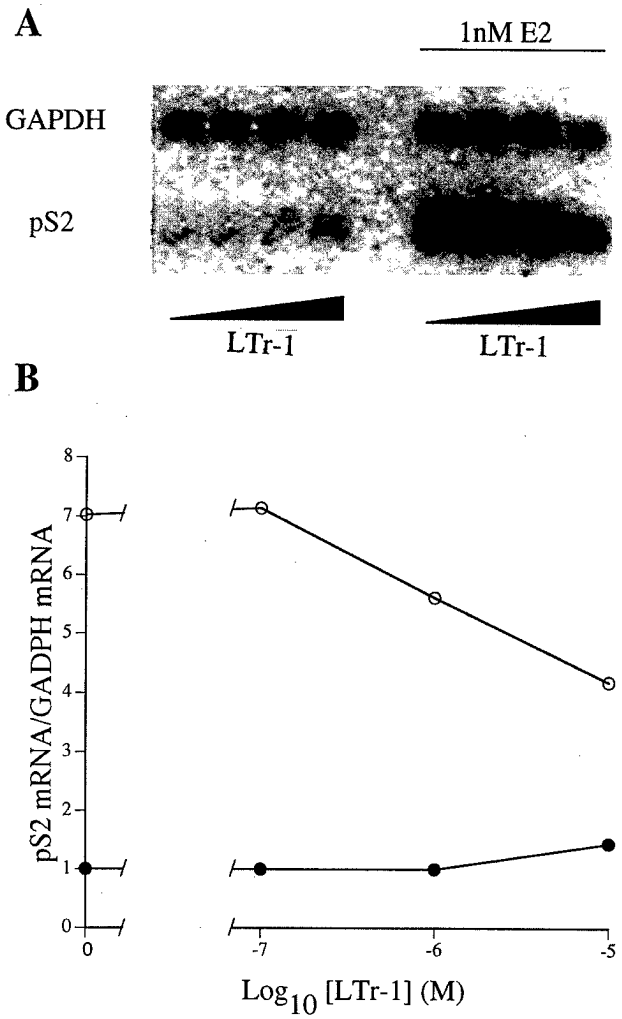

FIG. 8. Effect of LTr-1 on pS2 mRNA expression. Estrogen-depleted MCF-7 cells were treated for 48 hr with LTr-1 at concentrations ranging from 0.1 to 10.0 μM, with (○) or without (●) E_2 (1 nM). pS2 mRNA levels were measured by northern blot analysis (A) and normalized using GADPH mRNA as an internal standard (B). Results are presented as fold induction over the DMSO control (averages of two independent determinations).

creased cell counts apparently were not due to a general toxicity of the trimer, since we saw no evidence of cell killing over the 5-day treatment period. Interestingly, LTr-1 exhibited no apparent effect on proliferation of MCF-7 cells in the absence of E_2.

Effects of LTr-1 on Estrogen Receptor Binding and Function

Because LTr-1 inhibited the E_2-induced proliferation of MCF-7 cells, we examined the effects of this indole derivative on components of the ER signal transduction pathway. The relative binding affinity of LTr-1 for the ER, as measured by a competitive binding assay, indicated an IC_{50} of approximately 70 μM compared with 200 and 3.0 nM measured for tamoxifen and E_2, respectively (Fig. 6). Thus, LTr-1 exhibits a weak affinity for the ER.

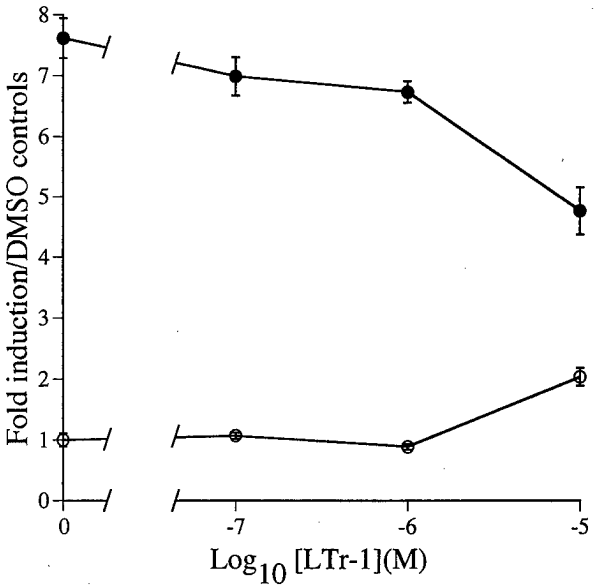

FIG. 9. Effect of LTr-1 on CAT expression from the ERE-vit-CAT reporter gene. MCF-7 cells were transiently transfected with the pERE-vit-CAT reporter plasmid and treated for 48 hr with LTr-1 at the concentrations indicated, in the presence (●) or absence (○) of E_2 (1 nM). CAT activity in cytosol preparations from individual plates was normalized for protein concentration. Results are presented as fold induction over the DMSO control (mean ± range of two independent determinations).

We next examined by gel mobility shift assay the effect of LTr-1 on the binding activity of ER to its cognate DNA motif. LTr-1 exhibited a strong concentration-dependent inhibitory effect on the E_2-induced binding of ER to a consensus ERE with nearly complete loss of the shifted band at 10 μM LTr-1 (Fig. 7). In the absence of E_2, however, LTr-1 exhibited weak agonist activity on ERE binding to DNA.

To determine whether LTr-1 can affect transcription of estrogen-responsive genes, we examined its effects on expression of the endogenous pS2 gene, often used as a marker of estrogen-responsive breast tumors, and on the pERE-vit-CAT reporter construct transiently transfected into MCF-7 cells. The pERE-vit-CAT construct contains the promoter and 5′-flanking region of the *Xenopus* vitellogenin gene upstream of the CAT structural gene. The results of northern blot analysis indicated that E_2-induced transcription of pS2 was inhibited in a concentration-dependent manner (approximately 50% at 10 μM) by LTr-1 (Fig. 8). In the absence of E_2, LTr-1 did not induce significant transcription of pS2. A similar inhibitory effect of LTr-1 was seen on E_2-induced expression of the pERE-vit-CAT reporter construct (Fig. 9). In this case, however, LTr-1 exhibited a weak activation of this reporter in the absence of E_2. Thus, LTr-1 could suppress activation of E_2-responsive genes at concentrations that inhibited breast tumor cell proliferation.

Effects of LTr-1 on Ah Receptor Signaling

We reported previously that LTr-1 has an appreciable affinity for the Ah receptor [23]. Since persistent activation of the Ah receptor is thought to be responsible for the toxic effects of certain ligands, including TCDD, we examined further the effects of LTr-1 on this pathway.

The effects of LTr-1 on binding of the Ah receptor to its cognate DNA motif, DRE, as determined by gel mobility shift assay, are represented in Fig. 10. At a concentration of 1 μM, LTr-1 promoted detectable binding of the Ah receptor to the DRE. At a concentration of 10 μM, binding was as strong as the positive control, ICZ, indicating that LTr-1 could efficiently transform the Ah receptor to a DNA binding form.

As shown in Fig. 11, LTr-1 was a weak inducer of Ah receptor responsive CYP1A1 activity in the concentration range of 1–10 μM, with a maximum induction of approximately 20% of the EROD activity induced by ICZ. We found also that LTr-1 was an inhibitor of induced CYP1A1 activity. As shown in Fig. 12, LTr-1 suppressed EROD activity with an ic_{50} of about 1.0 μM. The result of the double-reciprocal plot analysis indicates that LTr-1 was a competitive inhibitor of EROD activity (K_i = 0.913 mM) (data not shown). Taken together, these results indicate

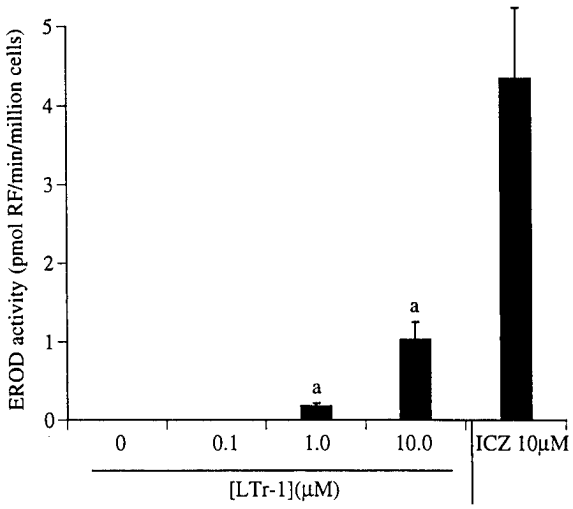

FIG. 11. Induction of expression of cytochrome P4501A1 by LTr-1. MCF-7 cells grown in 10% FBS-DMEM were treated with LTr-1 or ICZ at the concentrations indicated for 24 hr. Expression of P4501A1 was measured by the EROD assay and normalized for cell number in individual plates. RF = resorufin. The statistical differences between groups were determined using ANOVA and Tukey's Studentized range test. The results are expressed as means ± SD for at least three replicate determinations for each experiment. Key: (a) significantly different ($P < 0.05$) from the ICZ control.

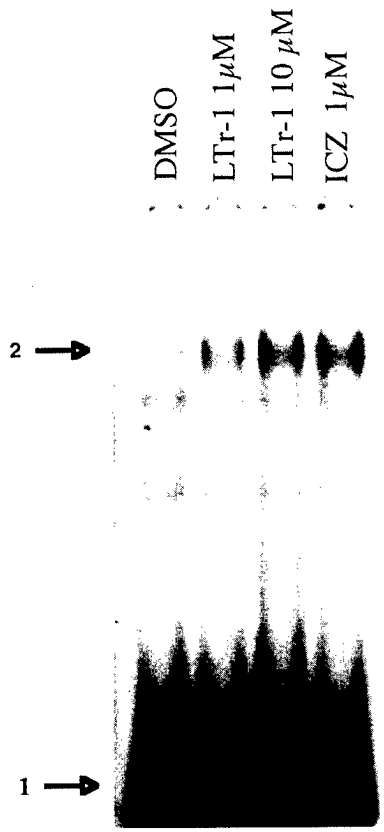

FIG. 10. Binding of nuclear proteins to the DRE. Gel mobility shift analysis of nuclear extracts from Hepa-1c1c-7 cells treated for 2 hr with DMSO, LTr-1, or ICZ. Arrows indicate the locations of the free labeled probe (arrow #1) and the ligand-responsive shifted band (arrow #2).

that LTr-1 is a weak but efficient agonist of Ah receptor function and an inhibitor of the Ah receptor-induced CYP1A1 enzyme activity.

DISCUSSION

Our results show that LTr-1 can inhibit ER function and activate Ah receptor function. In this respect, LTr-1 appears to produce effects similar to those of potent Ah receptor ligands including TCDD and ICZ. However, whereas LTr-1 can inhibit the estrogen-dependent proliferation of MCF-7 cells and the estrogen-independent proliferation of MDA-MB-231 cells, this indole produced little effect on the estrogen-independent proliferation of MCF-7 cells. These antiproliferative effects of LTr-1 are in contrast to those of TCDD, which strongly inhibits the estrogen-induced growth of MCF-7 cells but, in the same concentration range, has little effect on the proliferation of MDA-MB-231 cells [22]. Thus, the antiproliferative effects of LTr-1 in the two cell lines appear to require processes in addition to, or other than, those activated by TCDD. Other possible explanations for these effects include differences in the metabolism of LTr-1 in the cell lines such that a more generally cytostatic metabolite accumulates in the MDA-MB-231 cells and not in the MCF-7 cells.

The biological effects of LTr-1 differ in several respects from those of DIM, which we will report elsewhere.* Whereas the antiproliferative effects of these substances on

* Riby JE, Chang GHF, Firestone GL and Bjeldanes LF, manuscript submitted for publication.

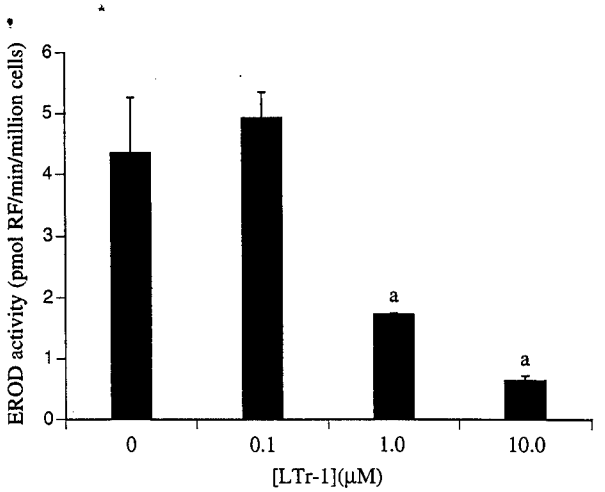

FIG. 12. Inhibition of EROD activity. MCF-7 cells that were 70–80% confluent were treated with 1 μM ICZ for 24 hr. LTr-1 was added to the cell suspension in the fluorometer cuvette to obtain final concentrations of 0.1, 1, and 10 μM, respectively, and incubated at room temperature for 5 min. Finally, 0.5 mL of 2.5 mM ethoxyresorufin was added to the cuvette, and the EROD activity was measured as described above. RF = resorufin. The statistical differences between groups were determined using ANOVA and Tukey's Studentized range test. The results are expressed as means ± SD for at least three replicate determinations for each experiment. Key: (a) significantly reduced ($P < 0.05$) from the DMSO control.

the E_2-dependent proliferation of MCF-7 cells and the E_2-independent proliferation of MDA cells were similar, LTr-1 exhibited little effect on the MCF-7 cells in the absence of E_2. In contrast, DIM showed a marked induction of MCF-7 cell proliferation under E_2-depleted conditions. Consistent with these growth effects, LTr-1 was primarily an antagonist in our assays of ER function, whereas DIM was consistently an agonist of this activity. Similar to DIM, LTr-1 was a weak agonist of Ah receptor function. Thus, in contrast to DIM, LTr-1 is a consistent inhibitor of breast tumor cell proliferation and shows little evidence that it might function as an agonist of ER-mediated transcriptional events. In this respect, the activities of LTr-1 in cultured cells are similar to the effects we observed for RXM. However, determination of whether LTr-1, DIM, or other RXM products can account for all or part of the effects of I3C administered orally requires further *in vivo* and *in vitro* studies of the individual and combinatorial effects of these substances.

Previous studies have established that LTr-1 and DIM are major *in vivo* products of orally administered I3C. Estimates of LTr-1 produced in the stomachs of rodents within several hours of oral administration of I3C range in yield from about 0.2 to 2.0% [23, 24]. These products appear to be absorbed to a similar extent from the gastrointestinal tract, since the relative concentrations of the two compounds found in the liver are similar to those found initially in the stomach. It is interesting to note that the concentrations of the two compounds found in the livers of treated rodents (up to 13 μM) [13] are within the range in which these substances are active in our cell proliferation and ER-dependent gene activation assays.

Efforts to estimate likely exposure to LTr-1 following ingestion of *Brassica* vegetables are difficult, since no direct measurements of glucobrassicin conversion to LTr-1 are available. Nevertheless, since it is well established that LTr-1 is a major product of I3C oligomerization *in vitro* and *in vivo*, in some cases exceeding DIM in yield, it is reasonable to estimate LTr-1 exposures based on estimates of DIM exposures. Thus, based on the published levels of glucobrassicin in fresh Brussels sprouts of about 1.4 g/kg and assuming a conversion of glucobrassicin of about 5%, the level of LTr-1 produced from a 100-g portion of vegetable is about 5–10 mg. On the assumption that absorption from the gastrointestinal tract is nearly complete, this would provide blood concentrations for an average person of as high as 8 μM. Thus, following ingestion of a 100-g portion of cruciferous vegetables, an average person may attain a blood concentration of LTr-1 of within an order of magnitude of the effective levels determined in this study.

Thus, these studies establish LTr-1 as a novel inhibitor of breast tumor cell proliferation that can affect both estrogen-dependent and -independent cellular pathways in cultured cells in a range of concentrations similar to concentrations found *in vivo* following ingestion of naturally occurring I3C. Further studies of the antiproliferative efficacy and modes of action of this compound are in progress.

This work was supported by the Department of Defense, Army Breast Cancer Research Program Grant DAMD17-96-1-6149 and by Grant CA69056 from the National Institutes of Health.

References

1. Wattenberg LW and Loub WD, Inhibition of polycyclic aromatic hydrocarbon-induced neoplasia by naturally occurring indoles. *Cancer Res* **38**: 1410–1415, 1978.
2. Nixon JE, Hendricks JD, Pawlowski NE, Pereira CB, Sinnhuber RO and Bailey GS, Inhibition of aflatoxin B_1 carcinogenesis in rainbow trout by flavone and indole compounds. *Carcinogenesis* **5**: 615–619, 1984.
3. Tanaka T, Kojima T, Morishita Y and Mori H, Inhibitory effects of the natural products indole-3-carbinol and sinigrin during initiation and promotion phases of 4-nitroquinoline 1-oxide-induced rat tongue carcinogenesis. *Jpn J Cancer Res* **83**: 835–842, 1992.
4. Morse MA, LaGreca SD, Amin SG and Chung FL, Effects of indole-3-carbinol on lung tumorigenesis and DNA methylation induced by 4-(methylnitrosamino)-1-(3-pyridyl)-1-butanone (NNK) and on the metabolism and disposition of NNK in A/J mice. *Cancer Res* **50**: 2613–2617, 1990.
5. Fong AT, Swanson HI, Dashwood RH, Williams DE, Hendricks JD and Bailey GS, Mechanisms of anti-carcinogenesis by indole-3-carbinol. Studies of enzyme induction, electrophile-scavenging, and inhibition of aflatoxin B_1 activation. *Biochem Pharmacol* **39**: 19–26, 1990.
6. Pence B, Buddingh H and Yang S, Multiple dietary factors in the enhancement of dimethylhydrazine carcinogenesis: Main effect of indole-3-carbinol. *J Natl Cancer Inst* **77**: 269–276, 1986.
7. Bailey GS, Hendricks JD, Shelton KW, Nixon JE and

Pawlowski NE, Enhancement of carcinogenesis by the natural anticarcinogen indole-3-carbinol. *J Natl Cancer Inst* **78**: 931–936, 1987.
8. Kim D, Han B, Ahn B, Hasegawa R, Shirai T, Ito N and Tsuda H, Enhancement by indole-3-carbinol of liver and thyroid gland neoplastic development in a rat medium-term multiorgan carcinogenesis model. *Carcinogenesis* **18**: 377–381, 1997.
9. Schmidt JV and Bradfield CA, Ah receptor signaling pathways. *Annu Rev Cell Dev Biol* **12**: 55–89, 1996.
10. Grubbs CJ, Steele VE, Casebolt T, Juliana MM, Eto I, Whitaker LM, Dragnev KH, Kelloff GJ and Lubet RL, Chemoprevention of chemically-induced mammary carcinogenesis by indole-3-carbinol. *Anticancer Res* **15**: 709–716, 1995.
11. Bradlow HL, Michnovicz JJ, Telang NT and Osborne MP, Effects of dietary indole-3-carbinol on estradiol metabolism and spontaneous mammary tumors in mice. *Carcinogenesis* **12**: 1571–1574, 1991.
12. Kojima T, Tanaka T and Mori H, Chemoprevention of spontaneous endometrial cancer in female Donryu rats by dietary indole-3-carbinol. *Cancer Res.* **54**: 1446–1449, 1994.
13. Grose KR and Bjeldanes LF, Oligomerization of indole-3-carbinol in aqueous acid. *Chem Res Toxicol* **5**: 188–193, 1992.
14. Stresser DM, Williams DE, Griffin DA and Bailey GS, Mechanisms of tumor modulation by indole-3-carbinol. Disposition and excretion in male Fischer 344 rats. *Drug Metab Dispos* **23**: 965–975, 1995.
15. Chen Y-H, Riby J, Srivastava P, Bartholomew J, Denison M and Bjeldanes L, Regulation of CYP1A1 by indolo[3,2-*b*]carbazole in murine hepatoma cells. *J Biol Chem* **270**: 22548–22555, 1995.
16. Chen I, Safe S and Bjeldanes L, Indole-3-carbinol and diindolymethane as aryl hydrocarbon (Ah) receptor agonists and antagonists in T47D human breast cancer cells. *Biochem Pharmacol* **51**: 1069–1076, 1996.
17. Stresser DM, Bjeldanes LF, Bailey GS and Williams DE, The anticarcinogen 3,3′-diindolylmethane is an inhibitor of cytochrome P-450. *J Biochem Toxicol* **10**: 191–201, 1995.
18. Chen I, McDougal A, Wang F and Safe S, Aryl hydrocarbon receptor-mediated antiestrogenic and antitumorigenic activity of diindolylmethane. *Carcinogenesis* **19**: 1631–1639, 1998.
19. Santell RC, Chang YC, Nair MG and Helferich WG, Dietary genistein exerts estrogenic effects upon the uterus, mammary gland and the hypothalamic/pituitary axis in rats. *J Nutr* **127**: 263–269, 1997.
20. Chang T-C, Nardulli AM, Lew D and Shapiro DJ, The role of estrogen response elements in expression of the *Xenopus laevis* vitellogenin B1 gene. *Mol Endocrinol* **6**: 346–354, 1992.
21. Seed B and Sheen JY, A simple phase-extraction assay for chloramphenicol acyltransferase activity. *Gene* **67**: 271–277, 1988.
22. Dohr O, Vogel D and Abel J, Different response of 2,3,7,8-tetrachlorodibenzo-*p*-dioxin (TCDD)-sensitive genes in human breast cancer MCF-7 and MDA-MB-231 cells. *Arch Biochem Biophys.* **321**: 405–412, 1995.
23. Bjeldanes L, Kim JY, Grose KR, Bartholomew JC and Bradfield CA, Aromatic hydrocarbon responsiveness-receptor agonists generated from indole-3-carbinol *in vitro* and *in vivo*: Comparisons with TCDD. *Proc Natl Acad Sci USA* **88**: 9543–9547, 1991.
24. De Kruif CA, Marsman JW, Venekamp JC, Falke HE, Noordhoek J, Blaauboer BJ and Wortelboer HM, Structure elucidation of acid reaction products of indole-3-carbinol: Detection *in vivo* and enzyme induction *in vitro*. *Chem Biol Interact* **80**: 303–315, 1991.

The Major Cyclic Trimeric Product of Indole-3-carbinol Is a Strong Agonist of the Estrogen Receptor Signaling Pathway

Jacques E. Riby, Chunling Feng, Yu-Chen Chang, Charlene M. Schaldach, Gary L. Firestone, and Leonard F. Bjeldanes

Division of Nutritional Sciences and Toxicology, and Department of Molecular and Cell Biology, University of California, Berkeley, California 94720

Biochemistry®

Reprinted from
Volume 39, Number 5, Pages 910–918

The Major Cyclic Trimeric Product of Indole-3-carbinol Is a Strong Agonist of the Estrogen Receptor Signaling Pathway†

Jacques E. Riby,‡ Chunling Feng,‡ Yu-Chen Chang,‡ Charlene M. Schaldach,‡ Gary L. Firestone,§ and Leonard F. Bjeldanes*,‡

Division of Nutritional Sciences and Toxicology, and Department of Molecular and Cell Biology, University of California, Berkeley, California 94720

Received August 23, 1999; Revised Manuscript Received November 15, 1999

ABSTRACT: Indole-3-carbinol (I3C), a component of *Brassica* vegetables, is under study as a preventive agent of cancers of the breast and other organs. Following ingestion, I3C is converted to a series of oligomeric products that presumably are responsible for the in vivo effects of I3C. We report the effects of the major trimeric product, 5,6,11,12,17,18-hexahydrocyclonona[1,2-*b*:4,5-*b*′:7,8-*b*″]triindole (CTr), on the estrogen receptor (ER) signaling pathways. Tumor-promoting effects of high doses of I3C may be due to activation of aryl hydrocarbon receptor (AhR)-mediated pathways; therefore, we also examined the effects of CTr on AhR activated processes. We observed that CTr is a strong agonist of ER function. CTr stimulated the proliferation of estrogen-responsive MCF-7 cells to a level similar to that produced by estradiol (E_2) but did not affect the growth of the estrogen-independent cell line, MDA-MD-231. CTr displaced E_2 in competitive-binding studies and activated ER-binding to an estrogen responsive DNA element in gel mobility shift assays with EC_{50}s of about 0.1 μM. CTr activated transcription of an E_2-responsive endogenous gene and exogenous reporter genes in transfected MCF-7 cells, also with high potency. CTr failed to activate AhR-mediated pathways, consistent with the low-binding affinity of CTr for the AhR reported previously. Comparisons of the conformational characteristics of CTr with other ER ligands indicated a remarkable similarity with tamoxifen, a selective ER antagonist used as a breast cancer therapeutic agent and suggest an excellent fit of CTr into the ligand-binding site of the ER.

Indole-3-carbinol (I3C),[1] a hydrolytic product of glucobrassicin found in common *Brassica* vegetables, is under study as a tumor preventive agent (*1*−*3*). Some of the most pronounced effects of I3C have been reported to be against tumor development in estrogen-responsive tissues. When administered prior to and during treatment with direct- and indirect-acting mammary carcinogens, I3C reduced tumor incidence by as much as 95% (*4*, *5*). I3C is also reported to inhibit spontaneous formation of tumors of the mammary gland and of the endometrium of rodents (*6*, *7*). At high doses, I3C promotes tumorigenesis in the thyroid gland, colon, pancreas, and liver of rodents when administered following treatment with a carcinogen (*8*−*10*). A recent report indicates that I3C exhibits tumor-promoting activity in the trout model in a range of concentrations below that which is required to induce the cytochrome P450 pathways thought to be important in the cancer protective effects of I3C (*11*). Clearly, if I3C is to be developed further as a cancer protective agent, its modes of action as a tumor-preventive and tumor-promoting agent must be thoroughly understood.

In our continuing efforts to examine the mechanisms of action of I3C, we have begun to determine the biological activities of the components of the acid reaction mixture (RXM) of I3C. It is now well-established that I3C is highly unstable in gastric acids and is rapidly converted to a mixture of oligomeric products following ingestion (*12*, *13*). I3C products found in vivo include indolo[3,2-*b*]carbazole (ICZ), a minor product that is a potent activator of Ah receptor pathways and exhibits antiestrogenic activities, DIM, a major product that is a potent inhibitor of carcinogen-induced mammary tumorigenesis in rodents and a weak activator of the Ah receptor, and LTr, a second major product and an antagonist of estrogen receptor function that inhibits proliferation of both estrogen-dependent and -independent cultured breast tumor cells (*14*−*19*). We report here the effects of the third major component of RXM, the cyclic trimeric product, 5,6,11,12,17,18-hexahydrocyclonona[1,2-*b*:4,5-*b*′:7,8-*b*″]triindole (CTr), on pathways mediated by the estrogen receptor and the Ah receptor in tumor cells. We show that this indole product is a strong agonist of estradiol (E_2) functions including estrogen receptor binding and activation and induction of proliferation of estrogen-dependent cultured breast tumor cells and transcriptional activation of E_2-

† This work was supported by the Department of Defense, Army Breast Cancer Research Program Grant DAMD17-96-1-6149 and by Grant CA69056 from the National Institutes of Health.

* Corresponding author: Leonard F. Bjeldanes, Division of Nutritional Sciences and Toxicology, 119 Morgan Hall, University of California at Berkeley, Berkeley, CA 94720. Telephone: 510-642-1601. Fax: 510-642-0535. E-mail: lfb@nature.berkeley.edu.

‡ Division of Nutritional Sciences and Toxicology.

§ Department of Molecular and Cell Biology.

[1] Abbreviations: I3C, indole-3-carbinol; CTr, 5, 6, 11, 12, 17, 18-hexahydrocyclonona[1, 2-*b*: 4, 5-*b*′: 7, 8-*b*″]triindole; E_2, 17-β-estradiol; ER, estrogen receptor; ERE, estrogen receptor responsive element; AhR, aryl hydrocarbon receptor; DIM, 3,3′-diindolylmethane; ICZ, indolo-[3, 2-*b*]carbazole; LTr-1, 2-(indol-3-ylmethyl)-3, 3′- diindolylmethane; EROD, ethoxyresorufin O-deethylase; OHT, 4-hydroxytamoxifen.

10.1021/bi9919706 CCC: $19.00
Published on Web 01/14/2000

responsive genes. In contrast, CTr exhibited weak activities in measures of Ah receptor activation that were consistent with the low-binding affinity we have reported previously for this receptor (*13*). Conformational comparisons indicated that CTr is similar to the established therapeutic agent, tamoxifen, and that CTr fits strickingly well into the ligand-binding site of the ER.

EXPERIMENTAL PROCEDURES.

Preparation of Acid Reaction Mixture (RXM). The procedure reported by Gross and Bjeldanes (*12*) was followed for the preparation of RXM. Briefly, I3C (100 mg, Aldrich Chemical Co., Milwaukee, WI) was suspended in 1 M HCl (100 mL) at room temperature for 15 min. The acid suspension was neutralized with aqueous ammonia to pH 7.0, and the precipitate was filtered and dried under vacuum to give RXM as a reddish powder.

Isolation CTr from RXM. RXM (200 mg) was dissolved in 1 mL of THF and fractionated initially by silica gel vacuum liquid chromatography. Mixtures of hexane/THF with increasing polarity were used as mobile phase to obtain the following five crude fractions: 100% hexane (A), hexane/THF 2:1 (B), hexane/THF 1:1 (C), hexane/THF 1:2 (D) and 100% THF (E). Fractions B and C, shown by analytical HPLC to contain CTr, were combined, extracted with hexane to remove highly lipophilic components, and resuspended in THF before injection onto semipreparative HPLC. HPLC purification of CTr was performed using a Shimadzu HPLC system (SCL-10A, Shimadzu Scientific Instruments, Inc., Japan) equipped with a C-18 bonded-phase semipreparative column (Beckman Ultrasphere-ODS, 10 × 250 mm, 5 mm) (Beckman, San Ramon, CA) and UV-vis detector (SPD-10AV, Shimadzu Scientific Instruments, Inc., Japan). Isocratic elution employed a mixture of acetonitrile/water (60:40) at a flow rate of 1.5 mL/min with the detector setting at 280 nm. The electron impact mass spectrometry analyses of the HPLC fractions of interest were performed at the Mass Spectrometry Facility of the College of Chemistry, University of California at Berkeley. The isolated CTr gave a single peak on analytical HPLC with the expected mass spectrum (*12*).

Cell Culture. The human breast adenocarcinoma cell lines, MCF-7 and MDA-MB-231, and the murine hepatoma cell line, Hepa-1c1c7, obtained from the American Type Culture Collection (ATCC, Maryland, U.S.A.), were grown as adherent monolayers in Dulbecco's modified Eagle's medium (DMEM), supplemented with 10% fetal bovine serum and passaged at approximately 80% confluence. Cultures of human cells were used in subsequent experiments for fewer than 25 passages.

Cell Proliferation. Before the beginning of the treatments, cells were depleted of estrogen for 7−10 days in medium composed of phenol-red-free DMEM supplemented with 5% calf serum twice stripped in dextran-coated charcoal, 0.1 nM nonessential amino acids, 2 mM glutamine and 10 ng/mL insulin. During the depletion period, medium was changed every other day. Treatments were administered by addition of 1 μL of 1000X solutions in DMSO per mL of medium. Once the treatment period started, medium was changed daily to counter possible loss of readily metabolized compounds. Cells were harvested by trypsinization and counted in a Coulter (Miami, FL) particle counter.

Estrogen Receptor (ER) Binding Assay. Rat uterine cytosol was prepared as described previously (*20*). Briefly, 2.5 g of uterine tissue from five Sprague−Dawley rats (12 weeks old) was excised and placed on ice. The fresh tissue was homogenized with 30 mL of ice-cold TEDG buffer (10 mM Tris, pH 7.4, 1.5 mM EDTA, 1 mM DTT, 10% glycerol) using a Polytron at medium speed for 1 min on ice. The homogenate was centrifuged at 1000*g* for 10 min at 4 °C. The supernatant solution was transferred to ultracentrifuge tubes and centrifuged at 100 000*g* for 90 min at 4 °C. The supernatant solution was divided into 1.0 mL aliquots, quickly frozen in a dry ice/ethanol bath, and stored at −80 °C. Protein concentration of the uterine cytosol was measured by the Bradford assay using bovine serum albumin as the standard. For each competitive-binding assay, 5 μL of 20 nM ^{3}H-E_2 in 50% ethanol, 10 mM Tris, pH 7.5, 10% glycerol, 1 mg/mL BSA, and 1 mM DTT was placed in a 1.5 mL microcentrifuge tube. Competitive ligands E_2 (0.1 nM−1.9 μM), ICI_{182780} (0.1 nM−5.0 μM), and CTr (1.0 nM−10 μM) were added as 1.0 μL of 100X solution in DMSO. After the solution was mixed, 95 μL of uterine cytosol was added, the solutions were vortexed and incubated at room temperature for 2−3 h. Proteins were precipitated by addition of 100 μL of 50% hydroxylapatite slurry equilibrated in TE (50 mM Tris, pH 7.4, 1 mM EDTA) and incubation on ice for 15 min with vortexing every 5 min to resuspend hydroxylapatite. The pellet was washed with 1.0 mL ice-cold wash buffer (40 mM Tris, pH 7.4, 100 mM KCl), and centrifuged for 5 min at 10 000 rpm at 4 °C. The supernatant was carefully aspirated and the pellet washed two more times with 1.0 mL of wash buffer. The final pellet was resuspended in 200 μL ethanol and transferred to a scintillation vial. The tube was washed with another 200 μL portion of ethanol, which was then added to the same counting vial. A negative control contained no uterine cytosol. Nonspecific binding was determined using 1000-fold excess of unlabeled E_2. Data points were connected by a Bezier curve and EC_{50} values were determined graphically as the concentration of competitor needed to reduce ^{3}H-E_2 binding by 50%.

Reporter Plasmids and Expression Vectors. The ER-responsive CAT reporter plasmids pERE-vit-CAT and pATC2 (*21*) were gifts from D. J. Shapiro (University of Illinois, Urbana-Champain). pERE-vit-CAT contains the 5′-flanking and promoter region (−596 to 21) of the *Xenopus* vitellogenin-B1 gene, including two imperfect endogenous EREs (at −302 and −334) and an exogenous consensus ERE (GGTCACAGTGACC) inserted at position −359. The simpler reporter pATC2 contains two copies of the consensus ERE coupled 38 bp from the TATA box of the vitellogenin-B1 promoter (−42 to 14). The luciferase reporter plasmid pS2-luc (*22*) containing the 5′-flanking region (−537 to −87) of the human pS2 gene upstream of the SV40 promoter and the firefly luciferase stuctural gene was a gift from T. Zacharewski (University of Western Ontario, London Ontario, Canada). The plasmid pCMV-hER constitutively expressing a fully functional human estrogen receptor (*23*) was a gift from B. S. Katzenellenbogen (University of Illinois, Urbana-Champain). The transfection efficiency control vector, pCMVβ constitutively expressing β-galactosidase, was obtained from ATCC.

Transient Transfections with Reporters. Transfections were done using Lipofectamine (Gibco BRL). Cells were grown in 10% FBS-DMEM until 80% confluent and transferred to 6.0 cm Petri plates 24 h before transfection. The plates were seeded with the appropriate number of cells to be 50−60% confluent at the time of transfection. For each 6 cm plate, 8 μL of lipofectamine was diluted with 92 μL of serum free medium. Plasmid DNA (0.1 μg luciferase reporter DNA per plate and 1.0 μg CAT reporter DNA per plate) was diluted in 100 μL of a serum-free medium. Lipid and plasmid dilutions were combined, mixed gently, and incubated at room temperature for 30−45 min. Meanwhile, the plates were washed with 4 mL serum free medium and 2 mL serum free medium was added to each plate. The 200 μL of the lipid/DNA suspension was added to each plate and mixed gently. The plates were returned to the incubator for 5−6 h and 2 mL of medium containing 10% calf serum was added. The next day, the plates were treated with fresh stripped medium without phenol-red (5% DCC−FBS) and the 48 h treatments were started by addition of 1 μL of 1000X solutions in DMSO per mL of medium. The transfection efficiency was determined using the constitutive galactosidase expression plasmid pCMVβ in an identical set of plates and was found to be unaffected by the treatments.

Chloramphenicol Acetyl Transferase (CAT) Assay. The CAT assay was done using a modification of the phase extraction assay described by Seed et al. (*24*). At the end of the 48 h treatment period, the transfected cells were harvested by scrapping with a rubber policeman, transferred with the medium to a conical 15 mL tube, centrifuged at 600*g* for 2 min, resuspended in 1 mL cold PBS, transferred to Eppendorf tubes, centrifuged at 600*g* for 2 min and washed in PBS a second time. Cell pellets were resuspended in 200 μL of Tris (0.1 M, pH 8.0) and lysed by 3 cycles of freeze−thaw treatment (alternating 5 min in a dry ice/alcohol bath and 5 min in a 37 °C bath). Cell lysates were incubated at 65 °C for 15 min to inactivate acylases and centrifuged at 14 000*g* for 8 min. A 165 μL aliquot of the cytosol was transferred to a 7 mL scintillation vial, and a 20 μL aliquot was reserved for determination of protein concentration by the Bradford assay. The substrate mixture (85 μL) was added to the scintillation vial for final concentrations of 100 mM Tris-HCl, pH 8.0, 250 nmoles chloramphenicol, 1 μCi ^{3}H-acetylCoA (200 mCi/mmol) in a total volume of 250 μL and mixed thoroughly. The organic scintillation fluid (4 mL) was added slowly and the vials were incubated at 37 °C for 1−2 h or until sufficient counts were obtained.

RNA Extraction and Northern Blot Analysis of pS2 Expression. Cells were lysed by addition of Tri-reagent (Molecular Research Center, Inc., Cincinnati, OH), and chloroform was used for phase separation. After centrifugation, the water-soluble upper phase was collected and total RNA was precipitated with 2-propanol, washed with 75% ethanol, and dissolved in DEPC-treated water. Total RNA was electrophoresed on a 1.2% agarose gel containing 3% formaldehyde, using MOPS as the running buffer. The gel was then washed gently with 10X SSC and blotted with a Zeta nylon membrane (Biorad, Hercules, CA) overnight. The RNA was fixed to the membrane by UV cross-linking. The hybridization probes were radio-labeled with (α^{32}P) dCTP using random primers and the pS2-cDNA and GAPDH-cDNA plasmids provided by ATCC as the template. Hybridization and quantitation of results were done as described previously (*15*). Specific pS2 mRNA levels were normalized using GAPDH as a standard.

Nuclear Extracts. Three near confluent (80−90%) cultures of MCF-7 cells in 100 mm Petri dishes were used for each treatment. CTr or E_2 was added as 1 μL of 1000X solution in DMSO per mL of medium. After 2 h of incubation at 37 °C, the plates were placed on ice and washed twice with 5 mL of hypotonic buffer (10 mM Hepes, pH 7.5) and incubated with 2 mL of the same buffer for 15 min. Cells were harvested in 1 mL of MDH buffer (3 mM $MgCl_2$, 1 mM DTT, 25 mM Hepes, pH 7.5) with a rubber scrapper, homogenized with a loose fitting Teflon pestle, and centrifuged at 1000*g* for 4 min at 4 °C. The pellets were washed twice with 3 mL of MDHK buffer (3 mM $MgCl_2$, 1 mM DTT, 0.1 M KCl, 25 mM Hepes, pH 7.5), resuspended in 1 mL of MDHK, and centrifuged at 600*g* for 4 min at 4 °C in a microcentrifuge. The pellets were resuspended in 100 μL of HDK buffer (25 mM Hepes, pH 7.5, 1 mM DTT, 0.4 M KCl), incubated for 20 min on ice with mixing every 5 min, and centrifuged at 14000*g* for 4 min at 4 °C. Glycerol was added to the supernatants to a concentration of 10% and aliquots of the nuclear extracts were stored at −80 °C.

Gel Mobility Shift Assay. The following set of complementary 31-mer oligonucleotides, 5′-GATCC*CAGGTCACAGTGACCTG*AGCTAAAAT-3′ and 5′-GATCATTTTAGCT*CAGGTCACTGTGACCTG*G-3′ containing the palindromic ERE consensus motif (italicized), was annealed and 5′-end labeled with (γ^{32}P)-ATP using T4 nucleotide kinase. The resulting labeled double-stranded DNA probe was purified on a Sephadex G50 spin-column, precipitated in ethanol, dissolved in TE buffer, and diluted in 25 mM Hepes, 1 mM DTT, 10% glycerol, 1 mM EDTA to contain approximately 25 000 cpm of ^{32}P/μL. Nuclear extracts (7 μg of proteins) were mixed with 90 ng poly-dIdC, 25 mM Hepes, 1 mM DTT, 10% glycerol, 1 mM EDTA, 160 mM KCl in a total volume of 21 μL. For antibody supershift experiments, 0.5 μg of monoclonal mouse-IgG anti-human-ER (Santa Cruz Biotechnology, Santa Cruz, CA) was added to the incubation mixture. After incubation for 15−20 min at room temperature, 4 μL (100 000 cpm) of an end-labeled ^{32}P-ERE probe was added and incubated for another 15 min at room temperature. After addition of 2.8 μL of 10X ficoll loading buffer (0.25% bromophenol blue, 25% ficoll type 400), 22 μL aliquots were loaded unto a pre-run, nondenaturing 4.0% polyacrylamide gel in TAE (67 mM Tris, 33 mM sodium acetate, 10 mM EDTA, pH 8.0) at 120 V for 2 h. The gel was then dried and autoradiographed.

Ethoxyresorufin O-Deethylase Assay. Enzymatic activity of cytochrome-P4501A1 was measured by the ethoxyresorufin O-deethylase (EROD) assay as described previously (*15*). Briefly, after the 18−24 h treatment, cells were trypsinized and 5 mL of PBS was added to the cells. The reaction was run at room temperature and the cells and the reaction solutions were first incubated at 37 °C. An aliquot of the cell suspension was counted to obtain the cell number and 1.5 mL of the cell suspension was added into a fluorometer cuvette, followed by the addition of 0.5 mL of 2.5 mM ethoxyresorufin (Sigma). The reaction mixture was mixed by inversion of the cuvette and fluorescence was measured

at the excitation wavelength of 510 nm and emission wavelength of 586 nm with a 20 nm slit width using a Perkin-Elmer 650−10S spectrofluorometer. Chart speed was recorded for time determination, and a standard curve was obtained using resorufin (RF) (Sigma) added to the heat-inactivated control cells. The enzyme activity was then presented as pmole RF produced/minute/10^6 cells.

Modeling of CTr-binding to the ER Ligand Binding Domain. Since CTr is a strong agonist of estrogen receptor function but exhibits no obvious structural similarity to E_2, we compared the structure of CTr to other classes of ER ligands. Our comparisons included size or "steric" considerations and also electrostatic charge distribution observations. Quantum mechanical geometry optimizations were performed using GAMESS (*25*) on 17β-estradiol, raloxifene, tamoxifen, and CTr molecules; solvent-accessible surfaces were then constructed surrounding these molecules to enable the solution of the Poisson−Boltzmann equation as described previously (*26*). The electronic distribution of the molecule is allowed to rearrange in response to the polarization of its interface with an aqueous environment. The polarization charge induced on these surface elements is mapped onto the nodes ("dots") from which the surface is comprised. These calculations were performed at the 6-31G**/MP2 level of theory allowing for an accurate depiction of the induced surface charge density. The 6-31G** nomenclature is used to describe the basis set used in the calculations, which includes Pople's N-31G split valence basis set. MP2 refers to the Møller−Plesset second-order perturbation theory method of inclusion of electronic correlation (*27*).

We next placed each of these molecules into the experimentally determined ER-binding sites obtained by Brzozowski et al. and Shiau et al. from their complexing of the ER with the specific ligand and determining the respective crystal structure (*28*, *29*). The minimum energy configurations of the molecules were determined by varying both the positions of their centers of mass and their three-dimensional angular orientation within the binding sites. Atoms comprising the binding site itself were not allowed to relax. Interatomic potentials required for this minimization were determined by pairwise summation using local density methods and reflect the electronic overlap repulsion between the atoms comprising the molecule and those in the appropriate receptor-binding site (*30*).

RESULTS

Cell Growth Assays. The effects of CTr were examined on the proliferation of the estrogen-responsive breast cancer cell line, MCF-7, and the estrogen-independent cell line, MDA-MB-231. The results indicate (Figure 1) that after a five-day period in complete medium (DMEM-10% FBS), the growth of MCF-7 cells was significantly increased compared to the vehicle (DMSO)-treated controls at CTr concentrations from 10 nM to 1 μM. The proliferation of the MDA-MB-231 cells was not affected by CTr in this concentration range. In MCF-7 cells grown in an estrogen-depleted medium (5% DCC−FBS DMEM), CTr produced a maximum increase in cell number that was similar to that produced by E_2. Co-treatment of MCF-7 cells in a depleted medium with a range of concentrations of CTr and at the maximum effective concentration of E_2 did not alter the E_2-induced growth rates. These results suggest that CTr may possess estrogenic activity.

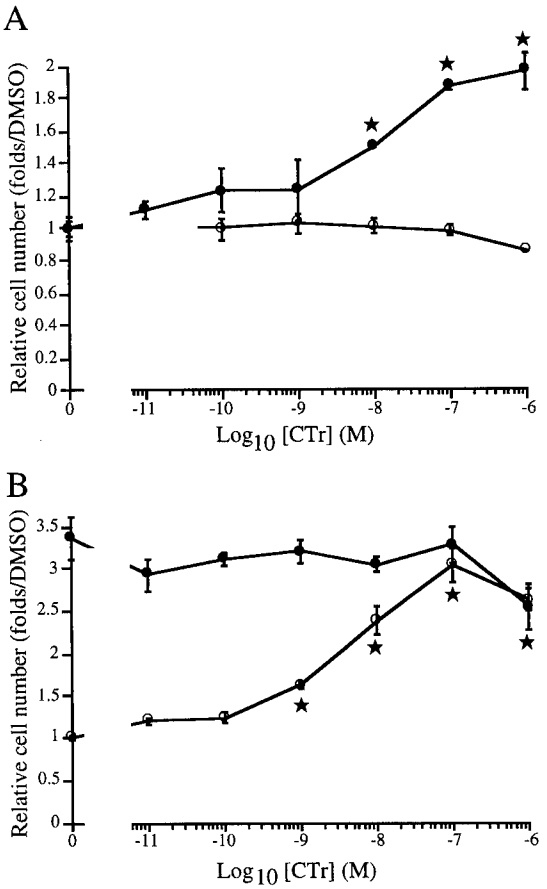

FIGURE 1: Effect of CTr on proliferation of breast cancer cells. Panel A: MCF-7 cells (closed circles) and MDA-MB-231 cells (open circles) were plated in 10% FBS-DMEM at a density of 10^5 cells per well in 6-well plates and treated with CTr at the concentrations indicated. Panel B: MCF-7 cells grown for 7 days in estrogen depleted medium were plated at a density of 10^5 cells per well in 6-well plates and treated with CTr at the concentrations indicated, in the presence (closed circles) or absence (open circles) of E_2 (1 nM). Duplicate aliquots of cells from individual wells were counted after 5 days. The results are shown as the average and standard deviation from three identical wells and expressed as the ratio of cell numbers over the corresponding DMSO controls. The statistical differences were determined using ANOVA and Tukey's Studentized Range test: (star) significantly different ($p < 0.05$) from DMSO control.

Competitive Estrogen Receptor (ER) Binding Assay. Because CTr exhibited estrogen-like activity in the cell proliferation assays, we examined the binding affinity of CTr with the ER using a competitive-binding assay. CTr displaced ^{3}H-labeled E_2 in a rat uterine cytosol binding assay producing a competitive-binding curve parallel to that of the other ER ligands and with an EC_{50} that was only 2 orders of magnitude greater than that of E_2 (Figure 2). The EC_{50} of the estrogen antagonist, ICI_{182780}, used as a positive control for this assay, correlates with its affinity for the ER. These results indicate that CTr is a strong ligand for the ER that binds to the E_2-binding site of the receptor.

Gel Mobility Shift Assay. To determine whether CTr can activate the binding of the ER to the corresponding estrogen-responsive element (ERE) in the regulatory region of E_2-responsive genes, we conducted a series of gel mobility shift assays. Nuclear protein extracts of MCF-7 cells grown in

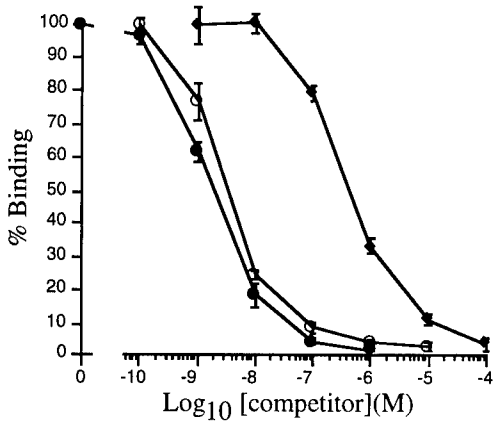

FIGURE 2: Competitive binding to the ER. The binding of $^3H-E_2$ (1 nM) to the ER from rat uterine cytosol was measured in the presence of the unlabeled competitors, E_2 (closed circles), ICI_{182780} (open circles), and CTr (closed diamond), at the concentrations indicated and reported as the percentage of binding in the absence of competitors. The results are shown as the average and standard deviation from three replicates. Relative binding affinities were calculated using the concentration of competitor needed to reduce ^3H-E_2 binding by 50% as compared to the concentration of unlabeled E_2 needed to achieve the same result.

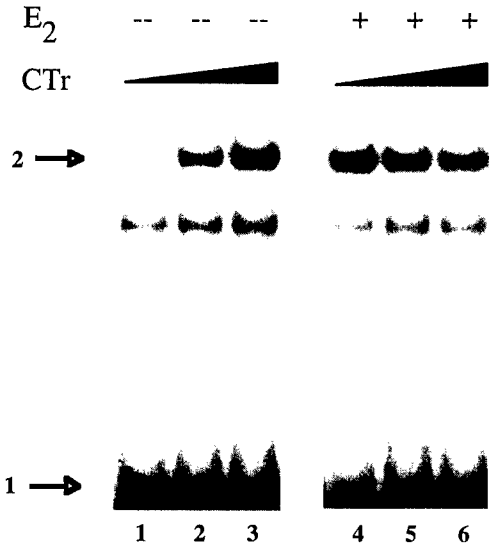

FIGURE 3: Binding of nuclear proteins to the ERE. Gel mobility shift analysis of nuclear extracts from estrogen depleted MCF-7 cells treated for 2 h with DMSO (lanes 1 and 4), CTr 10 nM (lanes 2 and 5), or CTr 100 nM (in lanes 3 and 6), and E_2 1 nM (lanes 4–6). A monoclonal antibody specific for the human ER was also added to the incubation mixture. Arrows indicate the locations of the free labeled probe (arrow # 1) and the ligand responsive antibody-super-shifted band (arrow # 2).

an estrogen-depleted medium for 7 days and treated for 2 h with CTr (10 nM and 100 nM) produced a shifted band with the ^{32}P-labeled consensus ERE oligonucleotide that was the same size as the ER–ERE complex induced by a 1 nM E_2 treatment. Figure 3 shows the complex supershifted by a monoclonal anti-ER antibody. The density of the shifted bands correlated with the concentrations of CTr and 100 nM CTr was as effective as 1 nM E_2. These results indicate that CTr can activate the ER into a DNA-binding form in a concentration range that corresponds to the binding affinity of CTr for the ER.

Activation of Transcription by CTr. To determine whether the binding of CTr with the ER produces a transcriptionally active complex with DNA, we examined by Northern blot assay whether CTr could activate expression of the endogenous E_2-responsive gene, pS2. Treatment of MCF-7 cells depleted of estrogen with CTr for 48 h at concentrations ranging from 10 nM to 1 μM induced accumulation pS2 mRNA in a concentration-dependent manner with 100 nM CTr as effective as 1 nM E_2 (Figure 4A). Co-treatment with CTr did not affect E_2-induced pS2 expression levels.

To examine whether the CTr-induced increase in pS2 mRNA levels could be attributed to an increase in transcriptional activity, we examined the effect of CTr on activities of three E_2-responsive reporter gene constructs in transiently transfected MCF-7 cells. ERE-vit-CAT contains the promoter and flanking regions of the frog vitallogenin-B1 gene upstream of the chloramphenicol-acetyltransferase structural gene. pATC2 contains only the promoter region of the vitallogenin gene and two consensus ERE motifs. pS2-luc contains the regulatory flanking region of the human pS2 gene upstream from the SV40 promoter and the luciferase gene. Our results show that all three reporters were induced by CTr with similar concentration dependency and with 100 nM CTr as effective as 1 nM E_2 (Figure 4, B–D). Co-treatment with CTr did not affect E_2 -induced expression levels. Taken together, these results indicate that the CTr-induced accumulation of mRNA of an endogenous E_2-responsive gene results from increased transcriptional activation and that CTr is equally effective in the activation of simple and complex ERE-containing promoters.

AhR Signaling Pathway. Because of the established effectiveness of orally administered I3C in the induction of CYP450 activities associated with the Ah receptor pathway and the well established role of activation of the Ah receptor in tumor promotion (*31*), we examined the effects of CTr on key indicators of Ah receptor function. We measured the ability of CTr to induce expression of both the CYP1A1-associated EROD activity in MCF-7 cells and of an AhR-responsive DRE-CAT reporter construct containing the promoter and flanking regions of the CYP1A1 gene stably transfected in murine hepatoma Hepa-1c1c7 cells (*15*). As expected (Figure 5), based on the relatively weak binding affinity of CTr for the AhR that we determined previously (*13*), CTr proved in both assays to be a very weak activator as compared to the ICZ positive control treatment.

Taken together, these results indicate that CTr functions as a classical agonist (*32*) of the ER signaling pathway with weak activity toward the AhR signal transduction pathway.

Structural Modeling of CTr Binding to the ER and Comparison with 4-Hydroxytamoxifen. Because CTr is without obvious stuctural similarity to E_2, we conducted a conformational analysis of CTr and computed its theoretical fit into the ER ligand-binding site. A comparison of the expected lowest energy conformation of CTr with conformations of other established ER ligands indicates a remarkable similarity with tamoxifen, a tissue-specific and promoter-specific estrogen antagonist. The structures of CTr and 4-hydroxytamoxifen (OHT) are shown in Figure 6A and Figure 6B, respectively. The portion of each of the molecules that fits into the 3-OH region of the ER ligand-binding site is shown oriented to the left. Of note is that the molecular dimensions of the two molecules are similar. For example, the distance between the C-6 positions of the lower two

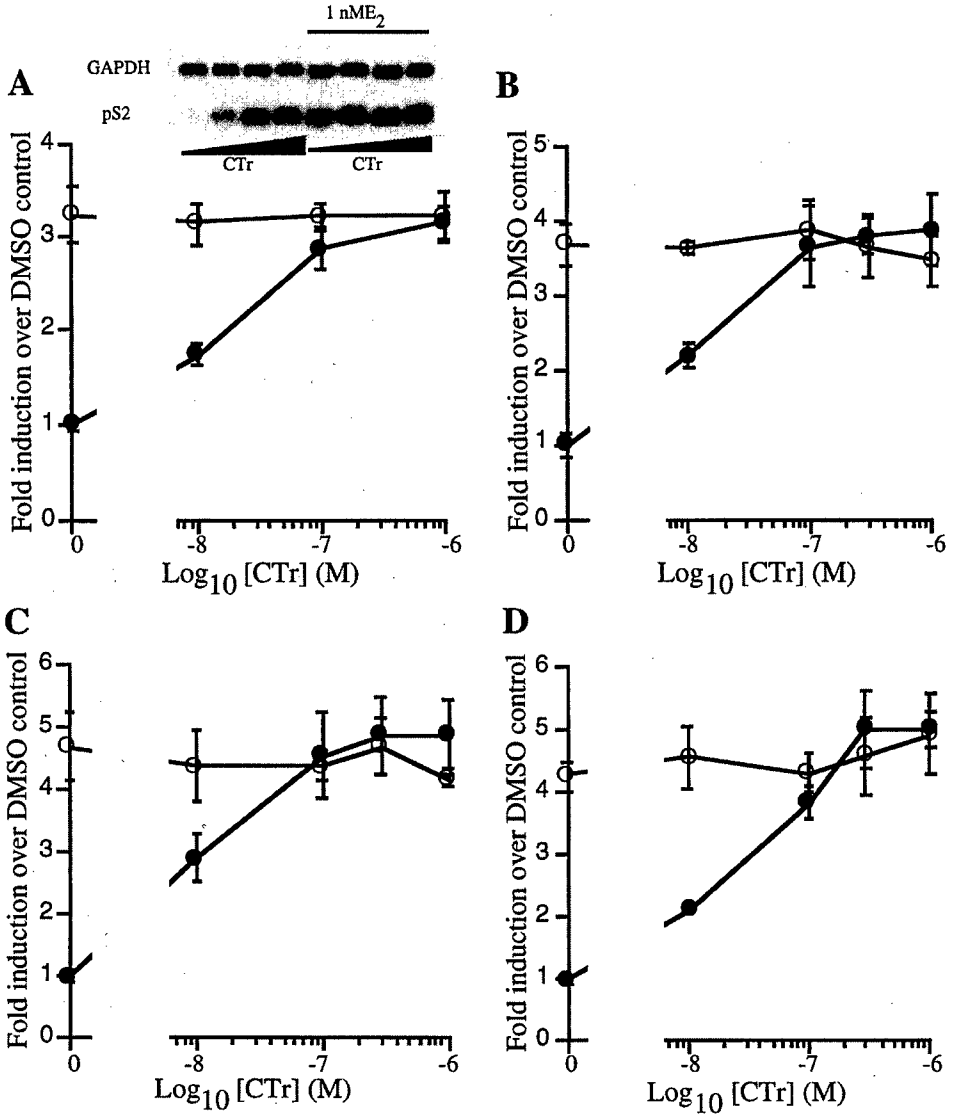

FIGURE 4: Effect of CTr on ER-responsive gene expression. Panel A shows the expression of endogenous pS2; estrogen-depleted MCF-7 cells were treated for 48 h with CTr-1 at concentrations ranging from 0.1 to 10.0 μM, with (open circles) or without (closed circles) E_2 (1 nM). pS2 mRNA levels were measured by Northern-blot analysis and normalized using GADPH mRNA as an internal standard. Results are presented as average and standard deviation of three experiments. A representative Northern blot is shown on top. Panels B, C, and D show transcription activity of reporter genes: MCF-7 cells were transiently transfected with 0.1 μg per plate of pS2-luc (B), or with 1.0 μg per plate of pERE-vit-CAT (C) and pATC2 (D). Transfected MCF-7 cells were treated for 48 h with CTr at concentrations ranging from 0.1 to 10.0 μM, with (open circles) or without (closed circles) E_2 (1 nM). Results are presented as fold induction over the DMSO control, as the average and standard deviation of four independent transfections.

indole moieties indicated in Figure 6A is 20 Å and thedistance of the corresponding hydroxyl carbon and the nitrogen atom in Figure 6B is 22.5 Å; this distance was also found to be 20.4 Å by crystal structure analysis of OHT (*29*). In addition, the aromatic substituents of the two molecules are similarly noncoplanar.

In Figure 6, C and D, we present the same molecules in identical orientations as above, including their solvent-accessible surfaces. The portion of each of the molecules, which fits into the 3-OH region of the ER ligand-binding site is shown oriented to the left. These figures provide a direct geometrical comparison of the properly oriented surfaces as well as a comparison of the polarization-induced charge on their solvent-accessible surfaces. The results indicate a similar charge pattern on the portion of each of the molecules, which fits into the 3-OH region of the binding site. It should be noted that, although only CTr and tamoxifen are shown, all four of the molecules examined, including E_2 and raloxifene, had a similar charge distribution on that region of the surface.

We next investigated the possibility of CTr binding to a site similar to that occupied by OHT in the ER-binding site. In Figure 6 (Panels E and F), we present two views of the overlapping solvent surfaces of the quantum mechanically derived CTr (shown as dots) and the experimentally determined OHT (*29*) (shown as a continuous gray surface), providing a direct comparison of the sizes and shapes of these two molecules. Panel E shows the molecules oriented as in panels A, B, C, and D, and Panel F shows them rotated by 90 degrees along the vertical axis. The OHT pocket is held rigid in these calculations; relaxation of the surrounding molecular environment would allow an even better accommodation of the two structures. The figures provide compelling evidence for the incorporation of CTr into the ER-binding site, both from "steric" (Panels E and F) and electrostatic (Panels C and D) considerations.

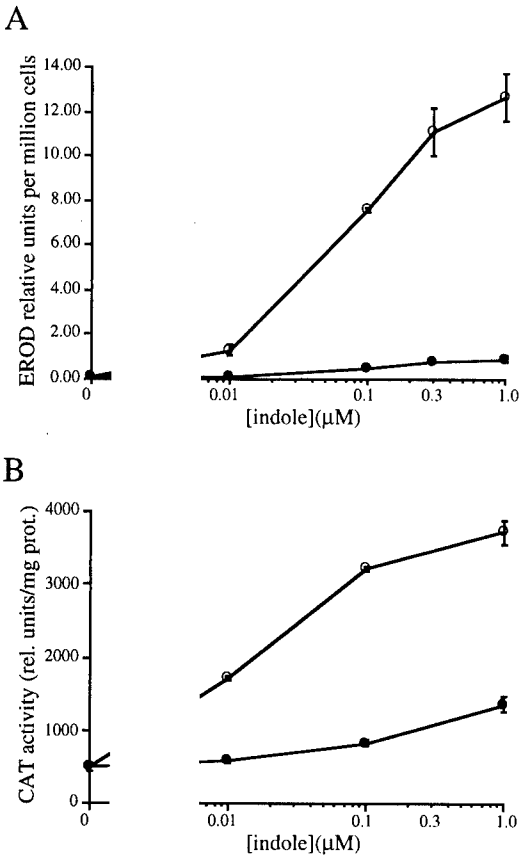

FIGURE 5: Effect of CTr on Ah-Receptor responsive gene expression. (A) Induction of endogenous cytochrome P450-1A1. MCF-7 cells were treated for 24 h with ICZ as a control (open circles) or with CTr (closed circles) at the concentrations indicated and EROD activity was measured. (B) Murine hepatoma cells Hepa-1c1c7 permanently transfected with a DRE-CAT reporter (clone M8) were treated with ICZ (open circles) or CTr (closed circles) at the concentrations indicated for 48 h.

DISCUSSION

Our results show that the novel diet-derived cyclic methylene indole trimer, CTr, behaves as an estrogenic substance in vitro and in cell culture. CTr binds to the ER, activates ER binding to the ERE, and initiates the transcription of an endogenous E_2-responsive gene as well as that of E_2-responsive reporter genes. The activity of CTr in these assays is as high as about 1% that of E_2.

To estimate the physiological significance of CTr production in vivo following oral administration of I3C, an analysis of reported tissue levels of CTr will be helpful. Published work by us and others indicates that the level of CTr produced following oral administration of I3C to rodents is comparable to levels of other major products, DIM and LTr-1. Using Sprague−Dawley rats, we readily detected CTr in the intestinal contents 5 h after treatment (*13*), occurring in about 50% the yield of the other major products. Consistent with these observations, Stresser et al. (*14*) provided chromatographic evidence for the accumulation of I3C acid products including CTr in the liver of Fisher rats 3 h following oral treatment with I3C to levels that again were roughly 50% the levels of DIM and LTr-1. These researchers estimated the levels of each of these major I3C products in rat liver to be in the range of 1−10 μM, which is well in excess of the concentrations (0.1 μM) we find necessary to activate the ER. Thus, it appears that CTr is produced in physiologically significant levels following ingestion of I3C.

Although CTr may attain active concentrations in vivo following administration of I3C, whether CTr contributes to the cancer-protective or cancer-promoting effects of I3C remains to be established. An intriguing possibility is that CTr may contribute to an overall estrogenic effect of oral I3C and that this estrogenic activity may account for the cancer-promoting effects of I3C in liver and for the cancer-protective effects of I3C in mammary glands. Williams et al. reported recently that oral I3C produced estrogenic effects in trout at doses below those required for Ah receptor activation. These investigators suggested that oral I3C may function as do other ER agonists in the promotion of carcinogen-induce liver tumors in the trout and rat models (*11*). CTr might also contribute to the cancer-protective effects of oral I3C against spontaneous mammary tumors by stimulation of mammary gland maturation resulting in decreased susceptibility to carcinogeneis, as suggested recently for the natural cancer-protective agent, genestein (*33*, *34*).

A comparison of the expected lowest energy conformation of CTr with conformations of other established ER ligands indicated a remarkable similarity with tamoxifen, a tissue and promoter specific estrogen antagonist currently under study as a breast cancer therapeutic agent (*35*). We found that the ER ligands compared quantum mechanically all have a similar charge distribution around the boundary region of the molecule that fits into the 3-OH region of the ER-binding site. Furthermore, overlapping surfaces of the CTr with those of experimentally established ligands show very little difference between CTr and tamoxifen, lending provocative evidence in support of the binding of CTr to the ER-binding site.

In light of the marked structural similarity of CTr and tamoxifen with regard to their interactions with the ligand-binding region of the ER, a comparison of the biological activities of CTr with those of tamoxifen and related substances is in order. Published data indicate that OHT, the activated form of tamoxifen, is a potent ligand for the human ER with a binding affinity in the range of 10 nM. In contrast to agonist activity, we observed for CTr, OHT is a potent inhibitor of MCF-7 cell proliferation (IC_{50} = 0.5 nM) (*36*). Whether CTr exhibits tissue and promoter specific agonist activities as does tamoxifen remains to be seen. It is interesting to note, however, that the activities of OHT, and other synthetic ER ligands, are highly dependent on the presence of a hydroxyl group in the position that corresponds to C-4 of tamoxifen (*37*, *38*). Loss of this substituent from OHT results in a 2 orders of magnitude decrease in ER-binding affinity to a level that is similar to the affinity we observe for CTr. This decrease in binding affinity is accompanied by a similar large decrease in potency against MCF-7 cell proliferation to a level of potency that is only about 10-fold greater than the concentration of CTr observed to inhibit MCF-7 cell proliferation (unpublished data). Addition of a hydroxyl group at the appropriate position(s) of CTr may produce a similar pronounced effect on the activity of this natural product. Further studies to explore

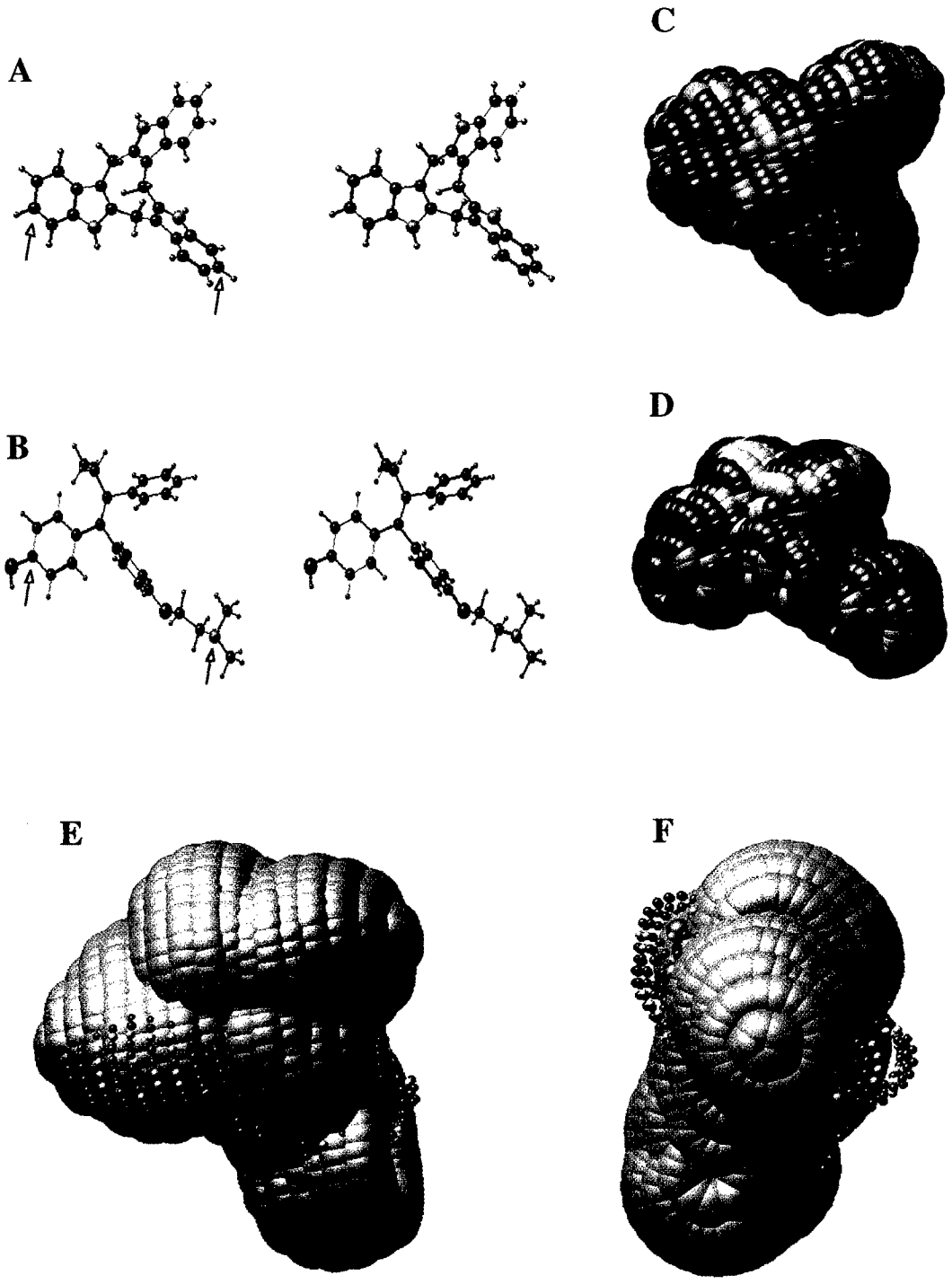

FIGURE 6: Stereoviews of CTr (A) and OHT (B). Structures were determined by quantum mechanical geometry optimization calculations. Comparison of polarization-induced charges on the surfaces of CTr (C) and OHT (D). Construction of a solvent-accessible surface around each of the QM-derived molecules shown in panels A and B allows solution of coupled Schrödinger and Poisson−Boltzmann equations, resulting in the polarization charge on the surface elements due to the aqueous environment. The electronic distribution of the molecule is allowed to rearrange in response to the polarization of its interface, resulting in an accurate depiction of the induced surface charge density. Blue indicates positive surface charge, red indicates negative surface charge, and gray indicates neutral areas. It should be noted that the sign of the surface charge, is essentially opposite that of the charge on the atom below the surface element. Comparison of the sizes and shapes of CTr and OHT. A solvent-accessible surface was created around the crystallographically determined OHT structure, as determined by Shiau et al. (25) and is shown as a continuous gray surface; the CTr structure, determined quantum mechanically, is shown as dots. In panel E, the molecules are oriented with the 4-OH of OHT on the left; in panel F, the molecules are rotated by 90 degrees, looking "down" the 4-OH end. The minimum energy conformation of the quantum mechanical CTr in the experimentally determined ER-binding site of OHT was determined by varying position and angular orientation of the CTr molecule within the OHT-binding site, while the atoms comprising the binding site itself were not allowed to relax. Interatomic potentials required for this minimization were determined by pairwise summation using local density methods and reflect the electronic overlap repulsion between the atoms comprising the CTr molecule and those in the receptor-binding site.

the possible metabolic activation and tissue specific activities of CTr and to further define the role of CTr in the cancer modulating activities of I3C are in progress in our laboratories.

REFERENCES

1. Nixon, J. E., Hendricks, J. D., Pawlowski, N. E, Pereira, C. B., Sinnhuber, R. O., and Bailey, G. S. (1984) *Carcinogenesis 5*, 615−619.
2. Tanaka, T., Kojima, T., Morishita, Y., and Mori, H. (1992) *Jpn. J. Cancer Res. 83*, 835−842.
3. Morse, M. A., LaGreca, S. D., Amin, S. G., and Chung, F. L.(1990) *Cancer Res. 50*, 2613−2617.
4. Wattenberg, L. W., and Loub, W. D. (1978) *Cancer Res. 38*, 1410−1415.
5. Grubbs, C. J., Steele, V. E., Casebolt, T., Juliana, M. M., Eto, I., Whitaker, L. M., Dragnev, K. H., Kellof, G. J., and Lubet, R. L. (1995) *Anticancer Research 15*, 709−716.
6. Bradlow, H. L., Michnovicz, J. J., Telang, N. T., and Osborne, M. P. (1991) *Carcinogenesis 12*, 1571−1574.
7. Kojima, T., Tanaka, T., and Mori, H. (1994) *Cancer Res. 54*, 446−1449.
8. Pence, B., Buddingh, H., and Yang, S. (1986) *J. Natl. Cancer Inst. 77*, 269−276.
9. Bailey, G. S., Hendricks, J. D., Shelton, K. W., Nixon, J. E., and Pawlowski, N. E. (1987) *J. Natl. Cancer Inst. 78*, 931−936.
10. Kim, D., Han, B., Ahn, B., Hasegawa, R., Shirai, T., Ito, N., and Tsuda, H. (1997) *Carcinogenesis 18*, 377−381.
11. Oganesian, A., Hendricks, J., Pereira, C., Orner, G., Bailey, G., and Williams, D., (1999) *Carcinogenesis 20*, 453−458.
12. Grose, K. R., and Bjeldanes, L. F. (1992) *Chem. Res. Toxicol. 5*, 188−193.
13. Bjeldanes, L. F., Kim, J. Y., Grose, K. R., Bartholomew, J. C. and Bradfield, C. A. (1991) *Proc. Natl. Acad. Sci. U.S.A. 88*, 9543−9547.
14. Stresser, D. M., Williams, D. E., Griffin, D. A., and Bailey, G. S. (1995) *Drug Metab. Disposition 23*, 965−975.
15. Chen, Y.-H., Riby, J., Srivastava, P., Bartholomew, J., Denison, M., and Bjeldanes, L. (1995) *J. Biol. Chem. 270*, 22548−22555.
16. Chen, I., Safe, S., and Bjeldanes, L. (1996) *Biochem. Pharm. 51*, 1069−1076.
17. Stresser, D. M., Bjeldanes, L. F., Bailey, G. S., and Williams, D. E. (1995) *J. Biochem. Toxicology 10*, 191−201.
18. Chen, I., McDougal, A., Wang, F., and Safe, S. (1998) *Carcinogenesis 19*, 1631−1639.
19. Chang, Y.-C., Riby, J., Chang, G., Peng, B., Firestone, G., and Bjeldanes, L. (1999) *Biochem. Pharm. 58*, 825−834.
20. Santell, R. C., Chang, Y. C., Nair, M. G., and Helferich, W. G. (1997) *J. Nutr. 127*, 263- 269.
21. Chang, T., Nardulli, A. M., Lew, D., and Shapiro, D. J. (1992) *Mol. Endocrinol. 6*, 346- 354.
22. Gillesby, B. E., Stanostefano M., Porter, W., Safe, S., Wu, Z. F., and Zacharewski, T. R. (1997) *Biochemistry 36*, 6080−6898.
23. Reese, J. C., and Katzenellenbogen, B. S. (1991) *Nucl Acids Res 19*, 6595−6602.
24. Seed, B., and Sheen, J. Y. (1988) *Gene 67*, 271−277.
25. Schmidt, M. W., Baldridge, K. K., Boatz, J. A., Elbert, S. T., Gordon, J. S., Jensen, J. J., Koseki, S., Matsunaga, N., Nguyen, K. A., Su, S., Windus, T. L., Dupuis, M., and Montgomery, J. A. (1993) *J. Comput. Chem. 14*, 1347−1363.
26. Wilson, W. D., Schaldach, C. M., and Bourcier, W. L. (1997) *Chem. Phys. Lett. 267*, 431−437.
27. Frisch, M. J., Head-Gordon, M., and Pople, J. A. (1990) *Chem. Phys. Lett. 166*, 275−280).
28. Brzozowski, A. M., Pike, A., Dauter, Z., Hubbard, R. E., Bonn, T., Engstrom, O., Ohman, L., Greene, G. L., Gustafsson, J.-A., and Carlquist, M. (1997) *Nature 389*, 753−758.
29. Shiau, A. K., Barstad, D. Loria, P. M., Cheng, L, Kushner, P. J., Agard, D. A., and Greene, G. L. (1998) *Cell 95*, 927−937.
30. Wilson, W. D., and Schaldach, C. M. (1998) *J. Colloid Interface Sci. 208*, 546−554.
31. Schmidt, J. V., and Bradfield, C. A. (1996) *Annu. Rev. Cell Dev. Biol. 12*, 55−89.
32. Wehling M. (1995) *J. Mol. Med. 73*, 439−47.
33. Hsieh, C. Y., Santell, R. C., Haslam, S. Z., and Helferich, W. G. (1998) *Cancer Res. 58*, 3833−3838.
34. Lamartiniere, C. A., Moore, J. B., Brown, N. M., Thompson, R., Hardin, M. J., and Barnes, S. (1995) *Carcinogenesis 16*, 2833−2840.
35. Watanabe, T., Inoue, S., Ogawa, S., Ishii, Y., Hiroi, H., Ikeda, K., Orimo, A., and Muramatsu, M. (1997) *Biochem. Biophys. Res. Comm. 236*, 140−145.
36. Grese, T., Sluka, J., Bryant, H., Cullinan, G., Glasebrook, A., Jones, C., Matsumoto, K., Palkowitz, A., Sato, M., Termine, J., Winter, M., Yang, N., and Dodge, J. (1997) *Proc. Natl. Acad. Sci. U.S.A. 94*, 14105−14110.
37. Grese, T. A., Cho, S., Finley, D. R., Godfrey, A. G., Jones, C. D., Lugar III, C. W., Martin, M. J., Matsumoto, K., Pennington, L., Winter, M., Adrian, M., Cole, H., Magee, D., Phillips, D., Rowley, E., Short, L., Glasebrook, A., and Bryant, H. (1997) *J. Med. Chem. 40*, 146−167.
38. Biberger, C., and von Angerer, E. (1996) *J. Steroid Biochem. Mol. Biol. 58*, 31−43

BI9919706

Biochemical Pharmacology, Vol. 58, pp. 1145–1153, 1999.

ELSEVIER

ISSN 0006-2952/99/$ matter
PII S0006-2952(99)00197-5

Modulation of Cytochrome P4501A1 Activity by Ascorbigen in Murine Hepatoma Cells

Pernille Uldall Stephensen,†‡ Christine Bonnesen,*†‡ Leonard F. Bjeldanes† and Ole Vang*§*

*Department of Life Sciences and Chemistry, Roskilde University, DK-4000 Roskilde, Denmark; and †Division of Nutritional Sciences and Toxicology, University of California, Berkeley, CA 94720, U.S.A.

ABSTRACT. Modulation of cytochrome P4501A1 (CYP1A1) activity is a mechanism whereby indoles present in cruciferous vegetables could affect the metabolism of xenobiotics. Ascorbigen (ASG) is the predominant indole formed during the degradation of glucobrassicin, although the mechanism by which ASG modulates CYP1A1 activity is not known. The major focus of this study was to examine the mechanism of CYP induction by ASG using a murine hepatoma-derived cell line (Hepa 1c1c7). ASG was shown to induce the activity of 7-ethoxyresorufin O-deethylase, a marker for CYP1A1, in a concentration-responsive manner with a maximum induction at 700 μM. Maximum ASG induction after 24-hr treatment was 7% of maximal CYP1A1 activity induced by the well-known potent CYP1A1 inducer, indolo[3,2-*b*]carbazole (ICZ) (1 μM), and the EC_{50} values differed by 2-fold. The CYP1A1 activity increased continuously up to 72 hr, where ASG showed an induction efficiency in the same range as for the positive control (1 μM ICZ) after 24 hr, whereas the CYP1A1 protein level, measured by Western blot analysis, was maximally induced after 24 hr. ASG significantly inhibited CYP1A1 activity in whole cells at concentrations above 1 μM. ASG increased the chloramphenicol acetyl transferase (CAT) activity via a CAT reporter construct containing a dioxin-responsive element in Hepa 1c1c7 cells, indicating involvement of the aryl hydrocarbon receptor. ASG was shown to be transformed into ICZ, or a compound with the same chromatographic mobility as ICZ, in the medium. Taken together, the results indicate that ASG inhibits CYP1A1 activity at low concentrations, but induces the same activity at higher concentrations. BIOCHEM PHARMACOL 58;7:1145–1153, 1999. © 1999 Elsevier Science Inc.

KEY WORDS. ascorbigen; indolo[3,2-*b*]carbazole; Hepa 1c1c7 cells, *Cyp1a1* induction; *Cyp1A1* inhibition; Ah receptor

A number of studies have demonstrated a decreased risk of cancer when consuming a diet containing substantial amounts of fresh fruits and vegetables, especially cruciferous vegetables of the *Brassica* genus, e.g. broccoli, cabbage, and Brussels sprouts [1–3]. The anticarcinogenic activity of cruciferous vegetables has been related to the content of the glucosinolates; for example, glucobrassicin is present in large amounts in broccoli [4]. On disruption of plant tissue, such as cutting and chewing, different indoles are formed as a result of the myrosinase (β-thioglucoside glucohydrolase, EC 3.2.3.1)-catalysed degradation of glucosinolates [5]. When glucobrassicin is degraded by myrosinase *in vitro*, I3C‖ is the main initial product formed at neutral pH. Under acidic conditions, condensation products of I3C, including DIM and ICZ, are formed (Fig. 1) [6, 7]. The yield of ICZ from the reactions of I3C under acidic conditions has been estimated to be 0.01% after 48 hr [8]. Glucobrassicin [9] and the degradation products formed have been shown to induce xenobiotic-metabolising enzymes, including the CYP1A1 enzyme, via the Ah receptor [8, 10]. By far the most potent Ah receptor agonist identified in the degradation mixture is ICZ [8].

Degradation of glucobrassicin in the presence of AA leads to the formation of ASG (Fig. 1) [11, 12]. AA is present in broccoli in amounts as high as 1.23 mg/g fresh broccoli [13], and it has been shown that ASG is the predominant indole compound in fresh, cooked, and fermented cabbage [7], about 7–10 times more abundant than I3C [7, 14]. Considering the abundance of ASG in vegetables of the *Brassica* genus, it seems that the biological effects of dietary ASG have been somewhat neglected. Thus far, only a few *in vivo* studies have investigated the effect of ASG on xenobiotic-metabolising enzymes [15]. McDanell *et al.* found that the EROD activity was increased by 45-fold in the small intestine and approximately 9-fold in the large intestine of rats fed a diet containing 1600 mg

‡ These authors contributed equally to the present study.

§ Corresponding author: Dr. Ole Vang, Department of Life Sciences and Chemistry, Roskilde University, DK-4000 Roskilde, Denmark. Tel. +45 4674 2552; FAX +45 4674 3011; E-mail: ov@virgil.ruc.dk

‖ *Abbreviations:* AA, ascorbic acid; Ah receptor, aryl hydrocarbon receptor; ASG, ascorbigen; CAT, chloramphenicol acetyl transferase; CYP, cytochrome P450; DIM, 3,3′-diindolylmethane; DRE, dioxin-responsive element; EROD, 7-ethoxyresorufin O-deethylase; ICZ, indolo[3,2-*b*]carbazole; I3C, indole-3-carbinol; RF, resorufin; and TCDD, 2,3,7,8-tetrachlorodibenzo-*p*-dioxin.

Received 25 August 1998; accepted 22 April 1999.

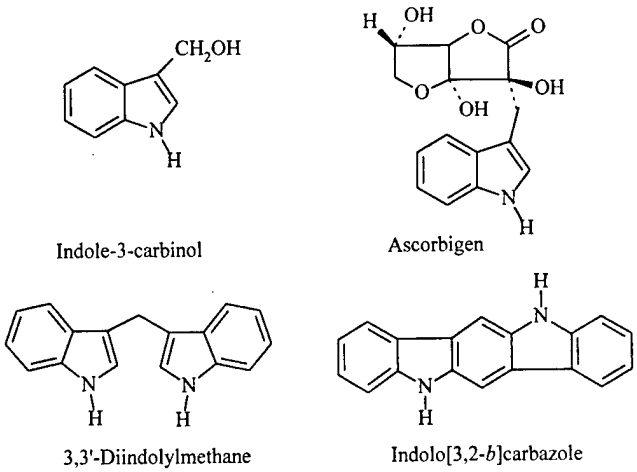

FIG. 1. Degradation products formed from glucobrassicin.

ASG/kg diet for 5 days, compared to controls [7]. Sepkovic *et al.* reported that ASG induces estradiol C-2 hydroxylation, primarily a CYP1A1 marker, about 1.5-fold in rats [16]. Inductions of CYP1A1-related activity have previously been observed for I3C and DIM in rats, and it has been suggested that this induction is responsible for altered carcinogen metabolism, leading to reduced tumour incidence [17]. The activity is most likely caused by oligomeric compounds formed from I3C and DIM, as I3C and DIM only weakly bind the Ah receptor and transcriptionally activate the *CYP1A* genes. It has also been shown that I3C and DIM both exhibit antagonist activity for the Ah receptor [18] and inhibit CYP activity. However, no results have been published on the mechanism by which ASG modulates CYP1A1 in cultured cells.

In the present study, we describe the CYP1A1-modulating activity of ASG using a murine hepatoma cell line (Hepa 1c1c7) and compare this activity with that of the potent CYP inducer, ICZ. Hepa 1c1c7 cells have been used in the present experiments as this cell line is stable, well characterised, and has been used for numerous experiments investigating Ah receptor-mediated induction of CYP1A1 [19].

MATERIALS AND METHODS

Chemicals

I3C was purchased from Aldrich Chemical Co. and recrystallised in toluene before use. ICZ and DIM were synthesised according to the procedure of Robinson [20] and Leete and Marion [21], respectively. TCDD was obtained from B. Ames (University of California, Berkeley, CA). 7-Ethoxyresorufin and RF were purchased from Sigma Chemical Co. and Aldrich Chemical Co., respectively. [RING,3,5-^{3}H] Chloramphenicol was purchased from Dupont New England Nuclear Co. *N*-Butyryl–coenzyme A lithium salt was from Sigma. All other organic solvents, chemicals, and biochemicals used in these studies were of the highest quality available from commercial sources.

General Methods

^{1}H-NMR spectra were measured at 300 MHz in methanol-d_4 on an AC-300 Brucker instrument. Chemical shift values were recorded relative to tetramethylsilane for all spectra. UV analysis was carried out on a Beckman UV/VIS spectrophotometer, model DU 530.

HPLC Analysis

For HPLC analysis, a C-18 bonded-phase column was used (Ultrasphere-ODS, 4.6 × 250 mm, particle size 5 μm, Beckman). The detector was either a Shimadzu UV-VIS spectrophotometer, model SPD-10A set at 280 nm, or a Perkin Elmer fluorescence spectrophotometer, model LS-4 set for excitation at 335 nm and emission at 415 nm. A gradient chromatographic and isocratic chromatographic system described by Aleksandrova *et al.* [14] and Kwon *et al.* [10], respectively, was used. The flow rate for both systems was 1 mL/min and the volume of injection 10 μL.

Synthesis of ASG

The synthesis was carried out according to the procedure of Kiss and Neukom [22], with some modifications. Briefly, 600 mg L-AA and 500 mg I3C were added to 125 mL H_2O and left stirred under nitrogen at room temperature for 2 hr. Light was avoided by wrapping the flask in foil. The solution was filtered and the aqueous phase neutralised with NaOH and extracted 3 times with ether. The aqueous phase was further extracted with ethylacetate and the extract was dried under reduced pressure (40°). Three hundred and fifty mg ASG was obtained as a white/pale yellow powder. The purity of ASG was assessed by HPLC and shown to be nearly 100%. AA, I3C, DIM, and ICZ were not detectable in preparations of ASG. The ^{1}H-NMR spectrum was identical to values reported previously [23]: ^{1}H-NMR (CHD_2-OH): δ 3.22 (1H, d), 3.40 (1H, d), 3.77 (1H, s), 3.98 (1H, dd), 4.10 (1H, dd), 4.20 (1H, dd), 6.97 (1H, t), 7.06 (1H, t), 7.20 (1H, s), 7.31 (1H, d), and 7.62 (1H, d). Additional parallel signals corresponding to about 10% isomeric ASG forms were observed in the NMR spectrum. The extinction coefficient for ASG was determined as 5650 $cm^{-1}M^{-1}$ at 280 nm.

Cell Culture Growth

The murine hepatoma cell line (Hepa 1c1c7 cells) and the Hepa cells stably transfected with the DRE reporter pMCAT 5.9 (M8 cells) were grown as monolayers at 37° in 95% air and 5% CO_2 in Dulbecco's modified Eagle's medium supplemented with 10% foetal bovine serum, 3.7 g/L sodium bicarbonate, and 3.0 g/L glucose. pMCAT 5.9 is a plasmid constructed by ligation of the −820 to −974 enhancer sequence from the mouse promoter in the pMCAT 5 plasmid [24] and was provided by Dr. J. P. Whitlock, Jr. (Stanford University, Palo Alto, CA).

EROD Activity

Hepa 1c1c7 cells were grown in 58-mm diameter plates. ASG and ICZ, dissolved in either DMSO or PBS, were added to the cells ($9-14 * 10^4$ cells/cm^2) and incubated for various lengths of time. Control cell cultures were incubated with DMSO or PBS. As positive controls, cell cultures were incubated with 1 μM ICZ in DMSO. At the end of the incubation, cells were washed in PBS, harvested by trypsination, and resuspended in PBS. Two hundred μL cell suspension was used for cell counting. To 1.5 mL cell suspension, 0.5 mL 2.5 μM 7-ethoxyresorufin was added, and the EROD activity was determined by measurement of the linear production of the fluorescent RF at 37° on a Perkin Elmer 650-105 spectrofluorometer with 510 nm excitation, 585 nm emission, and a slit width of 20 nm. The amount of RF formed was determined by comparison with a standard curve (0–6.3 nM RF in PBS). The specific activity was calculated based on the actual number of cells.

Microsome Preparation and Inhibition of EROD Activity

Confluent Hepa 1c1c7 cells, treated for 24 hr with 1 μM ICZ, were washed twice in ice-cold PBS and harvested by use of a rubber policeman in PBS. The cells were sedimented and the pellet resuspended in phosphate buffer (50 mM $NaPO_4$, pH 7.4, 0.1 mM EDTA, 10% glycerol). The suspension was sonicated twice for 10 sec while kept on ice and the lysate centrifuged for 15 min at 10,000 *g* and 4°. The supernatant was further centrifuged for 1 hr at 100,000 *g* and 4° and the microsomal pellet resuspended in storage buffer (0.154 M KCl, 10 mM Tris–HCl, pH 7.4, 1 mM EDTA, 20% glycerol). Microsomal protein concentration was determined by a Lowry assay using BSA as protein standard. The EROD inhibition assay was measured as an end point assay. Five hundred microliters of reaction mixtures consisting of 1.2 mg/mL BSA and 50 μg microsomes were prepared, dissolved in 0.1 M Tris–HCl buffer, pH 7.8, and incubated in a shaking waterbath at 37° with increasing concentrations of ASG (5–200 μM) for 10 min, following determination of the EROD activity. To the blank sample 1.25 mL MeOH was added, while 1 μM substrate solution (500 μM 7-ethoxyresorufin, dissolved in MeOH:H_2O, 1:1) and 0.5 mM NADPH were added to all samples, which were further incubated for 10 min. The reaction was stopped by addition of 1.25 mL ice-cold MeOH, and the samples were cooled at −20° for 30 min and centrifuged at 1800 *g* for 20 min. To one mL aliquots of the supernatants was added 10 μL 1 N NaOH and fluorescence was measured (Perkin-Elmer LS50B Luminescence Spectrometer) at excitation 530 and emission 585 nm. The standard curve was made using RF concentrations in the range 0–750 nM RF.

Western Blotting

The level of CYP1A1 protein in ASG-treated cells was determined using Western blotting and the enhanced chemiluminescence system (Amersham International plc). Following treatment, the cells were harvested in reporter lysis 5X buffer (Promega) and the lysates were resolved electrophoretically on a 12% constant SDS-PAGE gel using a Protean II system (Bio-Rad). The proteins were transferred to Hybond-P membrane (Amersham International plc) using a semi-dry blotting system [25]. Rabbit–anti-rat CYP1A1 from XenoTech LLC was used as primary antibody. The incubation and detection of the signals was performed as described by the manufacturer.

CAT Assay

Near confluent ($9-14 * 10^4$ cells/cm^2) M8 cells, Hepa 1c1c7 cells stably transfected with a CAT reporter gene, were treated for 19 hr with various concentrations of ASG (dissolved in DMSO) in the media ranging from 1 to 700 μM. The final concentration of DMSO in the media was 0.1% (v/v). Cells treated with DMSO or 1 μM ICZ were included as controls. CAT activity was measured in cell extracts by the two-phase extraction assay described by Seed and Sheen [26]. Briefly, cells were harvested and incubated for 5 min at room temperature in 5.0 mL buffer (20 mM Tris–HCl, pH 7.5, 2 mM $MgCl_2$). The buffer was aspirated and replaced by 100 μL of the buffer containing 0.1% Triton X-100. After 5-min incubation at room temperature, the lysate was centrifuged for 2 min to collect the supernatant. Assays were performed by incubating supernatants at 65° for 10 min. Fifty μL substrate was added to a final concentration of 100 mM Tris–HCl, pH 8.0, 100 μM [^{3}H]chloramphenicol (0.2 μCi), and 250 μM *N*-butyryl–coenzyme A. The mixture was incubated at 37° for 30 min and the reactions stopped by addition of 200 μL of 2,6,10,14-tetramethylpentadecane/xylene (2:1). After centrifugation, the organic phase was transferred to scintillation vials and counted.

Detection of ICZ Formed from ASG

Media from ASG kinetics experiments at 24 and 72 hr were extracted three times with ethylacetate and the organic phases evaporated to dryness. Samples were redissolved in 1 or 5 mL acetonitrile and analysed by HPLC. In parallel, the transformation of ASG in cell-free medium or PBS was estimated after various times of incubation at 37° or room temperature. Media were extracted and analysed as described above, whereas the PBS samples were analysed by HPLC without prior extraction. Authentic ICZ was used as a reference for determination of retention time and spiking of samples. To quantitate ICZ levels, authentic ICZ was added at various concentrations (10 nM–100 nM) to control cells preincubated for 24 or 72 hr before extraction.

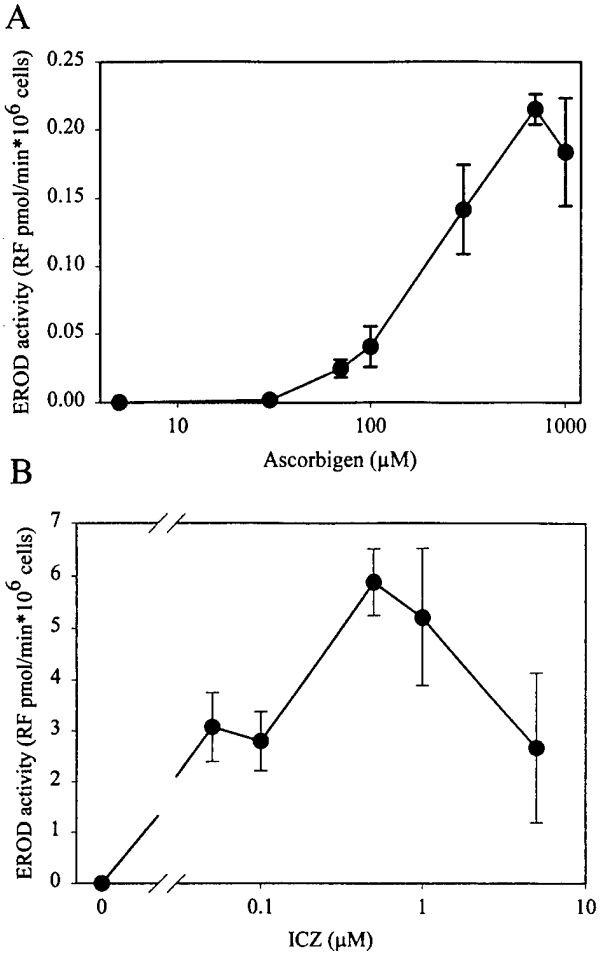

FIG. 2. Effect of ASG and ICZ on EROD activity in Hepa 1c1c7 cells. Cells were treated with increasing concentrations of ASG (1–1000 μM), panel A, or ICZ (0.05–5 μM), panel B, for 24 hr. The cells were then harvested for analysis of enzyme activity. Activity induced by solvent (DMSO) was subtracted for each concentration point. A positive control (1 μM ICZ) was included in the ASG experiment (panel A), i.e. 3.0 RF pmol/min/10^6 cells. Bars indicate mean values of three (panel A) or two (panel B) measurements ± SD (panel A) or range (panel B). The ASG induction experiment (panel A) was conducted twice with similar results.

RESULTS

Concentration-Dependent Induction of CYP1A1 Enzymatic Activity

The concentration–response effect of EROD activity induced by ASG and ICZ is shown in Fig. 2. The maximum induction response after 24 hr was achieved at 700 μM ASG, and the inducing efficiency of ASG was 7% of the EROD activity induced by the positive control, 1 μM ICZ. The EC_{50} values differed by nearly 2000-fold (Fig. 2, A and B). ASG is likely to modulate CYP1A1 activity in a manner similar to what has been reported for the other indoles derived from glucobrassicin. For example, ICZ binds to the Ah receptor and transcriptionally modulates CYP1A1 activity. To examine the effects of ASG on the Ah receptor, Hepa 1c1c7 cells transfected with a CAT reporter gene were treated with doses of ASG up to 700 μM

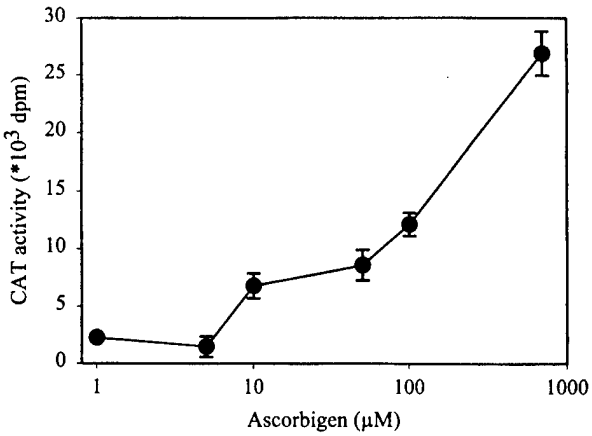

FIG. 3. Effect of ASG on DRE-driven CAT reporter gene activity in Hepa 1c1c7 cells. CAT reporter-transfected Hepa 1c1c7 cells (M8 cells) were treated for 19 hr with inducer at the indicated range of concentrations. Activity induced by solvent (DMSO) was subtracted for each concentration point. The CAT activity for the positive control (1 μM ICZ) was 67 * 10^3 dpm. Bars indicate mean values of two measurements ± range. The experiment was conducted twice with similar results.

(Fig. 3). Cells treated with 0.1% DMSO or 1 μM ICZ were included as controls. The CAT assay shows a concentration-responsive, ASG-induced CAT activity. Surprisingly, the activity of 700 μM ASG was approximately 40% of the CAT activity induced by 1 μM ICZ. A significant CAT activity was already observed at 10 μM ASG, i.e. approximately 25% of the highest observed activity at 700 μM ASG. Transcription of *Cyp1a1* requires a binding of the activated Ah receptor to DRE, which is located in the regulatory region of the *Cyp1a1* gene. Induction of CAT activity by ASG in the present experiment therefore indicates that the Ah receptor is involved in the ASG induction of *Cyp1a1*.

Concentration-Dependent Inhibition of EROD Activity

The greater efficacy exhibited by ASG for CAT induction compared to EROD induction, relative to ICZ, may arise from a strong inhibition of EROD activity by ASG. The inhibitory effect of ASG on microsomal EROD activity is shown in Fig. 4A. The result shows that ASG is an effective inhibitor of EROD activity above 50 μM in the ICZ-induced murine hepatoma microsomal system, as the activity declined with increasing ASG concentrations to 20% at the highest concentration of ASG analysed (200 μM). These results are in accordance with an experiment where Hepa 1c1c7 cells were co-treated with 1 nM TCDD, a highly potent inducer of EROD activity, and ASG at various concentrations for 24 hr, which gave a concentration-dependent decrease in EROD activity. The TCDD-induced EROD activity was significantly inhibited at concentrations above 1 μM ASG (Fig. 4B), thereby demonstrating the overall effect (induction and inhibition) of ASG on CYP1A1 activity. In conclusion, the results show

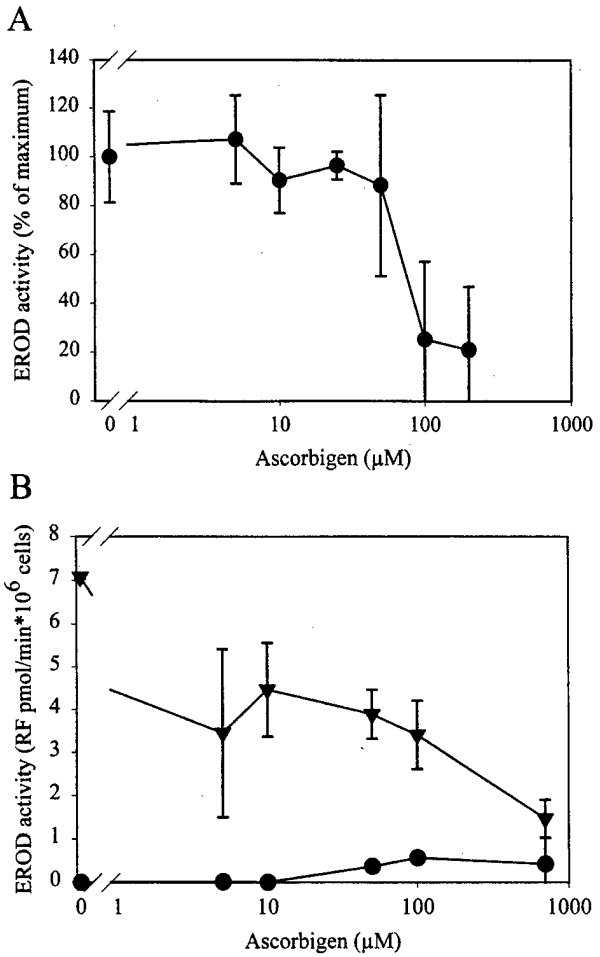

FIG. 4. Inhibitory effect of ASG on CYP1A1 enzymatic activity in microsomes and in whole cells. (A) Fifty μg ICZ-induced microsomes of Hepa 1c1c7 cells were treated with increasing concentrations of ASG 10 min before and throughout the determination of EROD activity. Bars indicate mean values of three measurements ± SD. The experiment was conducted twice with similar results. (B) Hepa 1c1c7 cells were treated with various concentrations of ASG alone (●) or co-treated with 1 nM TCDD and various concentrations of ASG (▼) for 24 hr followed by determination of EROD activity. EROD activity caused by DMSO was subtracted from each concentration point. Bars indicate mean values of two measurements ± range.

that beside activation of the Ah receptor, ASG also inhibits CYP1A1 activity.

Kinetics of Induction of EROD Activity by ASG

To investigate the kinetics of EROD induction by ASG, Hepa 1c1c7 cells were treated with 700 μM ASG for up to 84 hr, and the EROD activity was determined at different time points. The results (Fig. 5) indicate that the activity increases for up to 72-hr incubation with ASG dissolved in DMSO. The EROD activity after 72 hr was about 4-fold higher than that observed after 24-hr incubation. Since the solvent, DMSO, produces a weak CYP1A1 induction peak with a maximum at 8–12 hr (data not shown), we also

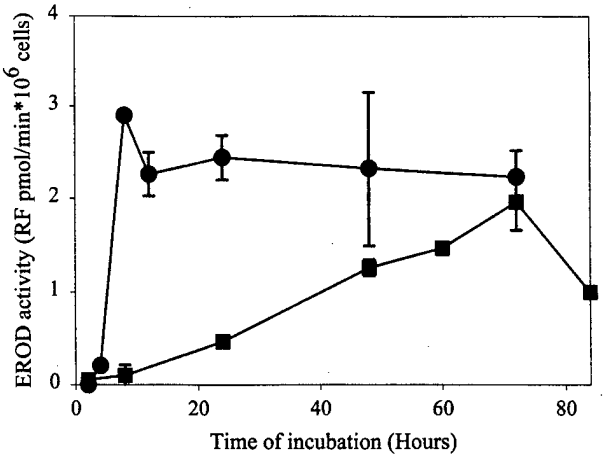

FIG. 5. Kinetics of EROD induction by ASG dissolved in DMSO or PBS in Hepa 1c1c7 cells. The cells were treated with 700 μM ASG dissolved in either DMSO (■) or PBS (●) and harvested at designated time points for analysis of enzyme activity. Activity induced by solvent (DMSO or PBS) was subtracted for each concentration point. Bars indicate mean values of two measurements ± range. The experiments were conducted twice with similar results.

analysed EROD activity kinetics in Hepa 1c1c7 cells exposed to ASG dissolved in PBS (Fig. 5). ASG (700 μM) induced EROD activity to a plateau (2.5 RF pmol/min/10^6 cells) after only 8 hr, which was the same activity obtained after 72 hr when using ASG dissolved in DMSO. This experiment shows that the kinetics for induction by ASG are different when DMSO and PBS are used as solvents.

Kinetics of Induction of CYP1A1 Protein Level by ASG

Hepa 1c1c7 cells were treated with 700 μM ASG, dissolved in DMSO, for up to 96 hr, and the CYP1A1 protein level was determined by Western blot analysis at different time points. The results (Fig. 6) show that the CYP1A1 level was maximally induced after 24 hr, with declining levels up to 96 hr. At 96 hr, the CYP1A1 protein level was reduced to 25% of the level at 24-hr ASG treatment, as determined by densitometric scanning. Comparison of the kinetics of EROD activity when ASG was dissolved in DMSO with the kinetics of the CYP1A1 protein level suggests that the time-dependent increase in EROD activity is caused by disappearance of the ASG from the medium, i.e. the inhibitory effect of ASG is reduced over time.

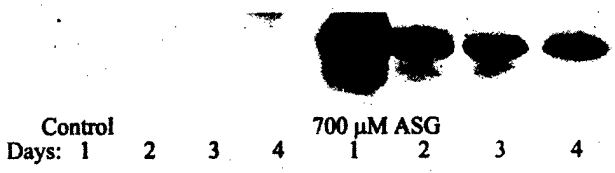

FIG. 6. Kinetics of CYP1A1 protein level induced by ASG. Hepa 1c1c7 cells were treated with 700 μM ASG, dissolved in DMSO, for 24, 48, 72, and 96 hr, and Western blot analysis was carried out on harvested cells using anti-CYP1A1 antibodies.

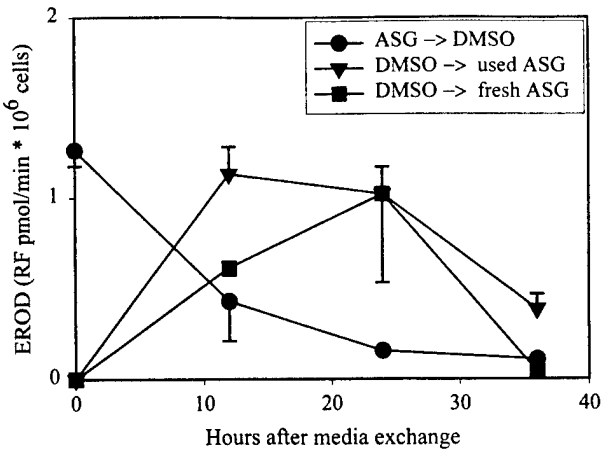

FIG. 7. Kinetics of EROD activity induced by degradation products of ASG. Cells were preincubated with 700 μM ASG (group 1, ●) or 0.1% DMSO (group 2, ▼, and group 3, ■) for 48 hr and EROD activity measured. At 48 hr, the media from group 1 and group 2 were swapped and further incubated for 36 hr. Group 3 was further incubated with fresh 700 μM ASG. EROD activity was measured at the designated time points. Bars indicate mean values of two measurements ± range.

EROD Induction by Degradation Products Formed from ASG during Incubation

To explain why a substance such as ASG, which only binds the Ah receptor weakly, may induce CYP1A1 activity, we suggest that ASG is transformed to an active inducer. Experiments to investigate this notion further were undertaken by determining the induction potential of preincubated ASG-containing medium (Fig. 7). Hepa 1c1c7 cells were preincubated with 700 μM ASG or DMSO for 48 hr followed by a media change as described below. EROD activity was analysed at different time points up to 36 hr after the media change. Cells were treated in three different ways. Cells in group 1 were exposed to ASG for 48 hr and then to an ASG-free medium. Two groups of cells were exposed to DMSO for 48 hr and then shifted to the 48-hr preincubated ASG-containing medium (group 2) or to a medium with fresh (700 μM) ASG (group 3). Figure 7 shows that EROD activity in cells preincubated with ASG decreased after exposure at 48 hr to the preincubated ASG-free medium (group 1). Twenty-four hours after replacement, the activity had decreased to 12% of that before replacement. In cells preincubated with solvent for 48 hr, the EROD activity 12 hr after the media exchange was virtually doubled when the 48-hr preincubated ASG medium (group 2) rather than the fresh ASG-containing medium was used (group 3). Cells exposed to preincubated ASG did show kinetics of EROD induction similar to those observed for CYP1A1 protein (Fig. 6). This experiment shows that preincubated ASG medium is a more effective inducer than fresh ASG, indicating transformation of ASG into a more active inducer. However, this experiment cannot exclude the possibility that the induction of EROD is in part caused by a simultaneous disappearance of ASG and thereby less inhibition of EROD activity.

HPLC Analysis of Degradation Products Formed from ASG

To test whether ASG was transformed into the potent EROD inducer, ICZ, in the cell media during incubation, 24- and 72-hr media from experiments where cells were exposed to ASG were analysed. The medium extracts were analysed by HPLC using fluorescence detection, since this method allows detection of many polycyclic aromatic compounds including ICZ. A peak with the same retention time as ICZ was observed and the identity of the peak was confirmed by spiking with authentic ICZ. The identity of this peak was not confirmed further. ICZ, or a substance with the same mobility, was detected in the medium after 24 hr, and the level was further increased about 5-fold at 72 hr. The level of ICZ or ICZ-like substance present in the ASG medium for 72 hr was estimated to be lower than 10 nM in comparison with controls (Fig. 8, A–C). In cell-free medium incubated with ASG for 2, 6, and 15 hr, ICZ was already detected after 2 hr (Fig. 8D) and found throughout the experiment.

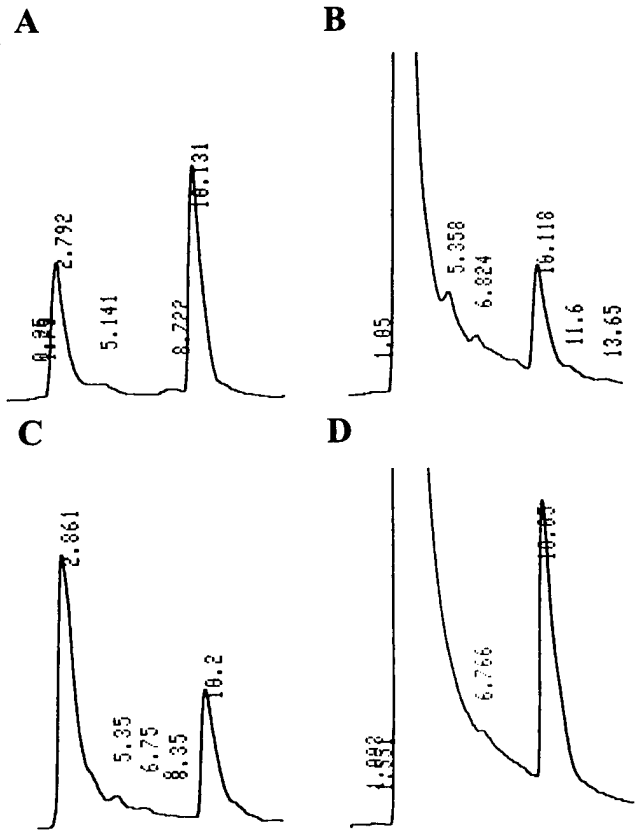

FIG. 8. HPLC analysis of extracts of media incubated with ASG. (A) Control medium to which ICZ (retention time 10.2 min) at the concentration 10 nM was added. (B) Medium from kinetic experiment at 24 hr with ASG dissolved in DMSO. (C) Medium from kinetic experiment at 72 hr with ASG dissolved in DMSO. (D) Cell-free medium incubated for 2 hr with ASG dissolved in DMSO. Following incubation, all media samples were extracted and redissolved in either 5 mL (samples A and C) or 1 mL (samples B and D) acetonitrile. HPLC conditions were as described in Materials and Methods.

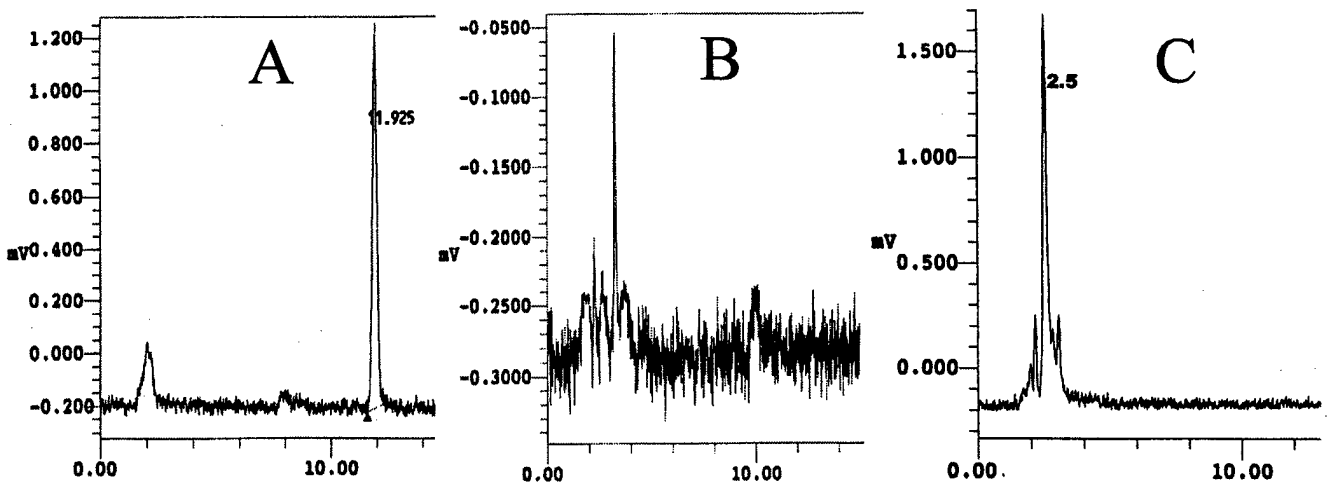

FIG. 9. HPLC analysis of PBS incubated with ASG. (A) Standard ICZ (5 nM). (B) 700 μM ASG incubated in PBS for 15 min at 37°. (C) 700 μM ASG incubated in PBS for 3 hr at 37°. HPLC conditions were as described in Materials and Methods.

In an attempt to account for the earlier EROD induction observed after exposure to ASG dissolved in PBS compared with DMSO, ASG dissolved in PBS was analysed by HPLC. No ICZ (retention time 11.9 min) was detected in the ASG–PBS solution either at room temperature or at 37° up to 24 hr. However, another fluorescent compound with a retention time of 2.5 min was found (Fig. 9). The fluorescent compound with a retention time of 2.5 min could also be formed in the ASG-containing medium, but detection of the compound was interfered with by the medium-specific signal with the same retention time. The fluorescent compound formed in PBS was not further characterised. In conclusion, ASG is transformed to ICZ (or a substance with an identical retention time) in the medium, but not in PBS buffer. However, the fluorescent compound found when ASG was incubated in PBS may be an EROD inducer or may be further transformed into ICZ.

DISCUSSION

It has been shown that broccoli contains high levels of the glucosinolate glucobrassicin and that this compound becomes degraded into I3C after the vegetable is processed. Under acidic conditions, as in the stomach, I3C will associate with the AA present in the vegetable to form ASG [27]. Numerous experiments have shown that I3C induces CYP1A1 activity following ingestion. As ASG is more prominent in cruciferous extracts, the inductive effect of ASG is of great interest. The purpose of this study was to investigate the mechanism of the *in vitro* modulation of CYP1A1 activity by ASG. ASG induced CYP1A1 activity in a concentration-dependent manner in the mouse hepatoma cell line, Hepa 1c1c7, with a maximum induction at 700 μM ASG. This concentration is about 700-fold higher than the maximum inducing concentration for ICZ found here (0.5–1 μM) and reported by Chen *et al.* [19]. The efficiency of ASG induction of CYP1A1 activity after 24 hr was 7% of the positive control (1 μM ICZ), whereas the level of ASG induced CAT activity corresponded to 40% of the ICZ-induced CAT activity. Moreover, the EC_{50} for induction of CAT activity was about one-half of the EC_{50} for induction of EROD, i.e. 120 μM and 210 μM, respectively. The promoter region of the CAT gene contains only one copy of mouse DRE whereas three DRE copies are found in the endogenous *Cyp1a1* promoter region, but these differences do not explain the observed differences in results obtained in the EROD and CAT assays. The likely explanation for these discrepancies could be that beside induction of EROD activity, ASG also exhibits an inhibitory effect on EROD activity. This assumption was confirmed in the present study, as ASG was shown to inhibit murine hepatoma microsomal EROD activity and TCDD-induced EROD activity in whole cells in a concentration-responsive manner. These profiles of responses Hepa 1c1c7 cells by ASG resemble those previously reported by Chen *et al.* [18] for I3C and DIM in T47D human breast cancer cells. These authors showed that both I3C and DIM are relatively weak Ah receptor agonists compared to ICZ and TCDD, since no induction of CYP1A1-dependent EROD activity was observed at concentrations as high as 125 and 31 μM, respectively [18], whereas I3C and DIM significantly inhibited TCDD-induced EROD activity in whole cells at concentrations of 31 and 1 μM, respectively. Furthermore, both I3C and DIM exhibited partial Ah receptor antagonist activity and significantly inhibited EROD activity in microsomes from TCDD-treated T47D cells at concentrations of 10 and 1 μM, respectively. In our experiments, the increase in EROD activity was shown to be caused by an induction of CYP1A1 protein by ASG, and the protein level was maximal after 24-hr exposure to ASG. Recently, Ciolino *et al.* [28] reported that another dietary constituent, curcumin, also has a dual property in being able to induce CYP1A1 in MCF-7 cells while also being an inhibitor of CYP1A1 activity.

The CAT experiment clearly indicates that ASG treatment activates the Ah receptor, which is a well-known

mechanism for induction of CYP1A1 protein and activity. Gillner *et al.* [29] previously demonstrated that the Ah receptor binding affinity of ASG, measured as IC_{50} values of the inhibition of specific [^{3}H]TCDD binding in rat liver cytosol, was more than 400 times lower than the corresponding value for ICZ and in the same range as for I3C. Since ASG has a very low affinity for the Ah receptor, it is likely that ASG is transformed into a more potent ligand and CYP1A1 inducer. ICZ, or a compound with an identical retention time, was detected in the ASG media at 24 and 72 hr. The possibility that other inducers are formed from ASG cannot be excluded. We therefore suggest that the induction of CYP1A1 protein by ASG is caused by transformation to the potent inducer ICZ and/or other potent products. Furthermore, it cannot be excluded from the present experiments that ASG may interact with other regulatory factors as well.

Preobrazhenskaya *et al.* [30] have previously shown that ASG incubated with gastric juice for 5 hr at 37° give rise to a very complex mixture containing ICZ, and that the concentration of ICZ in gastric juice was approximately 20 times higher after incubation under these conditions with ASG than after incubation with I3C. Our experiments indicate that ICZ may also be formed from ASG under physiological conditions at neutral pH. In contrast, ASG dissolved in PBS caused an EROD induction with the same efficiency at 8 hr as found for the positive control at 24 hr. This induction pattern corresponds to the ICZ-induced EROD activity shown by Chen *et al.* [19]. One can therefore speculate that ASG is transformed to ICZ in the aqueous buffer before addition to the medium. However, ICZ was not detected using HPLC in the ASG–PBS solution when incubated at 37° for up to 24 hr, whereas another fluorescent, more polar compound was detected. The identity of this compound has not been established but the ASG oligomers do not exhibit fluorescence, and the unidentified compound is likely to be a polycyclic polar product. The early response in EROD activity observed when using PBS as ASG solvent is therefore not caused by the presence of ICZ in the initial PBS solution. Furthermore, the low level of ICZ detected in the media cannot by itself account for the entire CYP1A1 induction observed. Degradation of ASG is likely to result in the release of AA, and the effect of AA on induction of CYP enzymes is not well characterised. It cannot be excluded that AA *in vitro* may enhance the inducing potential of ASG/ICZ. The observed EROD kinetic is a combination of a fast induction by ICZ or an ICZ-like compound, ASG, and other potential inducers formed from ASG and a slow disappearance of the inhibitor ASG from the medium over time. The half-life of ICZ is about 10 min [19], and the effect presented here is likely caused by a continuous formation of ICZ from an excess amount of ASG. Induction of CAT is observed above 10 μM ASG, but because of a significant ASG-mediated inhibition in whole cells above 1 μM, a significant induction of EROD is only observed above 50 μM ASG.

In conclusion, our results show that exposure to ASG induces CYP1A1 expression in Hepa 1c1c7 cells. ASG treatment induces Ah receptor-driven CAT activity and therefore presumably induces CYP1A1 via activation of the Ah receptor. According to the literature, ASG acts as a weak Ah receptor agonist compared to ICZ or an ICZ-like substance, but the induction may in part be explained by the transformation of ASG to the more potent inducer ICZ. In addition to inducing EROD activity, ASG also inhibits this activity. As ASG is the main transformation product from glucobrassicin in the presence of AA, the observation that ICZ, or an ICZ-like substance, may also be formed at neutral pH is of great interest.

We thank Charlene Schaldach (University of California, Berkeley, CA) for undertaking the CAT assay, Dr. Simon Bolvig (University of California, Berkeley, CA) for the NMR analysis, and Dr. Niels Agerbirk (The Royal Veterinary and Agricultural University, Denmark) for helpful discussions on ASG synthesis. Valuable comments on the manuscript from Dr. Hanne-Cathrine Bisgaard (Roskilde University) are appreciated. This work was supported by the Danish Cancer Society (P. U. S.), the Wedell-Wedellsborg Foundation (P. U. S., C. B., O. V.), The Foundation for Disease Treatment without use of Animal Experiments (O. V.), the US Department of Defense, Army Breast Cancer Research Program Grant DAMD17-96-1-6149 (L. F. B.) and NIH Grant CA 69056 (L. F. B.).

References

1. Steinmetz KA and Potter JD, Vegetables, fruit, and cancer. I. Epidemiology. *Cancer Causes Control* **2:** 325–357, 1991.
2. McDanell R, McLean AEM, Hanley AB, Heanley RK and Fenwick GR, Chemical and biological properties of indole glucosinolates (glucobrassicins): A review. *Food Chem Toxicol* **26:** 59–70, 1988.
3. Prochaska H, Santamaria AB and Talalay P, Rapid detection of inducers of enzymes that protect against carcinogens. *Proc Natl Acad Sci USA* **89:** 2394–2398, 1992.
4. Bjerg B and Sørensen H, Isolation of intact glucosinolates by column chromatography and determination of their purity. In: *Glucosinolates in Rapeseeds: Analytical Aspects.* (Ed. Wathelet J), pp. 59–75. Martinus Nyhoff, Dordrecht/Boston/Lancaster, 1987.
5. Sørensen H, Glucosinolates: Structure-Properties-Function. In: *Rapeseed/Canola: Production, Chemistry, Nutrition and Processing Technology* (Ed. Shahidi F), pp. 149–172. Van Nostrand Reinhold, New York, 1990.
6. Bradfield CA and Bjeldanes LF, Dietary modifications of xenobiotic metabolism: Contribution of indolylic compounds present in *Brassica oleracae*. *J Agr Food Chem* **35:** 896–900, 1987.
7. McDanell R, McLean AEM, Hanley AB, Heaney RK and Fenwick GR, Differential induction of mixed-function oxidase (MFO) activity in rat liver and intestine by diets containing processed cabbage: Correlation with cabbage levels of glucosinolates and glucosinolate hydrolysis products. *Food Chem Toxicol* **25:** 363–368, 1987.
8. Bjeldanes LF, Kim J, Grose KR, Bartholomew JC and Bradfield CA, Aromatic hydrocarbon responsiveness-receptor agonists generated from indole-3-carbinol *in vitro* and *in vivo*: Comparison with 2,3,7,8-tetrachlorodibenzo-*p*-dioxin. *Proc Natl Acad Sci USA* **88:** 9543–9547, 1991.
9. Bonnesen C, Stephensen PU, Andersen O, Sørensen H and

Vang O, Modulation of cytochrome P-450 and glutathione S-transferase isoform expression *in vivo* by intact and degraded indolyl glucosinolates. *Nutr Cancer* **33:** 178–187, 1999.
10. Kwon C, Grose KR, Riby J, Chen Y and Bjeldanes LF, *In vivo* production and enzyme-inducing activity of indolo[3,2-*b*]carbazole. *J Agr Food Chem* **42:** 2536–2540, 1994.
11. Kutacek M, Prochazka Z and Veres K, Biogenesis of glucobrassicin, the *in vitro* precursor of ascorbigen. *Nature* **194:** 393–394, 1962.
12. Preobrazhenskaya MN, Korolev AM, Plikhtyak IL, Yartseva IV, Efimov SA, Lazhko EI and Alexandrova LG, Chemistry and biology of acsorbigens. In: *Heterocycles in Bio-organic Chemistry* (Eds. Bergman J, Van der Plas HC and Simonyi M), pp. 68–86. The Royal Society of Chemistry, Cambridge, 1991.
13. Moller A, *Levnedsmiddeltabeller* 4. revised ed. (Ed. Saxholt E). National Food Agency, ISBN 87-601-4742-3, 1996.
14. Aleksandrova LG, Korolev AM and Preobrazhenskaya MN, Study of natural ascorbigen and related compounds by HPLC. *Food Chem* **45:** 61–69, 1992.
15. Vang O and Dragsted L, *Naturally Occurring Antitumourigens—III. Indoles*. The Nordic Council of Ministers, Copenhagen, 1996.
16. Sepkovic DW, Bradlow HL, Michnovicz J, Murtezani S, Levy I and Osborne MP, Catechol estrogen production in rat microsomes after treatment with indole-3-carbinol, ascorbigen, or β-naphthaflavone: A comparison of stable isotope dilution gas chromatography-mass spectrometry and radiometric methods. *Steroids* **59:** 318–323, 1994.
17. Wattenberg LW, Inhibition of neoplasia by minor dietary constituents. *Cancer Res* **43:** 2448–2453, 1983.
18. Chen I, Safe S and Bjeldanes LF, Indole-3-carbinol and diindolylmethane as aryl hydrocarbon (Ah) receptor agonists and antagonists in T47D human breast cancer cells. *Biochem Pharmacol* **51:** 1069–1076, 1996.
19. Chen Y, Riby J, Srivastava P, Bartholomew J, Denison M and Bjeldanes LF, Regulation of CYP1A1 by indolo[3,2-*b*]carbazole in murine hepatoma cells. *J Biol Chem* **270:** 22548–22555, 1995.
20. Robinson B, The Fisher indolisation of cyclohexane-1,4-dione bisphenylhydrazone. *J Soc Chem* **:** 3097–3099, 1963.
21. Leete E and Marion L, The hydrogenolysis of 3-hydroxymethylindole and other indole derivates with lithium aluminium hydride. *Can J Chem* **31:** 775–784, 1953.
22. Kiss G and Neukom H, Uber die struktur des ascorbigens. *Helv Chim Acta* **49:** 989–992, 1996.
23. Agerbirk N, Olsen CE and Sørensen H, Initial and final products, nitriles and ascorbigens produced in myrosinase catalysed hydrolysis of indole glucosinolates. *J Agr Food Chem* **46:** 1563–1571, 1998.
24. Fisher JM, Wu L, Denison MS and Whitlock JP Jr, Organization and function of a dioxin-responsive enhancer. *J Biol Chem* **265:** 9676–9681, 1990.
25. Vang O, Jensen H and Autrup H, Induction of cytochrome P-450IA1, IA2, IIB1, IIB2 and IIE1 by broccoli in rat liver and colon. *Chem Biol Interact* **78:** 85–96, 1991.
26. Seed B and Sheen J, A simple phase-extraction assay for chloramphenicol acyltransferase activity. *Gene* **67:** 271–277, 1988.
27. Piironen E and Virtanen AI, The synthesis of ascorbigen from ascorbic acid and 3-hydroxymethylindole. *Acta Chem Scand* **5:** 1286–1287, 1962.
28. Ciolino HP, Daschner PJ, Wang TT and Yeh GC, Effect of curcumin on the aryl hydrocarbon receptor and cytochrome P450 1A1 in MCF-7 human breast carcinoma cells. *Biochem Pharmacol* **56:** 197–206, 1998.
29. Gillner M, Bergman J, Cambillau C, Fernström B and Gustafsson J, Interactions of indoles with specific binding sites for 2,3,7,8-tetrachlorodibenzo-*p*-dioxin in rat liver. *Mol Pharmacol* **28:** 357–363, 1985.
30. Preobrazhenskaya MN, Korolev AM, Lazhko EI and Aleksandrova LG, Ascorbigen as a precursor of 5,11-dihydroindolo[3,2-*b*]carbazole. *Food Chem* **48:** 57–62, 1993.

NUTRITION AND CANCER, 36(1), 112–121

N-Methoxyindole-3-Carbinol Is a More Efficient Inducer of Cytochrome *P*-450 1A1 in Cultured Cells Than Indol-3-Carbinol

Pernille Uldall Stephensen, Christine Bonnesen, Charlene Schaldach, Ole Andersen, Leonard F. Bjeldanes, and Ole Vang

Abstract: *The well-documented reduction of cancer risk by high dietary cruciferous vegetable intake may in part be caused by modulation of cytochrome* P-*450 (CYP) expression and activity by indoles. The purpose of the present experiments was to study the mechanism of CYP 1A1 induction by* N-*methoxyindole-3-carbinol (NI3C) in cultured cells and to compare the CYP-inducing potential of NI3C and indole-3-carbinol (I3C) administered to rats. NI3C induced 7-ethoxyresorufin-*O*-deethylase (EROD) activity in Hepa-1c1c7 cells in a concentration-dependent manner with 10-fold higher efficiency than I3C. Inasmuch as NI3C induced binding of the aryl hydrocarbon receptor (AhR) to the dioxin-responsive element and induced expression of endogenous CYP 1A1 mRNA and an AhR-responsive chloramphenicol acetyl transferase construct, we conclude that NI3C can activate the AhR. Besides the induction of CYP 1A1, we observed an inhibition of EROD activity, with a concentration causing 50% inhibition of 6 μM. Oral administration of NI3C at 570 μmol/kg body wt to male Wistar rats increased the hepatic CYP 1A1 and 1A2 protein levels, as well as the EROD and 7-methoxyresorufin* O*-demethylase activities at 8 and 24 hours after administration, but the responses were less pronounced than after administration of I3C at 570 μmol/kg body wt. Furthermore, NI3C did not induce hepatic 7-pentoxyresorufin O-depentylase activity, as I3C did. Ascorbigen, another indolylic compound formed during degradation of glucobrassicin in the presence of ascorbic acid, was tested in the same animal model, and ascorbigen only weakly induced hepatic CYP 1A1 and 1A2, but not CYP 2B1/2. In conclusion, NI3C is a more efficient inducer of CYP 1A1 in cultured cells than I3C but is less active when administered to rodents.*

Introduction

Consumption of vegetables from the family Cruciferae, including broccoli, cauliflower, and brussels sprouts, leads to increased levels of hepatic and extrahepatic xenobiotic-metabolizing enzymes in experimental animals (1) and humans (2). An increased metabolism of xenobiotics may in part explain the well-documented reduced cancer incidences in population groups with a high dietary intake of cruciferous vegetables (3,4). This anticarcinogenic effect has been suggested to be associated with the high content of indolyl glucosinolates in these vegetables (5). Besides the indolyl glucosinolates, several other glucosinolates from cruciferous vegetables may have anticarcinogenic potentials, including sinigrin (6), glucoraphanin, from which sulphoraphane is formed (7), and gluconasturtiin, which is degraded to phenethyl isothiocyanate (8). Moreover, other potentially anticarcinogenic substances are found in these vegetables, and mechanisms other than modulations of cytochrome *P*-450 (CYP) activities are likely. The degradation of the indolyl glucosinolate glucobrassicin (GB; Figure 1) has been studied extensively, and effects on xenobiotic metabolism of one of the degradation products, indole-3-carbinol (I3C; Figure 1), have been investigated *in vivo* (9) and *in vitro* (10). From these experiments, it has been concluded that I3C acts as a very weak inducer of CYP 1A1 activity in cultured cells, but when given orally, I3C is transformed *in vivo* into more active, oligomeric products in the gastric juice. These oligomeric products, including indolo[3,2-*b*]carbazole (ICZ) and 3,3′-diindolylmethane (DIM), induce CYP 1A activities by binding to and activation of the aryl hydrocarbon receptor (AhR) (10). Neoglucobrassicin (NeoGB; Figure 1), another indolyl glucosinolate found in cruciferous vegetables, is present in relatively high concentrations, especially in broccoli. Levels of the degradation product *N*-methoxyindole-3-carbinol (NI3C; Figure 1) may be as high as the amount of I3C in this vegetable. Hence, the CYP 1A-modulating effects of cruciferous vegetables may be caused by NeoGB-NI3C and GB-I3C. Our laboratory recently showed that purified GB and NeoGB induced hepatic CYP 1A1 and 7-ethyoxyresorufin-*O*-deethylase (EROD) activity in rats (11). Considering the relatively

P. U. Stephensen, C. Bonnesen, O. Andersen, and O. Vang are affiliated with the Department of Life Sciences and Chemistry, Roskilde University, DK-4000 Roskilde, Denmark. P. U. Stephensen, C. Bonnesen, C. Schaldach, and L. F. Bjeldanes are affiliated with the Department of Nutrition, University of California, Berkeley, CA 94720.

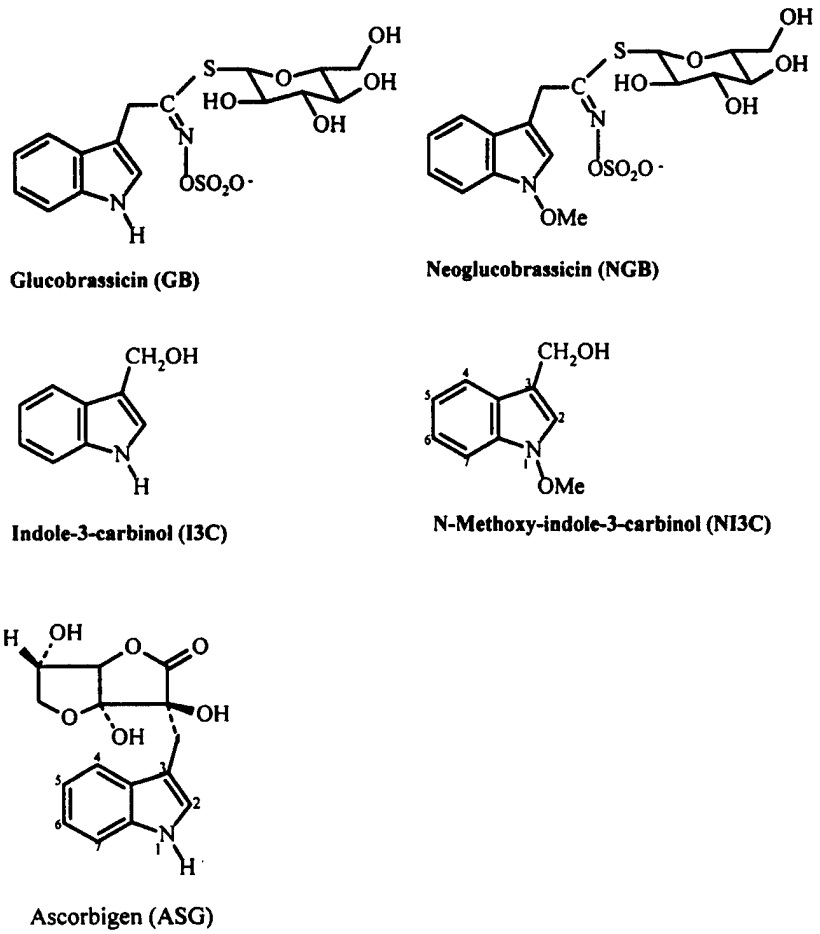

Figure 1. Structures of glucobrassicin, neoglucobrassicin, and derived indoles.

high concentrations of NeoGB in cruciferous vegetables, it seems that the possible effects of this compound and its degradation products have been somewhat neglected. Another degradation product of NeoGB, *N*-methoxyindole-3-ylcarbaldehyde, which is the oxidized form of NI3C, induced CYP 1A1 activity twofold in mice, slightly higher than I3C (12). In rats, *N*-methoxyindole-3-ylcarbaldehyde was a twofold stronger inducer of hepatic EROD activity than the analog formed from GB, indole-3-ylcarbaldehyde (9). On the other hand, NI3C significantly increased hepatic CYP 1A1 activity but had only one-half the inducing capacity of I3C in the same rat model (9). Studies on the CYP 1A1-modulating effects of NI3C in cultured cells have not been published. The present study describes the CYP 1A1-modulating activity of NI3C in a murine hepatoma cell line (Hepa-1c1c7) and the effect on hepatic CYP 1A and 2B1/2 expression in male Wistar rats. The effects of NI3C are compared with those of I3C. Furthermore, ascorbigen (ASG; Figure 1), which is formed during the degradation of GB in the presence of ascorbic acid, was tested in the same animal model. Ascorbic acid is present in cruciferous vegetables in high concentrations, and it has been shown that ASG is the predominant indole compound in fresh, cooked, and fermented cabbage (13). The biological effects of dietary ASG are therefore of great interest.

Materials and Methods

Chemicals

I3C and resorufin (RF) were purchased from Aldrich Chemical (Milwaukee, WI), and I3C was recrystallized from toluene before use. 7-Ethoxyresorufin, NADPH, *N*-butyryl coenzyme A, lithium salt, tris(hydroxymethyl)aminomethane (Tris), and bovine serum albumin were purchased from Sigma Chemical (St. Louis, MO). [*ring*,3,5-^{3}H]chloramphenicol was purchased from Dupont New England Nuclear (Boston, MA). 2,3,7,8-Tetrachlorodibenzo-*p*-dioxin (TCDD) was a kind gift from Prof. B. Ames (University of California, Berkeley, CA). All other organic solvents, chemicals, and biochemicals were of the highest quality available from commercial sources. ASG was synthesized according to the procedure of Kiss and Neukom (14) with the modifications described by Stephensen and co-workers (15).

High-Performance Liquid Chromatography Analysis

For high-performance liquid chromatography (HPLC) analysis, a C_{18} bonded-phase column was used (Ultrasphere-ODS, 4.6 × 250 mm, particle size 5 µm, Beckman, San Ramon, CA). The detector was a UV-VIS spectrophotometer

(model SPD-10A, Shimadzu) set at 280 nm. An isocratic system was used with HPLC-grade water modified with 60% acetonitrile as mobile phase.

Synthesis of NI3C

NI3C was synthesized by a three-step procedure starting with the synthesis of *N*-methoxyindole according to the method of Acheson and colleagues (16,17) using the modifications previously described by this laboratory (12). *N*-methoxyindole-3-ylcarbaldehyde was subsequently synthesized as described by Acheson and colleagues (16) and finally reduced to NI3C by the procedures of Leete (18) and Hanley and Parsley (19). Briefly, a solution of *N*-methoxyindole-3-ylcarbaldehyde (150 mg) in methanol-ethanol (1:8, 1.5 ml) was treated with 65 mg of sodium borohydride, and the mixture was stirred at room temperature for three hours. The solvent was removed by evaporation under reduced pressure, and the residue was treated with 1.5 ml of 0.1 M NaCl and extracted three times with 4.5 ml of diethyl ether. The organic fraction was dried with Na_2SO_4 and evaporated to dryness to afford a crude alcohol. NI3C was obtained as a yellow oil at an overall yield of 6%. The purity of NI3C was assessed by HPLC to be 94%. C, H, and N elementary analysis carried out on an elementary analyzer (model 2400, Perkin-Elmer) showed a composition of 67.4% C, 6.1% H, and 7.7% N compared with theoretical values of 67.8% C, 6.2% H, and 7.9% N. ^1H nuclear magnetic resonance spectra were measured at 300 MHz in D_4-methanol on an AC-300 Brucker instrument. Chemical shift values were recorded relative to tetramethylsilane for all spectra. The nuclear magnetic resonance spectrum was consistent with previously recorded values (19): δ_H 4.09 (s, OCH_3), 4.85 (s, CH_2), 7.16 (m, 6-H), 7.28 (m, 5-H), 7.28 (s, 2-H), 7.44 (dt, 4-H), and 7.71 (dt, 7-H) (see Figure 1 for proton numbering).

Cell Culture

Murine hepatoma cell lines, wild-type Hepa-1c1c7 cells, AhR nuclear transport (Arnt) protein-deficient mutant (B13) cells, and M8 cells, which are Hepa-1c1c7 cells stably transfected with the dioxin-responsive chloramphenicol acetyl transferase (CAT) reporter pMCAT 5.9, were grown as monolayers at 37°C in 95% air-5% CO_2 in Dulbecco's modified Eagle's medium containing 10% fetal bovine serum, 3.7 g/l sodium bicarbonate, and 4.0 g/l glucose. pMCAT 5.9 is a plasmid constructed by ligation of the −820 to −974 enhancer sequence from the mouse promoter, which contains one dioxin-responsive element (DRE) in the pMCAT 5 plasmid (20) and was generously provided by Dr. J. P. Whitlock, Jr. (Stanford University, Palo Alto, CA).

EROD Activity in Intact Cells

Hepa-1c1c7 cells and B13 cells were grown in 58-mm-diameter plates. NI3C or I3C dissolved in dimethyl sulfoxide (DMSO) was added to the cells (9–14 × 10^4 cells/cm^2), and the cells were incubated for 24 hours. Control cell cultures were incubated with DMSO. As positive controls, cell cultures were incubated with the potent CYP 1A1 inducer ICZ. At the end of the incubation, cells were washed in phosphate-buffered saline (PBS), harvested by trypsination, and resuspended in PBS. Two hundred microliters of cell suspension were used for cell counting. One-half milliliter of 1 μM 7-ethoxyresorufin was added to 1.5 ml of cell suspension that had been preincubated for a few minutes at 37°C. The EROD activity was determined as the linear production of the fluorescent RF at 37°C with a spectrofluorometer (model 650-105, Perkin-Elmer) with 510-nm excitation, 585-nm emission, and 20-nm slit width. The amount of RF formed was determined by comparison with a standard curve (0–6.3 nM RF in PBS).

CAT Assay

Near-confluent M8 cells (9–14 × 10^4 cells/cm^2) were treated for 19 hours with NI3C in DMSO at 1–100 μM. The final DMSO concentration in the medium was 0.1% (vol/vol). Cells treated with DMSO or 1 μM ICZ were included as controls. CAT activity was measured in cell extracts by the two-phase extraction assay described previously (21). Briefly, cells were harvested and incubated for five minutes at room temperature in 5.0 ml of buffer (20 mM Tris·HCl, pH 7.5, 2 mM $MgCl_2$). The buffer was aspirated and replaced by 100 μl of the buffer containing 0.1% Triton X-100. After five minutes of incubation at room temperature, the lysate was centrifuged for two minutes to collect the supernatant. Assays were performed by incubating supernatants at 65°C for 10 minutes. Fifty microliters of substrate were added to a final concentration of 100 mM Tris·HCl, pH 8, 100 μM [^3H]chloramphenicol (0.2 μCi), and 250 μM butyryl coenzyme A. The mixture was incubated at 37°C for 30 minutes, and the reaction was stopped by addition of 200 μl of 2,6,10,14-tetra-methyl-pentadecane-xylene (2:1). After centrifugation, the organic phase was transferred to scintillation vials and counted.

mRNA Expression

Near-confluent Hepa-1c1c7 cells were treated with 50 μM NI3C or DMSO, and after various lengths of time (2–24 h), total RNA was isolated from the cells by using the TRI Reagent (Molecular Research Center, Cincinnati, OH). RNA was separated on a formaldehyde gel, transferred to a Zeta Probe nylon membrane (Bio-Rad, Hercules, CA), probed with a ^{32}P-labeled CYP 1A1 probe (American Type Culture Collection, Manassas, VA), and normalized by a glyceraldehyde 3-phosphate dehydrogenase (GADPH) probe (a generous gift from Prof. G. L. Firestone, University of California, Berkeley, CA).

Gel Mobility Retardation Assay

Hepa-1c1c7 cells were incubated with NI3C (1–100 μM), ICZ (1 μM), or DMSO for one hour, and nuclear extracts

were prepared as described previously (22,23). A complementary pair of synthetic oligonucleotides containing the sequence 5′-GATCTGGCTCTTCTCACGCAACTCCG-3′ and 5′-GATCCGGAGTTGCGTGAGAAGAGCCA-3′ (corresponding to the AhR-binding site of DRE-3 and designated the wild-type DRE oligonucleotide) and 5′-GATCTGGCTCTTCTCACACAACTCCG-3′ and 5′-GATCCGGAGTTGTGTGAGAAGAGCCA-3′ [identical to the wild-type DRE oligonucleotide but containing a single substitution (underlined) within the DRE core consensus sequence that eliminates binding of the transformed ligand-AhR complex and designated the mutant DRE oligonucleotide] were synthesized, purified, annealed, and radiolabeled with [γ-^{32}P]ATP, as described previously (24).

In Vitro Inhibition of Microsomal EROD Activity

Microsomes were prepared from near-confluent Hepa-1c1c7 cells treated for 24 hours with 1 μM ICZ. The cells were harvested in PBS with a rubber policeman and sonicated in a phosphate buffer (50 mM $NaPO_4$, pH 7.4, 0.1 mM EDTA, 10% glycerol) twice for 10 seconds while kept on ice. The lysate was centrifuged for 15 minutes at 10,000 *g* and 4°C, the supernatant was further centrifuged for 1 hour at 100,000 *g* at 4°C, and the microsomal pellet was resuspended in storage buffer (0.154 M KCl, 10 mM Tris·HCl, pH 7.4, 1 mM EDTA, 20% glycerol). Microsomal protein concentration was determined by a Lowry method, with bovine serum albumin as protein standard. The EROD activity was measured as described above using 2 ml of 0.1 M potassium phosphate buffer, pH 7.8, containing 30 μg of microsomes, 0.05 μM 7-ethoxyresorufin, 0.5 mM NADPH, and different concentrations of inhibitor. The microsomes were mixed with the inhibitor and pretreated for five minutes at 37°C before addition of NADPH and substrate.

Treatment of Animals

Male Wistar rats (4 wk old, approx 150 g body wt; Møllegaard Breeding and Research Center) were kept as described previously (25) with free access to a semisynthetic diet (18% protein, 70% carbohydrate, 12% fat, polyunsaturated-to-saturated fat ratio = 0.7) and water for two weeks. The test compounds were dissolved in plant oil and given by oral intubation at a concentration of 570 μmol indole/kg body wt 8 or 24 hours before sacrifice. Control rats received similar amounts of plant oil. The rats were sacrificed, and livers were excised, weighed, and stored at −80°C until preparation of liver microsomes.

Hepatic Microsome Preparation

Liver microsomes were prepared from the tissue stored at −80°C. Approximately 2 g of frozen liver were homogenized (Potter-Elvehjem glass-Teflon homogenizer) in 8 ml of homogenization buffer (0.154 M KCl, 10 mM Tris·HCl, 1 mM EDTA, 0.25 mM phenylmethylsulfonyl fluoride, pH 7.4). The homogenized tissue was centrifuged at 9,000 *g* at 4°C for 30 minutes, and the supernatant was further centrifuged at 105,000 *g* at 4°C for 60 minutes. The microsomal pellet was redissolved in 5 ml of homogenization buffer containing 20% glycerol and stored at −80°C. The microsomal protein concentration was determined by a Lowry assay with bovine serum albumin as standard.

EROD Activity of Hepatic Microsomes

One-milliliter reaction mixtures were prepared consisting of 0.5 mM NADPH, 1.2 mg/ml bovine serum albumin, 50 μg/ml microsomal protein, 1 μM 7-ethoxyresorufin, and 0.1 M Tris·HCl (pH 7.8). The samples were preincubated in a shaking water bath at 37°C for one to two minutes. After addition of the substrates, the samples were incubated for 10 minutes, and the reaction was stopped by addition of 2.5 ml of ice-cold methanol. The samples were cooled at −20°C for 30 minutes and centrifuged at 3,000 rpm at 4°C for 20 minutes. To 1-ml aliquots of the supernatants, 10 μl of 1 M NaOH were added, and fluorescence was measured (LS50B Luminescence Spectrometer, Perkin-Elmer) at 530-nm excitation and 585-nm emission. The specific activity was calculated from a standard curve with RF in the concentration range 0–750 nM.

Western Blotting

The levels of CYP proteins were determined using Western blotting and the enhanced chemiluminescence system (Amersham Pharmacia Biotech Europe). Microsomal protein was resolved electrophoretically on a 12% constant sodium dodecyl sulfate-polyacrylamide gel with a Protean II system (Bio-Rad). The proteins were transferred to a polyvinylidene difluoride membrane (Amersham Pharmacia Biotech) with a semidry blotting system (1). As primary antibodies, rabbit anti-rat CYP 1A1 (XenoTech) and rabbit anti-rat CYP 2E, 2B, and 1A2 (Amersham Pharmacia Biotech) were used. The incubation and detection of the signals were performed as described by the manufacturer.

Statistics

Student's *t*-test was used to test the concentrations significantly different from the lowest concentration used in the particular *in vitro* experiments. The *in vivo* results were analyzed for statistically significant differences by using the logarithmically transformed values in analysis of variance and Bonferoni post hoc tests in the Systat 6.0.1 computer program (SPSS). In all cases, significance is assumed when $p < 0.05$.

Results

Concentration-Dependent Induction of CYP 1A1 Enzymatic Activity *In Vitro*

We compared the EROD-inducing effects of NI3C and I3C and found both compounds to cause induction in a con-

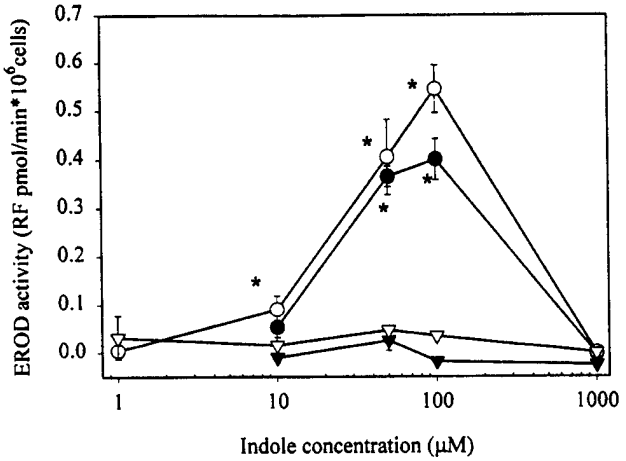

Figure 2. Inducing effect of *N*-methoxyindole-3-carbinol (NI3C) and indole-3-carbinol (I3C) on 7-ethoxyresorufin-*O*-deethylase (EROD) activity in Hepa-1c1c7 cells. Cultures of Hepa-1c1c7 cells were exposed to different concentrations (1–1,000 μM) of NI3C (*filled circles*) and I3C (*filled inverted triangles*) for 24 or 48 h (*open circles* and *open inverted triangles*), and EROD activity was determined in intact cells. Activity of positive control {1 μM indolo[3,2-*b*]carbazole (ICZ)} was 4.5 pmol resorufin (RF)/min × 10^6 cells. Activities obtained in dimethyl sulfoxide (DMSO)-treated cells are subtracted. Values are means of 2 measurements ± ranges, and experiment was conducted twice with similar results. *, Significantly different from 10 μM (24 h) or 1 μM (48 h).

centration-dependent manner (Figure 2) after 24 and 48 hours. The maximum responses occurred at 50 and 100 μM for I3C and NI3C, respectively. A comparison of the inductions caused by NI3C and I3C with the included positive control, 1 μM ICZ, showed that NI3C was a more efficient inducer than I3C: the maximum induction after 24 hours by I3C was 0.8% of the positive control value, whereas it was 8.9% for NI3C. In the Arnt protein-deficient Hepa-1 mutant B13 cells, up to 100 μM NI3C did not induce the EROD activity (data not shown), verifying that a functional AhR pathway is required for NI3C induction of CYP 1A1 activity. Cytotoxic effects were observed at 1,000 μM after 24 hours, but 50 μM NI3C was not found to reduce DNA synthesis or to reduce the number of Hepa-1c1c7 cells up to 72 hours (data not shown).

NI3C-Induced CYP 1A1 Activity by the AhR Pathway

It is likely that NI3C induces CYP 1A1 activity in a manner similar to that reported for the indoles derived from GB, e.g., ICZ and DIM, by binding to the AhR and transcriptionally activating the *cyp* 1A1 gene. To examine the effects of NI3C on the AhR pathway, we analyzed nuclear extracts of NI3C-induced Hepa-1c1c7 cells in a gel-mobility shift assay and found that NI3C induced the binding of the AhR to the wild-type DRE in a concentration-dependent fashion (Figure 3). The AhR binding could be displaced by an excess of cold DRE, but only partly by the mutant DRE, confirming the specificity of the AhR-DRE complex. To examine the interaction of NI3C with the AhR pathway further, we treated Hepa-1c1c7 cells stably transfected with an

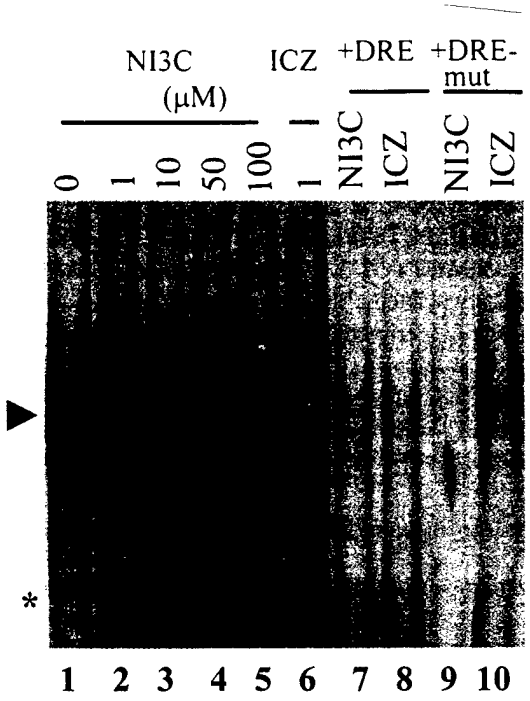

Figure 3. NI3C induces aryl hydrocarbon receptor (AhR)-dioxin-response element (DRE) complex formation. Nuclear extracts were prepared from Hepa-1c1c7 cells exposed to different concentrations of NI3C (0, 1, 10, 50, and 100 μM) and 1 μM ICZ and analyzed in a gel mobility assay. Lanes 1–5, cells treated with increasing amounts of NI3C; Lane 6, cells treated with 1 μM ICZ. Nuclear extracts of 100 μM NI3C- or 1 μM ICZ-treated cells incubated with 200-fold excess of unlabeled DRE are shown in Lanes 7 and 8, respectively; those treated with 200-fold excess of unlabeled mutant DRE (DRE-mut) are shown in Lanes 9 and 10, respectively. Arrowhead, position of AhR-DRE complex. *, Loading in Lanes 1, 9, and 10 is slightly lower than in other lanes.

AhR-responsive CAT reporter gene construct, M8 cells, with up to 100 μM NI3C (Figure 4). Cells treated with 0.1% DMSO or 1 μM ICZ were included as controls. The CAT activity was induced concentration dependently by NI3C, and

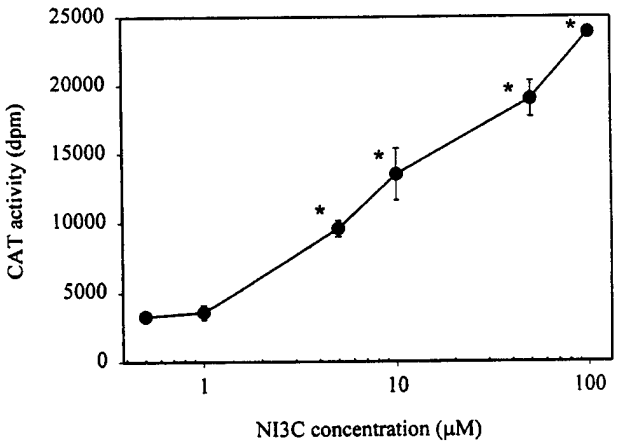

Figure 4. NI3C induces DRE-driven chloramphenicol acetyl transferase (CAT) reporter gene activity in Hepa-1c1c7 cells. Cultures of transfected Hepa-1c1c7 (M8) cells were exposed for 24 h to NI3C in indicated range of concentrations. Activity in DMSO-exposed cells was subtracted. CAT activity for positive control (1 μM ICZ) was 67,000 disintegrations/min (dpm). Values are means of 2 measurements ± ranges. *, Significantly different from 0.5 μM.

the activity induced by 100 μM NI3C was approximately 36% of the induction by the positive control. Inasmuch as the CAT reporter gene contains a single DRE, this experiment also suggests that the AhR is involved in the NI3C induction of *cyp* 1A1 expression. In studies of the transcriptional activation of CYP 1A1 by Northern analysis, we observed that CYP 1A1 mRNA was induced by 50 μM NI3C with a maximum CYP 1A1 mRNA level four to eight hours after the initiation of treatment with NI3C (Figure 5). Similar kinetics were observed for the EROD activity, which peaked at 8–12 hours with an activity level about fourfold that observed after 24 hours (results not shown). An induction peak of CYP 1A1 mRNA by DMSO and increased EROD activity were observed at four hours, but the explanation for this induction is unclear.

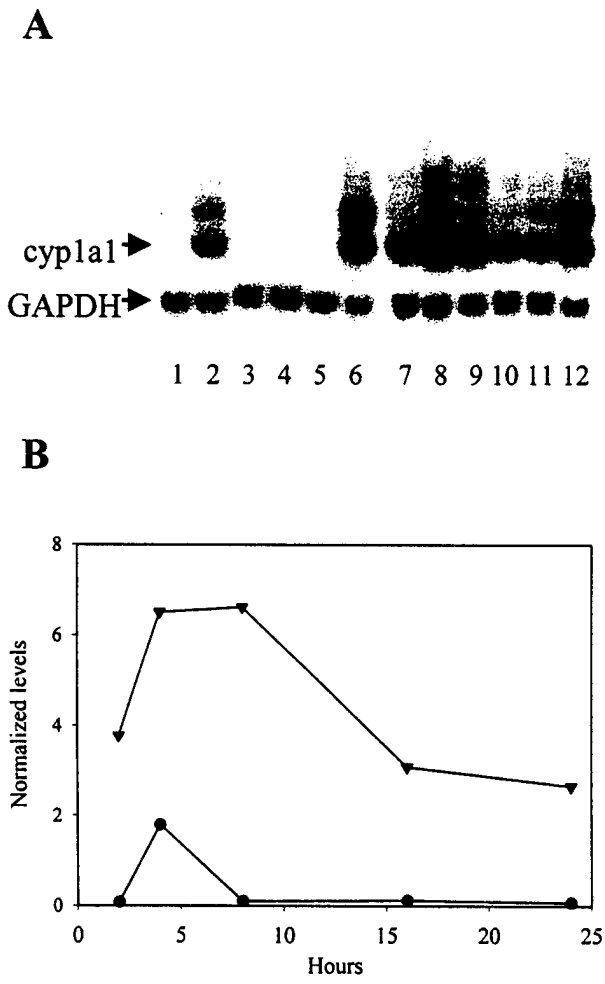

Figure 5. Induction of cytochrome *P*-450 (CYP) 1A1 mRNA in Hepa-1c1c7 cells by NI3C. Hepa-1c1c7 cells, exposed to 50 μM NI3C, were harvested at different time points (2–24 h), and total RNA was isolated. A: Northern blots. Lanes 1–5, 20 μg of RNA from DMSO-treated cells; Lanes 7–11, 20 μg of RNA from NI3C-treated cells; Lanes 6 and 12, 10 μg of RNA from cells exposed to 1 μM ICZ for 4 h as a control. Lanes 1 and 7, 2 h; Lanes 2 and 8, 4 h; Lanes 3 and 9, 8 h; Lanes 4 and 10, 16 h; Lanes 5 and 11, 24 h. B: quantitation of signals (DMSO, *filled circles*; NI3C, *filled inverted triangles*) obtained by PhosphorImager. CYP 1A1 signals are shown relative to glyceraldehyde 3-phosphate dehydrogenase (GAPDH) signals. Experiment was performed twice with identical results.

NI3C Is an Inhibitor of EROD Activity *In Vitro*

The relatively low level of EROD activity induced by NI3C compared with the induced CAT activity may be caused by a concomitant inhibition of the EROD activity by NI3C. Cotreatment of Hepa-1c1c7 cells with 1 nM TCDD, a highly potent inducer of EROD activity, and various concentrations of NI3C for 24 hours gave a concentration-dependent decrease in the EROD activity (Figure 6A). NI3C significantly inhibited TCDD-induced EROD activity at ≥10 μM NI3C with a concentration causing 50% inhibition (IC_{50}) of 58 μM. With use of a Hepa-1c1c7 microsomal system, NI3C significantly inhibited EROD activities at >3.3 μM in a concentration-dependent fashion (Figure 6B) with an IC_{50}

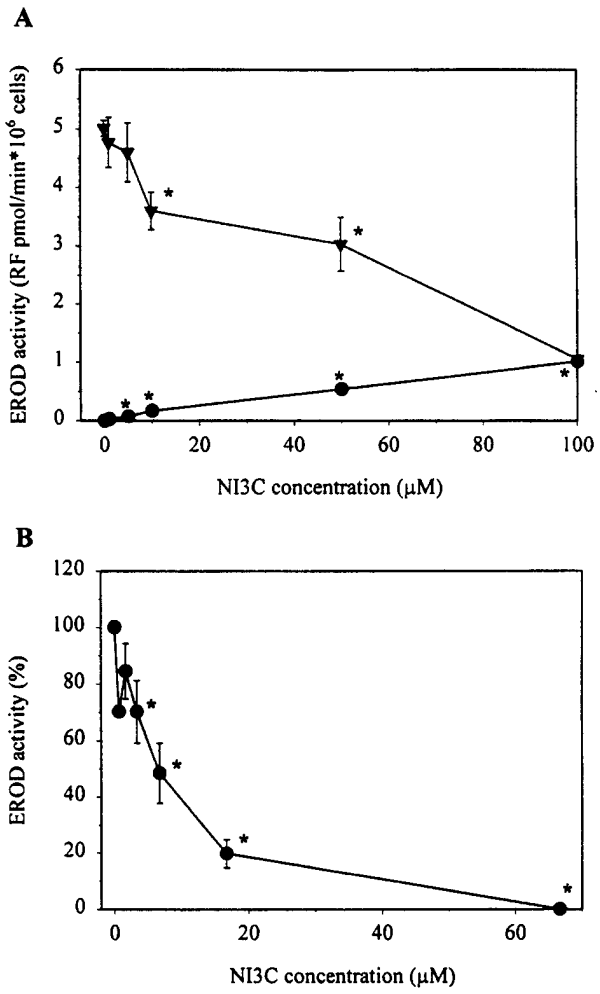

Figure 6. Inhibitory effect of NI3C. A: inhibition of 2,3,7,8-tetrachlorodibenzo-*p*-dioxin (TCDD)-induced EROD activity in intact cells by cotreatment with NI3C. Hepa-1c1c7 cells were exposed to various concentrations of NI3C alone (*filled circles*) or NI3C + 1 nM TCDD (*filled inverted triangles*) for 24 h, then EROD activity was determined. EROD activity in DMSO-treated cells was subtracted. Bars indicate mean values for 2 measurements ± range. *, Significantly different from controls (without NI3C). B: inhibition of microsomal EROD activity. Microsomes prepared from Hepa-1c1c7 cells exposed to 1 μM ICZ for 24 h were exposed to increasing concentrations of inhibitor, NI3C, added 5 min before determination of EROD activity. Values are means ± SEM of 3 separate experiments. *, Significantly different from control (without NI3C).

of 6 μM, indicating that, besides activation of the AhR, NI3C also inhibits the CYP 1A1 activity. The higher IC_{50} in the intact cells than in the microsomal system, particularly since the EROD activity is transient, may indicate a degradation of NI3C in the cells over time.

EROD Activities in Livers From Rats Exposed to NI3C or I3C for 8 or 24 Hours

To analyze the effect of NI3C *in vivo*, we exposed male Wistar rats orally to NI3C or I3C (570 μmol/kg body wt). The microsomal CYP 1A1 protein level was induced 60-fold by NI3C after eight hours, whereas I3C caused a 90-fold increase. The CYP 1A1 protein level was further increased to 135-fold induction 24 hours after administration of I3C, whereas the CYP 1A1 protein level had decreased to a 45-fold induction in animals treated with NI3C (Figure 7A). The EROD activity was induced 11-fold by NI3C, whereas I3C caused a 40-fold increase in the EROD activity at eight hours. The EROD activity decreased to sixfold induction by NI3C after 24 hours, whereas the inducing effect of I3C was almost the same after 24 hours as after 8 hours (Figure 8A). The induction of hepatic EROD by NI3C is consistent with the *in vitro* observation of EROD activity. NI3C significantly induced the expression of CYP 1A2 protein (9-fold) and 7-methoxyresorufin-*O*-demethylase (MROD) activity (3.5-fold) at 8 hours and MROD activity at 24 hours (4.5-fold) (Figures 7B and 8B). I3C enhanced the CYP 1A2 protein level and MROD activity at both time points to higher levels than NI3C. The CYP 1A2 protein level was induced 14- and 18-fold at 8 and 24 hours, respectively, by I3C, whereas the MROD activity was increased 10- and 18-fold after 8 and 24 hours, respectively. Neither the CYP 2B1/2 protein nor the 7-pentoxyresorufin- *O*-depentylase (PROD) activity was induced significantly by NI3C, whereas I3C enhanced the CYP 2B1/2 level by 3- to 6-fold and the PROD activity by 20-fold (Figures 7C and 8C) compared with control animals. There were no simple explanations why NI3C treatment reduced the level of CYP 2B1/2 protein, whereas the PROD activity was unchanged, and for the differences in the hepatic CYP 2B protein levels compared with PROD activity in rats treated with I3C. ASG is formed during the degradation of GB in the presence of ascorbic acid and is a potent inducer of CYP 1A1 in cultured cells (15), and ASG was tested in the same animal model. One single administration of ASG (570 μmol/ kg body wt po) only enhanced CYP 1A2 after 8 hours (3-fold) and CYP 1A1 after 24 hours (14-fold) but did not alter CYP 2B1/2 protein (Figures 7 and 8).

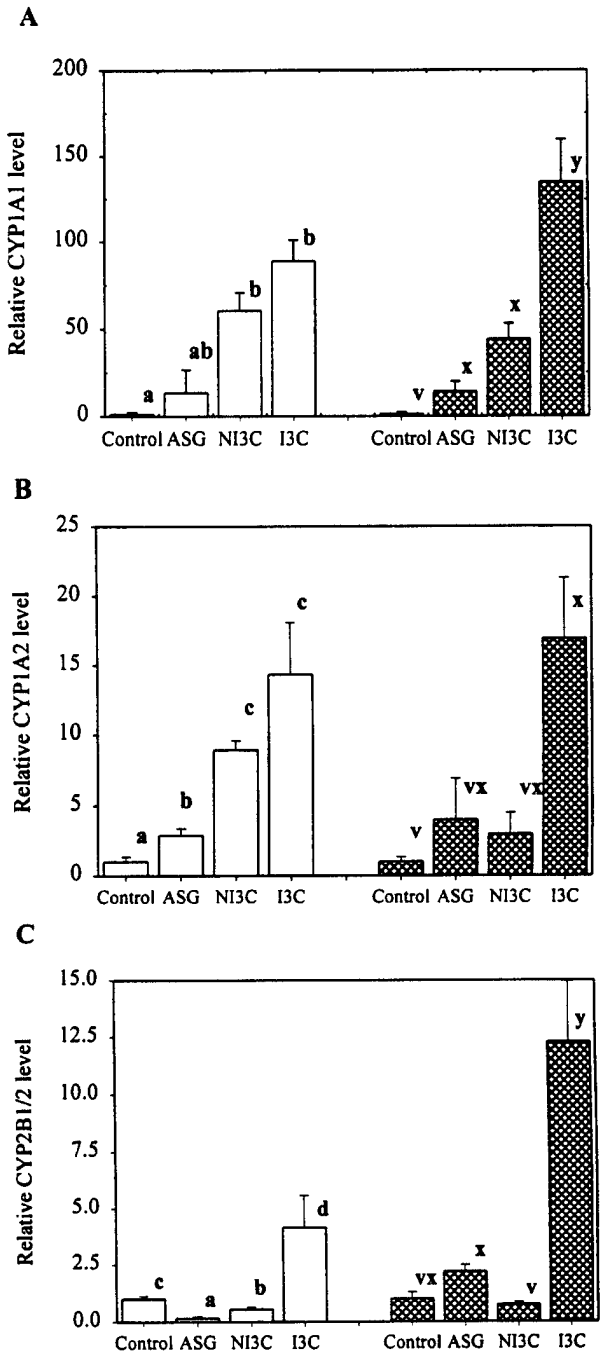

Figure 7. Hepatic CYP 1A1 (A), 1A2 (B), and 2B1/2 (C) levels in rats orally dosed with NI3C, I3C, or ascorbigen (ASG). Male Wistar rats, 4 in each group, were given 570 μmol of NI3C, I3C, or ASG orally in corn oil. Controls received corn oil. Groups of rats were killed at 8 and 24 h after dosage, and hepatic microsomes were isolated. Samples were analyzed by Western blotting. Bars show means ± SEM of each treatment after 8 (*open bars*) and 24 h (*cross-hatched bars*). Bars sharing different letters (a–d,v,x, y) at 1 time point are statistically significantly different at $p < 0.05$.

Discussion

The purpose of this study was to investigate the capacity of NI3C as a mediator of CYP 1A1 gene expression in animals and in cultured cells and, thereby, to assess its potential for regulating carcinogen metabolism. This is the first mechanistic study of the induction of *cyp* 1A1 by NI3C, whereas one previous study has investigated the effect of NI3C on EROD activity in rat liver (9), and our recent study describes induction of CYP 1A protein and EROD and MROD by the glucosinolate NeoGB (11).

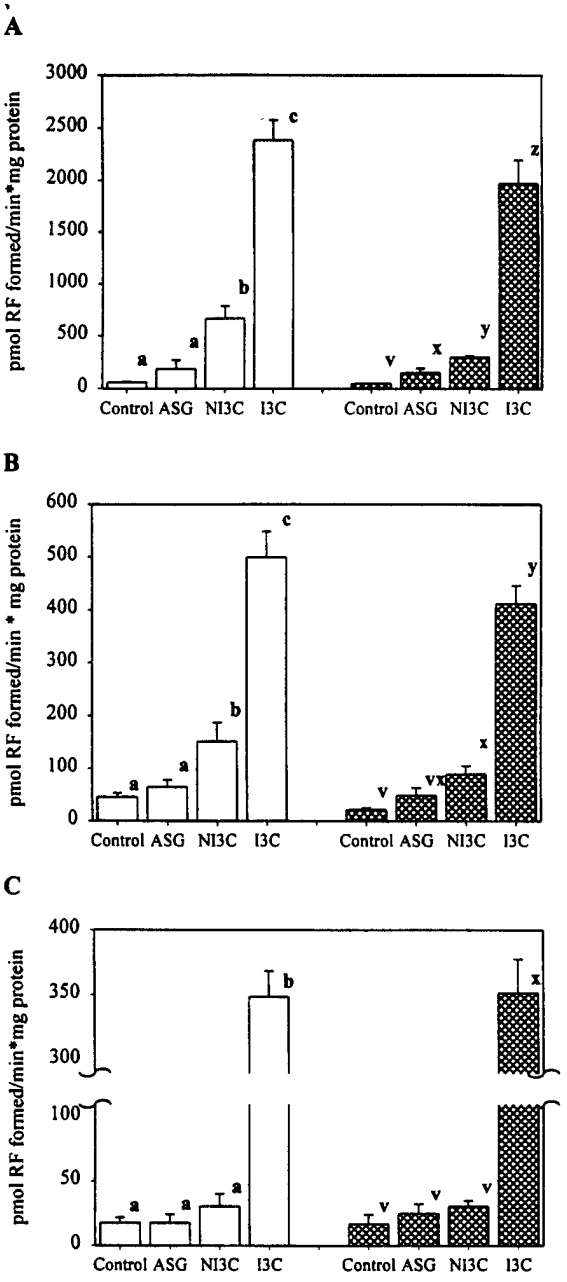

Figure 8. Hepatic EROD (A), 7-methoxyresorufin-*O*-demethylase (B), and 7-pentoxyresorufin-*O*-depentylase (C) activities in rats orally dosed with NI3C, I3C, and ASG. Male Wistar rats, 4 in each group, were given 570 μmol of NI3C, I3C, or ASG orally in corn oil. Controls received corn oil. Groups of rats were killed at 8 and 24 h after dosage, hepatic microsomes were isolated, and enzyme activities were determined. Bars show means ± SEM of each treatment after 8 (*open bars*) and 24 h (*cross-hatched bars*). Bars sharing different letters (a–c, v, x–z) at 1 time point are statistically significantly different at $p < 0.05$.

The expression of CYP 1A1 is generally considered to be regulated by the AhR pathway. Several results of this study indicated that this was the case for NI3C as well: 1) NI3C induced the AhR-DRE complex formation, 2) EROD activity was not induced by NI3C in the Arnt-deficient Hepa-1 mutant cell line B13, 3) NI3C induced CAT activity in cells stably transfected with a DRE-CAT reporter, and 4) CYP 1A1 mRNA was detected early after exposure of Hepa-1c1c7 cells to NI3C. NI3C does not have a structural similarity to the presently known indolylic AhR ligands, but a recent report has indicated that several types of AhR ligands exist (26). We therefore suggest that *N*-substitution with a methoxy group leads to a more potent inducer, as was observed in this study by comparison of *cyp* 1A1 inductions caused by NI3C and I3C.

Besides its EROD-inducing activity, NI3C also inhibited the EROD activity. A similar bifunctional activity has been observed for ICZ, I3C, and DIM (27). Various synthetic compounds (e.g., α-naphthoflavone) and naturally occurring compounds (e.g., flavonoids, coumarins, polyphenols) inhibit EROD activity. The inhibitory potency, expressed as IC_{50}, was 0.7–0.8 μM for the flavonoids, flavone, and tangeritine (28). The IC_{50} for NI3C is only 10-fold higher, indicating that this compound is a relatively strong inhibitor of EROD activity in cultured cells. NI3C is about three times more potent as an inhibitor of EROD activity than I3C, in comparison with results obtained in T47D cells by Chen and co-workers (10).

The induction of CYP 1A1 mRNA by NI3C and ICZ at their maximum response concentrations is in the same range, but a much lower induced EROD activity was observed after exposure to NI3C than to ICZ. The reason for this discrepancy is not clear, but the NI3C still present in the cells may have some inhibitory activity on EROD. It cannot be excluded from the present experiments that NI3C also may have an AhR antagonistic activity. However, it is not possible from the present experiments to elucidate whether NI3C causes competitive binding to the AhR besides inhibiting CYP 1A1 activity. AhR-binding experiments are needed to answer this question.

Our *in vivo* experiments clearly show that I3C is a more potent inducer than NI3C of hepatic CYP 1A1, 1A2, and 2B1/2 protein levels and their activities. This observation is in accordance with the response previously reported by Bradfield and Bjeldanes (9), who found that 31 μmol of I3C induced hepatic EROD activity 14-fold, whereas 31 μmol of NI3C caused only a 6-fold increase after 24 hours. Oral administrations of higher I3C concentrations, 500 μmol/kg body wt, caused a 36-fold increase in hepatic EROD activity and a 7-fold increase in PROD activity (29), which fit well with our present data. Recent data from our laboratory show that the inducing effect of pure NeoGB on rat hepatic CYP 1A protein and related enzyme activities is minor compared with that of pure GB (11). These data therefore support the results presented here. We suggest that the differences in inducing effects of NI3C and I3C *in vivo* may be explained by different stabilities of the compounds. The transformation products are believed to be responsible for the CYP 1A1-inducing effects of GB and I3C *in vivo*. Of the I3C products, only ICZ, DIM, and trimeric indoles have a significant binding affinity for the AhR (30). Small amounts of the potent CYP 1A1 inducer ICZ, as well as DIM (31), are formed from GB and I3C under acidic conditions, as in the stomach.

Similar transformation products formed from NI3C under acidic conditions are not well characterized. A dimer of NI3C, di(*N*-methoxyindole-3-yl)methane, was detected besides NI3C after myrosinase-catalyzed degradation of NeoGB at pH 5.6 in the absence of ascorbic acid (32). However, the formation of a compound analogous to ICZ formed from I3C has not been reported from NI3C. Furthermore, we recently found that acid treatment of NI3C leads to a lower yield of reaction products than the yield from I3C treated under similar reaction conditions (results not shown) in accordance with Agerbirk (33). This indicates that under acidic conditions, as in the stomach, less pronounced formation of the more potent oligomeric products would occur from NI3C than from I3C. The lower reactivity of NI3C than I3C may be caused by lower stability of the resonance-stabilized *N*-methoxyindole-3-ylmethyl carbonium ion because of the electron-withdrawing property of the *N*-methoxy group.

When the effects of NI3C and I3C in animals and in cultured cells are compared, it seems likely that the differences in chemical reactivity in the gastric juice may explain why NI3C is a more potent inducer in cultured cells but not a strong inducer in rat liver compared with I3C. NI3C and I3C are assumed to affect the CYP 1A1 activity in Hepa-1c1c7 cells without further transformation to other indole products. On the other hand, I3C will transform into more potent inducers *in vivo*, and it seems likely that NI3C will undergo similar transformations but at a slower rate, leading to less pronounced formation of more potent inducers.

Recently, we showed that ASG is more potent than I3C as an inducer of EROD activity in Hepa-1c1c7 cells (15). In the present animal model, a single dose of ASG (570 μmol/kg body wt po) had only small effects on the CYP 1A enzyme levels or their activities. McDanell and co-workers (13) found that about 500 μmol ASG/kg body wt/day for 5 days slightly decreased rat hepatic EROD activity compared with that in control animals. In the same study the intestinal EROD activity was increased by ASG. Sepkovic and colleagues (34) found that a diet containing 2,000 ppm ASG (500 μmol/kg body wt/day) enhances the 2- and 4-hydroxylation of estradiol and the 2-hydroxylation of estrone in rats, all activities partly related to CYP 1A enzymes. The effect of ASG was comparable to that of I3C. Compared with the present study and the work of McDanell and associates (13), the different responses obtained by Sepkovic and colleagues may be caused by different gender, strain, longer time of exposure, and induction of CYP enzymes other than CYP 1A and 2B. Recent data from our laboratory showed that although ASG induced CYP 1A1 activities in cultured cells, it also inhibited microsomal EROD activities (15). It is not known why ASG is not an inducer of rat hepatic CYP 1A1, inasmuch as ICZ is formed from ASG in stomach juice *in vitro* (35).

In conclusion, our results show that NI3C is more efficient as a CYP 1A1 inducer than I3C in cultured cells, whereas I3C is a much stronger inducer in rodents *in vivo*. Therefore, NI3C seems to play a minor role in the regulation of CYP 1A and 2B metabolism of xenobiotics *in vivo* compared with I3C. However, the present results from cultured cells indicate that NI3C may be a more potent inhibitor of CYP 1A enzymes than I3C, and preliminary results indicate that NI3C may modulate other chemopreventive biomarkers, i.e., inhibition of cell proliferation in cultured cells (unpublished results). ASG, which previously was shown to be an inducer in cultured cells, is only a weak inducer of CYP 1A protein *in vivo*.

Acknowledgments and Notes

P. U. Stephensen and C. Bonnesen contributed equally to the present study. The authors thank A. Maarup and G. Clausing for technical assistance. This work was supported by the Danish Cancer Society (P. U. Stephensen), the Wedell-Wedellsborg Foundation (C. Bonnesen and P. U. Stephensen), US Department of Defense, Army Breast Cancer Research Program Grant DAMD 17-96-1-6149, and National Cancer Institute Grant CA-69056 (L. F. Bjeldanes). Address reprint requests to Ole Vang, Dept. of Life Sciences and Chemistry, Roskilde University, Universitetsvej 1, Bld 18-2, PO Box 260, DK-4000 Roskilde, Denmark.

Submitted 15 March 1999; accepted in final form 30 August 1999.

References

1. Vang, O, Jensen, H, and Autrup, H: Induction of cytochrome *P*-450 IA1, IA2, IIB1, IIB2 and IIE1 by broccoli in rat liver and colon. *Chem Biol Interact* **78,** 85–96, 1991.
2. Kall, MA, Vang, O, and Clausen, J: Effects of dietary broccoli on human *in vivo* drug metabolizing enzymes: evaluation of caffeine, oestrone and chlorzoxazone metabolism. *Carcinogenesis* **17,** 793–799, 1996.
3. Steinmetz, KA, and Potter, JD: Vegetables, fruit, and cancer prevention: a review. *J Am Diet Assoc* **96,** 1027–1039, 1996.
4. *WCRF/AICR, Food, Nutrition and Prevention of Cancer: a Global Perspective.* Washington, DC: World Cancer Research Fund/Am Inst Cancer Res, 1997.
5. Sørensen, H: Glucosinolates: structure-properties-function. In *Canola and Rapeseed. Production, Chemistry, Nutrition and Processing Technology,* F Shahidi (ed). New York: Van Nostrand Reinhold, 1990, pp 149–172.
6. Tanaka, T, Kojima, T, Morishita, Y, and Mori, H: Inhibitory effects of the natural products indole-3-carbinol and sinigrin during initiation and promotion phases of 4-nitroquinoline 1-oxide-induced rat tongue carcinogenesis. *Jpn J Cancer Res* **83,** 835–842, 1992.
7. Zhang, Y, Kensler, TW, Cho, CG, Posner, GH, and Talalay, P: Anticarcinogenic activities of sulforaphane and structurally related synthetic norbornyl isothiocyanates. *Proc Natl Acad Sci USA* **91,** 3147–3150, 1994.
8. Nishikawa, A, Furukawa, F, Uneyama, C, Ikezaki, S, Tanakamaru, Z, et al.: Chemopreventive effects of phenethyl isothiocyanate on lung and pancreatic tumorigenesis in *N*-nitrosobis(2-oxopropyl)amine-treated hamsters. *Carcinogenesis* **17,** 1381–1384, 1996.
9. Bradfield, CA, and Bjeldanes, LF: Structure-activity relationships of dietary indoles: a proposed mechanism of action as modifiers of xenobiotic metabolism. *J Toxicol Environ Health* **21,** 311–323, 1987.
10. Chen, I, Safe, S, and Bjeldanes, L: Indole-3-carbinol and diindolylmethane as aryl hydrocarbon (Ah) receptor agonists and antagonists in T47D human breast cancer cells. *Biochem Pharmacol* **51,** 1069–1076, 1996.
11. Bonnesen, C, Stephensen, PU, Andersen, O, Sørensen, H, and Vang, O: Modulation of cytochrome *P*-450 and glutathione *S*-transferase

isoform expression *in vivo* by intact and degraded indolyl glucosinolates. *Nutr Cancer* **33,** 178–187, 1999.

12. Bradfield, CA, and Bjeldanes, LF: Dietary modification of xenobiotic metabolism: contribution of indolylic compounds present in *Brassica oleracea*. *J Agric Food Chem* **35,** 896–900, 1987.
13. McDanell, R, McLean, AE, Hanley, AB, Heaney, RK, and Fenwick, GR: Differential induction of mixed-function oxidase (MFO) activity in rat liver and intestine by diets containing processed cabbage: correlation with cabbage levels of glucosinolates and glucosinolate hydrolysis products. *Food Chem Toxicol* **25,** 363–368, 1987.
14. Kiss, G, and Neukom, H: Formation of an ascorbigen-like product from *p*-hydroxybenzyl alcohol and L-ascorbic acid. *Experientia* **24,** 326, 1968.
15. Stephensen, PU, Bonnesen, C, Bjeldanes, LF, and Vang, O: Modulation of cytochrome P450 1A1 activity by ascorbigen in murine hepatoma cells. *Biochem Pharmacol* **58,** 1145–1153, 1999.
16. Acheson, RM, Hunt, PG, Littelwood, DM, Murrer, BA, and Rosenberg, HE: The synthesis, reactions, and spectra of 1-acethoxy-, 1-hydroxy-, and 1-methoxy-indoles. *J Chem Soc Perkin Trans I* **10,** 1117–1125, 1978.
17. Acheson, RM, Aldridge, GN, Choi, MCK, Nwanko, JO, Ruscoe, MA, et al.: An improved preparation of 1-hydroxyindole and the synthesis of some related 3-carboxylic acids and 1-methoxyindole-3-acetonitrile. *J Chem Res* **4,** 1301–1319, 1984.
18. Leete, E: 3-Hydroxymethylindoles. *J Am Chem Soc* **81,** 6023–6026, 1959.
19. Hanley, AB, and Parsley, KR: Identification of 1-methoxyindol-3-methyl isothiocyanate as an indole glucosinolate breakdown product. *Phytochemistry* **29,** 769–771, 1990.
20. Fisher, JM, Wu, L, Denison, MS, and Whitlock, JPJ: Organization and function of a dioxin-responsive enhancer. *J Biol Chem* **265,** 9676–9681, 1990.
21. Seed, B, and Sheen, J: A simple phase-extraction assay for chloramphenicol acetyltransferase activity. *Gene* **67,** 271–277, 1988.
22. Denison, MS, Fisher, JM, and Whitlock, JP: Inducible, receptor-dependent protein-DNA interactions at a dioxin-responsive transcriptional enhancer. *Proc Natl Acad Sci USA* **85,** 2528–2532, 1988.
23. Denison, MS, Fisher, JM, and Whitlock, JP: The DNA recognition site for the dioxin-Ah receptor complex nucleotide sequence and functional analysis. *J Biol Chem* **263,** 17221–17224, 1988.
24. Yao, EF, and Denison, MS: DNA sequence determinants for binding of transformed Ah receptor to a dioxin-responsive enhancer. *Biochemistry* **31,** 5060–5067, 1992.
25. Vang, O, Rasmussen, BF, Sørensen, H, Clausen, J, and Andersen, O: The effect of dietary broccoli on oxidative stress biomarkers. *Clin Chem* **41,** 1910–1911, 1995.
26. Heath-Pagliuso, S, Rogers, WJ, Tullis, K, Seidel, SD, Cenijn, PH, et al.: Activation of the Ah receptor by tryptophan and tryptophan metabolites. *Biochemistry* **37,** 11508–11515, 1998.
27. Chen, YH, Riby, J, Srivastava, P, Bartholomew, J, Denison, M, et al.: Regulation of CYP 1A1 by indolo[3,2-*b*]carbazole in murine hepatoma cells. *J Biol Chem* **270,** 22548–22555, 1995.
28. Obermeier, MT, White, RE, and Yang, CS: Effects of bioflavonoids on hepatic P450 activities. *Xenobiotica* **25,** 575–584, 1995.
29. Park, JY, and Bjeldanes, LF: Organ-selective induction of cytochrome *P*-450-dependent activities by indole-3-carbinol-derived products: influence on covalent binding of benzo[*a*]pyrene to hepatic and pulmonary DNA in the rat. *Chem Biol Interact* **83,** 235–247, 1992.
30. Bjeldanes, LF, Kim, JY, Grose, KR, Bartholomew, JC, and Bradfield, CA: Aromatic hydrocarbon responsiveness-receptor agonists generated from indole-3-carbinol *in vitro* and *in vivo*: comparisons with 2,3,7,8-tetrachlorodibenzo-*p*-dioxin. *Proc Natl Acad Sci USA* **88,** 9543–9547, 1991.
31. Bradfield, CA, and Bjeldanes, LF: Modification of carcinogen metabolism by indolylic autolysis products of *Brassica oleraceae*. *Adv Exp Med Biol* **289,** 153–163, 1991.
32. Agerbirk, N, Olsen, CE, and Sørensen, H: Initial and final products, nitriles, and ascorbigens produced in myrosinase-catalyzed hydrolysis of indole glucosinolates. *J Agric Food Chem* **46,** 1563–1571, 1998.
33. Agerbirk, N: *Products of the Myrosinase Catalyzed Hydrolysis of Glucosinolates in Rape and* Brassica *Vegetables* (thesis). Copenhagen: Chemistry Department, Royal Veterinary and Agricultural University, 1997.
34. Sepkovic, DW, Bradlow, HL, Michnovicz, J, Murtezani, S, Levy, J, et al.: Catechol estrogen production in rat microsomes after treatment with indole-3-carbinol, ascorbigen, or β-naphthoflavone: a comparison of stable isotope dilution gas chromatography-mass spectrometry and radiometric methods. *Steroids* **59,** 318–323, 1994.
35. Preobrazhenskaya, MN, Korolev, AM, Lazhko, EI, Aleksandrova, LG, Bergman, J, et al.: Ascorbigen as a precursor of 5,11-dihydroindolo[3,2-*b*]carbazole. *Food Chem* **48,** 57–62, 1993.

Biochemical Pharmacology, Vol. 60, pp. 167–177, 2000.

ISSN 0006-2952/00/$–see front
PII S0006-2952(00)00307-5

Ligand-Independent Activation of Estrogen Receptor Function by 3,3′-Diindolylmethane in Human Breast Cancer Cells

Jacques E. Riby, Grace H. F. Chang,* Gary L. Firestone† and Leonard F. Bjeldanes*‡*

*Division of Nutritional Sciences and Toxicology, and †Department of Molecular and Cell Biology, University of California, Berkeley, CA 94720, U.S.A.

ABSTRACT. 3,3′-Diindolylmethane (DIM), a major *in vivo* product of acid-catalyzed oligomerization of indole-3-carbinol (I3C), is a promising anticancer agent present in vegetables of the *Brassica* genus. We investigated the effects of DIM on estrogen-regulated events in human breast cancer cells and found that DIM was a promoter-specific activator of estrogen receptor (ER) function in the absence of 17β-estradiol (E_2). DIM weakly inhibited the E_2-induced proliferation of ER-containing MCF-7 cells and induced proliferation of these cells in the absence of steroid, by approximately 60% of the E_2 response. DIM had little effect on proliferation of ER-deficient MDA-MB-231 cells, suggesting that it is not generally toxic at these concentrations. Although DIM did not bind to the ER in this concentration range, as shown by a competitive ER binding assay, it activated the ER to a DNA-binding species. DIM increased the level of transcripts for the endogenous pS2 gene and activated the estrogen-responsive pERE-vit-CAT and pS2-tk-CAT reporter plasmids in transiently transfected MCF-7 cells. In contrast, DIM failed to activate transcription of the simple E_2- and diethylstilbesterol-responsive reporter construct pATC2. The estrogen antagonist ICI 182780 (7α-[9-[(4,4,5,5,5-pentafluoropentyl)sulfonyl-]nonyl]-estra-1,3,5(10)-triene-3,17β-diol) was effective against DIM-induced transcriptional activity of the pERE-vit-CAT reporter, which further supports the hypothesis that DIM is acting through the ER. We demonstrated that ligand-independent activation of the ER in MCF-7 cells could be produced following treatment with the D1 dopamine receptor agonist SKF-82958 [(±)6-chloro-7,8-dihydroxy-3-allyl-1-phenyl-2,3,4,5-tetrahydro-1H-3-benzazepinehydrobromide]. We also demonstrated that the agonist effects of SKF-82958 and DIM, but not of E_2, could be blocked by co-treatment with the protein kinase A (PKA) inhibitor H-89 (*N*-[2-(*p*-bromocinnamylamino)ethyl]-5-isoquinolinesulfonamide). These results have uncovered a promoter-specific, ligand-independent activation of ER signaling for DIM that may require activation by PKA, and suggest that this major I3C product may be a selective activator of ER function. BIOCHEM PHARMACOL **60**;2: 167–177, 2000. © 2000 Elsevier Science Inc.

KEY WORDS. estrogen receptor; agonist; breast cancer; diindolylmethane; ligand independent

I3C§ (Fig. 1), a hydrolysis product of glucobrassicin found in *Brassica* plants, including turnips, kale, broccoli, Brussels sprouts, and cauliflower, is a potential cancer protective agent. Oral administration of I3C reduced BP-induced neoplasia of the forestomach and total covalent binding of BP and *N*-nitrosodimethylamine to hepatic DNA in mice [1–3]. In trout, oral I3C reduced aflatoxin B1-induced hepatocarcinogenesis when administered prior to and during carcinogen treatment [4]. Similarly, in rodents, oral I3C reduced DMBA-induced mammary tumor incidence by 70–80% [1, 5], and reduced by 50% the incidence and multiplicity of spontaneous mammary tumors [6]. In a screen of 90 potential chemopreventive agents in a series of six short-term bioassays relevant to initiation and post-initiation phases of carcinogenesis, I3C was found to be one of only eight compounds that tested positive in all assays [7]. Some evidence suggests, however, that whereas I3C mitigates mammary carcinogenesis, it may also enhance tumorigenesis in other organs under certain conditions. Thus, oral administration of high doses of I3C to rodents or trout following exposure to certain organ-selective carcinogens resulted in increased tumor incidence of the liver [8],

‡ Corresponding author: Dr. Leonard F. Bjeldanes, Division of Nutritional Sciences and Toxicology, 119 Morgan Hall, University of California, Berkeley, CA 94720. Tel. (510) 642-1601; FAX (510) 642-0535; E-mail: lfb@nature.berkeley.edu

§ *Abbreviations*: AhR, aryl hydrocarbon receptor; BP, benzo[*a*]pyrene; CAT, chloramphenicol acetyltransferase; CDK, cyclin-dependent kinase; CYP, cytochrome P450; DES, diethylstilbesterol; DIM, 3,3′-diindolylmethane; DMBA, dimethylbenzanthracene; DMEM, Dulbecco's modified Eagle's medium; DTT, dithiothreitol; E_2, 17β-estradiol; ER, estrogen receptor; ERE, estrogen response element; EROD, ethoxyresorufin O-deethylase; FBS, fetal bovine serum; GAPDH, glyceraldehyde phosphate dehydrogenase; I3C, indole-3-carbinol; ICZ, indolo[3,2-*b*]carbazole; and PKA, protein kinase A.

Received 8 September 1999; accepted 29 November 1999.

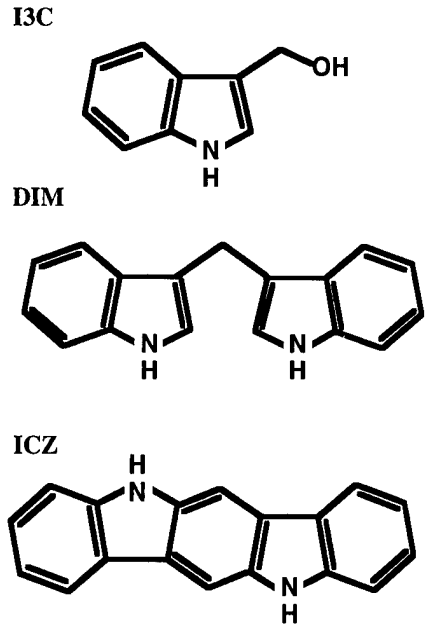

FIG. 1. Molecular structures of I3C, DIM, and ICZ.

colon [9], or thyroid gland [10]. These findings emphasize the importance of determining the mechanism of action of I3C before it is used in long-term cancer prophylaxis.

In a detailed analysis of the effects of I3C on cell proliferation and on components of the cell cycle regulation pathway, we showed that at high concentration, I3C produced a nearly complete but reversible G_1 cell cycle arrest in a manner that did not affect cell viability [11]. This arrest was accompanied by a selective repression of CDK6 expression, an inhibition of phosphorylation of retinoblastoma protein, and an increased expression of the CDK inhibitor proteins p21 and p27. Importantly, these effects were independent of the ER, since they also could be produced in an ER-deficient breast cancer cell line. These results suggest that I3C itself is not the cause of the antiestrogenic and tumor-promoting effects of orally administered I3C.

Of central importance to the *in vivo* biological activity of I3C is its facile conversion to other products on contact with acid. We have shown that the I3C induction of cytochrome P450 activity, and possibly other responses as well, is dependent on the route of administration. Whereas I3C fails to induce cytochrome P450 when administered by intraperitoneal injection into rats, thus bypassing contact with gastric acids, it is an active enzyme inducer when administered by oral intubation [12]. Acid treatment of I3C produces a mixture that is active by either route of administration. Analyses of this reaction mixture have indicated the presence of many minor oligomeric I3C products including ICZ, and several major products including DIM [13]; these products are also produced in the gastrointestinal tracts of rodents following oral treatment with I3C [14, 15].

ICZ is a planar pentacyclic compound (Fig. 1) that, in contrast to I3C, binds with high affinity to the AhR and is both a potent (but transient) inducer of AhR-regulated CYP1A1 expression and an inhibitor of CYP1A1-dependent enzyme activity [16]. Since the persistent activation of AhR-dependent pathways is thought to be responsible for the tumor-promoting effects of ligands such as 2,3,7,8-tetrachlorodibenzo-*p*-dioxin (TCDD) [17], conversion of I3C to ICZ and other potent AhR ligands may contribute to the adverse chronic effects resulting from high doses of I3C. DIM inhibits carcinogen-induced mammary tumor formation in rats [1] and weakly induces hepatic CYP1A enzymes *in vivo* [5, 18]. DIM is a weak ligand for the AhR, an antagonist of AhR-mediated gene transcription [19], and an inhibitor of CYP1A1 enzyme activity [20], suggesting that activation of AhR-dependent pathways may not be important in the protective effects of DIM against mammary cancer.

In the present study, we investigated, in human breast cancer cell lines, the interactions of DIM with E_2-regulated biological events including cell proliferation, binding affinity to the ER, and transcriptional expression of an endogenous gene and of transiently transfected reporter genes. We demonstrated that DIM acts as an agonist of E_2 function. DIM antagonized weakly the effects of E_2 on cell proliferation and transcriptional activation of a reporter gene, and DIM activated these responses in the absence of E_2. Although DIM did not bind to the ER, it produced a clear concentration-related activation of the ER to a DNA-binding species. We showed that the effects of DIM on ER-dependent transcription are promoter specific and may result from a PKA-related mechanism of ER activation.

MATERIALS AND METHODS

Materials

DMEM, Opti-MEM, and Lipofectamine were supplied by Gibco/BRL. Phenol red-free DMEM, FBS, calf serum, tamoxifen, and E_2 were supplied by the Sigma Chemical Co. ICI 182780 (7α- [9-[(4,4,5,5,5-pentafluoropentyl]sulfonyl]nonyl]-estra-1,3,5 [10]-triene-3,17β-diol) was supplied by Tocris. [γ-^{32}P]ATP and [^{3}H]acetyl-CoA were supplied by New England Nuclear. SKF-82958 [(±)6-chloro-7,8-dihydroxy-3-allyl-1-phenyl-2,3,4,5-tetrahydro-1*H*-3-benzazepinehydrobromide] was purchased from RBI, and H-89 (*N*-[2-(*p*-bromocinnamylamino)ethyl]-5-isoquinolinesulfonamide) was obtained from LC Laboratories. DIM was prepared from I3C as described [12–14] and recrystallized in toluene. All other reagents were of the highest grade available.

Cell Culture

The human breast adenocarcinoma cell lines MCF-7 and MDA-MB-231, obtained from the American Type Culture Collection, were grown as adherent monolayers in DMEM, supplemented to 4.0 g/L of glucose and 3.7 g/L of sodium bicarbonate, in a humidified incubator at 37° and 5% CO_2,

and passaged at approximately 80% confluence. Cultures used in subsequent experiments were at less than 25 passages.

Cell Proliferation

Before the beginning of the treatments, cells were depleted of estrogen for 7–10 days in medium composed of DMEM base without phenol red (Sigma), with 4 g/L of glucose, 3.7 g/L of sodium bicarbonate, and 5% calf serum twice stripped in dextran-coated charcoal and microfiltered, supplemented with non-essential amino acids (Gibco), 2 mM glutamine, and 10 ng/mL of insulin. During the depletion period, medium was changed every other day. Treatments were administered by the addition of 1 μL of 1000x solution in DMSO/mL of medium. Once the treatment period started, medium was changed daily to counter possible loss of readily metabolized compounds.

Cell Counting

Cells were harvested by trypsinization and resuspended in complete medium. Aliquots were diluted 50-fold in Isoton II (Coulter Corp.), and 500-μL duplicates were counted in a model Z1 Coulter particle counter and averaged.

ER Binding Assay

Rat uterine cytosol was prepared as described previously [21]. Briefly, 2.5 g of uterine tissue from five Sprague–Dawley rats (12 weeks old) was excised and placed on ice. The fresh tissue was homogenized with 30 mL of ice-cold TEDG buffer (10 mM Tris, pH 7.4, 1.5 mM EDTA, 1 mM DTT, 10% glycerol) using a Polytron apparatus at medium speed for 1 min on ice. The homogenate was centrifuged at 1000 *g* for 10 min at 4°. The supernatant solution was transferred to ultracentrifuge tubes and centrifuged at 100,000 *g* for 90 min at 4°. The supernatant solution was divided into 1.0-mL aliquots, quickly frozen in a dry-ice/ethanol bath, and stored at −80°. Protein concentration of the uterine cytosol was 3 mg/mL, as measured by the Bradford assay using BSA as the standard. For each competitive binding assay, 5 μL of 20 nM [^{3}H]E_2 in 50% ethanol, 10 mM Tris, pH 7.5, 10% glycerol, 1 mg/mL of BSA, and 1 mM DTT was placed in a 1.5-mL microcentrifuge tube. Competitive ligands were added as 1.0 μL of 100x solution in DMSO. After mixing, 95 μL of uterine cytosol was added, and the solutions were vortexed and incubated at room temperature for 2–3 hr. Proteins were precipitated by the addition of 100 μL of 50% hydroxylapatite slurry equilibrated in TE (50 mM Tris, pH 7.4, 1 mM EDTA) and incubated on ice for 15 min with vortexing every 5 min to resuspend hydroxylapatite. The pellet was washed with 1.0 mL of ice-cold wash buffer (40 mM Tris, pH 7.4, 100 mM KCl), and centrifuged for 5 min at 10,000 *g* at 4°. The supernatant was aspirated carefully, and the pellet was washed two more times with 1.0 mL of wash buffer. The final pellet was resuspended in 200 μL ethanol and transferred to a scintillation vial. The tube was washed with another 200 μL ethanol, which then was added to the same counting vial. A negative control contained no uterine cytosol. Nonspecific binding was determined using 100-fold (0.1 μM) excess unlabeled E_2. Relative binding affinities were calculated using the concentration of competitor needed to reduce [^{3}H]E_2 binding by 50% as compared with the concentration of unlabeled E_2 needed to achieve the same result.

CYP1A1 Activity

CYP1A1 activity was measured by the EROD assay as described previously [16]. Briefly, after the 18- to 24-hr treatment of near-confluent (80%) cultures in 60-mm diameter dishes, cells were trypsinized and resuspended in 5 mL PBS. The cells and the substrate solution were preincubated at 37°. An aliquot of the cell suspension was counted to obtain the cell number, and 1.5 mL of the cell suspension was placed into a fluorometer cuvette, followed by the addition of 0.5 mL of 2.5 μM ethoxyresorufin (Sigma). The reaction mixture was mixed by inversion of the cuvette, and the fluorescence produced was recorded at the excitation wavelength of 510 nm and the emission wavelength of 586 nm with a 20-nm slit width using a Perkin-Elmer 650–10S spectrofluorometer at a calibrated chart speed. A standard curve was obtained using different amounts (0, 2.5, 5, 7.5, and 10 pmol) of resorufin (Sigma) added to the control cells in a total volume of 2.0 mL. The enzyme activity was presented as picomoles resorufin produced per minute per million cells.

Plasmid Reporters and Expression Vectors

The ER-responsive CAT reporter plasmids pERE-vit-CAT and pATC2 [22] were gifts from D. J. Shapiro (University of Illinois). pERE-vit-CAT contains the 5′-flanking and promoter region (−596 to 21) of the *Xenopus* vitellogenin-B1 gene, including two imperfect endogenous EREs (at −302 and −334) and an exogenous consensus ERE (GGT CACAGTGACC) inserted at position −359. The simpler reporter pATC2 contains two copies of the consensus ERE coupled 38 bp from the TATA box of the vitellogenin-B1 promoter (−42 to 14). The reporter plasmid pS2-tk-CAT, containing the promoter and flanking region (−1100 to 10) of the human pS2 gene [23], was obtained from P. Chambon (University of Strasbourg). The plasmid pCMV-hER, constitutively expressing a fully functional human ER [24], was a gift from B. S. Katzenellenbogen (University of Illinois). The transfection efficiency control vector, pCMVβ, constitutively expressing β-galactosidase, was obtained from the American Type Culture Collection.

Transient Transfections with Reporters

Transfections were performed by the lipofection method using Lipofectamine (Gibco). Cells were grown in 10% FBS–DMEM to sub-confluence and transferred to 6.0-cm Petri plates 24 hr before transfection. The plates were seeded with the appropriate number of cells to become 50–60% confluent at the time of transfection. For each 6-mm plate, 8 μL of Lipofectamine was diluted with 92 μL of Opti-MEM serum-free medium (Gibco). Plasmid DNA (0.1 to 1.0 μg) was diluted in 100 μL of serum-free medium. Lipid and plasmid dilutions were combined, mixed gently, and incubated at room temperature for 30–45 min. Meanwhile, the cells were washed with 4 mL of serum-free medium, and 2 mL of serum-free medium was added to each plate. Next, 200 μL of the lipid–DNA suspension was added to each plate and mixed gently. The plates were returned to the incubator for 5–6 hr, and 2 mL of medium containing 10% calf serum was added. The next day, the cells were refed with fresh depleted medium without phenol red (5% dextran-coated charcoal-stripped FBS), and the 48-hr treatments were started by the addition of 1 μL of 1000x solutions in DMSO/mL of medium. The transfection efficiency was determined using the constitutive galactosidase expression plasmid CMVβ in an identical set of plates and was found to be unaffected by the treatments.

CAT Assay

The CAT assay was performed using a modification of the phase extraction assay described by Seed and Sheen [25]. At the end of the 48-hr treatment period, the transfected cells were harvested by scraping with a rubber policeman, transferred with the medium to a conical 15-mL tube, centrifuged at 600 *g* for 2 min, resuspended in 1 mL of cold PBS, transferred to Eppendorf tubes, centrifuged at 600 *g* for 2 min, and washed in PBS a second time. Cell pellets were resuspended in 200 μL of 0.1 M Tris, pH 8.0, and lysed by three cycles of freeze/thaw treatment (alternating 5 min in a dry-ice/alcohol bath and 5 min in a 37° bath). Cell lysates were incubated at 65° for 15 min to inactivate acylases and centrifuged at 14,000 *g* for 8 min. A 165-μL aliquot of the cytosol was transferred to a 7-mL scintillation vial, and a 20-μL aliquot was reserved for determination of protein concentration by the Bradford assay. The substrate mixture (85 μL) was added to the scintillation vial to obtain final concentrations of 100 mM Tris–HCl, pH 8.0, 250 nmol chloramphenicol, 1 μCi [^{3}H]acetyl-CoA (200 mCi/mmol) in a total volume of 250 μL and mixed thoroughly. The organic scintillation fluid (4 mL) was added slowly to avoid mixing with the aqueous phase, and the vials were incubated at 37° for 1–2 hr or until sufficient counts were obtained.

RNA Extraction and Northern Blot Analysis

Cells were lysed by the addition of Tri-reagent (Molecular Research Center, Inc.), and chloroform was used for phase separation. After centrifugation, the aqueous upper phase was collected, and total RNA was precipitated by isopropanol, washed with 75% ethanol, and dissolved in diethylpyrocarbonate-treated water. Total RNA was electrophoresed on a 1.2% agarose gel containing 3% formaldehyde, using MOPS as the running buffer. The gel was washed gently with 10x SSC (sodium chloride/sodium citrate (buffer); 20x SSC: 3 M NaCl, 0.3 M sodium citrate, pH 7.0) and blotted with a Zeta nylon membrane (Bio-Rad) overnight to transfer the RNA onto the membrane. The RNA was fixed to the membrane by UV cross-linking. The hybridization probes were labeled with ^{32}P using random primers and the pS2-cDNA and GADPH-cDNA plasmids provided by the American Type Culture Collection as the template. Hybridization and quantitation of results were performed as described previously [16]. Specific pS2 mRNA levels were normalized using GADPH as a standard.

Nuclear Extracts

Three near-confluent (80–90%) cultures of MCF-7 cells in 100-mm Petri dishes were used for each treatment. DIM or E_2 was added as 1 μL of 1000x solution in DMSO/mL of medium. After 2 hr of incubation at 37°, the plates were placed on ice, washed twice with 5 mL of hypotonic buffer (10 mM HEPES, pH 7.5), and incubated with 2 mL of HEPES for 15 min. Cells were harvested in 1 mL of MDH buffer (3 mM $MgCl_2$, 1 mM DTT, 25 mM HEPES, pH 7.5) with a rubber scraper, homogenized with a loose-fitting Teflon pestle, and centrifuged at 1000 *g* for 4 min at 4°. The pellets were washed twice with 3 mL of MDHK buffer (3 mM $MgCl_2$, 1 mM DTT, 0.1 M KCl, 25 mM HEPES, pH 7.5), resuspended in 1 mL of MDHK, and centrifuged at 600 *g* for 4 min at 4° in a microcentrifuge. The pellets were resuspended in 100 μL of HDK buffer (25 mM HEPES, pH 7.5, 1 mM DTT, 0.4 M KCl), incubated for 20 min on ice with mixing every 5 min, and centrifuged at 14,000 *g* for 4 min at 4°. Glycerol was added to the supernatants to a concentration of 10%, and aliquots of the nuclear extracts were stored at −80°.

Gel Mobility Shift Assay

The following two complementary 31-mer oligonucleotides:

5′-GATCCCAGGTCACAGTGACCTGAGCTAAAAT-3′ and 5′-GATCATTTTAGCTCAGGTCACTGTGACCTGG-3′ containing the palindromic ERE consensus motif (underlined) were annealed and 5′ end-labeled with [γ-^{32}P]ATP using T4 nucleotide kinase. The resulting labeled double-stranded DNA probe was purified on a Sephadex G50 spin-column, precipitated in ethanol, dissolved in TE buffer, and diluted in 25 mM HEPES, 1 mM DTT, 10% glycerol, 1 mM EDTA to contain approximately 25,000 cpm of ^{32}P/μL. Nuclear extracts (7 μg of proteins), were mixed with 90 ng poly(dIdC), 25 mM HEPES, 1 mM DTT, 10% glycerol, 1 mM EDTA, 160 mM KCl in a total

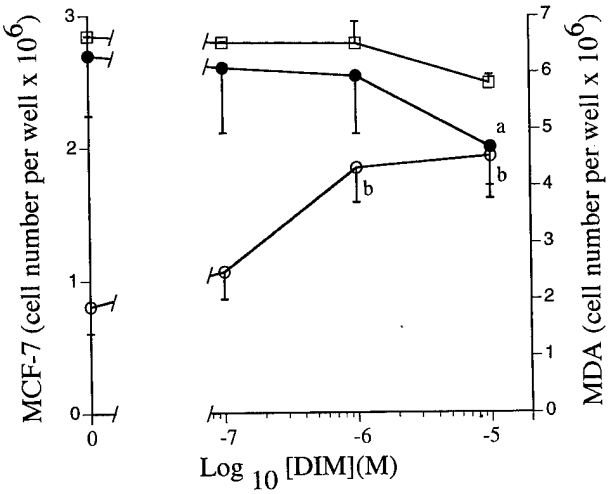

FIG. 2. Effect of DIM on proliferation of breast cancer cells. Estrogen-depleted MCF-7 cells were plated at a density of 10^5 cells/well in 6-well plates and treated with DIM at the concentrations indicated, in the presence (●) or absence (○) of E_2 (1 nM). MDA cells (□) grown in 10% FBS–DMEM were plated at a density of 10^5 cells/well in 6-well plates and treated with DIM at the concentrations indicated. Duplicate aliquots of cells from individual wells were counted after 7 days. Data from three identical wells are averaged. Results are shown as the means ± SD for four separate experiments. Key: (a) significantly reduced ($P < 0.05$) from the E_2-induced control; and (b) significantly different ($P < 0.05$) from the DMSO control.

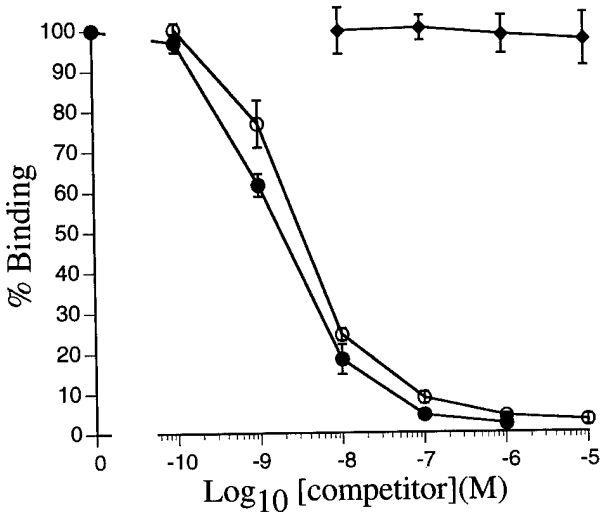

FIG. 3. Competitive binding to the ER. The binding of [^{3}H]E_2 (1 nM) to the ER from rat uterine cytosol was measured in the presence of the unlabeled competitors E_2 (●), ICI (○), and DIM (♦) at the concentrations indicated and reported as the percentage of binding in the absence of competitors. Results are shown as the means ± SD for four separate determinations. Relative binding affinities were calculated using the concentration of competitor needed to reduce [^{3}H]E_2 binding by 50% as compared with the concentration of unlabeled E_2 needed to achieve the same result.

volume of 21 μL. For antibody supershift experiments, 0.5 μg of monoclonal mouse IgG anti-human-ER (Santa Cruz Biotechnology) was added to the incubation mixture. After incubation for 15–20 min at room temperature, 4 μL (100,000 cpm) of end-labeled [^{32}P]ERE probe was added and incubated for another 15 min at room temperature. After the addition of 2.8 μL of 10x Ficoll loading buffer (0.25% bromophenol blue, 25% Ficoll type 400), 22-μL aliquots were loaded onto a pre-run, non-denaturing 4.0% polyacrylamide gel in TAE (67 mM Tris, 33 mM sodium acetate, 10 mM EDTA, pH 8.0) at 120 V for 2 hr. Finally, the gel was dried and autoradiographed.

RESULTS

DIM-Induced Growth of MCF-7 Cells in E_2-Depleted Medium

The effects of DIM on cell proliferation were examined in estrogen-treated and untreated MCF-7 cells over a 7-day time course. Treatment of cells with DIM in E_2-stripped medium produced a concentration-dependent increase in cell proliferation that at 10 μM reached a maximum of 60% of the growth produced in the absence of DIM in cells grown in complete, E_2-rich medium (Fig. 2). Co-treatment of cells with DIM (10 μM) in the E_2-rich medium, however, weakly inhibited estrogen-stimulated cell growth. DIM had no significant effect on proliferation of the ER-deficient breast cancer cell line MDA-MB-231 (Fig. 2). Taken together, these results suggested that DIM may affect breast tumor cell proliferation via an interaction with the ER and that DIM is not generally cytotoxic at the antiproliferative concentrations.

ER Affinity for DIM and Activation of ER Binding to the ERE

Based on our observation of a proliferative response, we assessed directly the ability of DIM to bind ER and activate its DNA-binding function. The relative binding affinity of DIM for the ER was measured by a competitive binding assay using 1.0 nM [^{3}H]E_2 as the labeled ligand (Fig. 3). The IC_{50} values, the concentrations of competitors necessary to displace the labeled ligand by 50%, were 2.0 and 4.0 nM for E_2 and ICI 182780 (ICI), respectively. DIM did not show significant affinity for the ER in the range of concentrations used.

We studied the binding of the ER to its cognate DNA motif (ERE) by a gel mobility shift assay using nuclear extracts from MCF-7 cells treated with E_2 or DIM. A 31-mer 5′-^{32}P-labeled double-stranded oligonucleotide containing the consensus ERE motif was used as the probe. Figure 4 shows that there was a clearly shifted band for the ERE from nuclear extracts of cells treated with E_2 or DIM, and that this band shift was obvious at a DIM concentration of only 1 μM. Pretreatment of these nuclear extracts with an anti-ER monoclonal antibody produced the supershifted band expected for the antibody–ER–ERE complex. These results demonstrate that DIM is capable of activating ER binding to the ERE by a mechanism that does not

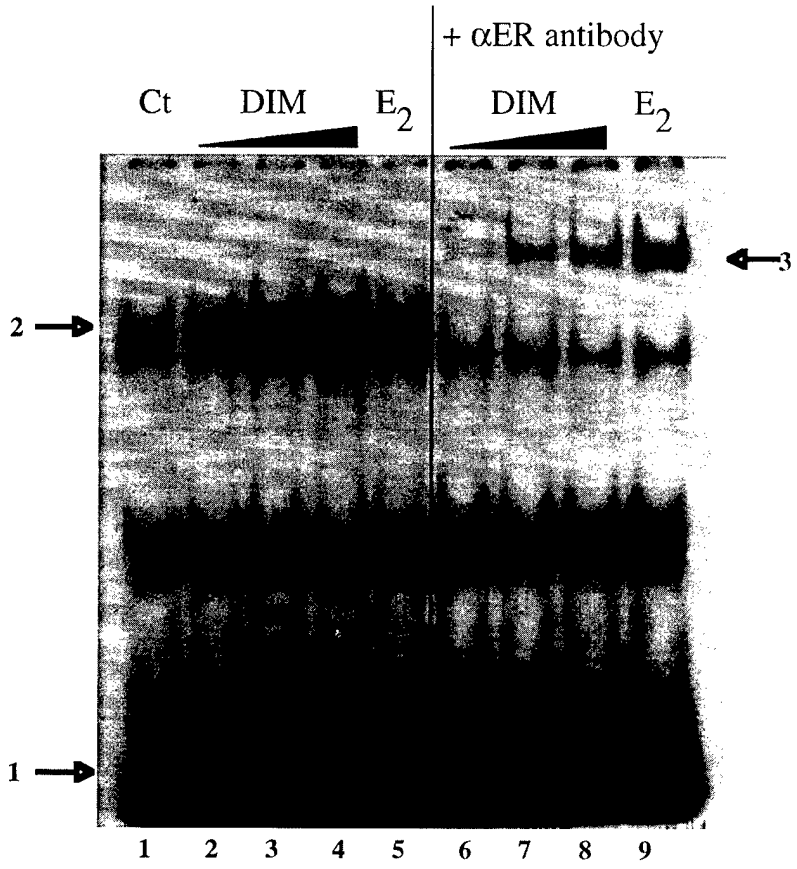

FIG. 4. Binding of nuclear proteins to the ERE. Gel mobility shift analysis of nuclear extracts from estrogen-depleted MCF-7 cells treated for 2 hr with DMSO (lane 1, control), DIM (0.1, 1.0, and 10.0 μM in lanes 2 and 6, 3 and 7, and 4 and 8, respectively), and E_2 (1 nM) (lanes 5 and 9). A monoclonal antibody specific for the human ER was also added to the incubation mixture for lanes 6–9. Arrows indicate the locations of the free labeled probe (arrow # 1), the ligand-responsive shifted band (arrow # 2), and the antibody supershifted band (arrow # 3).

require the binding of DIM to the ligand-binding domain of the ER.

Promoter Specificity of DIM Activation of ER-Responsive Genes and Sensitivity to a Standard Antiestrogen

To assess the effects of DIM on estrogen-responsive gene expression, MCF-7 cells were treated with DIM in the presence or absence of E_2 for 2 days, and northern blots were probed for E_2-responsive pS2 gene expression (Fig. 5). We found that when added to E_2-depleted medium, DIM induced the expression of endogenous pS2 mRNA in a concentration-dependent manner. However, co-treatment of cells with E_2 and DIM produced no statistically significant effect on the level of pS2 mRNA expression over that produced by E_2 treatment alone.

To examine whether the effects of DIM on E_2-responsive genes were affected by promoter conformation, cells were transfected transiently with the ERE-containing CAT-reporter plasmids pERE-vit-CAT or pS2-tk-CAT. DIM stimulated CAT activity of both reporters when administered in the absence of E_2 and weakly reduced E_2-induced expression of both of these reporters (Fig. 6). Thus, DIM functioned at the level of transcriptional activation of these two complex promoters. We did not observe the agonist effects of DIM, however, when cells were transfected with the simpler ERE-CAT reporter, pATC2, which was responsive to E_2 and to the synthetic estrogen DES (Fig. 7). Nevertheless, the weak antagonist effect of DIM on E_2-induced expression was also seen with this construct. These observations indicate that the agonist effects of DIM are restricted to a subset of E_2-responsive constructs.

Effects of Antiestrogens and Overexpression of ER on the Agonist Effects of DIM

Next, we examined whether the ER is essential to the agonist effects of DIM. First, we determined the effects of the pure antiestrogen ICI on DIM-induced activation of the pERE-vit-CAT reporter. The results presented in Fig. 8 show that ICI inhibited the activities of both DIM and E_2, and that ICI was a more effective inhibitor of DIM-induced activity than of E_2-induced activity. Whereas ICI produced a 90% reduction in E_2-induced activity, the combination of

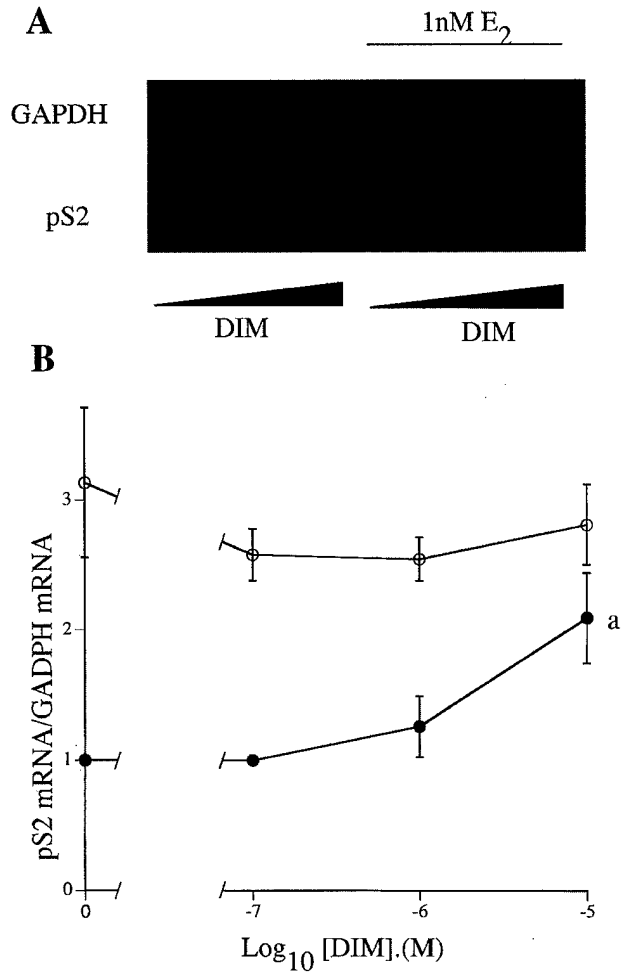

FIG. 5. Effect of DIM on pS2 mRNA expression. Estrogen-depleted MCF-7 cells were treated for 48 hr with DIM at concentrations ranging from 0.1 to 10.0 μM, with (○) or without (●) E_2 (1 nM). pS2 mRNA levels were measured by northern-blot analysis and normalized using GADPH mRNA as an internal standard. (A) Typical autoradiograph. (B) Results are presented as fold induction over the DMSO control, as the means ± SD for three separate experiments. Key: (a) significantly different ($P < 0.05$) from the DMSO control.

DIM and ICI reduced the activity to below the control values and resulted in greater than a 100% reduction of DIM-induced activity. These relative effects of E_2, DIM, and ICI on pERE-vit-CAT expression were unchanged by high levels of ER produced by co-transfection of MCF-7 cells with the pCMV-hER constitutive ER expression vector (data not shown). Taken together, these results provide further evidence that the ER plays a key role in the agonist effects of DIM.

Ligand-Independent Transcriptional Activation in MCF-7

To begin to examine the mode of ligand-independent activation of ER by DIM, we verified that ligand-independent transcriptional activation of the ER could be demonstrated with the ERE-vit-CAT reporter assay. Transfected cells were treated with a specific D1-dopamine receptor agonist, SKF-82958, shown previously to have that activity

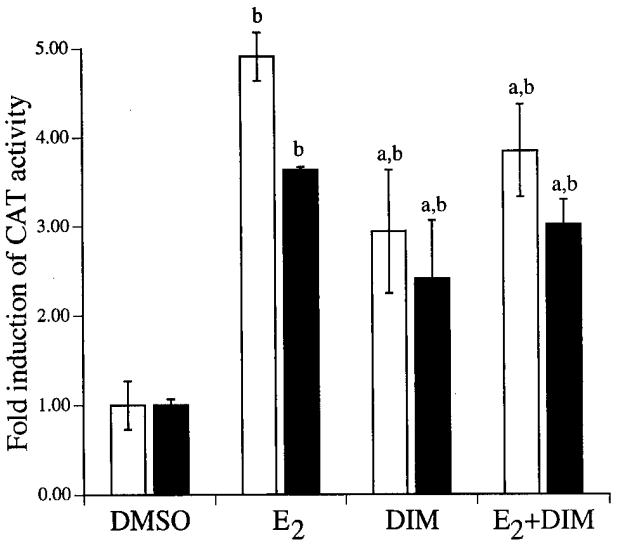

FIG. 6. Effect of DIM on CAT expression from the ERE-vit-CAT and pS2-tk-CAT reporters. MCF-7 cells were transfected transiently with the ERE-vit-CAT (black bars) or the pS2-tk-CAT (white bars) reporter plasmid and treated for 48 hr with vehicle control, E_2 (1 nM), DIM (10 μM), or a combination of the two. CAT activity in cytosol preparations from individual plates was normalized for protein concentration. Data are presented as fold induction over the DMSO control (means ± SD of four independent determinations). Key: (a) significantly reduced ($P < 0.05$) from E_2-induced; and (b) significantly different ($P < 0.05$) from the DMSO control.

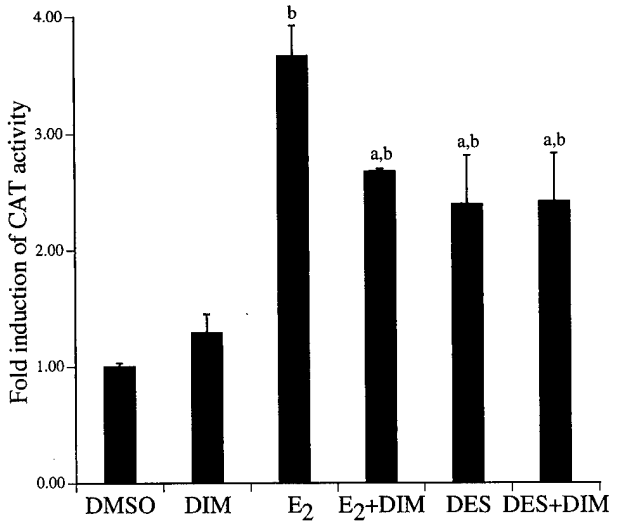

FIG. 7. Effect of DIM on CAT expression from the pATC2 reporter. MCF-7 cells were transiently transfected with the pATC2 reporter plasmid and treated for 48 hr with vehicle control, E_2 (1 nM), DES (1 nM), DIM (10.0 μM), or in combinations of E_2 or DES with DIM. Data are presented as fold induction over the DMSO control (means ± SD of four independent determinations). Key: (a) significantly reduced ($P < 0.05$) from E_2-induced, and (b) significantly different ($P < 0.05$) from the DMSO control.

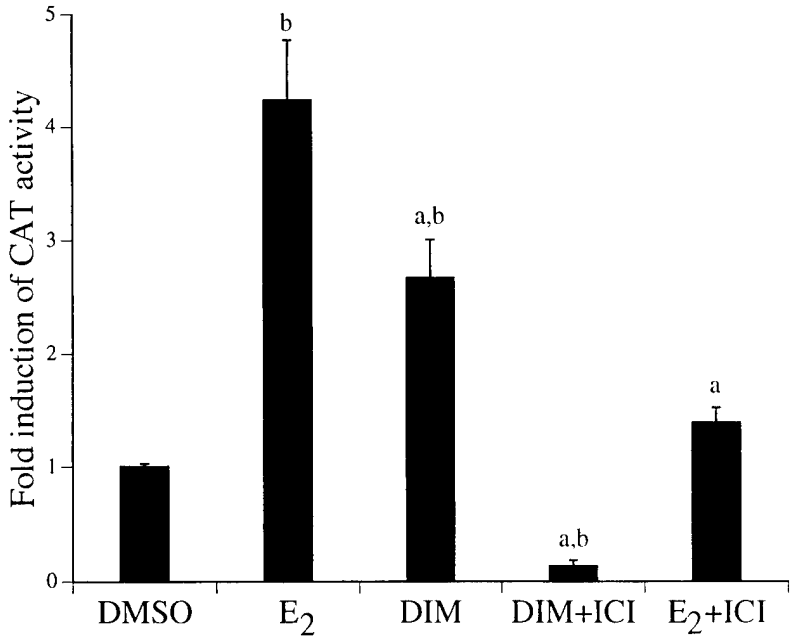

FIG. 8. Effect of antiestrogen on DIM- or E_2-induced CAT expression from the ERE-vit-CAT reporter. MCF-7 cells transiently transfected with the ERE-vit-CAT reporter plasmid were treated for 48 hr with DIM (10.0 μM) or E_2 (1 nM), with or without ICI (0.1 μM). Data are presented as fold induction over the DMSO control (means ± SD of four independent determinations). Key: (a) significantly reduced ($P < 0.05$) from E_2-induced; and (b) significantly different ($P < 0.05$) from the DMSO control.

in a neuroblastoma-derived cell line [26]. Figure 9 shows that 10 μM SKF-82958 induced transcription of the reporter gene to the same level as did E_2. This dopaminergic effect on ER function was blocked by the PKA inhibitor H-89. Importantly, H-89 completely ablated the response to DIM but exhibited no effect on the response to E_2, clearly indicating different modes of ER activation by the two substances. These results suggest that DIM-mediated activation of the ER may involve a PKA activation pathway.

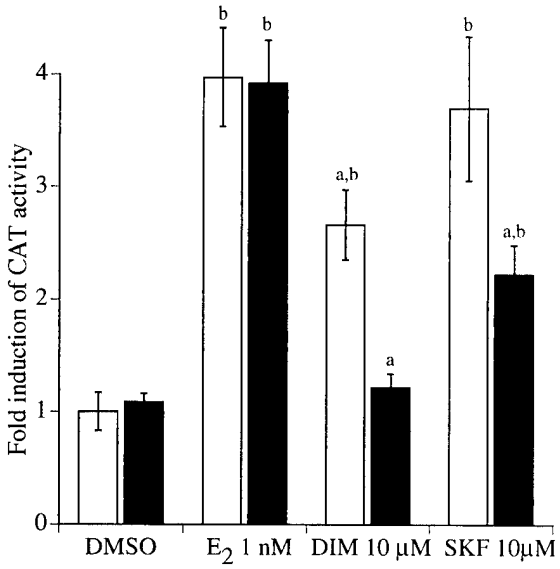

FIG. 9. Ligand-independent activation of transcription of an ER-responsive reporter gene. MCF-7 cells transiently transfected with the ERE-vit-CAT reporter plasmid were treated for 48 hr with DIM (10.0 μM), E_2 (1 nM), or SKF-82958 (10.0 μM) with (black bars) or without (white bars) the PKA inhibitor H-89 (10.0 μM). Data are presented as fold induction over the DMSO control (means ± SD of four independent determinations). Key: (a) significantly reduced ($P < 0.05$) from E_2-induced; and (b) significantly different ($P < 0.05$) from the DMSO control.

DISCUSSION

Our results show that at concentrations of up to 10 μM, DIM exhibited primarily agonist activity on cell proliferation and transcriptional activation of E_2-responsive endogenous and transfected reporter genes. Although DIM did not interact with the ligand-binding site of the ER, DIM activated the ER to a form that binds *in vitro* to the consensus ERE. In the absence of E_2, DIM promoted a level of cell proliferation in the E_2-responsive MCF-7 cell line that was approximately 60% of the maximum rate produced by E_2, but reduced the maximum E_2-induced proliferation rate of this cell line by about 40%. At the concentrations effective against proliferation of MCF-7 cells, however, DIM had very little effect on the proliferation of the E_2-independent cell line MDA-MB-231. Thus, under the conditions used in this study, the proliferative effects of DIM were cell type-specific and may require interaction with the ER.

In addition to the effects of DIM on cell proliferation, DIM could also function as an activator of E_2-responsive reporter genes and endogenous gene expression. In the absence of E_2, DIM exhibited pronounced agonist activities

with E_2-responsive genes regulated by complex promoters (ERE-vit-CAT, pS2-tk-CAT, endogenous pS2). DIM, however, had little effect on activation of a basal E_2-responsive reporter construct, pATC2. DIM did not affect significantly the E_2-induced expression of the endogenous pS2 gene and was a weak antagonist of E_2-induced expression of all three reporter constructs. The agonist effects of DIM were efficiently blocked by the antiestrogen ICI. ICI, considered a pure antiestrogen, functions specifically by binding to and inactivating the ER. These results indicate that the agonist effects of DIM require a pathway that involves both the activation of the ER and the presence of a *cis*-acting DNA element in addition to the consensus ERE or the core promoter. The consistently weak but generally significant antagonist effects of DIM on E_2 functions in E_2-responsive breast tumor cells are less dependent on promoter context and thus, may be important in long-term cancer prophylaxis.

The results emphasize the potential importance of an interaction of I3C-derived indoles on E_2-activated cellular processes, independent of possible effects of indoles on E_2 metabolism. Several studies have appeared suggesting that a major antiestrogenic mode of action of dietary indoles is via the metabolic deactivation of E_2 by an indole-induced increase in the activities of certain cytochrome P450 oxidative enzymes [27]. DIM, on the contrary, has been shown to competitively inhibit the activities associated with CYP1A1, CYP1A2, and CYP2B1 enzymes, and is an antagonist of AhR-mediated gene activation [19]. Our observation of the ER agonist effects of DIM strongly suggests that DIM can interact directly with the ER pathway and that the tumor growth inhibitory effects of I3C products may arise from effects in addition to or independent of increased E_2 metabolism.

There has been considerable recent concern over the presence of hormonally active contaminants in the environment [28]. These so-called endocrine disrupters have been suggested to be involved in various hormone-related abnormalities including decreased sperm count, birth defects, and breast cancers. To adequately assess the relative significance of such substances, it is important to consider their activities relative to the natural background of such activities produced by plant products including DIM and other hormonally active substances in the diet. Agonist activities on estrogen-dependent growth of breast tumor cells also have been reported for several other phytochemicals including certain flavonoids, such as genistein and apigenin, and lignins such as enterolactone [29]. As a result, the total dose of natural, estrogenically active substances from the diet can be substantial. For example, the amount of I3C in a 100-g portion of broccoli is about 50 mg, which would be expected to provide between 5 and 10 mg of DIM following ingestion and acid-catalyzed conversion in the stomach. The total dose of estrogenically active substances from a typical Western diet is estimated to be in excess of 1 g/day, which, when estrogenic potency is considered, is far in excess of the estrogen equivalent dose from environmental contaminants [29].

The results presented here are an interesting extension to results of related studies that report antiproliferative and apoptotic effects of DIM [30]. In a recent study by Chen *et al.* [31] DIM was reported to behave as an antagonist of estrogen function: at concentrations below 10 μM, DIM strongly inhibited the proliferation of a variant of cultured MCF-7 cells selected for their sensitivity to TCDD. At higher concentrations, DIM inhibited E_2-induced expression of a vitellogenin A2 gene promoter–CAT reporter construct co-transfected with an ER expression plasmid into MCF-7 cells. Also, in contrast with our results, these investigators reported that in gel mobility shift analyses of extracts of cells cultured in complete medium, the higher concentrations of DIM decreased the intensity of the ER–ERE bands. We observed strong antiproliferative effects on E_2-responsive MCF-7 cells and in E_2-nonresponsive MDA-MB-231 cells at DIM concentrations above 10 μM. However, since treatment with these concentrations was accompanied by considerable cell death and possible induction of apoptosis, we restricted the present studies to the lower concentrations. It is interesting to note that the proliferative effects of DIM reported in the aryl hydrocarbon-nonresponsive MCF-7BaPr cells [30] are similar to the effects we observed in our wild-type estrogen-responsive MCF-7 cells, i.e. DIM-induced proliferation in the absence of E_2 and weak inhibition of E_2-induced proliferation. Since the AhR signal transduction pathway is functional in our wild-type cells, as shown by the ICZ-induced expression of EROD activity (data not shown), it appears that the reported low concentration antagonistic effects of DIM are dependent on factors other than or in addition to a functional AhR.

The importance of the promoter- and cell-specific agonist effects of DIM reported here to the well-established protective effects of I3C against carcinogen-induced mammary cancer is yet to be defined. An overall picture is emerging, however, suggesting that the biological effects of oral I3C and of the major acid products of I3C are primarily estrogenic. We reported previously on the activities of two other major acid condensation products of I3C, namely the linear trimeric product, LTr-1, and the cyclic trimeric product, CTr. We observed that LTr-1 exhibited weak ER antagonist activities in the breast tumor cells that required concentrations in excess of 10 μM [32]. In contrast, we observed that CTr was a potent ligand for the ER and exhibited strong ER agonist activities at concentrations as low as 0.1 μM [33]. An important indication of the combined *in vivo* effects of the I3C acid products was reported recently by Oganesian *et al.* [34]. These investigators showed that oral I3C produces clearly estrogenic effects in trout. It is possible, therefore, that I3C may function in a manner similar to that suggested for the anticarcinogenic isoflavone genistein. Hsieh *et al.* [35] reported that genistein is a strong ER agonist and at physiological concentrations produces an estrogenic stimulation of mam-

mary development and enhanced proliferation of implanted MCF-7 cells in rodents. Lamartiniere *et al.* [36] and Hsieh *et al.* [35] suggest that the cancer protective effects of estrogen agonists such as genistein may result from effects on the maturation of the mammary gland. It is possible that the protective effects of I3C and DIM may arise from a similar estrogenic mechanism.

The case for the agonist effect of DIM occurring through a ligand-independent activation of the ER is strongly supported by the fact that DIM has no affinity for the ligand binding site but causes ER to bind to its cognate DNA motif and to activate transcription of E_2 responsive genes. The fact that this transcriptional activation was totally blocked by the specific ER antagonist ICI establishes the central role of the ER in this process. Our observation that the PKA inhibitor H-89 blocked the DIM-induced activity of the ERE-vit-CAT reporter but had no effect on the E_2-mediated activation of this reporter suggests a role for PKA in the observed agonist activities of DIM. Several reports of ligand-independent activation of the ER have appeared and show that the human ER responds to certain growth factors, phosphatase inhibitors, kinase activators, and neurotransmitters [26]. Whether DIM triggers similar physiologically important pathways and whether these pathways are involved in the cancer protective effects of DIM are important objectives of our ongoing research in this area.

This work was supported by the Department of Defense, Army Breast Cancer Research Program Grant DAMD17–96-1–6149, and by Grant CA69056 from the National Institutes of Health.

References

1. Wattenberg LW and Loub WD, Inhibition of polycyclic aromatic hydrocarbon-induced neoplasia by naturally occurring indoles. *Cancer Res* **38:** 1410–1415, 1978.
2. Shertzer HG, Protection by indole-3-carbinol against covalent binding of benzo[a]pyrene metabolites to mouse liver DNA and protein. *Food Chem Toxicol* **21:** 31–36, 1983.
3. Shertzer HG, Indole-3-carbinol protects against covalent binding of benzo[a]pyrene and N-nitrosodimethylamine metabolites to mouse liver macromolecules. *Chem Biol Interact* **48:** 81–90, 1984.
4. Dashwood RH, Arbogast DN, Fong AT, Hendricks JD and Bailey GS, Mechanisms of anti-carcinogenesis by indole-3-carbinol: Detailed *in vivo* DNA binding dose-response studies after dietary administration with aflatoxin B1. *Carcinogenesis* **9:** 427–432, 1988.
5. Grubbs CJ, Steele VE, Casebolt T, Juliana MM, Eto I, Whitaker LM, Dragnev KH, Kelloff GJ and Lubet RL, Chemoprevention of chemically-induced mammary carcinogenesis by indole-3-carbinol. *Anticancer Res* **15:** 709–716, 1995.
6. Bradlow HL, Michnovicz JJ, Telang NT and Osborne MP, Effects of dietary indole-3-carbinol on estradiol metabolism and spontaneous mammary tumors in mice. *Carcinogenesis* **12:** 1571–1574, 1991.
7. Sharma S, Stutzman JD, Kelloff GJ and Steele VE, Screening of potential chemopreventive agents using biochemical markers of carcinogenesis. *Cancer Res* **54:** 5848–5855, 1994.
8. Bailey GS, Hendricks JD, Shelton KW, Nixon E and Pawlowski NE, Enhancement of carcinogenesis by the natural anticarcinogen indole-3-carbinol. *J Natl Cancer Inst* **78:** 931–936, 1987.
9. Pence B, Buddingh H and Yang S, Multiple dietary factors in the enhancement of dimethylhydrazine carcinogenesis: Main effect of indole-3-carbinol. *J Natl Cancer Inst* **77:** 269–276, 1986.
10. Kim D, Han B, Ahn B, Hasegawa R, Shirai T, Ito N and Tsuda H, Enhancement by indole-3-carbinol of liver and thyroid gland neoplastic development in a rat medium-term multiorgan carcinogenesis model. *Carcinogenesis* **18:** 377–381, 1997.
11. Cover CM, Hsieh SJ, Tran SH, Hallden G, Kim GS, Bjeldanes LF and Firestone GL, Indole-3-carbinol inhibits the expression of cyclin dependent kinase-6 and induces a G_1 cell cycle arrest of human breast cancer cells independent of estrogen receptor signaling. *J Biol Chem* **273:** 3838–3847, 1998.
12. Bradfield CA and Bjeldanes LF, Structure-activity relationships of dietary indoles: A proposed mechanism of action as modifiers of xenobiotic metabolism. *J Toxicol Environ Health* **21:** 311–323, 1987.
13. Grose KR and Bjeldanes LF, Oligomerization of indole-3-carbinol in aqueous acid. *Chem Res Toxicol* **5:** 188–193, 1992.
14. Bjeldanes LF, Kim JY, Grose KR, Bartholomew JC and Bradfield CA, Aromatic hydrocarbon responsiveness-receptor agonists generated from indole-3-carbinol *in vitro* and *in vivo*: Comparisons with TCDD. *Proc Natl Acad Sci USA* **88:** 9543–9547, 1991.
15. Kwon CS, Grose KR, Riby J, Chen Y-H and Bjeldanes LF, *In vivo* production and enzyme-inducing activity of indolo[3,2-*b*]carbazole. *J Agric Food Chem* **42:** 2536–2540, 1994.
16. Chen Y-H, Riby J, Srivastava P, Bartholomew J, Denison M and Bjeldanes LJ, Regulation of CYP1A1 by indolo[3,2-*b*]carbazole in murine hepatoma cells. *J Biol Chem* **270:** 22548–22555, 1995.
17. Whitlock J Jr, Genetic and molecular aspects of 2,3,7,8-tetrachlorodibenzo-p-dioxin action, *Annu Rev Pharmacol Toxicol* **30:** 251–277, 1990.
18. Jellinck H, Forket PG, Riddick DS, Okey AB, Michnovicz JJ and Bradlow HL, Ah receptor binding properties of indole carbinols and induction of hepatic estradiol hydroxylation. *Biochem Pharmacol* **43:** 1129–1136, 1993.
19. Chen I, Safe S and Bjeldanes L, Indole-3-carbinol and diindolylmethane as aryl hydrocarbon (Ah) receptor agonists and antagonists in T47D human breast cancer cells. *Biochem Pharmacol* **51:** 1069–1076, 1996.
20. Stresser DM, Bjeldanes LF, Bailey GS and Williams DE, The anticarcinogen 3,3′-diindolylmethane is an inhibitor of cytochrome P-450. *J Biochem Toxicol* **10:** 191–201, 1995.
21. Santell RC, Chang YC, Nair MG and Helferich WG, Dietary genistein exerts estrogenic effects upon the uterus, mammary gland and the hypothalamic/pituitary axis in rats. *J Nutr* **127:** 263–269, 1997.
22. Chang T-C, Nardulli AM, Lew D and Shapiro DJ, The role of estrogen response elements in the *Xenopus laevis* vitellogenin B1 gene. *Mol Endocrinol* **6:** 346–354, 1992.
23. Jeltsch JM, Roberts M, Schatz C, Garnier JM, Brown AMC and Chambon P, Structure of the human estrogen-responsive gene pS2. *Nucleic Acids Res* **15:** 1401–1414, 1987.
24. Reese JC and Katzenellenbogen BS, Differential DNA-binding abilities of estrogen receptor occupied with two classes of antiestrogens: Studies using human estrogen receptor over expressed in mammalian cells. *Nucleic Acids Res* **19:** 6595–6602, 1991.
25. Seed B and Sheen J-Y, A simple phase extraction assay for

chloramphenicol acetyltransferase activity. *Gene* **67:** 271–277, 1988.
26. Gangolli EA, Conneely OM and O'Malley BW, Neurotransmitters activate the human estrogen receptor in a neuroblastoma cell line. *J Steroid Biochem Mol Biol* **61:** 1–9, 1997.
27. Telang NT, Katdare M, Bradlow HL, Osborne MP and Fishman J, Inhibition of proliferation and modulation of estradiol metabolism: Novel mechanisms for breast cancer prevention by the phytochemical indole-3-carbinol. *Proc Soc Exp Biol Med* **216:** 246–252, 1997.
28. Colborn T, Von Saal F and Soto A, Developmental effects of endocrine-disrupting chemicals in wildlife and humans. *Environ Health Perspect* **101:** 378–384, 1993.
29. Safe S, Environmental and dietary estrogens and human health: Is there a problem? *Environ Health Perspect* **103:** 346–351, 1995.
30. Ge X, Yannai S, Rennert G, Gruener N and Fares FA, 3,3′-Diindolylmethane induces apoptosis in human cancer cells. *Biochem Biophys Res Commun* **228:** 153–158, 1996.
31. Chen I, McDougal A, Wang F and Safe S, Aryl hydrocarbon receptor-mediated antiestrogenic and antitumorigenic activity of diindolylmethane. *Carcinogenesis* **19:** 1631–1639, 1998.
32. Chang Y-C, Riby J, Chang GH-F, Peng BC, Firestone G and Bjeldanes LF, Cytostatic and antiestrogenic effects of 2-(indol-3-ylmethyl)-3,3′-diindolylmethane, a major *in vivo* product of dietary indole-3-carbinol. *Biochem Pharmacol* **58:** 825–834, 1999.
33. Riby JE, Feng C, Chang Y-C, Schaldach CM, Firestone GL and Bjeldanes LF, The major cyclic trimeric product of indole-3-carbinol is a strong agonist of the estrogen receptor signaling pathway. *Biochemistry* **39:** 910–918, 2000.
34. Oganesian A, Orner GA, Hendricks JD, Pereira C, Bailey GS and Williams DE, The potency of indole-3-carbinol as a promoter of aflatoxin B_1-initiated hepatocarcinogenesis. *Carcinogenesis* **20:** 453–458, 1999.
35. Hsieh CY, Santell RC, Haslam SZ and Helferich WG, Estrogenic effects of genistein on the growth of estrogen receptor-positive human breast cancer (MCF-7) cells *in vitro* and *in vivo*. *Cancer Res* **58:** 3833–3838, 1998.
36. Lamartiniere CA, Moore JB, Brown NM, Thompson R, Hardin MJ and Barnes S, Genistein suppresses mammary cancer in rats. *Carcinogenesis* **16:** 2833–2840, 1995.

Biochemical Pharmacology, Vol. 51, pp. 1069–1076, 1996.

ELSEVIER

ISSN 0006-2952/96/$15.00 + 0.00
PII S0006-2952(96)00060-3

Indole-3-carbinol and Diindolylmethane as Aryl Hydrocarbon (Ah) Receptor Agonists and Antagonists in T47D Human Breast Cancer Cells

Ichen Chen, Stephen Safe*† and Leonard Bjeldanes‡*

*Veterinary Physiology and Pharmacology, Texas A&M University, College Station, TX 77843-4466; and ‡Department of Nutritional Sciences, University of California, Berkeley, CA 94720, U.S.A.

ABSTRACT. Indole-3-carbinol (I3C) is a major component of *Brassica* vegetables, and diindolylmethane (DIM) is the major acid-catalyzed condensation product derived from I3C. Both compounds competitively bind to the aryl hydrocarbon (Ah) receptor with relatively low affinity. In Ah-responsive T47D human breast cancer cells, I3C and DIM did not induce significantly CYP1A1-dependent ethoxyresorufin O-deethylase (EROD) activity or CYP1A1 mRNA levels at concentrations as high as 125 or 31 μM, respectively. A 1 nM concentration of 2,3,7,8-tetrachlorodibenzo-*p*-dioxin (TCDD) induced EROD activity in these cells, and cotreatment with TCDD plus different concentrations of I3C (1–125 μM) or DIM (1–31 μM) resulted in a > 90% decrease in the induced response at the highest concentration of I3C or DIM. I3C or DIM also partially inhibited (< 50%) induction of CYP1A1 mRNA levels by TCDD and reporter gene activity, using an Ah-responsive plasmid construct in transient transfection assays. In T47D cells cotreated with 5 nM [^{3}H]TCDD alone or in combination with 250 μM I3C or 31 μM DIM, there was a 37 and 73% decrease, respectively, in formation of the nuclear Ah receptor. The more effective inhibition of induced EROD activity by I3C and DIM was due to *in vitro* inhibition of enzyme activity. Thus, both I3C and DIM are partial Ah receptor antagonists in the T47D human breast cancer cell line. BIOCHEM PHARMACOL 51;8:1069–1076, 1996.

KEY WORDS. indole-3-carbinol; diindolylmethane; T47D cells; Ah receptor antagonist

Several studies have reported that laboratory animals fed a diet containing cruciferous vegetables are protected from the development of various spontaneous and carcinogen-induced tumors [1–3]. For example, there is a decreased incidence and growth of DMBA§-induced mammary tumors in female Sprague–Dawley rats maintained on a diet containing brussels sprouts [2]. I3C is a major secondary metabolite found in cruciferous vegetables, and this compound also exhibits a broad spectrum of anticarcinogenic activities [4–9]. I3C inhibits several carcinogen-induced tumors at various sites in rodent models [5–9] and also decreases the development of spontaneous mammary and endometrial tumors in female C3H/OuJ mice [4] and Donryu rats [7], respectively. I3C induces phase I and phase II drug-metabolizing enzymes in both laboratory animals and humans, and these include several CYP isoforms and their dependent enzyme activities: glutathione S-transferase, glucuronosyl transferase, NAD(P)H:quinone oxidoreductase, and epoxide hydrolase [10–18]. In studies with carcinogens such as benzo[*a*]pyrene and aflatoxin B_1, the induction of these enzyme activities correlates with altered metabolism and decreased levels of carcinogen-DNA and other adducts [19, 20]. Several studies have also demonstrated that I3C undergoes acid-catalyzed self-condensation to give several products including DIM and ICZ [17, 21, 22]. These I3C-derived compounds bind with variable affinities to the Ah receptor and thereby constitute one of the major classes of endogenous or natural compounds that bind to this receptor [15, 17, 23]. For example, competitive Ah receptor binding studies, using TCDD as the radioligand, give relative binding affinities of 1.0, 3.7×10^{-2}, 7.8×10^{-5}, and 2.6×10^{-7} for TCDD, ICZ, DIM, and I3C, respectively [17]. Similar results were also reported by Jellinck and coworkers [15]. Many of the induction responses observed in animals treated with I3C are consistent with the activity of this compound and related heteropolynuclear aromatic hydrocarbons as Ah receptor agonists, which typically induce CYP1A1- and CYP1A2-dependent glutathione S-transferase, UDP-glucuronosyl transferase and NAD(P)H:quinone oxidoreductase activities [24–27]. Previous

† Corresponding author. Tel. (409) 845-5988; FAX (409) 862-4929.

§*Abbreviations:* Ah, aryl hydrocarbon; CAT, chloramphenicol acetyltransferase; DIM, diindolylmethane; DMBA, 7,12-dimethylbenzanthracene; EROD, ethoxyresorufin O-deethylase; I3C, indole-3-carbinol; ICZ, indolo[3,2-*b*]carbazole; MCDF, 6-methyl-1,3,8-trichlorodibenzofuran; PCDDs, polychlorinated dibenzo-*p*-dioxins; PCDFs, polychlorinated dibenzofurans; SSC, 0.15 M sodium chloride + 0.015 M sodium citrate; TCDD, 2,3,7,8-tetrachlorodibenzo-*p*-dioxin; and TCDF, 2,3,7,8-tetrachlorodibenzofuran.

Received 15 September 1995; accepted 6 December 1995.

studies have also demonstrated that TCDD and related compounds exhibit antiestrogenic activity in mammalian cells in culture [28–34] and inhibit mammary tumor growth or formation in rodent models [29, 35, 36] and possibly in humans [37]. Similarly, I3C and ICZ also exhibit antiestrogenic activity in the MCF-7 human breast cancer cell line [38, 39], and inhibition of both carcinogen-induced and spontaneous mammary tumors and endometrial cancer in rodents may also be Ah receptor mediated [2, 4, 7]. I3C induces CYP1A2-dependent estradiol-2-hydroxylase activity in rodents and humans, and this metabolic pathway may also be associated with decreased risk from estrogen-dependent tumors [4, 40].

It has been shown previously that Ah receptor agonists with moderate to weak binding affinity for the receptor may also exhibit partial antagonist activity [41–46]. This study reports the Ah receptor agonist and partial antagonist activities of I3C and DIM in the T47D human breast cancer cell line. T47D cells treated with TCDD form the nuclear Ah receptor complex, and the induction of CYP1A1-dependent EROD activity is among the highest observed in human or rodent cancer cell lines. Results of studies reported in this paper demonstrated that both I3C and DIM exhibit Ah receptor antagonist activity in T47D human breast cancer cells.

MATERIALS AND METHODS

Cells, Chemicals, and Biochemicals

T47D human breast cancer cells were obtained from the American Type Culture Collection (Rockville, MD). DIM was prepared as previously described [14, 17, 21]. I3C was purchased from the Sigma Chemical Co. (St. Louis, MO). Solutions of I3C and DIM were stored carefully in the dark due to their photolability. [^{3}H]TCDD (37 Ci/mmol) was prepared by chlorination of [1,6-$^3H_2$]dibenzo-*p*-dioxin and purified by high pressure liquid chromatography to greater than 95% purity. Unlabeled TCDD and TCDF are prepared routinely in this laboratory (> 98% pure by gas chromatographic analysis). All other chemicals and biochemicals used in these studies were the highest quality available from commercial sources.

Cell Growth and Formation of Nuclear Receptor Complexes in T47D Cells Treated with [^{3}H]TCDD

Cells were grown as monolayer cultures in α-Eagle's Minimum Essential Medium supplemented with 2.2 g/L sodium bicarbonate, 5% fetal bovine serum, and 10 mL antibiotic-antimycotic solution (Sigma). Cells were maintained in 150-cm^2 culture flasks in an air:carbon dioxide (95:5) atmosphere at 37°. After reaching confluence, the cultures were trypsinized and washed once with used culture medium. The washed cells were resuspended in this medium in 25-cm^2 flasks at a cell concentration of 3×10^6 cells/mL (final volume 10 mL). The cells were incubated with 5 nM [^{3}H]TCDD in the presence or absence of 31 μM DIM and 250 μM I3C in DMSO (0.1% final concentration). Nuclear extract baselines were obtained by cotreatment of the cells with [^{3}H]TCDD plus a 200-fold excess of TCDF. The flasks were incubated by gentle shaking for 2 hr at 37°. After incubation, the suspended cells were decanted into 50-mL centrifuge tubes and centrifuged at 400 *g*. This and all subsequent procedures were performed at 4°.

Isolation and Analysis of Nuclear Extracts

Harvested cells were washed twice in 20 mL of HEGD buffer (25 mM HEPES, 1.5 mM EDTA, 10% glycerol, 1.0 mM dithiothreitol; pH 7.6). The washed cell pellet was resuspended in 3 mL of HED buffer (HEDG without glycerol) and incubated for 10 min. After incubation, the cells were pelleted and resuspended with an additional 1.5 mL of HEGD buffer and homogenized using a tight Teflon pestle/drill apparatus. The homogenate was transferred to a centrifuge tube in 20 mL of HEGD buffer and centrifuged at 1500 *g* for 10 min. The pellet was then resuspended in 3 mL of HEGD buffer containing 0.5 M potassium chloride (pH 8.5) and allowed to stand at 4° for 1 hr. Nuclei prepared by this method were found to be intact and were greater than 90% free of extranuclear cellular contamination, as determined by microscopic examination and trypan-blue staining. Aliquots (200 μL) of the samples were layered onto linear sucrose gradients (5–25%) prepared in HED buffer containing 0.4 M potassium chloride. Gradients were centrifuged at 4° for 2.5 hr at 404,000 *g*. After centrifugation, 30 fractions were collected from each gradient, and the radioactivity of each fraction was determined by liquid scintillation counting. ^{14}C-Labeled BSA (4.4S) and catalase (11.3S) were used as the markers for determining sedimentation values.

EROD Activity

EROD activity was assayed as described [47] with some modifications. Trypsinized cells were plated into 25-cm^2 tissue culture flasks (10^5 cells/mL), allowed to attain 60% confluency, and treated with 1 nM TCDD, 1–31 mM DIM, 1–125 mM I3C, and combinations of TCDD plus DIM or I3C for 24 hr. Cells were harvested by manual scraping from the plate, centrifuged at 400 *g* for 5 min at 4°, and resuspended in 100 μL of Tris–sucrose buffer (38 mM Tris–HCl, 0.2 M sucrose; pH 8.0). Aliquots (50 μL) of the cells were incubated with 1.15 mL cofactor solution (1 mg BSA, 0.7 mg NADH, 0.7 mg NADPH, 1.5 mg $MgSO_4$ in 0.1 M HEPES buffer; pH 7.5) in a 37° water bath for 2 min. The reaction was started by adding 50 μL ethoxyresorufin (1 mg ethoxyresorufin/40 mL methanol). After incubation for 15 min, the reaction was stopped by adding 2.5 mL methanol. Samples were centrifuged for 10 min at 1500 *g*. The supernatant was used for fluorescence measurement at an excitation wavelength of 550 nm and an emission wavelength of 595 nm.

Northern Blot Analysis

Cells were plated into 100 mm Petri dishes, and when 60% confluent, the cells were treated with 1 nM TCDD, DIM, and I3C alone or their combinations for 24 hr. After trypsinization, cells were pelleted by centrifugation at 500 *g* for 5 min at 4°. To the cell pellet, 700 μL of a solution containing 4 M guanidinium thiocyanate, 10% sarcosyl, 3 M sodium acetate (pH 5.2), and 0.1% 2-mercaptoethanol was added. The cell pellet was resuspended immediately with a 1-mL syringe and a 22-gauge needle. To the cell homogenate, 0.5 mL of water-saturated phenol was added and mixed thoroughly. A solution of chloroform:isoamyl alcohol (24:1) was added, vortexed, and then allowed to incubate at 4° for 15 min. Samples were then centrifuged at 10,000 *g* for 15 min, and 600 μL of the upper aqueous phases was extracted carefully. After addition of 1 vol. of isopropyl alcohol, the RNA was allowed to precipitate overnight at −20°. After precipitation, the samples were centrifuged at 10,000 *g* for 15 min, and the RNA was washed with cold ethanol once and 70% ethanol once. Samples were evaporated and redissolved in 15–20 μL of deionized formamide. The murine CYP1A1 cDNA probe was obtained from the American Type Culture Collection. The plasmid pGMB1.1 was a gift from Dr. Don Cleveland (Johns Hopkins University) and carries the mouse β-tubulin cDNA cloned into the *Eco* RI site of pGMB1.1. Digestion of the plasmid yielded a 1.3-kb fragment that was used to detect β-tubulin mRNA.

The RNA (10 μg) was mixed with sample buffer, electrophoresed on a denaturing agarose gel (1.2%), and transferred to a nylon membrane as previously described [41]. The membrane was then exposed to UV light for 5 min to cross-link RNA to the membrane and baked at 80° for 2 hr. The membrane was then prehybridized in a solution containing 0.1% BSA, 0.1% Ficoll, 0.1% polyvinyl pyrrolidine, 10% dextran sulfate, 1% SDS and 5× SSPE (0.75 M NaCl, 50 mM NaH_2PO_4, 5 mM EDTA) for 18–24 hr at 65°. Probes were ^{32}P-labeled using a Boehringer-Mannheim kit. The membrane was hybridized for approximately 24 hr in the prehybridization solution with the addition of 10^6 cpm/mL ^{32}P-labeled CYP1A1 cDNA probe. After hybridization, the membrane was washed twice at 20° in 1 × SSC, 1% SDS, and again twice for 45 min at 65°. After two additional rinses in 0.1 × SSC, 1% SDS at 20°, the membrane was sealed in a plastic bag, quantitated on a Betagen Betascope 603 blot analyzer imaging system, and visualized by autoradiography. The membrane was stripped by washing twice in stripping buffer (0.1 × SSC, 0.5% SDS) at 100° and rehybridized. The CYP1A1 mRNA was standardized relative to β-tubulin mRNA [41].

Transient Transfection Assays

The plasmid pRNH11c contains the regulatory human CYP1A1 region from the *Taq* I site at −1142 to the Bcl I site at +24 fused to the bacterial CAT reporter gene [48]. Cells were seeded in 100-mm Petri dishes and grown as described above in the proliferation assays until 70% confluent. Five micrograms of the pRNH11c plasmid and 20 μg polybrene/mL were incubated for 6 hr; cells were then shocked using 15% glycerol. After 18 hr, cells were treated with 1 nM TCDD, 31 μM DIM, and 125 μM I3C for 30 hr. Cells were then washed with PBS and scraped from the plates. Cell lysates were prepared in 0.16 mL of 0.25 M Tris-HCl, pH 7.5, by three freeze–thaw-sonication cycles (3 min/each cycle) to ensure maximum levels of CAT activity. Cell lysates were incubated at 56° for 7 min to remove endogenous deacetylase activity. CAT activity was determined using 0.2 mCi *d*-threo-[*dichloroacetyl*-1-^{14}C]chloramphenicol and 4 mM acetyl-CoA as substrates. The protein concentrations were determined using BSA as a standard. Following TLC, acetylated products were visualized and quantitated using a Betascope 603 blot analyzer. CAT activity was calculated as the percentage of that observed in cells treated with DMSO alone, and results are expressed as means ± SD. The experiments were carried out at least in triplicate.

Isolation of Microsomes from T47D Cells

After treatment with 1 nM TCDD for 24 hr, T47D cells were homogenized in HEGD buffer using a Teflon pestle/drill apparatus. The homogenates were centrifuged at 10,000 *g* for 20 min. The resulting supernatant was centrifuged further at 105,000 *g* for 30 min. The microsomal pellet was resuspended in 100 μL Tris–sucrose buffer (38 mM Tris–HCl, 0.2 M sucrose; pH 8.0) and stored at −80°. Test compounds were incubated with TCDD-induced microsomes, BSA, NADH, and NADPH at 3° for 2, 10, or 20 min, and EROD activity was determined fluorimetrically [47].

Statistical Analysis

All the experiments were carried out in triplicate, and the results are expressed as means ± SD. Statistical significance was determined by performing ANOVA using Student's *t*-test.

RESULTS

The results in Fig. 1 summarize the concentration-dependent induction of EROD activity by I3C and DIM in T47D cells. At concentrations of I3C and DIM as high as 31 and 125 μM, respectively, no significant induction was observed for either compound. In contrast, EROD activity in cells treated with 1 nM TCDD was 300–400 pmol/min/mg. Cotreatment of T47D cells with 1 nM TCDD and I3C or DIM gave a concentration-dependent decrease in induced EROD activity. I3C significantly inhibited TCDD-induced EROD activity at a concentration of 31 μM, and this activity was decreased to less than 10% of the maximal response at the highest concentration of I3C (125 μM). Sim-

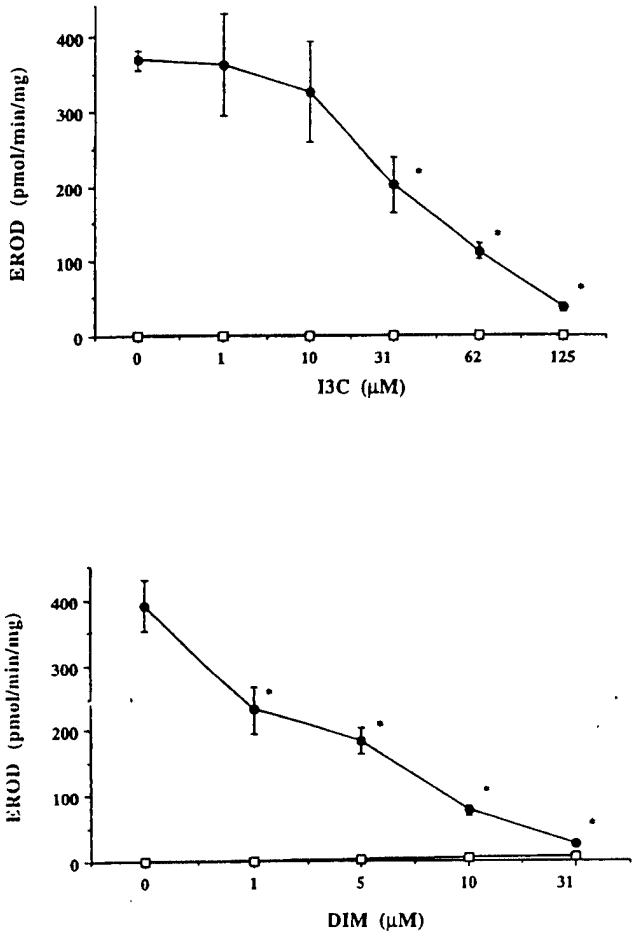

FIG. 1. Inhibition of TCDD-induced EROD activity in T47D cells by I3C (top) and DIM. T47D cells were treated with 1 nM TCDD, different concentrations of I3C (□, top) or DIM (□, bottom) alone or cotreated with 1 nM TCDD plus different concentrations of I3C (●, top) or DIM (●, bottom) for 24 hr. Cells were isolated, and EROD activity was determined as described in Materials and Methods. Results are expressed as means ± SD for 3 separate determinations for each data point. I3C and DIM significantly inhibited ($P < 0.05$) induced EROD activity at concentrations as low as 31 and 1 μM, respectively.

ilar results were also observed for DIM in which 1 μM DIM significantly decreased induced EROD activity (Fig. 1, bottom). The results in Fig. 2 summarize the effects of 1 nM TCDD, 1 and 31 μM DIM, 10 and 125 μM I3C, and TCDD plus DIM or I3C on CYP1A1 mRNA levels in T47D cells. DIM alone caused a small but marked increase (62%) in CYP1A1 mRNA levels at the highest concentration (31 μM), whereas I3C did not induce CYP1A1 mRNA levels significantly. In T47D cells cotreated with 1 nM TCDD and 1 or 31 μM DIM, there was a 53% decrease in TCDD-induced CYP1A1 mRNA levels. Similarly, in T47D cells cotreated with 1 nM TCDD and 10 or 125 μM I3C, there was a 58% decrease in TCDD-induced CYP1A1 mRNA levels only at the 125 μM concentration of I3C. The results in Fig. 3 summarize the effects of 1 nM TCDD, 31 μM DIM, 125 μM I3C, and TCDD plus DIM or I3C on CAT activity in T47D cells transiently transfected with the pRNH11c plasmid. CAT activity was induced 6- to 10-fold by TCDD (in two separate experiments), whereas 125 μM I3C and 31 μM DIM alone caused a 3.4- and 2.7-fold increase in activity, respectively. In cells cotreated with TCDD plus DIM or I3C, there was a significant decrease in CAT activity compared with results obtained with TCDD alone.

The results in Fig. 4 illustrate the velocity sedimentation analysis of nuclear extracts from T47D cells treated with 5 nM [^{3}H]TCDD alone and in the presence of 250 μM I3C, 31 μM DIM or 1 μM TCDF. A higher concentration of [^{3}H]TCDD was used in this experiment to ensure that sufficient specifically bound nuclear extract could be obtained for sucrose density gradient centrifugation. Preliminary studies showed that with the higher concentration of [^{3}H]TCDD, cotreatment with 125 μM unlabeled I3C resulted in only minimal decreases in accumulation of the radiolabeled nuclear Ah receptor; however, cotreatment with 250 μM I3C resulted in a 37% decrease in the [^{3}H]TCDD nuclear Ah receptor complex. In cells cotreated with 5 nM [^{3}H]TCDD plus 31 μM DIM, there was a 73% decrease in the radiolabeled nuclear Ah receptor complex.

The *in vitro* effects of I3C on CYP1A1-dependent activ-

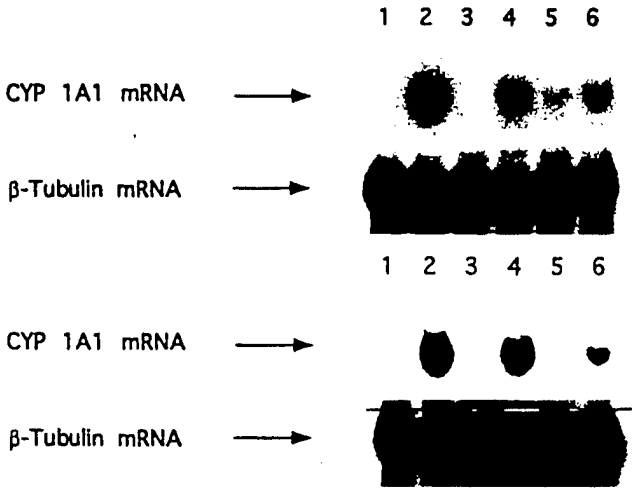

FIG. 2. Induction of CYP1A1 mRNA levels by TCDD, I3C, DIM, and TCDD plus I3C (top) or DIM (bottom) in T47D cells. T47D cells were treated with DMSO, 1 nM TCDD, 10 μM I3C, 10 μM I3C plus 1 nM TCDD, 125 μM I3C, and 125 μM I3C plus 1 nM TCDD (top, lanes 1 through 6, respectively) for 24 hr. Cells were treated with DMSO, 1 nM TCDD, 1 μM DIM, 1 μM DIM plus 1 nM TCDD, 31 μM DIM, 31 μM DIM plus 1 nM TCDD (bottom, lanes 1 through 6, respectively) for 24 hr. Cells were harvested, and mRNA was isolated and analyzed by northern blot analysis as described in Materials and Methods. CYP1A1 mRNA levels were standardized relative to β-tubulin mRNA, and the values (means ± SD for 3 determinations) were: (top) 1.00 ± 0.15, 4.07 ± 0.75, 0.94 ± 0.08, 3.22 ± 0.49, 1.18 ± 0.10, and 1.96 ± 0.01 (lanes 1 through 6, respectively); (bottom) 1.00 ± 0.19, 6.27 ± 0.86, 1.35 ± 0.09, 5.30 ± 0.29; 1.62 ± 0.15, and 2.94 ± 0.35 (lanes 1 through 6, respectively). Quantitation of induced bands was determined using a Betagen Betascope 603 blot analyzer.

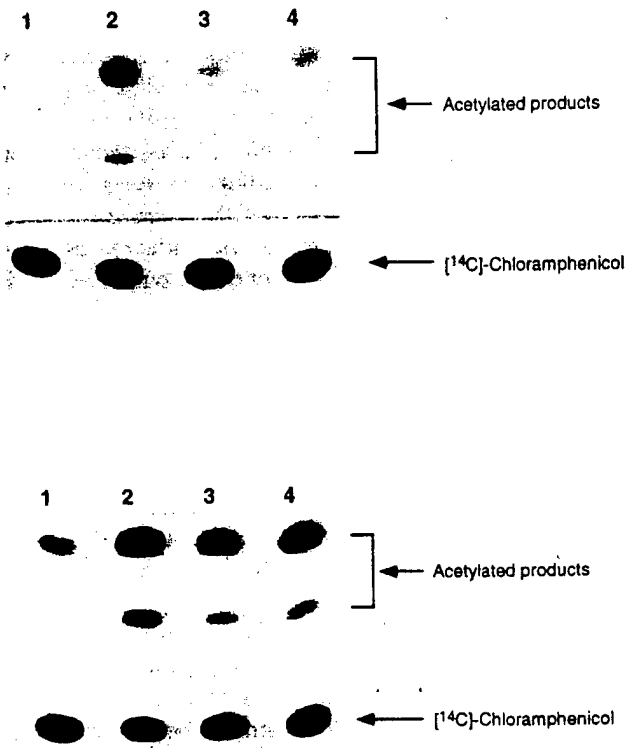

FIG. 3. Induction of CAT activity in T47D cells by TCDD, I3C, DIM, and their combinations. T47D cells were transiently transfected with pRNH11c and treated with the various chemical combinations for 24 hr; CAT activity was determined as described in Materials and Methods. In two separate experiments, CAT activity was induced 6- to 10-fold by 1 nM TCDD (lane 2) compared with activity in cells treated with DMSO (lane 1). The relative intensities of the acetylated products in cells with 1 nM TCDD, 125 μM I3C, and TCDD plus I3C (lanes 2 through 4, respectively, top) were: 100 ± 4, 34 ± 3, and 67 ± 8%. The relative intensities of acetylated products in cells treated with 1 nM TCDD, 31 μM DIM, and TCDD plus DIM (lanes 2 through 4, respectively, bottom) were: 100 ± 25, 42 ± 16, and 59 ± 20%. I3C (top) and DIM (bottom) alone significantly induced CAT activity and also significantly inhibited the TCDD-induced response ($P < 0.005$). The relative intensities (means ± SD for 3 separate determinations) of the acetylated products were determined using a Betagen Betascope 603 blot analyzer.

ity (Fig. 5) were determined by incubating different concentrations of I3C (10, 63, and 125 μM) or DIM (1, 10, or 31 μM) with microsomes from T47D cells treated with 1 nM TCDD for 2, 10, or 20 min. The results showed that both I3C and DIM caused a concentration- and time-dependent decrease in EROD activity using a complete microsomal enzyme incubation system and that DIM was the more potent inhibitor. In the absence of the reduced nucleotide cofactors, comparable inhibitory responses were observed (data not shown).

DISCUSSION

MCDF and related 6-alkyl-1,3,8-trichlorodibenzofurans have been characterized previously as weak Ah receptor agonists for the induction of CYP1A1 and for several toxic responses including immunotoxicity, porphyria, and fetal cleft palate formation in mice [44–46]. Moreover, in cells or in mice cotreated with an effective (or toxic) dose of TCDD plus MCDF, there was a significant inhibition of these same TCDD-induced responses. Surprisingly, MCDF did not inhibit TCDD-induced antiestrogenic responses in the rat uterus or in human breast cancer cell lines but exhibited Ah receptor agonist activity for this response [49–51]. The combination of low toxicity but high antiestrogenic activity suggests that MCDF and related compounds may be useful clinically as antiestrogens [51]. Previous studies have shown that I3C exhibits several properties similar to those described for MCDF; I3C binds with low affinity to the Ah receptor and at high doses or concentrations, I3C induces CYP1A1/1A2-dependent activity [11–17]. For example, 500 μM I3C induces immunoreactive CYP1A1 protein in MCF-7 breast cancer cells [52], whereas minimal induction responses are observed at lower concentrations. Similar results were observed in this study using T47D cells, since 125 μM I3C induced only a minimal increase in CYP1A1 mRNA levels (Fig. 2). It was reported previously that lower concentrations of I3C also inhibit several estrogen (E_2)-induced responses including cell proliferation and nuclear estrogen receptor binding [38, 39]. This profile of responses in MCF-7 cells, namely antiestrogenic activity and minimal induction of CYP1A1-dependent EROD activity, resembled those previously reported for MCDF, and therefore the major objective of this study was to determine if I3C or its major dimerization product, DIM [52], also exhibited Ah receptor antagonist activity.

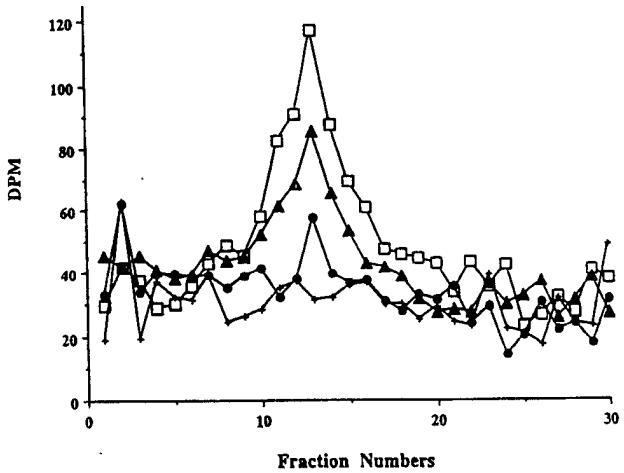

FIG. 4. Velocity sedimentation analysis of nuclear extracts from T47D cells treated with [^{3}H]TCDD plus I3C or DIM. Cells in suspension were treated with 5 nM [^{3}H]TCDD alone (□) or in combination with 250 μM I3C (▲), 31 μM DIM (●) or 1 μM TCDF (+) for 2 hr; nuclear extracts were isolated and analyzed on sucrose density gradients as described in Materials and Methods. Relative nuclear Ah receptor levels in cells treated with [^{3}H]TCDD alone, [^{3}H]TCDD plus I3C, and [^{3}H]TCDD plus DIM were 100 ± 17, 63 ± 13, and 27 ± 12%, respectively. Representative gradients are shown.

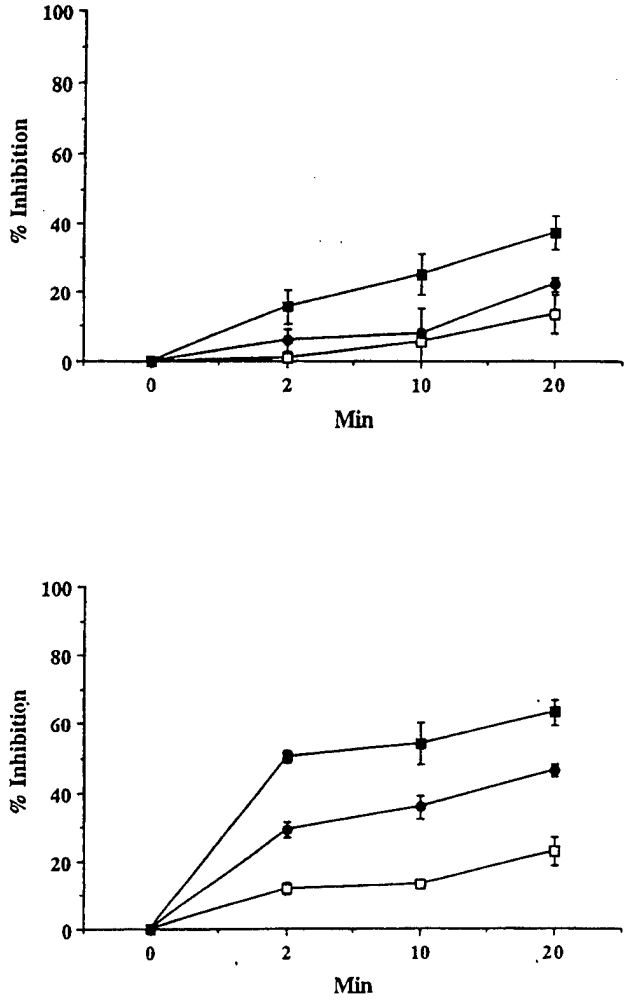

FIG. 5. *In vitro* inhibition of EROD activity by I3C (top) or DIM (bottom). Microsomes from T47D cells treated with 1 nM TCDD for 24 hr were incubated with 10 (□), 63 (●), or 125 (■) μM I3C (top) and 1 (□), 10 (●), or 31 (■) μM DIM (bottom) for 2, 10, or 20 min, and EROD activity was determined fluorimetrically as described in Materials and Methods. The results are expressed as means ± SD for each data point (3 separate determinations). Significant inhibition ($P < 0.05$) was observed for all concentrations of I3C and DIM after incubation with microsomes from T47D cells, and similar inhibitory effects were observed using induced rat hepatic microsomes (data not shown). The induced EROD activity was 437 pmol/min/mg.

T47D human breast cancer cells were utilized in this study because of the reported high inducibility of CYP1A1-dependent EROD activity [53].

The results in Figs. 1 and 2 confirmed that both I3C and DIM are relatively weak Ah receptor agonists since at concentrations as high as 125 and 31 μM, respectively, no induction of EROD activity was observed. I3C (125 μM) caused a small but insignificant increase in CYP1A1 mRNA levels in T47D cells, whereas 31 μM DIM markedly induced mRNA levels (Fig. 2); similar results were observed in transient transfection assays using pRNH11c, an Ah-responsive plasmid that contains a dioxin-responsive element enhancer sequence (Fig. 3). These data are consistent with results of previous studies showing that DIM is more potent than I3C as an Ah receptor agonist; however, both compounds are much less active than either ICZ or TCDD [15, 17].

In T47D cells treated with 1 nM TCDD, there was a significant induction of EROD activity; however, in cells cotreated with TCDD plus I3C or DIM, there was a concentration-dependent decrease in the induced response and, at the highest concentrations of these compounds (125 and 31 μM, respectively), < 10% of induced activity was observed. I3C and DIM also markedly inhibited TCDD-induced CYP1A1 mRNA levels (Fig. 2) and CAT activity (Fig. 3) in cells transiently transfected with pRNH11c. The inhibitory effects of I3C and DIM on TCDD-induced responses in T47D cells also correlated with the decreased accumulation of the radiolabeled nuclear Ah receptor complex in cells cotreated with I3C or DIM (Fig. 4). These results are similar to those previously observed for other Ah receptor antagonists, such as α-naphthoflavone and MCDF, which also decrease formation of the radiolabeled nuclear Ah receptor complex in cells cotreated with [^{3}H]TCDD plus the antagonists [41–45].

The results of this study demonstrate that both I3C and DIM are weak Ah receptor agonists that also exhibit partial Ah receptor antagonist activity for the induction of *CYP1A1* gene expression by TCDD. However, there was a disparity between the > 90% inhibition of TCDD-induced EROD activity (Fig. 1) and the < 50% inhibition of CYP1A1 mRNA levels (Fig. 2). Jellinck and coworkers [15] noted that several Ah receptor agonists which induce CYP1A1/1A2 *in vivo* inhibit the induced microsomal enzyme activity *in vitro*. The results in Fig. 5 demonstrate that I3C and DIM caused a concentration- and time-dependent decrease in EROD activity using microsomes from T47D cells treated with 1 nM TCDD for 24 hr. Thus, the *in vitro* activity of DIM and I3C as inhibitors of CYP1A1-dependent EROD activity is consistent with the >90% inhibition of this induced response in cells cotreated with TCDD plus I3C or DIM (Fig. 1).

I3C and related hetero-polynuclear aromatic hydrocarbons in vegetables represent a class of endogenous Ah receptor agonists ("natural dioxins") that are consumed in the diet along with industrial and combustion-derived halogenated aromatic compounds, such as TCDD, which are also Ah receptor agonists (exodioxins). Levels of PCDDs and PCDFs in the human diet vary from 1000 to 2000 pg/day or 80 to 120 pg/day of toxic (or TCDD) equivalents. Moreover, in the general population, average background levels of TCDD equivalents are estimated to be 58 ng/kg serum lipid [54]. For individuals who consume an average of 25 g of *Brassica* vegetables each day, the intake levels of I3C are in excess of 700,000,000 pg/day [17]. Since I3C, DIM, and related compounds exhibit both Ah receptor agonist and partial antagonist activities, risk assessment of low level dietary exposure to exodioxins should also take into account the possible inhibitory or additive effects of dietary compounds that also bind to the Ah receptor. The inter-

actions (additive or inhibitory) between I3C and related condensation products with exodioxins will depend on their relative serum levels; however, at present, the values of I3C-derived compounds are unknown. Moreover, due to rapid metabolism of I3C and related indoles, serum levels of these compounds will be highly variable, and this may also influence interactions with TCDD and related exodioxins. Current ongoing studies in this laboratory are investigating the relative potencies of TCDD, I3C, DIM, and other "natural dioxins" and their interactions for several other Ah receptor-mediated responses.

The financial assistance of the National Institutes of Health (ES04917) and the Texas Agriculture Experiment Station is gratefully acknowledged. S. Safe is a Sid Kyle Professor of Toxicology.

References

1. Wattenburg LW and Loub WD, Inhibition of aromatic hydrocarbon-induced neoplasia by naturally occurring indoles. *Cancer Res* **38:** 1410–1413, 1978.
2. Stoewsand GS, Anderson JL and Munson L, Protective effect of dietary brussels sprouts against mammary carcinogenesis in Sprague-Dawley rats. *Cancer Lett* **39:** 199–207, 1988.
3. Wattenberg LW, Inhibition of chemical carcinogenesis. *J Natl Cancer Inst* **60:** 11–18, 1978.
4. Bradlow HL, Michnovicz JJ, Telang NT and Osborne MP, Effects of dietary indole-3-carbinol on estradiol metabolism and spontaneous mammary tumors in mice. *Carcinogenesis* **12:** 1571–1574, 1991.
5. Morse MA, LaGreca SD, Amin SG and Chung FL, Effects of indole-3-carbinol on lung tumorigenesis and DNA methylation induced by 4-(methylnitrosamino)-1-(3-pyridyl)-1-butanone (NNK) and on the metabolism and disposition of NNK in A/J mice. *Cancer Res* **50:** 2613–2617, 1990.
6. Nixon JE, Hendricks JD, Pawlowski NE, Pereira CB, Sinnhuber RO and Bailey GS, Inhibition of aflatoxin B_1 carcinogenesis in rainbow trout by flavone and indole compounds. *Carcinogenesis* **5:** 615–619, 1984.
7. Kojima T, Tanaka T and Mori H, Chemoprevention of spontaneous endometrial cancer in female Donryu rats by dietary indole-3-carbinol. *Cancer Res* **54:** 1446–1449, 1994.
8. Tanaka T, Mori Y, Morishita Y, Hara A, Ohno T, Kojima T and Mori H, Inhibitory effect of sinigrin and indole-3-carbinol in diethylnitrosamine-induced hepatocarcinogenesis in male ACI/N rats. *Carcinogenesis* **11:** 1403–1406, 1990.
9. Tanaka T, Kojima T, Morishita Y and Mori H, Inhibitory effects of the natural products indole-3-carbinol and sinigrin during initiation and promotion phases of 4-nitroquinoline 1-oxide-induced rat tongue carcinogenesis. *Jpn J Cancer Res* **83:** 835–842, 1992.
10. Loub WD, Wattenberg LW and Davis DW, Aryl hydrocarbon hydroxylase induction in rat tissues by naturally occurring indoles of cruciferous plants. *J Natl Cancer Inst* **54:** 985–988, 1975.
11. Vang O, Jensen MB and Autrup H, Induction of cytochrome P450IA1 in rat colon and liver by indole-3-carbinol and 5,6-benzoflavone. *Carcinogenesis* **11:** 1259–1263, 1990.
12. Michnovicz JJ and Bradlow HL, Induction of estradiol metabolism by dietary indole-3-carbinol in humans. *J Natl Cancer Inst* **82:** 947–949, 1990.
13. Bradfield CA and Bjeldanes LF, Effect of dietary indole-3-carbinol on intestinal and hepatic monooxygenase, glutathione S-transferase and epoxide hydrolase activities in the rat. *Food Chem Toxicol* **22:** 977–997, 1984.
14. Bradfield CA and Bjeldanes, LF, Structure–activity relationships of dietary indoles: A proposed mechanism of action as modifiers of xenobiotic metabolism. *J Toxicol Environ Health* **21:** 311–323, 1987.
15. Jellinck PH, Forkert PG, Riddick DS, Okey AB, Michnovicz JJ and Bradlow HL, Ah receptor binding properties of indole carbinols and induction of hepatic estradiol hydroxylation. *Biochem Pharmacol* **45:** 1129–1136, 1993.
16. Baldwin WS and LeBlanc GA, The anti-carcinogenic plant compound indole-3-carbinol differentially modulates P450-mediated steroid hydroxylase activities in mice. *Chem Biol Interact* **83:** 155–169, 1992.
17. Bjeldanes LF, Kim J-Y, Grose KR, Bartholomew JC and Bradfield CA, Aromatic hydrocarbon responsiveness-receptor agonists generated from indole-3-carbinol *in vitro* and *in vivo*: Comparisons with 2,3,7,8-tetrachlorodibenzo-*p*-dioxin. *Proc Natl Acad Sci USA* **88:** 9543–9547, 1991.
18. Bogaards JJP, Verhagen H, Willems MI, van Poppel G and van Bladeren PJ, Consumption of Brussels sprouts results in elevated α-class glutathione *S*-transferase levels in human blood plasma. *Carcinogenesis* **15:** 1073–1075, 1994.
19. Shertzer HG, Indole-3-carbinol protects against covalent binding of benzo[*a*]pyrene and *N*-nitrosodimethylamine metabolites to mouse liver macromolecules. *Chem Biol Interact* **48:** 81–90, 1984.
20. Fong AT, Swanson HI, Dashwood RH, Williams DE, Hendricks JD and Bailey GS, Mechanisms of anti-carcinogenesis by indole-3-carbinol: Studies of enzyme induction, electrophile-scavenging, and inhibition of aflatoxin B_1 activation. *Biochem Pharmacol* **39:** 19–26, 1990.
21. Grose KR and Bjeldanes LF, Oligomerization of indole-3-carbinol in aqueous acid. *Chem Res Toxicol* **5:** 188–193, 1992.
22. De Kruif CA, Marsman JW, Venekamp JC, Falke HE, Noordhoek J, Blaauboer BJ and Wortelboer HM, Structure elucidation of acid reaction products of indole-3-carbinol: Detection *in vivo* and enzyme induction *in vitro*. *Chem Biol Interact* **80:** 303–315, 1991.
23. Gillner M, Bergman J, Cambillau C, Alexandersson M, Fernström B and Gustafsson JA, Interactions of indolo[3,2-*b*]carbazoles and related polycyclic aromatic hydrocarbons with specific binding sites for 2,3,7,8-tetrachlorodibenzo-*p*-dioxin in rat liver. *Mol Pharmacol* **44:** 336–345, 1993.
24. Poland A and Knutson JC, 2,3,7,8-Tetrachlorodibenzo-*p*-dioxin and related halogenated aromatic hydrocarbons. Examinations of the mechanism of toxicity. *Annu Rev Pharmacol Toxicol* **22:** 517–554, 1982.
25. Goldstein JA and Safe S, Mechanism of action and structure–activity relationships for the chlorinated dibenzo-*p*-dioxins and related compounds. In: *Halogenated Biphenyls, Naphthalenes, Dibenzodioxins and Related Compounds* (Eds. Kimbrough RD and Jensen AA), pp. 239–293. Elsevier-North Holland, Amsterdam, 1989.
26. Okey AB, Riddick DS and Harper PA, The Ah receptor: Mediator of the toxicity of 2,3,7,8-tetrachlorodibenzo-*p*-dioxin (TCDD) and related compounds. *Toxicol Lett* **70:** 1–22, 1994.
27. Whitlock JP Jr, Genetic and molecular aspects of 2,3,7,8-tetrachlorodibenzo-*p*-dioxin action. *Annu Rev Pharmacol Toxicol* **30:** 251–277, 1990.
28. Gierthy JF, Lincoln DW, Gillespie MB, Seeger JI, Martinez HL, Dickerman HW and Kumar SA, Suppression of estrogen-regulated extracellular plasminogen activator activity of MCF-7 cells by 2,3,7,8-tetrachlorodibenzo-*p*-dioxin. *Cancer Res* **47:** 6198–6203, 1987.
29. Gierthy JF, Bennett JA, Bradley LM and Cutler DS, Correlation of *in vitro* and *in vivo* growth suppression of MCF-7 human breast cancer by 2,3,7,8-tetrachlorodibenzo-*p*-dioxin. *Cancer Res* **53:** 3149–3153, 1993.

30. Gierthy JF and Lincoln DW, Inhibition of postconfluent focus production in cultures of MCF-7 breast cancer cells by 2,3,7,8-tetrachlorodibenzo-*p*-dioxin. *Breast Cancer Res Treat* **12:** 227–233, 1988.
31. Biegel L and Safe S, Effects of 2,3,7,8-tetrachlorodibenzo-*p*-dioxin (TCDD) on cell growth and the secretion of the estrogen-induced 34-, 52- and 160-kDa proteins in human breast cancer cells. *J Steroid Biochem Mol Biol* **37:** 725–732, 1990.
32. Krishnan V and Safe S, Polychlorinated biphenyls (PCBs), dibenzo-*p*-dioxins (PCDDs) and dibenzofurans (PCDFs) as antiestrogens in MCF-7 human breast cancer cells: Quantitative structure–activity relationships. *Toxicol Appl Pharmacol* **120:** 55–61, 1993.
33. Harper N, Wang X, Liu H and Safe S, Inhibition of estrogen-induced progesterone receptor in MCF-7 human breast cancer cells by aryl hydrocarbon (Ah) receptor agonists. *Mol Cell Endocrinol* **104:** 47–55, 1994.
34. Zacharewski TR, Bondy KL, McDonell P and Wu ZF, Antiestrogenic effect of 2,3,7,8-tetrachlorodibenzo-*p*-dioxin on 17β-estradiol-induced pS2 expression. *Cancer Res* **54:** 2707–2713, 1994.
35. Holcomb M and Safe S, Inhibition of 7,12-dimethylbenzanthracene-induced rat mammary tumor growth by 2,3,7,8-tetrachlorodibenzo-*p*-dioxin. *Cancer Lett* **82:** 43–47, 1994.
36. Kociba RJ, Keyes DG, Beger JE, Carreon RM, Wade CE, Dittenber DA, Kalnins RP, Frauson LE, Park CL, Barnard SD, Hummel RA and Humiston CG, Results of a 2-year chronic toxicity and oncogenicity study of 2,3,7,8-tetrachlorodibenzo-*p*-dioxin (TCDD) in rats. *Toxicol Appl Pharmacol* **46:** 279–303, 1978.
37. Bertazzi PA, Pesatori AC, Consonni D, Tironi A, Landi MT and Zocchetti C, Cancer incidence in a population accidentally exposed to 2,3,7,8-tetrachlorodibenzo-*p*-dioxin. *Epidemiology* **4:** 398–406, 1993.
38. Liu H, Wormke M, Safe S and Bjeldanes LF, Indolo[3,2-*b*]carbazole: A dietary factor which exhibits both antiestrogenic and estrogenic activity. *J Natl Cancer Inst* **86:** 1758–1765, 1994.
39. Tiwari RK, Guo L, Bradlow HL, Telang NT and Osborne MP, Selective responsiveness of breast cancer cells to indole-3-carbinol, a chemopreventative agent. *J Natl Cancer Inst* **86:** 126–131, 1994.
40. Bradlow HL, Telang NT, Osborne MP and Michnovicz JJ, Selective induction of cytochrome P450 enzymes in the prevention of breast cancer. In: *The New Biology of Steroid Hormones* (Eds. Hochberg RB and Naftolin F), pp. 127–143. Raven Press, New York, 1992.
41. Merchant M, Morrison V, Santostefano M and Safe S, Mechanism of action of aryl hydrocarbon receptor antagonists: Inhibition of 2,3,7,8-tetrachlorodibenzo-*p*-dioxin-induced *CYP1A1* gene expression. *Arch Biochem Biophys* **298:** 389–394, 1992.
42. Merchant M, Krishnan V and Safe S, Mechanism of action of α-naphthoflavone as an Ah receptor antagonist in MCF-7 human breast cancer cells. *Toxicol Appl Pharmacol* **120:** 179–185, 1993.
43. Gasiewicz TA and Rucci G, α-Naphthoflavone acts as an antagonist of 2,3,7,8-tetrachlorodibenzo-*p*-dioxin by forming an inactive complex with the Ah receptor. *Mol Pharmacol* **40:** 607–612, 1991.
44. Harris M, Zacharewski T, Astroff B and Safe S, Partial antagonism of 2,3,7,8-tetrachlorodibenzo-*p*-dioxin-mediated induction of aryl hydrocarbon hydroxylase by 6-methyl-1,3,8-trichlorodibenzofuran: Mechanistic studies. *Mol Pharmacol* **35:** 729–735, 1989.
45. Astroff B, Zacharewski T, Safe S, Arlotto MP, Parkinson A, Thomas P and Levin W, 6-Methyl-1,3,8-trichlorodibenzofuran as a 2,3,7,8-tetrachlorodibenzo-*p*-dioxin antagonist: Inhibition of the induction of rat cytochrome P-450 isozymes and related monooxygenase activities. *Mol Pharmacol* **33:** 231–236, 1988.
46. Bannister R, Biegel L, Davis D, Astroff B and Safe S, 6-Methyl-1,3,8-trichlorodibenzofuran (MCDF) as a 2,3,7,8-tetrachlorodibenzo-*p*-dioxin antagonist in C57BL/6 mice. *Toxicology* **54:** 139–150, 1989.
47. Pohl RJ and Fouts JR, A rapid method for assaying the metabolism of 7-ethoxyresorufin by microsomal subcellular fractions. *Anal Biochem* **107:** 150–155, 1980.
48. Hines RN, Mathis JM and Jacob CS, Identification of multiple regulatory elements on the human cytochrome P450IA1 gene. *Carcinogenesis* **9:** 1599–1605, 1988.
49. Astroff B and Safe S, Comparative antiestrogenic activities of 2,3,7,8-tetrachlorodibenzo-*p*-dioxin and 6-methyl-1,3,8-trichlorodibenzofuran in the female rat. *Toxicol Appl Pharmacol* **95:** 435–443, 1988.
50. Zacharewski T, Harris M, Biegel L, Morrison V, Merchant M and Safe S, 6-Methyl-1,3,8-trichlorodibenzofuran (MCDF) as an antiestrogen in human and rodent cancer cell lines: Evidence for the role of the Ah receptor. *Toxicol Appl Pharmacol* **13:** 311–318, 1992.
51. Safe S, MCDF, 6-methyl-1,3,8-trichlorodibenzofuran. *Drugs Future* **17:** 564–565, 1992.
52. Niwa T, Swaneck G and Bradlow HL, Alterations in estradiol metabolism in MCF-7 cells induced by treatment with indole-3-carbinol and related compounds. *Steroids* **59:** 523–527, 1994.
53. Harris M, Piskorska-Pliszczynska J, Zacharewski T, Romkes M and Safe S, Structure-dependent induction of aryl hydrocarbon hydroxylase in human breast cancer cell lines and characterization of the Ah receptor. *Cancer Res* **49:** 4531–4535, 1989.
54. DeVito MJ, Birnbaum LS, Farland WH and Gasiewicz TA, Comparisons of estimated human body burdens of dioxinlike chemicals and TCDD body burdens in experimentally exposed animals. *Environ Health Perspect* **103:** 820–831, 1995.

TCDD
been w
TCDD
respons
toxicol
haloger
worker
rably a
from C
ceptor,
man tis

‡ Curren
Unionda
§ Corr
‖ Abbr
dioxin-re
hydroxyl
2,3,7,8-t
zofuran.
Recei

[CANCER RESEARCH 59, 1244–1251, March 15, 1999]

Indole-3-Carbinol and Tamoxifen Cooperate to Arrest the Cell Cycle of MCF-7 Human Breast Cancer Cells[1]

Carolyn M. Cover, S. Jean Hsieh, Erin J. Cram, Chibo Hong, Jacques E. Riby, Leonard F. Bjeldanes, and Gary L. Firestone[2]

Department of Molecular and Cell Biology and The Cancer Research Laboratory [C. M. C., S. J. H., E. J. C., G. L. F.] and Department of Nutritional Sciences [C. H., J. E. R., L. F. B.], The University of California at Berkeley, Berkeley, California 94720-3200

ABSTRACT

The current options for treating breast cancer are limited to excision surgery, general chemotherapy, radiation therapy, and, in a minority of breast cancers that rely on estrogen for their growth, antiestrogen therapy. The naturally occurring chemical indole-3-carbinol (I3C), found in vegetables of the *Brassica* genus, is a promising anticancer agent that we have shown previously to induce a G_1 cell cycle arrest of human breast cancer cell lines, independent of estrogen receptor signaling. Combinations of I3C and the antiestrogen tamoxifen cooperate to inhibit the growth of the estrogen-dependent human MCF-7 breast cancer cell line more effectively than either agent alone. This more stringent growth arrest was demonstrated by a decrease in adherent and anchorage-independent growth, reduced DNA synthesis, and a shift into the G_1 phase of the cell cycle. A combination of I3C and tamoxifen also caused a more pronounced decrease in cyclin-dependent kinase (CDK) 2-specific enzymatic activity than either compound alone but had no effect on CDK2 protein expression. Importantly, treatment with I3C and tamoxifen ablated expression of the phosphorylated retinoblastoma protein (Rb), an endogenous substrate for the G_1 CDKs, whereas either agent alone only partially inhibited endogenous Rb phosphorylation. Several lines of evidence suggest that I3C works through a mechanism distinct from tamoxifen. I3C failed to compete with estrogen for estrogen receptor binding, and it specifically down-regulated the expression of CDK6. These results demonstrate that I3C and tamoxifen work through different signal transduction pathways to suppress the growth of human breast cancer cells and may, therefore, represent a potential combinatorial therapy for estrogen-responsive breast cancer.

INTRODUCTION

I3C[3] is a naturally occurring compound found in vegetables of the *Brassica* genus, such as broccoli and Brussels sprouts (1, 2), and it has been shown to reduce the incidence of spontaneous and carcinogen-induced mammary tumors in rodents (3, 4). When ingested, the stomach acid catalyzes the conversion of I3C into a number of derivatives. Two of the most prevalent derivatives that have been identified are 3,3′-diindolymethane and indolo[3,2-*b*]carbazole (5). These compounds are thought to be responsible for the long-term antiestrogenic biological activities of ingested I3C that may contribute to protection against mammary tumor formation. We have documented that the treatment of MCF-7 human breast cancer cells with I3C but not with its acid-catalyzed derivatives rapidly suppresses cell growth. This reversible G_1 cell cycle arrest is preceded by a decrease in the expression of CDK6 and is independent of estrogen receptor signaling (6). However, many of the molecular details of this antiproliferative pathway are unknown and an understanding of the mechanism of I3C action in human breast cancer cells could potentially lead to a novel approach to control breast cancer. Currently, the only specific therapy for breast cancer is antiestrogen treatment, and this treatment is only effective on tumors that rely on estrogen for their growth. Because I3C has been shown to suppress the growth of both estrogen-dependent and estrogen-independent human breast cancer cell lines (6), a combination of these two growth suppressors may potentially provide beneficial effects for breast cancer patients.

Tamoxifen has been a clinically useful antiestrogen for breast cancer patients for >20 years (7–9). Tamoxifen, a nonsteroidal triphenyl ethylene, can adopt a structural conformation that resembles steroids in the nucleus and act as a competitive inhibitor of E2 binding to the estrogen receptor (10, 11). Although tamoxifen generally acts as an estrogen receptor antagonist in breast cancer cells, in certain other cell types, tamoxifen can act as an estrogen receptor agonist (reviewed in Ref. 12). Several mechanisms are proposed for the modulation of breast cancer cell proliferation by tamoxifen, including down-regulation of oncogenes, modulation of growth factor signaling, and regulation of the cell cycle machinery (13–15). Regulated changes in the expression and/or activity of cell cycle components that act within G_1 have been closely associated with alterations in the proliferation rate of normal and transformed mammary epithelial cells (16). Regulation of these events by both antiproliferative and proliferative extracellular signals are well documented. For example, progesterone inhibition of breast cancer cell growth has been linked to the inactivation of G_1 CDKs by modulating the components of the CDK complex (17). Also, the estrogen-induced activation of CDK4 and CDK2 during progression of human breast cancer cells between the G_1 and S phases is accompanied by the increased expression of cyclin D1 and decreased association of the CDK inhibitors with the cyclin E-CDK2 complex (18).

The sequential activation of CDKs and subsequent phosphorylation of specific substrates govern progress through the cell cycle on multiple levels. CDKs are inactive in the absence of cyclin binding; therefore, cyclin abundance is a major determinant of cyclin-CDK activity (19–22). Each cyclin is typically present for only a restricted portion of the cell cycle, and alterations in cyclin abundance are sufficient to alter the rate of cell cycle progression (19, 21, 22). CDK activity is also regulated by a network of kinases and phosphatases (reviewed in Ref. 20), which can either activate or inactivate the complex. A further level of control results from the actions of two families of specific CDK-inhibitory proteins. Members of the p16INK4 family specifically target the kinases that associate with the D-type cyclins, CDK4 and CDK6 (21, 23, 24). Members of the p21 (WAF1, Cip1) family interact with a broader range of CDKs, including CDK2, CDK4, and CDK6 (25, 26). One of the key endogenous substrates of the G_1 CDKs is the retinoblastoma protein (Rb). Its phosphorylation is an important step in the transition between the G_1 and S phases of the cell cycle because, when sufficiently phospho-

Received 7/15/98; accepted 1/13/99.

The costs of publication of this article were defrayed in part by the payment of page charges. This article must therefore be hereby marked *advertisement* in accordance with 18 U.S.C. Section 1734 solely to indicate this fact.

[1] Supported by Department of Defense Army Breast Cancer Research Program Grant DAMD17-96-1-6149 (to L. F. B.) and by University of California Breast Cancer Research Program Grant 31B-0110 (to G. L. F.). C. M. C. is a recipient of a predoctoral fellowship supported by NIH National Research Service Grant CA-09041. E. J. C. is a recipient of a predoctoral fellowship supported by the United States Army Medical Research and Materiel Command Breast Cancer Research Program Award BC971062.

[2] To whom requests for reprints should be addressed, at Department of Molecular and Cell Biology, 591 LSA, University of California at Berkeley, Berkeley, CA 94720-3200. Phone: (510) 642-8319; Fax: (510) 643-6791; E-mail: glfire@uclink4.berkeley.edu.

[3] The abbreviations used are: I3C, indole-3-carbinol; CDK, cyclin-dependent kinase; E2, β-estradiol; FBS, fetal bovine serum; IP, immunopreciptation; GST, glutathione *S*-transferase.

rylated, Rb releases a transcription factor of the E2F family that drives cells into S phase (27).

Tamoxifen has been shown to decrease the activity of the estrogen receptor, and it does not have an antiproliferative effect on estrogen receptor-negative cell lines. In contrast, I3C can suppress the growth of cells regardless of estrogen receptor status (6). Taking into account the known features of the growth suppression cascades induced by I3C or tamoxifen, we tested the combinatorial effects of these two breast cancer cell growth suppressors in estrogen-responsive MCF-7 cells. Most significantly, a combination of tamoxifen and I3C displayed a more effective growth suppression response, a more stringent inhibition of CDK2 specific activity, and more endogenous Rb phosphorylation than either compound alone. Our results suggest the possibility of developing I3C and tamoxifen as a potential combinatorial therapy to control estrogen-responsive breast cancers.

MATERIALS AND METHODS

Materials. DMEM, FBS, calcium- and magnesium-free PBS, L-glutamine, and trypsin-EDTA were supplied by BioWhittaker (Walkersville, MD). Insulin (bovine) and tamoxifen ([Z]-1-[*p*-dimethylaminoethoxyphenyl]-1,2-diphenyl-1-butene) citrate salt were obtained from Sigma Chemical Co. (St. Louis, MO). [^{3}H]Thymidine (84 Ci/mmol) and [γ-^{33}P]ATP (3,000 Ci/mmol) were obtained from NEN Life Science Products (Boston, MA). I3C was purchased from Aldrich (Milwaukee, WI). I3C was recrystallized in hot toluene prior to use. The sources of other reagents used in the study are either listed below or were of the highest purity available.

Cell Culture. The MCF-7 human breast adenocarcinoma cell line was obtained from the American Type Culture Collection (Manassas, VA). MCF-7 cells were grown in DMEM supplemented with 10% FBS, 10 μg/ml insulin, 50 units/ml penicillin, 50 units/ml streptomycin, and 2 mM L-glutamine and maintained at subconfluency at 37°C in humidified air containing 5% CO_2. I3C and tamoxifen were dissolved in DMSO (99.9% high-performance liquid chromatography grade; Aldrich) at concentrations that were 1000-fold higher than the final medium concentration. In all experiments, 1 μl of the concentrated agent was added per 1 ml of medium, and for the vehicle control, 1 μl of DMSO was added per 1 ml of medium.

Estrogen Receptor Binding. Rat uterine cytosol was prepared as described (28). Briefly, 2.5 g of uterine tissue from five 12-week-old Sprague Dawley rats were excised and homogenized for 1 min with 30 ml of ice cold TEDG buffer [10 mM Tris, 1.5 mM EDTA, 1 mM DTT, and 10% glycerol (pH 7.4)], using a Polytron homogenizer at medium speed. The homogenate was centrifuged at 2800 rpm for 10 min at 4°C, transferred to a new tube, and centrifuged at 39,000 rpm for 90 min at 4°C. The supernatant was quickly frozen in a dry ice/ethanol bath and stored at −80°C.

For the competitive binding assay, 1 μl of competitor (100× solution in DMSO) was added to 5 μl of [^{3}H]E2 mixture [20 nM [^{3}H]E2 (NEN) in 50% ethanol, 5 mM Tris (pH 7.5), 5% glycerol, 0.5 mg/ml BSA, and 0.5 mM DTT] and incubated at room temperature with 95 μl of uterine cytosol (3 mg/ml) for 2 h. The range of concentrations of competitive ligand were 0.1 nM–1 μM for E2, 10 nM–10 μM for tamoxifen, and 10 μM–1 mM for I3C. The reaction was then incubated on ice for 15 min with 100 μl of 50% HAP slurry (hydoxylapatite; Bio-Rad BioGel HTP) rinsed and swelled overnight in TE buffer [50 mM Tris and 1 mM EDTA (pH 7.4)] and then adjusted to 50%. The slurry was vortexed to resuspend HAP every 5 min. Next, 1.0 ml of ice-cold wash buffer [40 mM Tris (pH 7.4), 100 mM KCl, 1 mM EDTA, and 1 mM EGTA] was added, and the mixture was vortexed and centrifuged for 5 min at 10,000 rpm at 4°C. The pellet was washed twice more with ice-cold wash buffer and then resuspended in 400 μl of ethanol and transferred to a scintillation vial for measurement. Relative binding affinities were calculated using the concentration of competitor needed to reduce [^{3}H]E2 binding by 50%, as compared to the concentration of unlabeled estrogen needed to achieve the same result.

[^{3}H]Thymidine Incorporation. MCF-7 cells were plated onto 24-well Corning tissue culture dishes. Triplicate samples of asynchronously growing mammary cells were treated for the indicated times with either vehicle control (1 μl of DMSO per 1 ml of medium) or varying concentrations of I3C and/or tamoxifen. The cells were pulsed for 3 h with 3 μCi of [^{3}H]thymidine (84 Ci/mmol), washed three times with ice-cold 10% trichloroacetic acid, and lysed with 300 μl of 0.3 N NaOH. Lysates (150 μl) were transferred into vials containing liquid scintillation cocktail, and radioactivity was quantitated by scintillation counting. Triplicates were averaged and expressed as cpm per well.

Crystal Violet Staining of Low Confluency Cultures. MCF-7 cells were plated onto 100-mm Corning tissue culture dishes (10,000 cells per plate). The cells were treated with the indicated concentrations of I3C and tamoxifen for 8 days. At the end of the treatment, the cells were washed with PBS and incubated in a solution of 0.5% crystal violet and 10% formalin for 10 min and then rinsed with water. The integrated density of the colonies on each plate was determined using NIH Image software.

Soft Agar Colony Formation. Two layers of Difco agar with different concentrations were set in individual wells of a 24-well plate. The lower layer contained 0.5 ml of 0.6% soft agar in medium with the indicated combinations of I3C and tamoxifen. The upper layer was composed of 0.5 ml of 0.3% soft agar in medium with MCF-7 cells (500 cells/well) and the corresponding combinations of I3C and tamoxifen in triplicate. After 4.5 weeks, all of the colonies that were <50 μm in diameter were counted.

Flow Cytometric Analyses of DNA Content. MCF-7 cells (4×10^4) were plated onto Corning six-well tissue culture dishes. Triplicate samples were treated with the indicated concentrations of I3C and tamoxifen. The medium was changed every 24 h. Cells were incubated for 96 h and hypotonically lysed in 1 ml of DNA staining solution (0.5 mg/ml propidium iodide, 0.1% sodium citrate, and 0.05% Triton X-100). Nuclear emitted fluorescence with wavelength of >585 nM was measured with a Coulter Elite instrument with laser output adjusted to deliver 15 mW at 488 nM. Nuclei (10,000) were analyzed from each sample at a rate of 300–500 nuclei/s. The percentages of cells within the G_1, S, and G_2-M phases of the cell cycle were determined by analysis with the Multicycle computer program provided by Phoenix Flow Systems in the Cancer Research Laboratory Microchemical Facility of the University of California, Berkeley.

Western Blot Analysis. After the indicated treatments, cells were harvested in radioimmunoprecipitation assay buffer (150 mM NaCl, 0.5% deoxycholate, 0.1% NP40, 0.1% SDS, and 50 mM Tris) containing protease and phosphatase inhibitors (50 μg/ml phenylmethylsulfonyl fluoride, 10 μg/ml aprotinin, 5 μg/ml leupeptin, 0.1 μg/ml NaF, and 10 μg/ml β-glycerophosphate). Equal amounts of total cellular protein were mixed with loading buffer [25% glycerol, 0.075% SDS, 1.25 ml of 14.4 M β-mercaptoethanol, 10% bromphenol blue, 3.13% 0.5 M Tris-HCl, and 0.4% SDS (pH 6.8)] and fractionated on 10% (7.5% for Rb) polyacrylamide/0.1% SDS resolving gels by electrophoresis. Rainbow marker (Amersham Life Sciences, Arlington Heights, IL) was used as the molecular weight standard. Proteins were electrically transferred to nitrocellulose membranes (Micron Separations, Inc., Westboro, MA) and blocked overnight at 4°C with Western wash buffer-5% NFDM [10 mM Tris-HCl (pH 8.0), 150 mM NaCl, and 0.05% Tween 20–5% nonfat dry milk). Blots were subsequently incubated for 1 h at room temperature for rabbit anti-CDK2, CDK4, CDK6, p16, p21, and cyclin D1 antibodies (Santa Cruz Biotechnology, Inc., Santa Cruz, CA) and overnight at 4°C for mouse anti-Rb and cyclin E antibodies (PharMingen, San Diego, CA). The working concentration for all antibodies was 1 μg/ml in Western wash buffer. Immunoreactive proteins were detected after incubation with horseradish peroxidase-conjugated secondary antibody diluted to 3×10^{-4} in Western wash buffer-1% NFDM [goat antirabbit IgG (Bio-Rad, Hercules, CA); rabbit antimouse IgG (Zymed, San Francisco, CA)]. Blots were treated with enhanced chemiluminescence reagents (NEN Life Science Products), and all proteins were detected by autoradiography. Equal protein loading was confirmed by Ponceau S staining of blotted membranes.

IP and CDK Kinase Assay. MCF-7 cells were cultured in growth medium with combinations of tamoxifen and I3C for the indicated times and then rinsed twice with PBS, harvested, and stored as dry pellets at −70°C. For the IP, cells were lysed for 15 min in IP buffer [50 mM Tris-HCl (pH 7.4), 200 mM NaCl, and 0.1% Triton X-100] containing protease and phosphatase inhibitors (50 μg/ml phenylmethylsulfonyl fluoride, 10 μg/ml aprotinin, 5 μg/ml leupeptin, 0.1 μg/ml NaF, 10 μg/ml β-glycerophosphate, and 0.1 mM sodium orthovanadate). Samples were diluted to 500 μg of protein in 1 ml of IP buffer. Samples were precleared for 30 min at 4°C with 20 μl of a 1:1 slurry of protein A-Sepharose beads (Pharmacia Biotech, Sweden) in IP buffer and 1 μg of rabbit IgG. After a brief centrifugation to remove precleared beads, 0.5 μg of

anti-CDK2 or anti-CDK6 antibody was added to each sample and incubated on a rocking platform at 4°C for 2 h. Then, 20 μl of protein A-Sepharose beads were added to each sample, and the slurries were incubated on the rocking platform at 4°C for 30 min. The beads were then washed five times with IP buffer and twice with kinase buffer (50 mM HEPES, 10 mM $MgCl_2$, 5 mM $MnCl_2$, 0.1 μg/ml NaF, 10 μg/ml β-glycerophosphate, and 0.1 mM sodium orthovanadate). Half of the immunoprecipitated sample was checked by Western blot analysis to confirm the IP.

For the kinase assay, the other half of the sample was resuspended in 25 μl of kinase buffer containing 20 mM ATP, 5 mM DTT, 0.21 μg of Rb COOH-terminal domain protein substrate (Santa Cruz Biotechnology), and 10 μCi of [γ-^{33}P]ATP (3000 Ci/mmol). Reactions were incubated for 15 min at 30°C and stopped by the addition of an equal volume of 2× loading buffer [10% glycerol, 5% β-mercaptoethanol, 3% SDS, 6.25 mM Tris-HCl (pH 6.8), and bromphenol blue]. Reaction products were boiled for 10 min and then electrophoretically fractionated in SDS-10% polyacrylamide gels. Gels were stained with Coomassie blue to monitor loading and destained overnight with 3% glycerol in 10% acetic acid. Subsequently, gels were dried and quantitated on a PhosphorImager (Molecular Dynamics, Sunnyvale, CA) and visualized by autoradiography.

Quantitation of Autoradiography. Autoradiographic exposures were scanned with a UMAX UC630 scanner, and band intensities were quantified using the NIH Image program. Autoradiographs from a minimum of three independent experiments were scanned per time point.

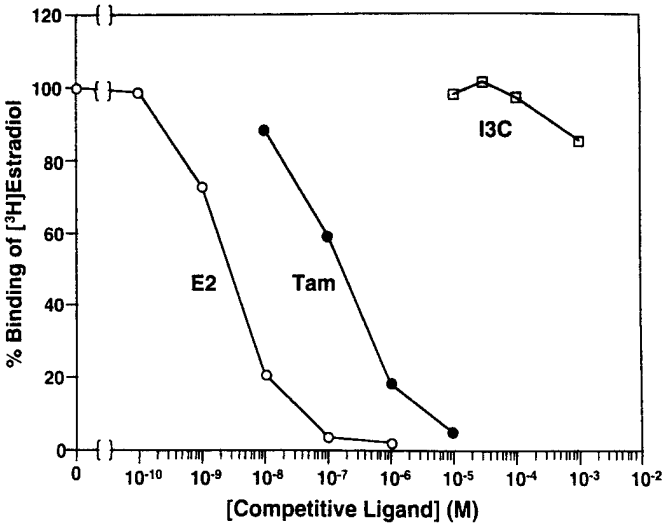

Fig. 2. Competitive binding to the estrogen receptor. The binding of [^{3}H]E2 (1 nM) to the estrogen receptor from rat uterine cytosol was measured in the presence of the unlabeled competitive ligands, E2 (○), Tam (●), and I3C (□), at the indicated concentrations as described in "Materials and Methods." The results are reported as the percentage of binding in the absence of competitors. Relative binding affinities were calculated using the concentration of competitor needed to reduce [^{3}H]E2 binding by 50% as compared to the concentration of unlabeled E2 to achieve the same result.

RESULTS

I3C and Tamoxifen Cooperate to Arrest the Growth of MCF-7 Cells. To determine the potential combinatorial effects of I3C and tamoxifen on the growth of an estrogen-dependent breast cancer cell line, MCF-7 cells were grown in medium supplemented with 10% FBS, which contains enough estrogen to support the proliferation of these cells. The cells were treated with 100 μM I3C, 1 μM tamoxifen, or a combination of I3C and tamoxifen over a 96-h time course (Fig. 1). These concentrations of I3C and tamoxifen were previously shown to decrease cell growth without affecting viability (6, 29). The cells were then pulse-labeled with [^{3}H]thymidine for 3 h at each time point to provide a measure of their proliferative state. Analysis of [^{3}H]thymidine incorporation revealed that tamoxifen caused a steady decrease in DNA synthesis over the time course with a 60% inhibition after 96 h of treatment. I3C treatment also resulted in a time-dependent decrease in DNA synthesis with a 90% inhibition after 96 h. The combination of I3C and tamoxifen yielded statistically similar results as I3C alone for the 24- and 48-h time points. However, by the 72- and 96-h time points, the combination of I3C and tamoxifen resulted in a more effective growth suppression than either agent alone, resulting in a 95% inhibition after 96 h of treatment.

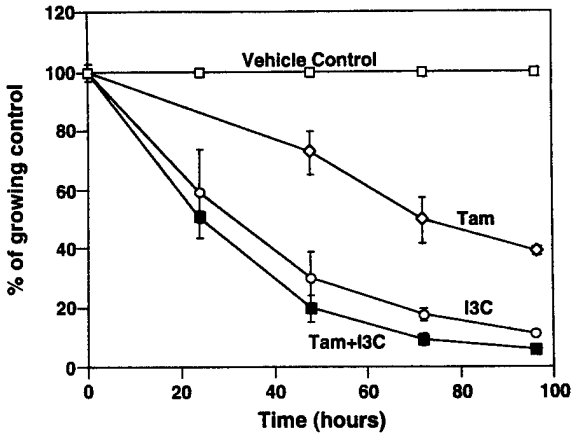

Fig. 1. Time course effects of I3C and tamoxifen on DNA synthesis in MCF-7 cells. MCF-7 cells cultured in 24-well dishes were treated for the indicated time with vehicle control (*Vehicle Control*; □), 1 μM tamoxifen (*Tam*; ◇), 100 μM I3C (*I3C*; ○), or a combination of tamoxifen and I3C (*Tam+I3C*; ■). Cells were labeled with [^{3}H]thymidine for 3 h, and the [^{3}H]thymidine incorporation into DNA was determined by acid precipitation as described in "Materials and Methods." The data are expressed as the percentage of growing control. This was calculated by dividing the value of the vehicle control-treated sample at each time point by the value of the drug-treated sample at the same time point. *Data points*, average of triplicate samples from six different experiments; *bars*, SE.

Because both I3C and the antiestrogen tamoxifen inhibited the growth of estrogen-responsive breast cancer cells, we wanted to determine whether I3C has any effect on estrogen receptor ligand binding. An *in vitro* competition binding assay for receptor-ligand interactions was used to examine the relative affinities of I3C and tamoxifen for the estrogen receptor. As a control and point of reference for the relative ligand affinity, unlabeled E2 was shown to effectively compete with [^{3}H]E2 binding to the estrogen receptor, with half-maximal competition occurring at ~3 nM (Fig. 2). As expected, tamoxifen has a relatively high affinity for the estrogen receptor with a half maximal [^{3}H]E2 displacement of ~200 nM. In contrast, I3C caused no significant displacement of [^{3}H]E2 binding to the estrogen receptor, even at 1 mM. For the remainder of this study, the highest concentration of tamoxifen used was 1 μM, which is within the range of E2 competition, and the highest concentration of I3C used was 100 μM, which does not compete with E2 for receptor binding.

Effects of I3C and Tamoxifen on Adherent Cell Growth and Anchorage-independent Cell Growth. To characterize the inhibitory effects of I3C and tamoxifen on adherent cell growth, MCF-7 cells were plated at low confluency (10,000 single cells per 100-mm plate) and grown for 8 days in medium containing the vehicle control or various doses of each agent alone or in combination. To visualize the cell colonies, the cells were stained and fixed in crystal violet/formalin. Representative plates of vehicle control, high doses of I3C (100 μM) or tamoxifen (1 μM) and the combination of I3C and tamoxifen are shown in Fig. 3*A*. The average integrated density of replicate areas on each plate was determined by NIH Image and normalized by dividing that value by the area that was measured on each plate. This measurement takes into account both the number and size of the colonies and is representative of the number of cells on each plate. Treatment with the high doses of I3C or tamoxifen alone inhibited cell colony formation by 80 and 65%, respectively, whereas

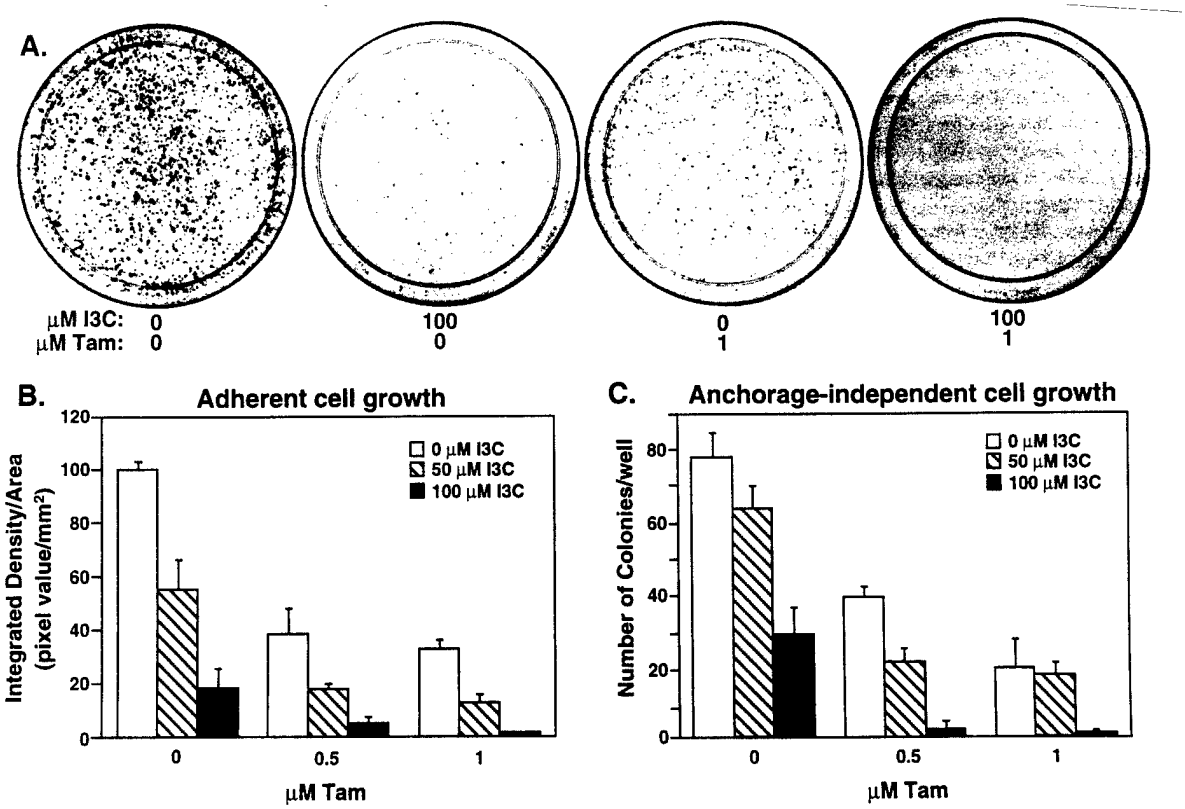

Fig. 3. Effects of I3C and tamoxifen on low confluency cell colony number in MCF-7 cells on plastic and in soft agar. *A*, four representative 100-mm plates of MCF-7 cells cultured for 8 days in the presence of the indicated concentrations of I3C and tamoxifen (*Tam*). At the end of the treatment the cells were fixed and stained as described in "Materials and Methods." *B*, quantification of the amount and size of the colonies on each plate treated with the indicated combination of I3C and tamoxifen was determined by calculating the integrated density using NIH Image. Data shown represent a detailed dose response. *Columns*, average of triplicate samples, expressed as integrated density in pixel value/area in mm^2; *bars*, SE. *C*, 500 MCF-7 cells were cultured in 0.3% soft agar as described in "Materials and Methods." After 4.5 weeks at the indicated concentrations of I3C and/or tamoxifen, colonies that were >50 μm in diameter were counted. *Columns*, average of triplicate samples; *bars*, SE.

a combination of both agents inhibited adherent cell growth by >95%. An expanded analysis of the dose-dependent suppression of adherent cell growth by I3C and tamoxifen is shown in Fig. 3*B*.

The effects of combinations of I3C and tamoxifen on the anchorage-independent growth of MCF-7 cells in soft agar was examined. Cells were cultured for 4.5 weeks in 0.3% agar and complete medium containing the vehicle control, I3C, tamoxifen, or a combination of both agents. Cell colonies that were >50 μm in diameter were counted. As shown in Fig. 3*C*, increasing doses of I3C or tamoxifen caused a decrease in cell colony formation, and consistent with the adherent cell growth properties, a combination of both agents caused a more pronounced decrease in cell colony formation. For both growth conditions, the combined inhibitory effect of suboptimal concentrations of I3C (50 μM) and tamoxifen (0.5 μM) approximated that observed with the highest doses of either I3C or tamoxifen alone.

Cell Cycle Effects of I3C and Tamoxifen. To assess the effect of combinations of I3C and tamoxifen on the cell cycle, MCF-7 cells were treated with the indicated concentrations of each compound for 96 h and then hypotonically lysed in the presence of propidium iodide to stain the nuclear DNA. Flow cytometry profiles revealed that treatment with increasing doses of I3C or tamoxifen lead to a dose-dependent shift in percentage of cells with a G_1-like DNA content. As shown in Fig. 4*A*, I3C or tamoxifen altered the DNA content of the MCF-7 cell population from an asynchronous population of growing cells in all phases of the cell cycle (61.4% in G_1, 29.0% in S, and 9.7% in G_2-M) to one in which most of the treated breast cancer cells were in the G_1 phase of the cell cycle (Fig. 4*A*, *top right* for I3C and *bottom left* for tamoxifen). Consistent with the cell growth studies, a combination of both agents caused a more striking shift to G_1 (Fig. 4*A*, *bottom right*). Incubation with suboptimal concentrations of both I3C and tamoxifen (Fig. 4*A*, *middle*) induced the G_1 shift to approximately the same extent as observed with the highest concentrations of either compound alone. As shown graphically in Fig. 4*B*, the I3C- and tamoxifen-mediated shift in number of G_1 cells (*top*) appeared to result from a decrease in S-phase cells (*middle*), whereas the G_2-M phase values did not significantly change (*bottom*).

The expression levels of specific cell cycle proteins that are responsible for progression through G_1 and/or transition into S phase were examined in cells treated for 96 h with combinations of 100 μM I3C and/or 1 μM tamoxifen. Western blot analysis revealed that I3C selectively decreased the level of CDK6 protein and increased the level of the p21 CDK inhibitor at this time point (Fig. 5). In contrast, tamoxifen had no effect on each of these cell cycle proteins under our cell culture conditions. Our previous studies show that I3C also slightly increases the level of the p27 CDK inhibitor protein (6), whereas tamoxifen has no effect on p27 protein levels (data not shown). The expression of the other cell cycle proteins tested, such as CDK2, CDK4, cyclin D1, and cyclin E, were not affected by either I3C or tamoxifen. The p16 CDK inhibitor was not detectable in the MCF-7 cells used for our study.

I3C and Tamoxifen Cooperate to Decrease the *in Vitro* Activity of CDK2 and the Phosphorylation of Endogenous Rb. The control of G_1 CDK enzymatic activity is critical for regulating cell cycle progression (22). The activity of specific CDKs is regulated, in part, by the composition of the holoenzyme, which includes the appropriate cyclin and/or CDK inhibitory proteins. Therefore, although the levels of CDK2 and CDK4 remain unaltered after I3C and/or tamoxifen treatment, we examined the potential effects of I3C and tamoxifen on

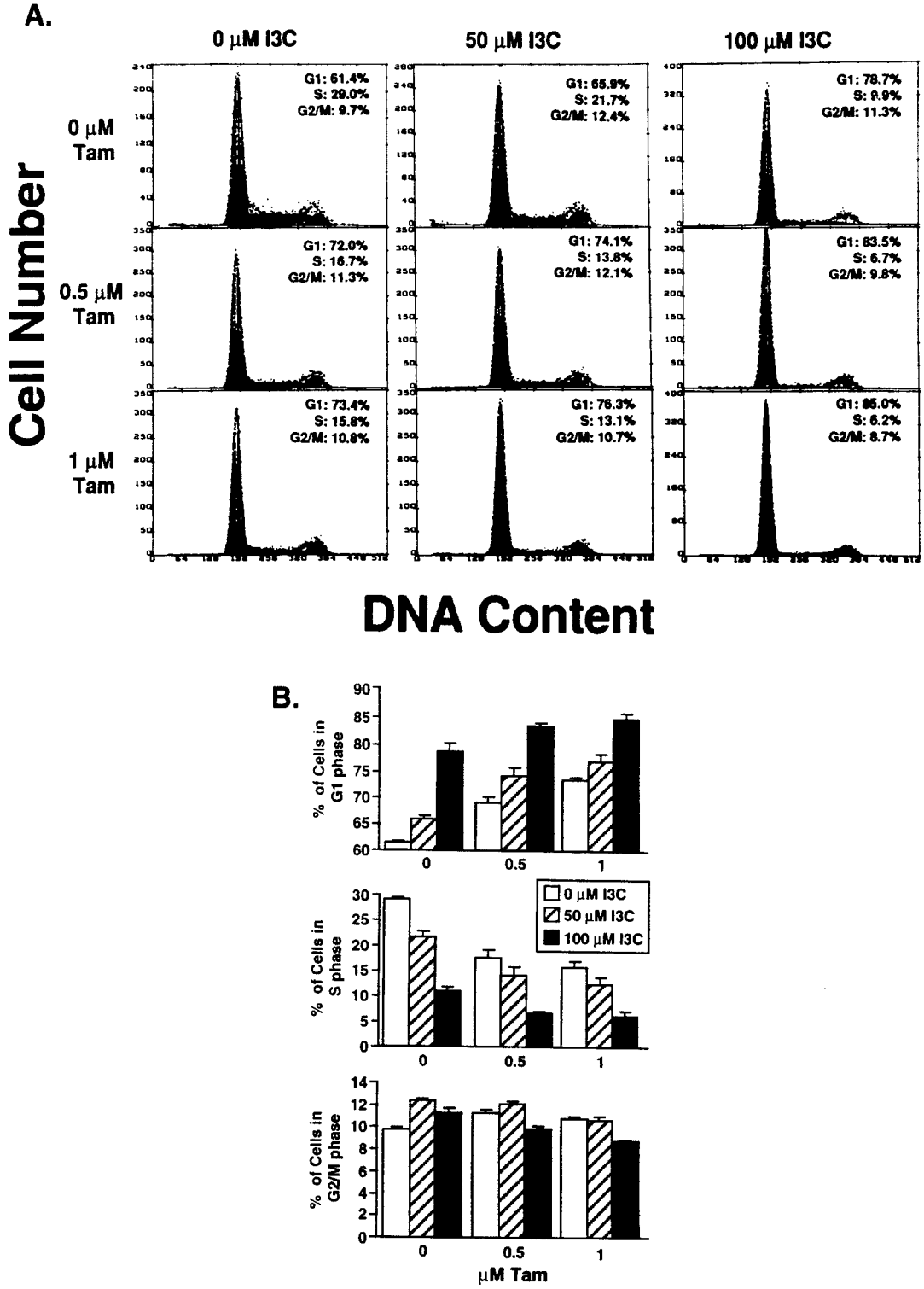

Fig. 4. Effects of I3C and tamoxifen on DNA content of MCF-7 cells. *A*, MCF-7 cells were treated with the indicated combinations of concentrations of I3C and tamoxifen (*Tam*) for 96 h. Cells were then stained with propidium iodide, and nuclei were analyzed for DNA content by flow cytometry with a Coulter Elite Laser. A total of 10,000 nuclei were analyzed from each sample, and the percentages of cells within G_1, S, and G_2-M were determined as described in "Materials and Methods." Representative profiles are shown for each condition, and the numbers in the upper right corner of the profiles are an average of triplicate samples. *B*, results from the flow cytometry profiles were converted into bar graphs. *Top*, G_1; *middle*, S; *bottom*, G_2-M, after the indicated treatments of doses of I3C and tamoxifen (*Tam*) for 96 h. *Bars*, SE.

G_1 CDK specific activities. Because one of the key endogenous substrates for the G_1 CDKs is the Rb protein, we determined the ability of the individual G_1 CDKs to phosphorylate Rb *in vitro*. MCF-7 cells were treated for 48 h with I3C and/or tamoxifen and then CDK2, CDK4, or CDK6 were immunoprecipitated from total cell extracts. For the kinase assays, half of each immunoprecipitated sample was incubated with the COOH-terminal domain of Rb fused to GST and [γ-^{33}P]ATP. The electrophoretically fractionated reaction products were quantitated on a PhosphorImager and then visualized by autoradiography. The other half of the immunoprecipitated samples were analyzed by Western blot and densitometry to confirm the efficiency and specificity of each IP. The CDK-specific activity was calculated by dividing the *in vitro* kinase activity by the corresponding protein expression. As shown in the CDK2 specific activity graph, increasing doses of I3C alone or tamoxifen alone resulted in dose-dependent decreases in CDK2-specific activity (Fig. 6). Treatment with combinations of these two growth inhibitors resulted in a more stringent decrease in CDK2-specific activity than either agent alone.

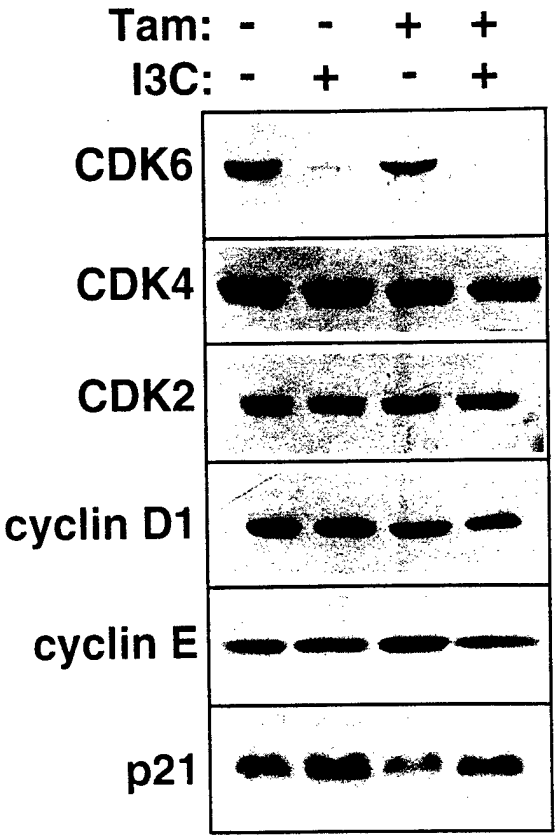

Fig. 5. Effects of I3C on expression of G_1 cell cycle proteins. MCF-7 cells were treated with 100 μM I3C and/or 1 μM tamoxifen (*Tam*) for 96 h, and the protein production of the G_1 cell cycle components was determined by Western blot analysis using specific antibodies. The same cell extracts were used for the analysis of each cell cycle protein, and equal sample loading was confirmed by Ponceau S staining of the Western blot membrane.

In contrast, I3C inhibited CDK6 protein expression, but the specific activity of the residual CDK6 protein remained unaltered. Tamoxifen had no effect on CDK6 protein expression or specific activity (Fig. 6). Thus, the decrease in CDK6 activity appears to result from the I3C-mediated decrease in CDK6 protein levels and not due to an effect on CDK6 enyzmatic activity. CDK4-specific activity was not affected by either tamoxifen or I3C (data not shown).

It was important to determine whether the *in vitro* kinase assay results reflected the phosphorylation status of endogenous Rb after treatment with the antiproliferative agents. Therefore, the levels of phosphorylated and hypophosphorylated Rb were examined in MCF-7 cells treated for 48 h with I3C, tamoxifen, or a combination of both agents. The extent of Rb phosphorylation was determined by probing Western blots with a Rb-specific antibody and analyzing the characteristic mobility shift of the hyperphosphorylated Rb protein. As shown in Fig. 7, I3C treatment, and to a lesser extent tamoxifen treatment, caused a decrease in total Rb protein levels and an increase in the relative levels of hypophosphorylated Rb (pRb). Most significantly, a combination of I3C and tamoxifen virtually ablated the expression of the hyperphosphorylated form of Rb (ppRb), which likely explains the more potent growth arrest observed in the presence of these two growth suppressors.

DISCUSSION

A wide range of extracellular signaling molecules either inhibit or stimulate the proliferation of mammalian cells through pathways that ultimately target specific components within G_1 (19, 22, 30). It is well established that tamoxifen can exert its growth-inhibitory effects in human breast cancer cells by antagonizing the estrogen receptor stimulation of cell cycle progression (18). We have recently documented that the dietary indole I3C can induce a G_1 block in cell cycle progression of breast cancer cell lines in the absence of estrogen receptor signaling (6). Depending on the antiproliferative pathways, cell cycle progression can be more effectively blocked through the coordinate actions of specific networks of cell cycle-regulated gene products (31). Our results have established that the antiproliferative cascades initiated by I3C and tamoxifen can cooperate to induce a more stringent growth suppression in breast cancer cells treated with a combination of both agents compared to treatment with either I3C or tamoxifen alone. We propose that the I3C- and tamoxifen-activated antiproliferative responses are mediated by distinct signal transduction pathways (see Fig. 8) that converge on the inhibition of CDK2-specific activity as a common target with a subsequent decrease in endogenous Rb phosphorylation.

The distinguishing feature of the I3C antiproliferative pathway is the rapid down-regulation of CDK6 expression (6), which accounts for the inhibition of total CDK6 activity in breast cancer cells. Tamoxifen had no apparent effect on either CDK6 protein levels or enzymatic activity. In contrast to tamoxifen, I3C did not compete with E2 for binding to the estrogen receptor and has been shown to exert its growth-suppressive effects in breast cancer cells irrespective of estrogen receptor status, such as in estrogen receptor-deficient breast cancer cells (6). The immediate cellular target for I3C or a specific metabolite is unknown. We propose (Fig. 8) that this extracellular signal binds to a target molecule that mediates the growth-inhibitory cascade. The sustained growth suppression of colonies in soft agar in the absence of a medium change for 4.5 weeks implies that I3C could be working through a stable compound that binds to a specific cellular component. I3C regulates several G_1-acting cell cycle components, including the down-regulation of CDK6 expression and the inhibition of CDK2-specific activity. Tamoxifen inhibited MCF-7 cell growth through its antiestrogenic effects because the cells were cultured in medium supplemented with 10% FCS, which contains enough endogenous estrogen to maintain the cells in a proliferative state. Other studies have shown that tamoxifen interferes with the estrogen stimulation of the cell cycle, which includes a disruption in the stimulation of CDK2 activity and Rb phosphorylation (32). Our results are consistent with these observations and we propose that the inhibition of CDK2-specific activity and Rb phosphorylation are common targets for both the I3C and tamoxifen pathways (Fig. 8) and, thereby, provides one mechanistic explanation for the more stringent growth suppression observed with both agents.

Several potential mechanisms could account the inhibition of CDK2-specific activity by the I3C and/or the tamoxifen pathways. For example, treatment with either agent could alter the composition of CDK2 holoenzyme complex resulting in inactive complexes that do not support the phosphorylation of Rb. Alternatively, because full activation of CDK2 requires phosphorylation on specific residues and removal of phosphates from other residues (17, 20, 33), the CDK2-specific kinases and phosphatases may be targets for either the I3C or tamoxifen pathways. The unique features of each pathway likely play a role in the more stringent inhibition of growth observed in cells treated with both I3C and tamoxifen. The I3C down-regulation of CDK6 expression could release other cell cycle factors contained within the CDK6 protein complexes and, thereby, shift the cellular equilibrium of these components in manner that alters the composition of the other G_1 CDK protein complexes. For example, enough CDK-inhibitory molecules could conceivably be released from the CDK6 protein complexes to negatively modulate the specific activity of CDK2. Furthermore, longer I3C treatments increase the level of the p21 CDK inhibitor, which could also influence CDK2-specific activ-

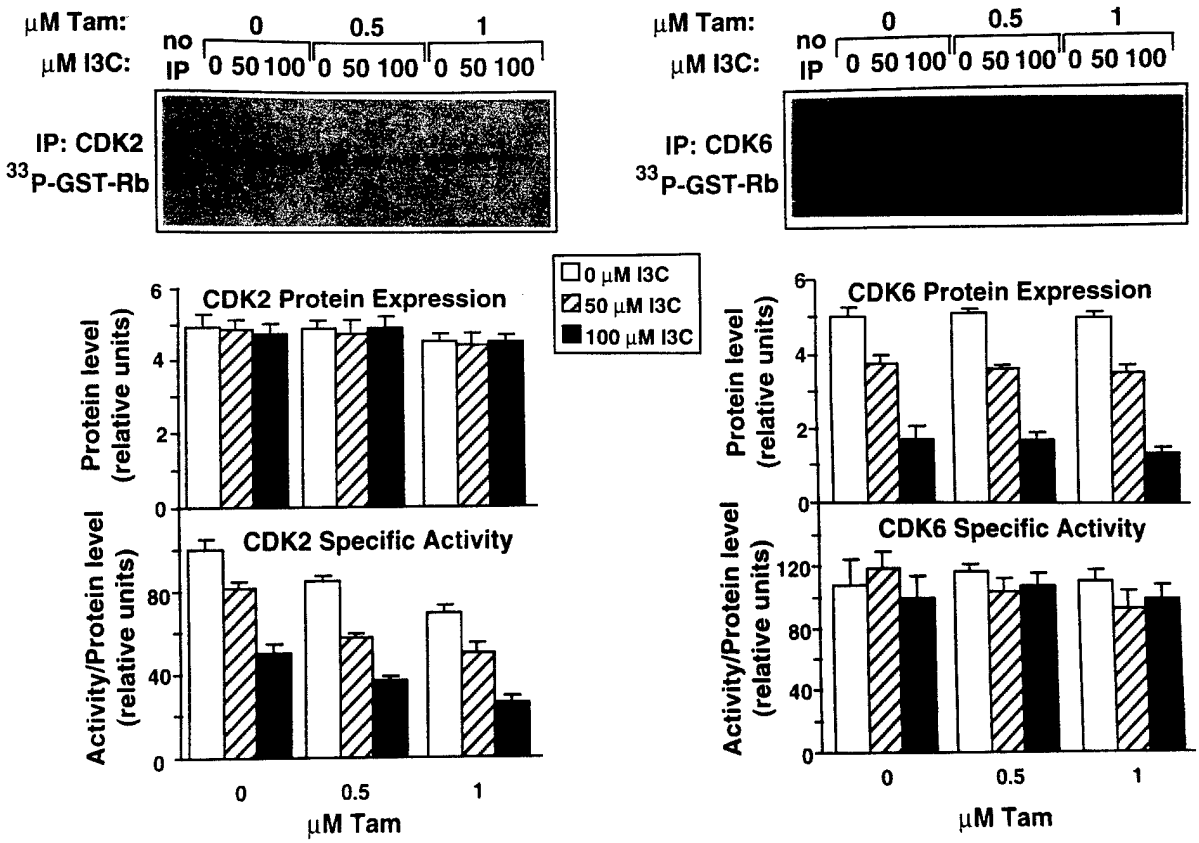

Fig. 6. Effects of I3C and tamoxifen on *in vitro* CDK2 and CDK6 kinase activity in MCF-7 cells. MCF-7 cells were treated with I3C and/or tamoxifen (*Tam*) for 48 h. CDK2 or CDK6 was immunoprecipitated from cell lysates and assayed for *in vitro* kinase activity using the COOH terminus of the Rb protein as a substrate (*GST-Rb*). One control immunoprecipitation (*no IP*) contained rabbit anti-IgG only in vehicle control-treated MCF-7 cell lysates. The kinase reaction mixtures were electrophoretically fractionated, and the level of [^{33}P]Rb (*pGST-Rb*) was quantitated by PhosphorImager analysis and visualized by autoradiography. The efficiency of the IP for each sample was confirmed and quantitated by Western blot analysis as described in "Materials and Methods." To normalize for IP efficiency, the specific activity was determined by dividing the values for the activity by the values for the protein level. *Columns*, average results of at least three kinase assays for each condition; *bars*, SE.

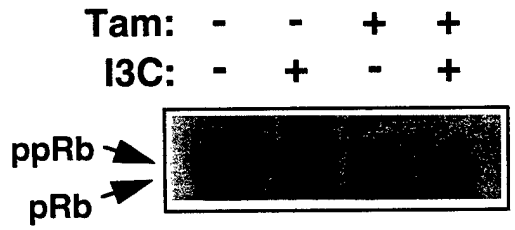

Fig. 7. Effects of I3C and tamoxifen on phosphorylation of endogenous Rb in MCF-7 cells. MCF-7 cells were treated with 100 μM I3C and/or 1 μM tamoxifen (*Tam*) for 48 h, the cell extracts were electrophoretically fractionated, and Western blots were probed with anti-Rb antibodies. The extent of endogenous Rb phosphorylation was determined by the characteristic migration of the hyperphosphorylated (*ppRb*) and hypophosphorylated (*pRb*) forms of Rb.

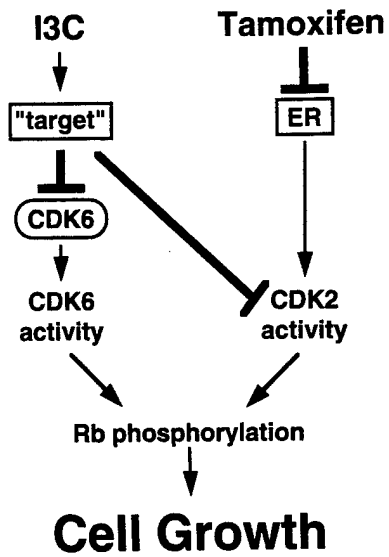

Fig. 8. Model for the comparison of the antiproliferative effects of I3C and tamoxifen in breast cancer cells. I3C potentially mediates its effects through a putative cellular target (*"target"*). I3C-induced breast cancer cell growth suppression is correlated with a rapid inhibition of CDK6 expression and activity and a decrease in the activity of CDK2. The inhibition of the activity of these two G_1-acting CDKs are most likely responsible for the decrease in retinoblastoma protein (Rb) phosphorylation and thereby results in the observed G_1 block in cell cycle progression. In contrast, tamoxifen mediates its effects by inhibiting the activity of the estrogen receptor, which prevents the estrogen-stimulated growth of breast cancer cells through a pathway that eventually converges on the activity of CDK2.

ity. However, within the 24-h time point when CDK2 activity is affected, neither p21 protein levels nor p21's ability to coimmunoprecipitate with CDK2 changes (data not shown). Thus, p21 does not appear to be responsible for I3C's ability to decrease CDK2 activity.

In addition to the differential cell cycle effects of I3C and tamoxifen, treatment with both compounds virtually eliminated colony formation in soft agar. This suggests the possibility that I3C could enhance the effectiveness of tamoxifen to control the growth of breast tumors *in vivo*. Tamoxifen has been shown to act as an estrogen agonist or antagonist, depending on cell type (reviewed in Ref. 12). The use of tamoxifen to treat estrogen-responsive breast cancers has extended the lives of many women (7–9). In addition, the preliminary

results of a clinical trial using tamoxifen as a preventative treatment for women that are at a high risk for breast cancer are very encouraging (34). However, approximately two-thirds of breast cancer patients have estrogen receptor-positive tumors, only half of which respond to tamoxifen therapy (35). Moreover, after 12–18 months of treatment, resistance to tamoxifen develops in all patients (36), and tamoxifen has been shown to actually stimulate the growth of breast cancer cells after prolonged treatment (37, 38). The molecular mechanism underlying the development of acquired resistance to antiestrogens is unclear, but continued exposure of cells to tamoxifen may select for cells able to grow without estrogen stimulation (39).

Our results suggest that I3C, in combination with tamoxifen, could overcome some of the drawbacks of tamoxifen therapy while capitalizing on the positive effects of this proven therapy. Lower doses and/or pulses of tamoxifen are two of the proposed methods of circumventing tamoxifen resistance (40). In this regard, our results showed that lower doses of tamoxifen and I3C inhibited MCF-7 cell growth and CDK2-specific activity to the same extent as higher doses of either agent added individually. In principle, this response could be exploited to circumvent acquired drug resistance to sustained high doses of tamoxifen. Alternatively, patients could conceivably receive intermittent pulses of tamoxifen while undergoing I3C treatment. I3C has been shown to reduce the formation of both spontaneous and carcinogen-induced mammary tumors in rodents with no apparent side effects (4, 41–43). Human subjects who ingested I3C also had no side effects (44, 45). To extend our current studies, we plan to examine the *in vivo* effectiveness of combinations of I3C and tamoxifen on the growth of tumors derived from estrogen-responsive and estrogen-nonresponsive breast cancer cell lines and to determine the mechanism by which the I3C and tamoxifen pathways cooperate to block cell cycle progression.

ACKNOWLEDGMENTS

We express our appreciation to members of both the Firestone and Bjeldanes laboratories for their helpful comments throughout the duration of this work. We also thank Jerry Kapler for his excellent photography and Peter Schow, Meredith L. Leong, Minnie Wu, and Tran Van for their technical assistance.

REFERENCES

1. Loub, W. D., Wattenberg, L. W., and Davis, D. W. Aryl hydrocarbon hydroxylase induction in rat tissues by naturally occurring indoles of cruciferous plants. J. Natl. Cancer Inst. (Bethesda), *54:* 985–988, 1975.
2. Wattenberg, L. W., and Loub, W. D. Inhibition of polycyclic aromatic hydrocarbon-induced neoplasia by naturally occurring indoles. Cancer Res., *38:* 1410–1413, 1978.
3. Morse, M. A., LaGreca, S. D., Amin, S. G., and Chung, F. L. Effects of indole-3-carbinol on lung tumorigenesis and DNA methylation induced by 4-(methylnitrosamino)-1-(3-pyridyl)-1-butanone (NNK) and on the metabolism and disposition of NNK in A/J mice. Cancer Res., *50:* 2613–2617, 1990.
4. Bradlow, H. L., Michnovicz, J., Telang, N. T., and Osborne, M. P. Effects of dietary indole-3-carbinol on estradiol metabolism and spontaneous mammary tumors in mice. Carcinogenesis (Lond.), *12:* 1571–1574, 1991.
5. Bjeldanes, L. F., Kim, J. Y., Grose, K. R., Bartholomew, J. C., and Bradfield, C. A. Aromatic hydrocarbon responsiveness-receptor agonists generated from indole-3-carbinol *in vitro* and *in vivo*: comparisons with 2,3,7,8-tetrachlorodibenzo-*p*-dioxin. Proc. Natl. Acad. Sci. USA, *88:* 9543–9547, 1991.
6. Cover, C. M., Hsieh, S. J., Tran, S. H., Hallden, G., Kim, G. S., Bjeldanes, L. F., and Firestone, G. L. Indole-3-carbinol inhibits the expression of cyclin-dependent kinase-6 and induces a G_1 cell cycle arrest of human breast cancer cells independent of estrogen receptor signaling. J. Biol. Chem., *273:* 3838–3847, 1998.
7. Pennisi, E. Drug's link to genes reveals estrogen's many sides. Science (Washington DC), *273:* 1171, 1996.
8. Powles, T. J. Efficacy of tamoxifen as treatment of breast cancer. Semin. Oncol., *24* (Suppl. 1): S1-48–S1-54, 1997.
9. Forbes, J. F. The control of breast cancer: the role of tamoxifen. Semin. Oncol., *24* (Suppl. 1): S1-5–S1-19, 1997.
10. Skidmore, J. R., Walpole, A. L., and Woodburn, J. Effect of some triphenylethylenes on oestradiol binding *in vitro* to macromolecules from uterus and anterior pituitary. J. Endocrinol., *52:* 289–298, 1972.
11. Jordan, V. C., and Prestwich, G. Binding of [^{3}H] tamoxifen in rat uterine cytosols. A comparison of swinging bucket and vertical tube rotor sucrose density gradient analysis. Mol. Cell. Endocrinol., *8:* 179–188, 1977.
12. Gallo, M. A., and Kaufman, D. Antagonistic and agonistic effects of tamoxifen: significance in human cancer. Semin. Oncol., *24* (Suppl. 1): S1-71–S1-80, 1997.
13. Tsai, L. C., Hung, M. W., Yuan, C. C., Chao, P. L., Jiang, S. Y., Chang, G. G., and Chang, T. C. Effects of tamoxifen and retinoic acid on cell growth and *c-myc* gene expression in human breast and cervical cancer cells. Anticancer Res., *17:* 4557–4562, 1997.
14. Lindner, D. J., Kolla, V., Kalvakolanu, D. V., and Borden, E. C. Tamoxifen enhances interferon-regulated gene expression in breast cancer cells. Mol. Cell. Biochem., *167:* 169–177, 1997.
15. Otto, A. M., Paddenberg, R., Schubert, S., and Mannherz, H. G. Cell-cycle arrest, micronucleus formation, and cell death in growth inhibition of MCF-7 breast cancer cells by tamoxifen and cisplatin. J. Cancer Res. Clin. Oncol., *122:* 603–612, 1996.
16. Hamel, P. A., and Hanley, H. J. G1 cyclins and control of the cell division cycle in normal and transformed cells. Cancer Invest., *15:* 143–152, 1997.
17. Musgrove, E. A., Swarbrick, A., Lee, C. S. L., Cornish, A. L., and Sutherland, R. L. Mechanisms of cyclin-dependent kinase inactivation by progestins. Mol. Cell. Biol., *18:* 1812–1825, 1998.
18. Prall, O., Sarcevic, B., Musgrove, E. A., Watts, C., and Sutherland, R. L. Estrogen-induced activation of Cdk4 and Cdk2 during G_1-S phase progression is accompanied by increased cyclin D1 expression and decreased cyclin-dependent kinase inhibitor association with cyclin E-Cdk2. J. Biol. Chem., *272:* 10882–10894, 1997.
19. Hunter, T., and Pines, J. Cyclins and cancer. II: cyclin D and CDK inhibitors come of age. Cell, *79:* 573–582, 1994.
20. Morgan, D. O. Principles of CDK regulation. Nature (Lond.), *374:* 131–134, 1995.
21. Sherr, C. J., and Roberts, J. M. Inhibitors of mammalian G1 cyclin-dependent kinases. Genes Dev., *9:* 1149–1163, 1995.
22. Sherr, C. J. Cancer cell cycles. Science (Washington DC), *274:* 1672–1677, 1996.
23. Hirai, H., Roussel, M. F., Kato, J. Y., Ashmun, R. A., and Sherr, C. J. Novel INK4 proteins, p19 and p18, are specific inhibitors of the cyclin D-dependent kinases CDK4 and CDK6. Mol. Cell. Biol., *15:* 2672–2681, 1995.
24. Reynisdottir, I., and Massague, J. The subcellular locations of p15(Ink4b) and p27(Kip1) coordinate their inhibitory interactions with cdk4 and cdk2. Genes Dev., *11:* 492–503, 1997.
25. Xiong, Y., Hannon, G. J., Zhang, H., Casso, D., Kobayashi, R., and Beach, D. p21 is a universal inhibitor of cyclin kinases. Nature (Lond.), *366:* 701–704, 1993.
26. Alessandrini, A., Chiaur, D. S., and Pagano, M. Regulation of the cyclin-dependent kinase inhibitor p27 by degradation and phosphorylation. Leukemia (Baltimore), *11:* 342–345, 1997.
27. Slansky, J. E., and Farnham, P. J. Introduction to the E2F family: protein structure and gene regulation. Curr. Top. Microbiol. Immunol., *208:* 1–30, 1996.
28. Santell, R. C., Chang, Y. C., Nair, M. G., and Helferich, W. G. Dietary genistein exerts estrogenic effects upon the uterus, mammary gland and the hypothalamic/pituitary axis in rats. J. Nutr., *127:* 263–269, 1997.
29. Bardon, S., Vignon, F., Derocq, D., and Rochefort, H. The antiproliferative effect of tamoxifen in breast cancer cells: mediation by the estrogen receptor. Mol. Cell. Endocrinol., *35:* 89–96, 1984.
30. Draetta, G. F. Mammalian G1 cyclins. Curr. Opin. Cell. Biol., *6:* 842–846, 1994.
31. Van heusden, J., Wouters, W., Ramaekers, F. C., Krekels, M. D., Dillen, L., Borgers, M., and Smets, G. The antiproliferative activity of all-*trans*-retinoic acid catabolites and isomers is differentially modulated by liarozole-fumarate in MCF-7 human breast cancer cells. Br. J. Cancer, *77:* 1229–1235, 1998.
32. Planas, S. M., and Weinberg, R. A. Estrogen-dependent cyclin E-cdk2 activation through p21 redistribution. Mol. Cell. Biol., *17:* 4059–4069, 1997.
33. Morgan, D. O. The dynamics of cyclin dependent kinase structure. Curr. Opin. Cell Biol., *8:* 767–772, 1996.
34. Smigel, K. Breast Cancer Prevention Trial shows major benefit, some risk. J. Natl. Cancer Inst. (Bethesda), *90:* 647–648, 1998.
35. Legha, S. S. Tamoxifen in the treatment of breast cancer. Ann. Intern. Med., *109:* 219–228, 1988.
36. Couillard, S., Gutman, M., Labrie, C., Belanger, A., Candas, B., and Labrie, F. Comparison of the effects of the antiestrogens EM-800 and tamoxifen on the growth of human breast ZR-75–1 cancer xenografts in nude mice. Cancer Res., *58:* 60–64, 1998.
37. Gottardis, M. M., and Jordan, V. C. Development of tamoxifen-stimulated growth of MCF-7 tumors in athymic mice after long-term antiestrogen administration. Cancer Res., *48:* 5183–5187, 1988.
38. Osborne, C. K., Coronado-Heinsohn, E. B., Hilsenbeck, S. G., McCue, B. L., Wakeling, A. E., McClelland, R. A., Manning, D. L., and Nicholson, R. I. Comparison of the effects of a pure steroidal antiestrogen with those of tamoxifen in a model of human breast cancer. J. Natl. Cancer Inst. (Bethesda), *87:* 746–750, 1995.
39. Wiebe, V. J., Osborne, C. K., Fuqua, S. A., and DeGregorio, M. W. Tamoxifen resistance in breast cancer. Crit. Rev. Oncol. Hematol., *14:* 173–188, 1993.
40. Lykkesfeldt, A. E. Mechanisms of tamoxifen resistance in the treatment of advanced breast cancer. Acta Oncol., *35* (Suppl. 5): 9–14, 1996.
41. Baldwin, W. S., and LeBlanc, G. A. The anti-carcinogenic plant compound indole-3-carbinol differentially modulates P450-mediated steroid hydroxylase activities in mice. Chem. Biol. Interact., *83:* 155–169, 1992.
42. Bradfield, C. A., and Bjeldanes, L. F. Effect of dietary indole-3-carbinol on intestinal and hepatic monooxygenase, glutathione *S*-transferase and epoxide hydrolase activities in the rat. Food Chem. Toxicol., *22:* 977–982, 1984.
43. McDanell, R., McLean, A. E., Hanley, A. B., Heaney, R. K., and Fenwick, G. R. The effect of feeding *Brassica* vegetables and intact glucosinolates on mixed-function-oxidase activity in the livers and intestines of rats. Food Chem. Toxicol., *27:* 289–293, 1989.
44. Michnovicz, J. J., and Bradlow, H. L. Induction of estradiol metabolism by dietary indole-3-carbinol in humans. J. Natl. Cancer Inst. (Bethesda), *82:* 947–949, 1990.
45. Bradlow, H. L., Michnovicz, J. J., Halper, M., Miller, D. G., Wong, G. Y., and Osborne, M. P. Long-term responses of women to indole-3-carbinol or a high fiber diet. Cancer Epidemiol. Biomark. Prev., *3:* 591–595, 1994.

THE JOURNAL OF BIOLOGICAL CHEMISTRY
Vol. 273, No. 7, Issue of February 13, pp. 3838–3847, 1998
Printed in U.S.A.

Indole-3-carbinol Inhibits the Expression of Cyclin-dependent Kinase-6 and Induces a G_1 Cell Cycle Arrest of Human Breast Cancer Cells Independent of Estrogen Receptor Signaling*

(Received for publication, July 21, 1997, and in revised form, October 29, 1997)

Carolyn M. Cover‡, S. Jean Hsieh, Susan H. Tran, Gunnell Hallden, Gloria S. Kim, Leonard F. Bjeldanes§, and Gary L. Firestone¶

From the Department of Molecular and Cell Biology and Cancer Research Laboratory and the §Department of Nutritional Sciences, University of California, Berkeley, California 94720

Indole-3-carbinol (I3C), a naturally occurring component of *Brassica* vegetables such as cabbage, broccoli, and Brussels sprouts, has been shown to reduce the incidence of spontaneous and carcinogen-induced mammary tumors. Treatment of cultured human MCF7 breast cancer cells with I3C reversibly suppresses the incorporation of [^{3}H]thymidine without affecting cell viability or estrogen receptor (ER) responsiveness. Flow cytometry of propidium iodide-stained cells revealed that I3C induces a G_1 cell cycle arrest. Concurrent with the I3C-induced growth inhibition, Northern blot and Western blot analyses demonstrated that I3C selectively abolished the expression of cyclin-dependent kinase 6 (CDK6) in a dose- and time-dependent manner. Furthermore, I3C inhibited the endogenous retinoblastoma protein phosphorylation and CDK6 phosphorylation of retinoblastoma *in vitro* to the same extent. After the MCF7 cells reached their maximal growth arrest, the levels of the p21 and p27 CDK inhibitors increased by 50%. The antiestrogen tamoxifen also suppressed MCF7 cell DNA synthesis but had no effect on CDK6 expression, while a combination of I3C and tamoxifen inhibited MCF7 cell growth more stringently than either agent alone. The I3C-mediated cell cycle arrest and repression of CDK6 production were also observed in estrogen receptor-deficient MDA-MB-231 human breast cancer cells, which demonstrates that this indole can suppress the growth of mammary tumor cells independent of estrogen receptor signaling. Thus, our observations have uncovered a previously undefined antiproliferative pathway for I3C that implicates CDK6 as a target for cell cycle control in human breast cancer cells. Moreover, our results establish for the first time that CDK6 gene expression can be inhibited in response to an extracellular antiproliferative signal.

Considerable epidemiological evidence suggests that high vegetable diets correlate with low breast cancer risk (1, 2). This phenomenon is likely due to the diverse spectrum of dietary and environmental compounds that can regulate the function and proliferation of mammalian cells by influencing hormone receptor signal transduction pathways (3, 4). Several classes of these naturally occurring hormone-like chemicals have been implicated in the control of tumor cell growth and as chemopreventative agents. One such substance is the dietary compound indole-3-carbinol (I3C),[1] an autolysis product of a glucosinolate, glucobrassicin, which occurs in *Brassica* vegetables such as cabbage, broccoli, and Brussels sprouts (5, 6). A recent screen of 90 potential chemopreventative agents in a series of six short term bioassays relevant to carcinogen-induced DNA damage, oxidative stress, and tumor initiation and promotion, revealed I3C to be one of only eight compounds effective in all assays (7). Several studies have shown that exposure to dietary I3C markedly reduces the incidence of spontaneous and carcinogen-induced mammary tumors in rodents (8, 9). For example, I3C administered in the diet or by oral intubation prior to treatment with carcinogen reduced the incidence of 7,12-dimethyl-benz(a)anthracene-induced mammary tumors in rodents by 70–90% (6, 10). Consistent with these results, dietary supplementation with cabbage or broccoli, vegetables that are good sources of I3C, also resulted in decreased mammary tumor formation in 7,12-dimethyl-benz(a)anthracene-treated rats (11). Also, in a long term feeding experiment, in which female mice consumed synthetic diets containing I3C, spontaneous mammary tumor incidence and multiplicity were reduced by 50% and tumor latency was prolonged compared with untreated control animals (9). I3C also has anticarcinogenic effects on other cancer types, such as hepatic tumors (12) and can reduce benzo(a)pyrene-induced neoplasia of the forestomach (6).

I3C has been shown to have an antiestrogenic activity *in vivo*, which has been proposed to account for some of its protective and antiproliferative effects on mammary tumor formation. Part of this effect may be due to alterations in estrogen metabolism, since oral administration of I3C to humans increased estradiol 2-hydroxylation by approximately 50% in both men and women (13) and also increased the levels of estradiol hydroxylation activity in female rats (14). In addition, I3C was shown to block the estradiol-induced proliferation of long term confluent cultures of human breast cancer cells (15).

* This work was supported by Department of Defense Army Breast Cancer Research Program Grant DAMD17-96-1-6149 (to L. J. B.), and in the later stages this work was also supported by University of California Breast Cancer Research Program Grant 31B-0110 (to G. L. F.). The costs of publication of this article were defrayed in part by the payment of page charges. This article must therefore be hereby marked "*advertisement*" in accordance with 18 U.S.C. Section 1734 solely to indicate this fact.

‡ Predoctoral trainee supported by National Institutes of Health National Research Service Grant CA-09041.

¶ To whom correspondence and reprint requests should be addressed: Dept. of Molecular and Cell Biology, 591 LSA, University of California, Berkeley, CA 94720. Tel.: 510-642-8319; Fax: 510-643-6791; E-mail: glfire@mendel.berkeley.edu.

[1] The abbreviations used are: I3C, indole-3-carbinol; Ah, aromatic hydrocarbon; BrdUrd, 5-bromo-2′-deoxyuridine; CAT, chloramphenicol acetyltransferase; CDK, cyclin-dependent kinase; CS, calf serum; DIM, 3,3′-diindolylmethane; ER, estrogen receptor; ERE, estrogen response element; FBS, fetal bovine serum; GAPDH, glyceraldehyde-3-phosphate dehydrogenase; ICZ, indolo(3,2-*b*)carbazole; NFDM, nonfat dry milk; PBS, phosphate-buffered saline; Rb, retinoblastoma; HPLC, high pressure liquid chromatography; IP, immunoprecipitation.

A major complication in interpreting the physiological results is that I3C is extremely unstable in acidic solution and does not withstand exposure to the low pH environment of the stomach (16). A relatively large fraction of I3C is converted into several acid-catalyzed derivatives with distinct biological activities that appear to mediate the antiestrogenic effects of I3C. Two of the most active acid products of I3C that have been identified are 3,3'-diindolylmethane (DIM) and indolo(3,2-*b*)carbazole (ICZ) (17).

A general picture has emerged indicating that many of the long term antiestrogenic biological activities of I3C probably result from the actions of one or more of its acid-catalyzed derivatives (17, 18). ICZ appears to mediate its antiestrogenic effects by the direct binding to the Ah receptor (aromatic hydrocarbon or dioxin receptor), inducing cytochrome P450 *CYP1A1* gene expression (19), which can alter estrogen metabolism, thereby effectively decreasing the amount of circulating estrogen. This reduction in circulating estrogen leads to the decreased growth of estrogen-responsive mammary tissue and, presumably, a protective effect against breast cancer. ICZ exhibits only a very weak affinity for the ER but is the most potent Ah receptor agonist among the characterized I3C acid-catalyzed derivative compounds. In contrast, I3C has approximately 100,000-fold lower affinity for the Ah receptor compared with ICZ (K_d of 190 pM) and 3000-fold lower affinity compared with DIM (K_d of 90 nM) (17). Thus, it is unlikely that I3C mediates its activities directly through the Ah receptor, and conceivably this dietary indole may exert many of its direct growth-inhibitory effects through a signal transduction pathway distinct from the antiestrogenic effects of its acid-catalyzed products. However, virtually nothing is known about the mechanism by which I3C mediates its antiproliferative effects on human breast cancer cells. The I3C-regulated cellular processes are likely to be complex, however, because both estrogen-independent and estrogen-dependent pathways may potentially be under indole control.

Analogous to most other antiproliferative signaling molecules in mammalian cells, the I3C growth suppression pathway probably targets specific components and stages within the cell cycle. The eukaryotic cell cycle is composed of four phases (G_1 (gap 1), DNA synthesis (S), G_2 (gap 2), and mitosis (M)) as well as an out of cycle quiescent phase designated G_0. In normal mammary epithelial cells, an intricate network of growth-inhibitory and -stimulatory signals are transduced from the extracellular environment and converge on G_1-acting components, which, through their concerted actions, stringently regulate cell cycle progression (20, 21). The final targets of these growth signaling pathways are specific sets of cyclin-cyclin-dependent kinase (CDK) protein complexes, which function at specific, but overlapping, stages of the cell cycle (22–24). An active CDK complex phosphorylates retinoblastoma (Rb) protein family members. Rb and its related proteins sequester the E2F transcription factor, and the phosphorylation of Rb proteins by the active CDKs releases E2F, which then induces the expression of genes involved in the initiation of DNA synthesis (25). In the G_1 phase of the cell cycle, certain cyclins (C, D1, D2, D3, E) are necessary for activation the G_1 CDKs (CDK2, CDK4, and CDK6), while, in a complementary manner, several of the small proteins associated with cyclin-CDK complexes (p15, p16/Ink4a, p21/Waf1/Cip1, p27/Kip1, p57/Kip2) have been shown to act as specific inhibitors of cyclin-dependent kinase activity (26–29). The loss of normal cell cycle control in G_1 has been implicated in mammary tumor development and proliferation. Up to 45% of human breast cancers show an aberrant expression and/or amplification of cyclin D1 or cyclin E (30, 31). In other studies, inappropriate expression and/or mutation of certain G_1-acting proto-oncogenes, growth factors, and their cognate receptors has been observed in both human and rodent mammary tumor cells (31–33). Furthermore, many tumors exhibit a loss in expression or function of certain tumor suppressor genes (such as p53), which modulate cell cycle events late in the G_1 phase (34, 35).

Regulated changes in the expression and/or activity of cell cycle components that act within G_1 have been closely associated with alterations in the proliferation rate of normal and transformed mammary epithelial cells (4). For example, the estrogen-induced activation of CDK4 and CDK2 during progression of human breast cancer cells between the G_1 and S phases is accompanied by the increased expression of cyclin D1 and decreased association of the CDK inhibitors with the cyclin E-CDK2 complex (36). In rat tumor cells derived from 7,12-dimethyl-benz(a)anthracene-induced mammary adenocarcinomas, glucocorticoids induce a G_1 cell cycle arrest and alter expression of cell cycle-regulated genes (37). Thus, it seemed likely that dietary indoles control the emergence and proliferation of breast cancer cells by regulating G_1-acting cell cycle components in mammary epithelial cells. In this study, we demonstrate that the dietary indole I3C, but not the acid-catalyzed derivative DIM or ICZ, inhibits the growth of human MCF7 breast cancer cells and induces a G_1 cell cycle arrest in an ER-independent manner. Strikingly, this growth arrest is accompanied by the selective inhibition in expression of CDK6 transcripts, CDK6 protein, and the activity of CDK6, which correlates with a decrease in endogenous Rb phosphorylation.

EXPERIMENTAL PROCEDURES

Materials—Dulbecco's modified Eagle's medium, fetal bovine serum (FBS), calf serum (CS), calcium-free and magnesium-free phosphate buffered saline (PBS), L-glutamine, and trypsin-EDTA were supplied by BioWhittaker (Walkersville, MD). Insulin (Bovine), 17β-estradiol, and tamoxifen ((*Z*)-1-(*p*-dimethylaminoethoxyphenyl)-1,2-diphenyl-1-butene) citrate salt were obtained from Sigma. [^{3}H]Thymidine (84 Ci/mmol), [γ-^{32}P]ATP (6,000 Ci/mmol), and [α-^{32}P]dCTP (3,000 Ci/mmol) were obtained from NEN Life Science Products. Indole-3-carbinol (I3C) was purchased from Aldrich. I3C was recrystallized in hot toluene prior to use, while ICZ and DIM were prepared and purified as described (17). The sources of other reagents used in the study are either listed in the following methods or were of the highest purity available.

Cell Culture—The human breast adenocarcinoma cell lines, MCF7 and MDA-MB-231, were obtained from the American Type Culture Collection (Rockville, MD). MCF7 cells were grown in Dulbecco's modified Eagle's medium supplemented with 10% FBS, 10 μg/ml insulin, 50 units/ml penicillin, 50 units/ml streptomycin, and 2 mM L-glutamine. MDA-MB-231 cells were grown in Dulbecco's modified Eagle's medium supplemented with 10% FBS, 50 units/ml penicillin, 50 units/ml streptomycin, and 2 mM L-glutamine. Both cell lines were maintained at 37 °C in humidified air containing 5% CO_2 at subconfluency. I3C, tamoxifen, and estradiol were dissolved in Me_2SO (99.9% HPLC grade, Aldrich) at concentrations 1000-fold higher than the final medium concentration. In all experiments, 1 μl of the concentrated agent was added per ml of medium, and for the vehicle control, 1 μl of Me_2SO was added per ml of medium.

[^{3}H]Thymidine Incorporation—Breast cancer cells were plated onto 24-well Corning tissue culture dishes. Triplicate samples of asynchronously growing mammary cells were treated for the indicated times with either vehicle control (1 μl of Me_2SO/ml of medium) or varying concentrations of I3C, estradiol, and/or tamoxifen. The cells were pulsed for 3 h with 3 μCi of [^{3}H]thymidine (84 Ci/mmol), washed three times with ice-cold 10% trichloroacetic acid, and lysed with 300 μl of 0.3 N NaOH. Lysates (150 μl) were transferred into vials containing liquid scintillation mixture, and radioactivity was quantitated by scintillation counting. Triplicates were averaged and expressed as counts/min/well.

Flow Cytometric Analyses of DNA Content—Breast cancer cells (4×10^4) were plated onto Corning six-well tissue culture dishes. A final concentration of 100 μM I3C was added to three of the wells, and vehicle control (1 μl of Me_2SO/ml of medium) was added to the other three. The medium was changed every 24 h. Cells were incubated for 96 h and hypotonically lysed in 1 ml of DNA staining solution (0.5 mg/ml propidium iodide, 0.1% sodium citrate, 0.05% Triton X-100). Nuclear emit-

ted fluorescence with wavelength greater than 585 nm was measured with a Coulter Elite instrument with laser output adjusted to deliver 15 milliwatts at 488 nm. Nuclei (10,000) were analyzed from each sample at a rate of 300–500 cells/s. The percentages of cells within the G_1, S, and G_2/M phases of the cell cycle were determined by analysis with the Multicycle computer program provided by Phoenix Flow Systems in the Cancer Research Laboratory Microchemical Facility of the University of California, Berkeley.

Western Blot Analysis—After the indicated treatments, cells were harvested in radioimmune precipitation buffer (150 mM NaCl, 0.5% deoxycholate, 0.1% Nonidet P-40, 0.1% SDS, 50 mM Tris) containing protease and phosphatase inhibitors (50 μg/ml phenylmethylsulfonyl fluoride, 10 μg/ml aprotinin, 5 μg/ml leupeptin, 0.1 μg/ml NaF, 10 μg/ml β-glycerophosphate). Equal amounts of total cellular protein were mixed with loading buffer (25% glycerol, 0.075% SDS, 1.25% 2-mercaptoethanol, 10% bromphenol blue, 3.13% stacking gel buffer) and fractionated by electrophoresis on 10% (7.5% for Rb) polyacrylamide, 0.1% SDS resolving gels. Rainbow marker (Amersham Life Sciences) was used as the molecular weight standard. Proteins were electrically transferred to nitrocellulose membranes (Micron Separations, Inc., Westboro, MA) and blocked overnight at 4 °C with Western wash buffer and 5% NFDM (10 mM Tris HCl, pH 8.0, 150 mM NaCl, 0.05% Tween 20, 5% nonfat dry milk) (PBS, 5% nonfat dry milk for Rb). Blots were subsequently incubated for 1 h at room temperature for rabbit anti-CDK2, -CDK4, -CDK6, and -ER antibodies (Santa Cruz Biotechnology, Inc. (Santa Cruz, CA), catalog numbers sc-163, sc-260, sc-177, and sc-543, respectively), 2 h at room temperature for goat anti-p21, rabbit anti-cyclin E, and rabbit anti-p27 antibodies (Santa Cruz Biotechnology, catalog numbers sc-397, sc-198, and sc-528, respectively), and overnight at 4 °C for mouse anti-cyclin D1 and mouse anti-Rb antibodies (Santa Cruz Biotechnology, catalog number sc-246; Pharmingen (San Diego, CA), catalog number 14001A, respectively). Working concentration for all antibodies was 1 μg/ml Western wash buffer (PBS for Rb). Immunoreactive proteins were detected after incubation with horseradish peroxidase-conjugated secondary antibody diluted to 3×10^{-4} in Western wash buffer, 1% NFDM (goat anti-rabbit IgG (Bio-Rad); rabbit anti-mouse IgG (Zymed, San Francisco, CA); donkey anti-goat IgG (Santa Cruz Biotechnology)). Blots were treated with ECL reagents (NEN Life Science Products), and all proteins were detected by autoradiography. Equal protein loading was ascertained by Ponceau S staining of blotted membranes.

Immunoprecipitation and CDK6 Kinase Assay—Breast cancer cells were cultured for 0, 15, 24, 48, or 96 h in growth medium with or without 100 μM I3C and then rinsed twice with PBS, harvested, and stored as dry pellets at −70 °C. For the immunoprecipitation, cells were lysed for 15 min in immunoprecipitation (IP) buffer (50 mM Tris-HCl, pH 7.4, 200 mM NaCl, 0.1% Triton X-100) containing protease and phosphatase inhibitors (50 μg/ml phenylmethylsulfonyl fluoride, 10 μg/ml aprotinin, 5 μg/ml leupeptin, 0.1 μg/ml NaF, 10 μg/ml β-glycerophosphate, 0.1 mM sodium orthovanadate). Samples were diluted to 500 μg of protein in 1 ml of IP buffer, and samples were precleared for 2 h at 4 °C with 40 μl of a 1:1 slurry of protein A-Sepharose beads (Pharmacia Biotech, Uppasala, Sweden) in IP buffer and 1 μg of rabbit IgG. After a brief centrifugation to remove precleared beads, 0.5 μg of anti-CDK6 antibody was added to each sample and incubated on a rocking platform at 4 °C for 2 h. Then 10 μl of protein A-Sepharose beads were added to each sample, and the slurries were incubated on the rocking platform at 4 °C for 30 min. The beads were then washed five times with IP buffer and twice with kinase buffer (50 mM HEPES, 10 mM $MgCl_2$, 5 mM $MnCl_2$, 0.1 μg/ml NaF, 10 μg/ml β-glycerophosphate, 0.1 mM sodium orthovanadate). Half of the immunoprecipitated sample was checked by Western blot analysis to confirm the immunoprecipitation.

For the kinase assay, the other half of the immunoprecipitated sample was resuspended in 25 μl of kinase buffer containing 20 mM ATP, 5 mM dithiothreitol, 0.21 μg of Rb carboxyl-terminal domain protein substrate (Santa Cruz Biotechnology, catalog number sc-4112), and 10 μCi of [γ-^{32}P]ATP (6000 Ci/mmol). Reactions were incubated for 15 min at 30 °C and stopped by adding an equal volume of 2 × loading buffer (10% glycerol, 5% β-mercaptoethanol, 3% SDS, 6.25 mM Tris-HCl, pH 6.8, and bromphenol blue). Reaction products were boiled for 10 min and then electrophoretically fractionated in SDS-10% polyacrylamide gels. Gels were stained with Coomassie Blue to monitor loading and destained overnight with 3% glycerol. Subsequently, gels were dried and visualized by autoradiography.

Isolation of Poly(A)$^+$ RNA and Northern Blot Analysis—Poly(A)$^+$ RNA was isolated from MCF7 cells treated with either 100 μM I3C or vehicle control (1 μl of Me_2SO/ml of medium) for 5 or 15 h as described previously (38). For Northern blot analysis, 10 μg of poly(A)$^+$ RNA was electrophoretically fractionated in 6% formaldehyde, 1% agarose gels, transferred onto Nytran nylon membranes (Schleicher and Schuell), and UV-cross-linked in a UV Stratalinker (Stratagene, La Jolla, CA). Membranes were preannealed with 100 μg/ml denatured salmon sperm DNA in hybridization buffer (5 × Denhardt's reagent, 5 × SSC, 50% formamide) and subsequently hybridized for 16–20 h with cDNA probes [α-^{32}P]dCTP-labeled by random primer extension (Boehringer Mannheim). For detection of CDK6 transcripts, the cDNA probe was added to the hybridization buffer at a concentration of 6 million cpm/ml. CDK6 membranes were washed twice for 10 min with 2 × SSC at room temperature followed by two 1-h-long washes with 0.2 × SSC, 0.1% SDS at 60 °C. For detection of glyceraldehyde-3-phosphate dehydrogenase (GAPDH), CDK2, and CDK4 transcripts, the cDNA probe was added to the hybridization buffer at a concentration of 2 million cpm/ml. These membranes were subsequently washed with 2 × SSC twice at room temperature for 10 min followed by two 30-min washes at 60 °C in 0.2 × SSC, 0.1% SDS. The membranes were placed under film and analyzed after 4-h to 6-day exposures at −80 °C. CDK2, -4, and -6 transcripts were detected using purified *Bam*HI fragments of the pCMVcdk2, pCMVcdk4, or pCMVcdk6 plasmids containing the respective cDNA for each of the CDKs. The CDK plasmids were a generous gift from Ed Harlow's laboratory as described (39). GAPDH transcripts were detected with a 560-base pair *Xba*I/*Hin*D III cDNA fragment of the corresponding cDNA.

Quantitation of Autoradiography—Autoradiographic exposures were scanned with a UMAX UC630 scanner and band intensities were quantified using the NIH Image program. Autoradiographs from a minimum of three independent experiments were scanned per time point.

Transfection Procedure—Subconfluent breast cancer cells were propagated for at least 1 week in either low (5% CS) or high serum (10% FBS) containing medium prior to plating onto 60-mm Corning dishes 24 h before transfection in the appropriate medium. DNA-lipofectamine (Life Technologies, Inc.) mixtures were prepared by mixing 1 μg of ERE-vit-CAT reporter (−596 to +21 of the *Xenopus laevis* vitellogenin B1 genomic clone plus a consensus estrogen response element (ERE) subcloned into the *Hin*dIII site upstream of the chloramphenicol acetyltransferase (CAT) reporter gene in the SVOCAT vector, a generous gift from D. J. Shapiro (University of Illinois)) with 5 μl of lipofectamine in a total volume of 100 μl for 15 min at room temperature. The cells were washed twice with serum-free medium, and 100 μl of the liposome complex was added to each plate. After a 5-h incubation at 37 °C, the transfection was terminated by adding an equal volume of 2 × media containing either 10% CS or 20% FBS. Complete medium was replaced 18–24 h post-transfection, at which time appropriate agents (*e.g.* estrogen, tamoxifen, and I3C) were added. pCAT-basic vector (Promega, Madison, WI), which contains the promoterless CAT cDNA, was used as a negative control to determine background CAT activity.

CAT Assay—Cells were harvested by washing in PBS, resuspended in 100 mM Tris-HCl, pH 7.8, and lysed by three freeze/thaw cycles, 5 min/cycle. Cell lysates were heated at 68 °C for 15 min and centrifuged at $1.4 \times 10^4 \times g$ for 10 min, and the supernatant fractions were recovered. CAT activity in the cell extracts containing 20–50 μg of lysate protein was measured by a quantitative nonchromatographic assay (40). The enzyme assay was carried out in 100 mM Tris-HCl, pH 7.8, 1 mM aqueous chloramphenicol, and 1 μCi of [^{3}H]acetyl coenzyme A (final reaction volume of 250 μl). The reaction mixture was overlaid with 4 ml of Econofluor scintillation fluorochrome (NEN Life Science Products). CAT activity was monitored by direct measurement of radioactivity by liquid scintillation counting. Measurements of CAT activity were in the linear range of the assay as determined by a standard curve using bacterial CAT enzyme (0.01 units; Pharmacia), the positive control for CAT enzymatic activity. Reaction mixtures were incubated at 37 °C for 2–6 h. Mock-transfected cells were used to establish basal level activity for both assays. The enzyme activity was expressed as CAT activity produced per μg of protein present in corresponding cell lysates as measured by a Bradford assay, and the results show averages of triplicate samples.

5-Bromo-2′-deoxyuridine (BrdUrd) Incorporation and Indirect Immunofluorescence—MCF7 cells grown on eight-well Lab-Tek Permanox slides (Nalge Nunc International, Naperville, IL) were treated for 96 h with either vehicle control (1 μl of Me_2SO/ml of medium), I3C, tamoxifen, or both I3C and tamoxifen at the indicated concentrations followed by incubation with fresh medium containing a final concentration of 100 μM BrdUrd (Sigma) at 37 °C for 2 h. Cells were washed with PBS, fixed for 30 min in 4% paraformaldehyde, and rinsed with PBS, and DNA was denatured by incubation in 0.12 N HCl at 37 °C for 1 h. After neutralization in two changes of 0.1 M borate buffer over 10 min, cells

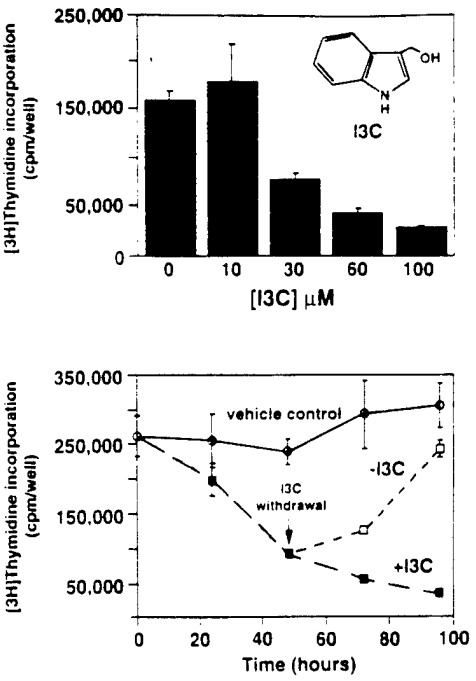

FIG. 1. **Effects of I3C on DNA synthesis in MCF7 breast cancer cells.** *Top panel*, MCF7 cells were plated at 20,000 cells/well on 24-well tissue culture dishes (forming a subconfluent monolayer) and treated with the indicated concentrations of I3C (see structure) for 48 h. Cells were labeled with [^{3}H]thymidine for 3 h, and the incorporation into DNA was determined by acid precipitation as described under "Experimental Procedures." The reported values are an average of triplicate samples. *Lower panel*, MCF7 cells were treated with 100 μM I3C (*+I3C*, ■) or with the Me_2SO vehicle control (*vehicle control*, □) for a 96-h time course. After 48 h of I3C treatment, the I3C-containing medium in a subset of the cell cultures was replaced with medium containing only the vehicle control (*−I3C*, □), and the time course continued for an additional 48 h. At the indicated time points for each condition, the cells were labeled with [^{3}H]thymidine for 3 h, and the incorporation into DNA was determined by acid precipitation. The reported values are an average of triplicate samples.

were washed in PBS and blocked for 5 min in PBS containing 4% normal goat serum (Jackson ImmunoResearch Laboratories, Inc., West Grove, PA). Cells were then incubated with mouse monoclonal anti-BrdUrd antibody (DAKO Corp. (Carpinteria, CA); diluted 1:80 in PBS) for 60 min at 25 °C. After five washes with PBS, cells were blocked for 5 min in PBS containing 4% normal goat serum. Cells were then incubated in anti-mouse rhodamine-conjugated secondary antibody (Jackson ImmunoResearch Laboratories; diluted 1:300 in PBS) at 4 °C for 30 min. Finally, cells were washed five times with PBS, mounted with 50% glycerol, 50 mM Tris (pH 8.0), and examined on a Nikon Optiphot fluorescence microscope. Images were captured using Adobe Photoshop 3.0.5 and a Sony DKC-5000 digital camera. Nonspecific fluorescence, as determined by incubation with secondary antibody alone, was negligible.

RESULTS

I3C Reversibly Inhibits the Growth and Induces a G_1 Cell Cycle Arrest of Human MCF7 Breast Cancer Cells—As an initial test to determine whether dietary indoles can directly regulate the growth of human breast cancer cells, MCF7 cells were cultured at subconfluency in medium supplemented with 10% FBS and 10 μg/ml insulin and treated with several concentrations of I3C for 48 h. Cells were then pulse-labeled with [^{3}H]thymidine for 3 h to provide a measure of their proliferation. Analysis of [^{3}H]thymidine incorporation revealed a strong dose-dependent inhibition of DNA synthesis with half-maximal response at approximately 30 μM I3C (Fig. 1, *upper panel*). Treatment with I3C above 200 μM was toxic to the cells. The lowest concentration of I3C that maximally inhibited the growth of MCF7 cells without affecting viability was 100 μM, and this level of the indole was therefore routinely used in subsequent experiments. HPLC analysis of the culture medium from I3C-treated cells revealed that this indole remained stable during the entire course of the experiment.[2] In the low pH environment of the stomach, I3C is converted into several acid-catalyzed products including DIM and ICZ, which bind to and activate the Ah receptor. Neither of these acid-catalyzed products had any significant effect on the incorporation of [^{3}H]thymidine into MCF7 breast cancer cells after 48-h treatments with concentrations that were above the K_d for the Ah receptor (data not shown). In multiple experiments, ICZ and DIM caused only an average of 10% inhibition of DNA synthesis under these conditions, which was not statistically significant.

Time course studies of I3C addition and withdrawal demonstrated that the I3C growth suppression of MCF7 breast cancer cells is completely reversible; therefore, this compound did not affect cell viability. For example, analysis of DNA synthesis over a 96-h time course revealed that 100 μM I3C inhibited [^{3}H]thymidine incorporation by 80% after 72 h and by greater than 90% after 96 h of treatment (Fig. 1, *lower panel*). The rate of [^{3}H]thymidine incorporation in untreated cells was approximately equal to the rate observed 48 h after indole withdrawal (Fig. 1, *lower panel*). Even after prolonged exposure (50 days), the I3C-induced growth arrest was readily reversible (data not shown).

To assess the cell cycle effects of I3C, MCF7 cells were treated with or without 100 μM I3C for 96 h and were then hypotonically lysed in the presence of propidium iodide to stain the nuclear DNA. Flow cytometry profiles of nuclear DNA content revealed that I3C induced a cell cycle arrest of these breast cancer cells. As shown in Fig. 2, I3C treatment altered the DNA content of the MCF7 cell population from an asynchronous population of growing cells (Fig. 2, *upper panel*) in all phases of the cell cycle (26% in G_1, 52% in S phase, and 22% in G_2/M phase) to one in which most (73%) of the I3C-treated breast cancer cells exhibited a 2n DNA content (Fig. 2, *lower panel*), which is indicative of a G_1 block in cell cycle progression. These results suggest that I3C suppresses cell growth by inducing a specific block in cell cycle progression.

I3C Rapidly Abolishes the Production and Activity of the CDK6 Cell Cycle Component and Reduces the Endogenous Phosphorylation of Rb—To determine potential downstream targets of the I3C-activated pathway that induces the cell cycle arrest, the expression of components that function within the G_1 phase of the cell cycle was examined during a time course of I3C treatment. MCF7 cells were treated with or without 100 μM I3C for the indicated time periods (Fig. 3), and the production of G_1 CDKs, cyclins, and CDK inhibitors was examined by Western blot analysis. Among the array of cell cycle components tested, only CDK6 protein levels were rapidly and significantly reduced in response to I3C treatment. The level of CDK6 is reduced within 24 h of indole treatment, and by 96 h, CDK6 production is essentially abolished (Fig. 3, *upper panel*). Importantly, no effect was observed on the expression of the two other G_1-acting cyclin-dependent kinases, CDK2 and CDK4. This result demonstrates the specificity of the I3C response. In addition, I3C did not alter the level of either cyclin D1 or cyclin E, both of which have been shown to be regulated in other studies. Estrogen and progesterone stimulate and antiestrogens inhibit cell cycle progression of the T47D human breast cancer cell line at a point in the early G_1 phase of the cell cycle with corresponding changes in cyclin D1 and p21 expression (41, 42). Quantitative analysis of autoradiographs from

[2] L. Bjeldanes, unpublished data.

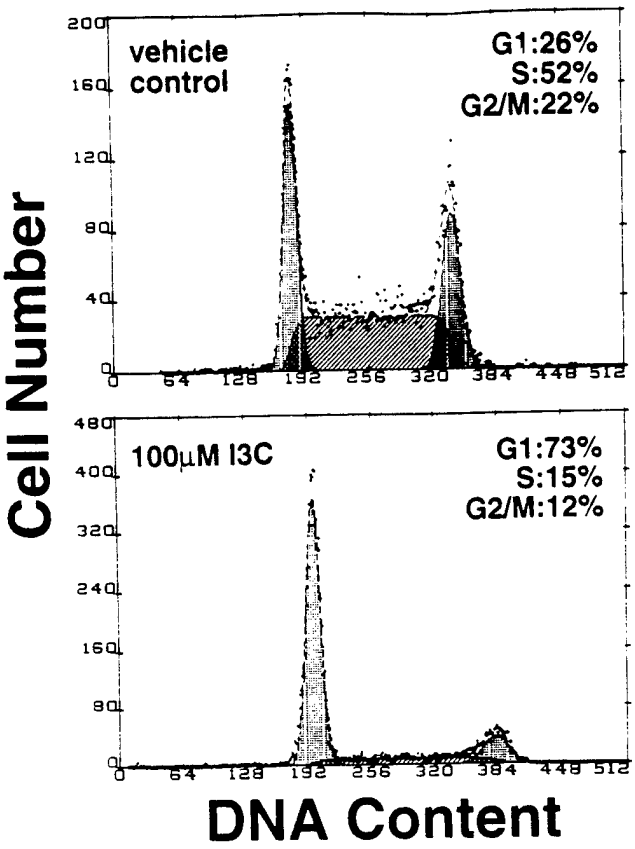

FIG. 2. **Effects of I3C on cell cycle phase distribution of MCF7 breast cancer cells.** MCF7 cells were treated with 100 μM I3C or with the vehicle control (Me_2SO) for 96 h. Cells were then stained with propidium iodide, and nuclei were analyzed for DNA content by flow cytometry with a Coulter Elite laser. A total of 10,000 nuclei were analyzed from each sample. The percentages of cells within the G_1, S, and G_2/M phases of the cell cycle were determined as described under "Experimental Procedures."

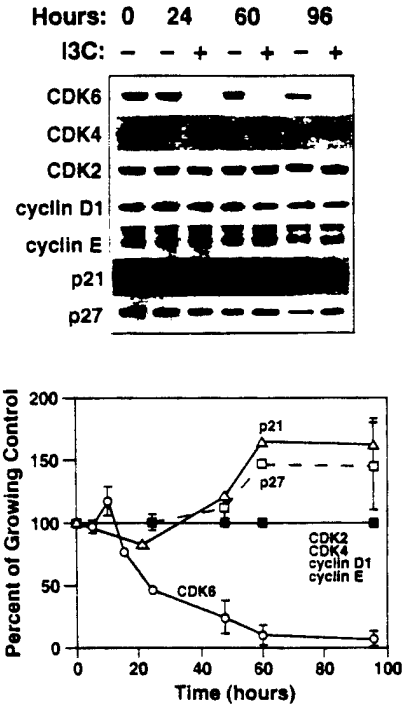

FIG. 3. **Effects of I3C on expression of G_1 cell cycle proteins in MCF7 breast cancer cells.** *Upper panel*, MCF7 cells were treated with 100 μM I3C or with the vehicle control (Me_2SO) for the indicated times, and the protein production of the G_1 cell cycle components was determined by Western blot analysis using specific antibodies. The same cell extracts were utilized for the analysis of each cell cycle protein, and equal sample loading was confirmed by Ponceau S staining of the Western blot membrane. *Lower panel*, the relative level of each cell cycle component shown in the representative Western blot in the *upper panel*, as well as from other Western blots with additional time points, was quantitated as described under "Experimental Procedures." The percentage of growing control was calculated by dividing the densitometry measurements of I3C-treated cells by the densitometry measurements of vehicle control-treated growing cells for each assay (CDK6 (○), p21 (△), p27 (□), CDK2, CDK4, cyclin D1, and cyclin E (■)).

more detailed time courses (Fig. 3, *lower panel*) revealed that of all the cell cycle components, only CDK6 protein levels changed early enough to coincide with the inhibition of DNA synthesis (see Fig. 1), suggesting a relationship between these two effects of I3C. Western blot analysis also demonstrated that I3C gradually stimulated the levels of the p21 and p27 cell cycle inhibitors by 50% only after the cells begin to display their maximal cell cycle arrest.

The phosphorylation of the Rb protein by the CDKs is critical for progression through the cell cycle, while in G_1 cell cycle-arrested cells, the Rb protein remains hypophosphorylated (43). To determine potential functional connections between the decreased expression of CDK6 and the cell cycle arrest, the effects of I3C on the ability of CDK6 to phosphorylate Rb *in vitro* and the level of total phosphorylated endogenous Rb protein were compared through a time course of I3C treatment. MCF7 cells were treated with and without I3C for a 96-h time course, and at specific time points, the immunoprecipitated CDK6 was assayed for Rb phosphorylation activity. As shown in Fig. 4 (*top panel*), the level of CDK6-mediated Rb phosphorylation activity was strongly inhibited by I3C in a manner consistent with the decreased expression of CDK6 protein. No change was observed in CDK6 activity at 15 h. However, by 24 h of treatment, there was a significant reduction in the ability of immunoprecipitated CDK6 to phosphorylate the GST-Rb fusion protein *in vitro*. The CDK6 activity in the I3C-treated cells remained low throughout the remainder of the time course. In a parallel experiment using I3C-treated and untreated MCF7 cells, the level of endogenous phosphorylated Rb protein was assessed in Western blots. The hyperphosphorylated and hypophosphorylated forms of Rb migrate at characteristic sizes in SDS-polyacrylamide gel electrophoresis (44, 45). As shown in Fig. 4 (*middle panel*), by 48 h of treatment, I3C causes a significant decrease in the amount of hyperphosphorylated Rb (*ppRb*) compared with untreated cells cultured for the same time period. The levels of *in vitro* CDK6 activity and endogenous phosphorylation of Rb were compared by quantitating the phosphorylation patterns at the 48-h time points. As shown in the *lower panel* of Fig. 4, I3C caused a similar inhibition of Rb phosphorylation in both assays. This result suggests a connection between the I3C-mediated decrease in CDK6 activity, the lack of endogenous Rb hyperphosphorylation, and the observed cell cycle arrest.

I3C Inhibition of CDK6 Transcript Expression—Because the level of CDK6 protein is rapidly reduced by indole treatment, it seemed likely that I3C regulates the level of CDK6 transcripts. Poly(A)$^+$ RNA was isolated from MCF7 breast cancer cells treated with and without 100 μM I3C for the indicated times, and electrophoretically fractionated samples were examined by Northern blot analysis. As shown in Fig. 5 (*upper left panel*), 15 h of treatment with I3C caused a specific reduction in the level of all three of the CDK6 transcripts. By 24 h of I3C treatment, the expression of CDK6 transcripts were undetectable (data not shown). Consistent with the unaltered protein production observed for CDK2 and CDK4, the transcript levels for these CDKs remained unchanged in either the presence or

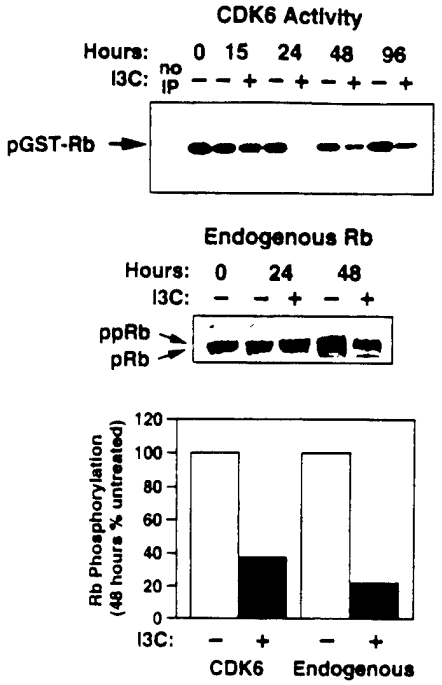

FIG. 4. **Effects of I3C on CDK6 kinase activity and endogenous Rb phosphorylation in MCF7 cells.** *Upper panel*, MCF7 cells were treated with 100 μM I3C or with the vehicle control (Me_2SO) for the indicated times. CDK6 was immunoprecipitated from cell lysates and assayed for *in vitro* kinase activity using the C terminus of the Rb protein as a substrate (GST-Rb). One control immunoprecipitation (*no IP*) contained rabbit anti-IgG with no added anti-CDK6 antibodies in untreated MCF7 cell lysates. The kinase reaction mixtures were electrophoretically fractionated, and the level of [^{32}P]Rb (*pGST-Rb*) was analyzed by autoradiography. *Middle panel*, MCF7 cells were treated with 100 μM I3C or with the vehicle control (Me_2SO) for the indicated times, the cell extracts were electrophoretically fractionated, and Western blots were probed with anti-Rb antibodies. The level of endogenous Rb phosphorylation was determined by the characteristic migration of the hyperphosphorylated (*ppRb*) and hypophosphorylated (*pRb*) forms of Rb. *Lower panel*, the levels of observed Rb phosphorylation at the 48-h time points from the CDK6 kinase assay and the Western blot were quantitated as described under "Experimental Procedures." The level of Rb phosphorylation in the untreated control was set at 100%, and the inhibition by I3C was determined by dividing the densitometry measurements of untreated cells by the densitometry measurements of I3C-treated cells for each assay.

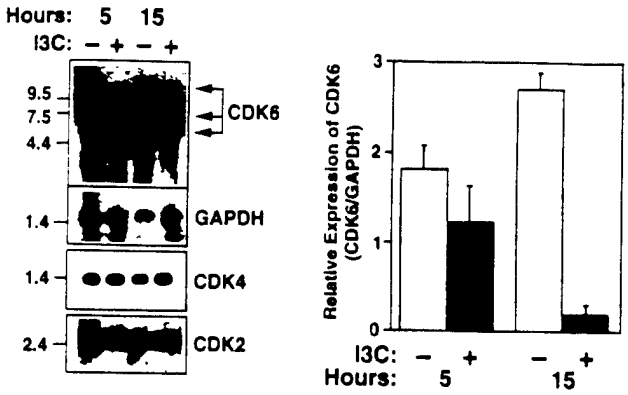

FIG. 5. **Effects of I3C on the expression of G_1 CDK transcripts in MCF7 breast cancer cells.** Poly(A)$^+$ RNA isolated from MCF7 cells treated with or without 100 μM I3C for 5 or 15 h. The RNAs were electrophoretically fractionated, and Northern blots were probed for CDK6, CDK4, and CDK2 transcripts (*left panels*) as described under "Experimental Procedures." As a loading control, the CDK6 Northern blots were reprobed for GAPDH, which is a constitutively expressed transcript. The x-ray film exposure times were 6 days for CDK6 and 2 h for CDK4, CDK2, and GAPDH. Molecular size standards in kilobases are indicated in the *left panel*. The band intensities of CDK6 and GAPDH transcripts for each condition were quantitated (*right panel*) as described under "Experimental Procedures." CDK6 mRNA levels were normalized to GAPDH mRNA levels by dividing the band intensities of CDK6 by the band intensity for GAPDH. The reported values represent an average of three independent experiments.

absence of I3C (Fig. 5, *lower left panels*). It is worth mentioning that MCF7 cells produce a significantly lower amount of CDK6 mRNA compared with the level of either CDK2 or CDK4 transcripts. A 6-day x-ray film exposure is required to detect the CDK6 mRNA bands with 10 μg of poly(A)$^+$ sample, whereas the same blot reprobed for CDK2 or CDK4 can be developed within 2 h. Autoradiographs from multiple experiments were quantitated, and CDK6 mRNA concentrations at each time point were normalized to the level of GAPDH transcripts, a constitutively expressed gene. No significant effect of I3C on CDK6 transcript levels was observed after 5 h of treatment. By 15 h, I3C caused a 5-fold reduction in CDK6 mRNA levels (Fig. 5, *right panel*). These changes in CDK6 transcript levels appear to account for the reduction in CDK6 protein because CDK6 protein levels begin to decrease in response to I3C between 15 and 21 h of treatment (Fig. 3, *lower panel*). Taken together, our results demonstrate that under conditions in which I3C induces a cell cycle arrest of MCF7 breast cancer cells, the gene expression and protein expression of CDK6, a G_1-acting cell cycle component, is selectively reduced.

The Regulation of CDK6 Production Is Specific for the Antiproliferative Effects of I3C—An important question is whether the I3C-induced reduction in CDK6 expression is a specific I3C response or whether it is a general consequence of the inhibition of cell growth. To distinguish these possibilities, the effects of I3C were compared with those of the antiestrogen tamoxifen, a well known inhibitor of the proliferation of estrogen-treated MCF7 cells (46). The I3C treatments were performed using MCF7 cells cultured in medium supplemented with 10% FBS, which contains enough estrogen and growth factors to maintain the cells in a proliferative state. To first demonstrate that tamoxifen can selectively inhibit an estrogen-responsive reporter plasmid in the presence of 10% FBS, ER expressing MCF7 breast cancer cells were transiently transfected with the ERE-vit-CAT reporter plasmid, which contains the vitellogenin promoter with four estrogen response elements linked upstream and driving the bacterial CAT gene. The cells were treated for 48 h with the indicated combinations of estrogen, tamoxifen, and/or I3C (Fig. 6), and the reporter gene activity was assayed by monitoring the conversion of [^{3}H]acetyl-CoA and unlabeled chloramphenicol into [^{3}H]acetylchloramphenicol. As shown in Fig. 6, the medium used for I3C-induced growth suppression (10% FBS) has endogenous estrogen and growth factors at a sufficient concentration to cause a high basal level of reporter gene activity in MCF7 cells transiently transfected with the ERE-vit-CAT reporter plasmid compared with the low serum (5% CS) condition. Low serum medium, as opposed to serum-free medium, was chosen because MCF7 cells cultured in serum-free conditions were not transfection-competent. Treatment with 100 nM estrogen further stimulated ERE-vit-CAT activity above each of the basal serum levels, whereas tamoxifen inhibited the serum-induced ERE-vit-CAT reporter plasmid activity by 70%. Treatment with I3C had no effect on the ER responsiveness of the ERE-vit-CAT activity; nor did this dietary indole modulate the antagonistic effects of tamoxifen (Fig. 6). Thus, under the FBS-containing conditions utilized to culture MCF7 cells, tamoxifen acts as a potent antagonist of ER responsiveness, while I3C has no apparent effects on ER function.

To test whether I3C and tamoxifen affected the absolute number of S phase cells, MCF7 cells were treated for 48 h with 100 μM I3C and/or 1 μM tamoxifen, and the cells were exposed

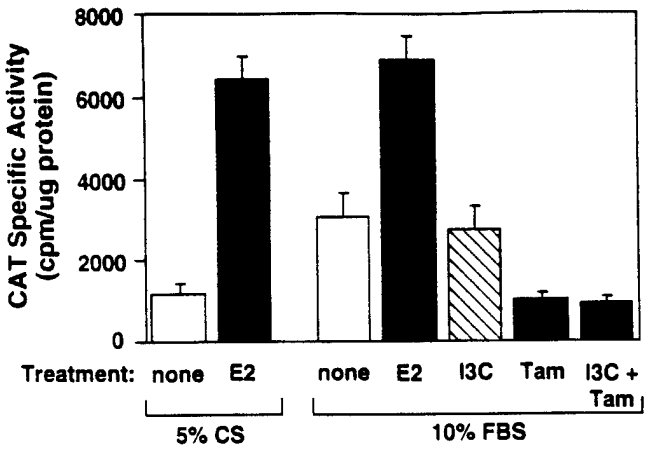

FIG. 6. **Effects of I3C and tamoxifen on the ERE-vit-CAT reporter plasmid activity in MCF7 breast cancer cells.** MCF7 cells were first cultured for 1 week in either 5% CS or 10% FBS. Cells were then transfected with the ERE-vit-CAT reporter plasmid, which encodes four EREs within the vitellogenin promoter linked upstream to and driving the bacterial CAT gene. Transfected cells were treated with the indicated combinations of 100 nM 17β-estradiol (*E2*), 100 μM I3C, and/or 10 μM tamoxifen (*Tam*) or with a vehicle control (*none*) for 48 h and assayed for CAT activity by a quantitative method that measures the conversion of [^{3}H]acetyl coenzyme A into [^{3}H]acetylchloramphenicol. CAT specific activity is the CAT activity produced per μg of protein present in the corresponding cell lysates. The reported values are an average of four independent experiments of triplicate samples.

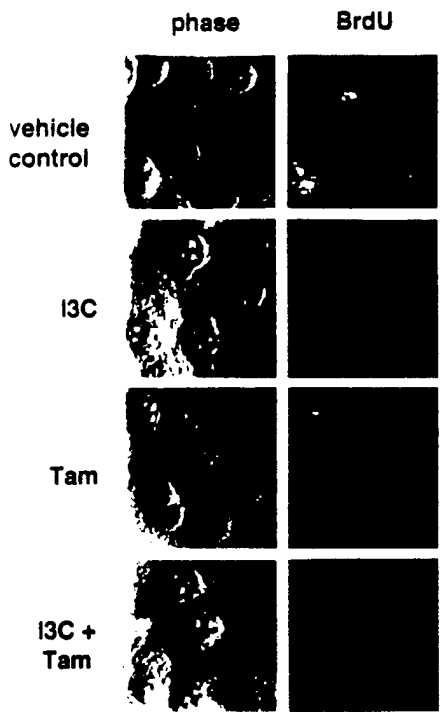

FIG. 7. **Single cell analysis of the effects of I3C and tamoxifen on DNA synthesis in MCF7 breast cancer cells.** MCF7 cells cultured on eight-well slides were treated with the indicated combinations of 100 μM I3C and/or 1 μM tamoxifen (*Tam*) or with only Me_2SO (vehicle control) for 96 h. Cells were then labeled with 100 μM BrdUrd for 2 h, fixed in paraformaldehyde, and incubated with mouse anti-BrdUrd antibodies. BrdUrd-incorporating cells were then visualized by fluorescence microscopy using anti-mouse rhodamine-conjugated secondary antibodies as described under "Experimental Procedures."

to a 2-h pulse of BrdUrd, which was used as a measure of DNA synthesis on a single cell level. The incorporation of BrdUrd was monitored by indirect immunofluorescence using BrdUrd-specific antibodies. Representative photographs are shown in Fig. 7. The number of BrdUrd-incorporating cells was quantitated by examining approximately 500–1000 cells/condition. In an asynchronous growing population, 21.5% of MCF7 cells incorporated BrdUrd. Treatment with either I3C or with tamoxifen suppressed BrdUrd incorporation to 4.7 and 12.3%, respectively, whereas treatment with both reagents induced a more effective growth suppression (3.8%) compared with either I3C or tamoxifen alone. Treatment with I3C or tamoxifen caused the cells to show a more flattened morphology, which is consistent with the effects of other antiproliferative agents (47, 48).

Because I3C and tamoxifen both inhibited cell growth, the effects of these two antiproliferative agents on CDK6 production were examined. MCF7 cells were treated with combinations of I3C and tamoxifen over a 96-h time course, and cell extracts were analyzed for CDK protein by Western blots. I3C, but not tamoxifen, reduced the level of CDK6 protein, whereas no effects were observed on CDK4 or CDK2 production with either reagent (Fig. 8). A combination of I3C and tamoxifen reduced CDK6 protein levels to approximately the same extent as I3C alone. These results indicate that the inhibition of CDK6 expression is a specific I3C response and not a general consequence of growth arrest in MCF7 cells. Because the effects of the antiestrogen tamoxifen and I3C differ, these results suggest that I3C may act, in part, through an ER-independent pathway to suppress breast cancer cell growth.

I3C Can Suppress the Growth and Reduce CDK6 Production in an ER-deficient Human Breast Cancer Cell Line—The ER-deficient MDA-MB-231 cells were utilized to demonstrate that I3C can suppress the growth of human breast cancer cells independent of any effects on ER responsiveness. Western blot analysis using antibodies to the human ER confirmed that the MDA-MB-231 breast cancer cells do not express ER protein, while MCF7 cells produce ER (Fig. 9, *upper panel*). Moreover, consistent with the lack of ER protein, neither estrogen nor

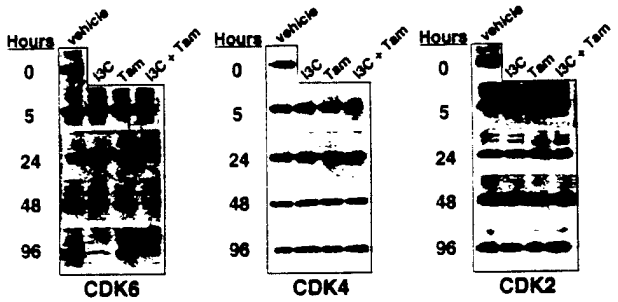

FIG. 8. **Effects of I3C and tamoxifen on the expression of G_1 CDK proteins in MCF7 breast cancer cells.** MCF7 cells were treated with combinations of 100 μM I3C and/or 1 μM tamoxifen or with the vehicle control (Me_2SO) for the indicated times. The protein production of CDK6, CDK4, and CDK2 was determined by Western blot analysis using specific antibodies. The same cell extracts were utilized for the analysis of each CDK protein, and equal sample loading was confirmed by Ponceau S staining of the Western blot membrane.

tamoxifen had any effects on ERE-vit-CAT reporter activity in transiently transfected MDA-MB-231 cells (data not shown). To test whether I3C can suppress the growth of human breast cancer cells in an ER-independent manner, MCF7 cells, which contain ERs, and MDA-MB-231 cells, which do not contain ERs, were treated with combinations of I3C and tamoxifen for 48 h, and DNA synthesis was assayed as a measure of the incorporation of [^{3}H]thymidine. As shown in Fig. 9, *middle panel*, treatment with either I3C or tamoxifen inhibited MCF7 DNA synthesis by approximately 70 and 60%, respectively, compared with vehicle controls. Consistent with a more stringent growth-inhibitory effect of both reagents, a combination of both I3C and tamoxifen inhibited [^{3}H]thymidine incorporation by more than 90%. In contrast, I3C, but not tamoxifen, strongly

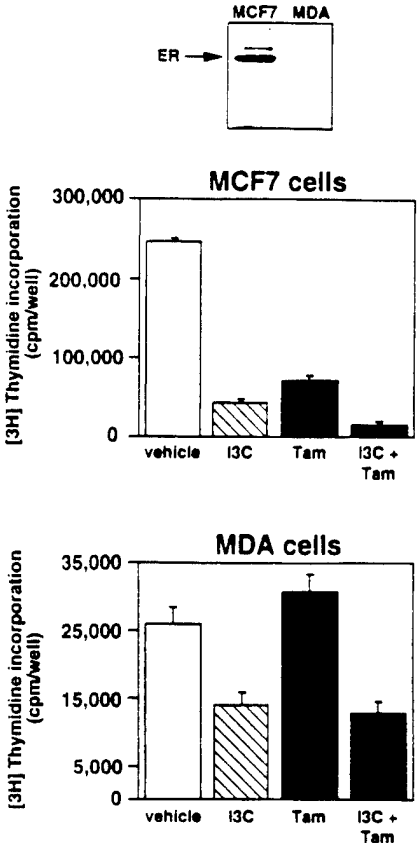

FIG. 9. **Effects of I3C and tamoxifen on DNA synthesis in ER-containing and ER-deficient breast cancer cells.** *Upper panel*, expression of ER was confirmed in ER-containing MCF7 cells and ER-deficient MDA-MB-231 (*MDA*) cells. ER protein expression was determined by Western blot analysis using specific antibodies, and equal sample loading was confirmed by Ponceau S staining of the Western blot membrane. *Lower panels*, MCF7 and MDA cells were plated at 20,000 cells/well on 24-well tissue culture dishes and treated with the indicated combinations of 100 μM I3C and/or 1 μM tamoxifen or with the vehicle control (Me_2SO) for 48 h. Cells were labeled with [^{3}H]thymidine for 3 h, and the incorporation into DNA was determined by acid precipitation as described under "Experimental Procedures." The reported values are an average of triplicate samples.

inhibited [^{3}H]thymidine incorporation in the ER-deficient MDA-MB-231 cells (Fig. 9, *lower panel*). A combination of I3C and tamoxifen suppressed DNA synthesis to approximately the same extent as I3C alone. This result demonstrates that I3C can suppress breast cancer cell growth independent of ER-mediated events.

The ER-positive MCF7 cells and ER-negative MDA-MB-231 cells were utilized to examine the relationship between the estrogen-independent suppression of cell growth by I3C and the reduction in CDK6 protein. Cells were treated with increasing concentrations of I3C for 48 h, and the level of G_1-acting CDK proteins was analyzed by Western blots. As shown in Fig. 10, *upper panels*, this indole can dose-dependently reduce CDK6 production in both cell lines, while in the same extracts, CDK4 and CDK2 protein levels remained unaffected. Quantitative analysis of the Western blots and a parallel analysis of [^{3}H]thymidine incorporation of the I3C dose response revealed that the inhibition of CDK6 protein levels approximately correlated with the I3C-mediated decrease in DNA synthesis (Fig. 10, *lower panels*). Consistent with the MDA-MB-231 cells not being as stringently growth-suppressed, I3C reduces CDK6 levels to a lesser extent compared with the MCF7 cells. Thus, I3C can suppress the growth and reduce CDK6 production in an ER-independent manner.

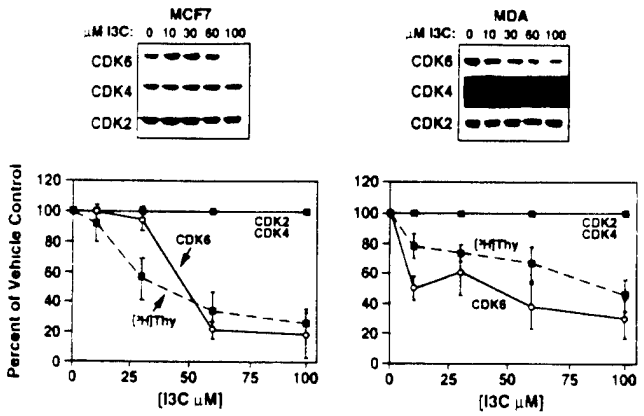

FIG. 10. **Dose-response effects of I3C on the expression of G_1 CDK proteins and DNA synthesis in ER-containing and ER-deficient breast cancer cells.** *Upper panels*, ER-containing MCF7 (*upper left*) and ER-deficient MDA-MB-231 (*upper right*) cells were treated with the indicated concentrations of I3C for 48 h. The protein production of CDK6 (○), CDK4 (△), and CDK2 (□) was determined by Western blot analysis using specific antibodies. The same cell extracts were utilized for the analysis of each CDK protein, and equal sample loading was confirmed by Ponceau S staining of the Western blot membrane. *Lower panels*, the relative level of each CDK shown in the representative Western blots in the upper panels, as well as from other Western blots, were quantitated as described under "Experimental Procedures." The reported values were calculated as the percentage of vehicle control-treated growing cells (0 μM I3C) by dividing the densitometry measurements of I3C-treated cells by the measurements of vehicle control cells for each assay. In parallel with the Western blots, triplicate sets of MCF7 and MDA-MB-231 cells were plated at 20,000 cells/well on 24-well tissue culture plates and treated with the indicated concentrations of I3C for 48 h. Cells were labeled with [^{3}H]thymidine for 3 h, and the incorporation into DNA was determined by acid precipitation as described under "Experimental Procedures" (*[^{3}H]Thy*, ■).

DISCUSSION

Extracellular regulators of cell proliferation, such as steroid and protein hormones, can transduce an intricate network of growth-inhibitory and -stimulatory signals that converge on specific sets of cell cycle components, which through their concerted actions, either drive cells through critical cell cycle transitions or inhibit cell cycle progression (3, 21). Dietary and environmental compounds that alter cell growth are likely to mediate many of their effects through signal transduction pathways analogous to the known mechanisms of hormone receptor signaling. Our results demonstrate the existence of a distinct growth-inhibitory pathway that establishes a direct link between the regulation of cell cycle control by the dietary indole I3C and the selective control of cell cycle components. The unique feature of this response is that the I3C-mediated growth arrest is accompanied by the specific inhibition of expression of CDK6 transcripts, protein, and activity. The selective regulation of CDK6 in mammary epithelial cells by I3C provides the basis to propose a biological mechanism by which dietary indoles potentially control the emergence and proliferation of breast cancer cells. In this regard, several recent studies have demonstrated that CDK6 expression and activity is altered in a manner that correlates with the transformed state. For example, tumor-specific amplification of CDK6 has recently been observed in human gliomas (49), and the activity of CDK6 is amplified in certain human squamous cell carcinoma lines (50).

Changes in cyclin or CDK inhibitor expression have been thought to be the key regulatory mechanisms controlling CDK function. A few recent studies have started to uncover examples of changes in expression of the G_1-acting CDKs under conditions that either inhibit or stimulate cell cycle progression (23, 51, 52). For example, staurosporine treatment of human

breast cancer cells causes a minor reduction in CDK6 protein levels that accompanies a G_1 cell cycle arrest (53). Treatment of T cells with the herbimycin A tyrosine kinase inhibitor reduces the stability of the CDK6 protein (54), while both CDK4 and CDK6 protein production were suppressed by the apopototic signaling through the sIgM surface antigen receptor in B cells (55).

CDK6 functions during progression through the G_1 phase of the cell cycle (56). However, relatively little is known about the influence on CDK6 expression by regulators of cell growth. In our studies with human MCF7 breast cancer cells, time course and dose-response assays with I3C revealed that the loss of CDK6 production and activity closely coincided with the reduction in cell proliferation, which implicates CDK6 as a direct target for cell cycle control in human breast cancer cells. The rapid I3C effect on CDK6 gene expression is unique, because it is the first report of a growth inhibitor decreasing the mRNA for CDK6. One other study has shown that the level of another G_1-acting CDK can be reduced in response to a specific antiproliferative signal. Under conditions in which retinoic acid suppresses the growth of MCF7 cells, the level of CDK2 mRNA was decreased within 8 h of retinoic acid treatment (57). In our study, the CDK6 transcript levels were significantly reduced between 5 and 15 h of I3C treatment, which appears to account for the decrease in CDK6 protein production. In contrast, no obvious changes were observed in the production of the other G_1-acting CDKs and cyclins.

Our results have established that I3C signaling can induce the G_1 cell cycle arrest of cultured human MCF7 breast cancer cells in an estrogen-independent manner. Most strikingly, the I3C-mediated cell cycle arrest and repression of CDK6 production were observed in ER-deficient MDA-MB-231 human breast cancer cells under conditions in which the antiestrogen tamoxifen had no effect on cell growth. In ER-containing MCF7 cells, tamoxifen suppressed DNA synthesis to approximately the same extent as I3C but had no effect on CDK6 expression. Moreover, while tamoxifen reduced the activity of an ERE-containing reporter plasmid in cells cultured with FBS-containing endogenous estrogens, I3C had no effect on ER responsiveness under these same culture conditions. Consistent with I3C and tamoxifen acting through distinct antiproliferative pathways, a combination of I3C and tamoxifen inhibited MCF7 cell growth to a greater extent compared with the effects of either agent alone.

Tamoxifen has been a clinically useful antiestrogen (58–60); however, 60–75% of patients with metastatic breast cancer have ER-positive tumors, and only approximately half of those patients will respond to tamoxifen therapy. Therefore, only 35% of metastatic breast cancer patients actually benefit from tamoxifen therapy (61). All patients who initially respond to therapy will eventually develop acquired tamoxifen resistance following prolonged administration. The cellular and molecular mechanisms underlying the development of acquired resistance to antiestrogens is unclear, but it has been proposed that continued exposure of cells to tamoxifen may select for hormone-independent, resistant cells (62). Our results suggest that I3C, in combination with tamoxifen, could prove to be an effective therapy. Patients could receive intermittent pulses of tamoxifen or lower doses of tamoxifen, both of which are proposed methods of circumventing tamoxifen resistance, while on I3C treatment. I3C has been shown to reduce the formation of both spontaneous and carcinogen-induced mammary tumors in rodents with no apparent side effects (9, 63–65), and human subjects treated with I3C also had no side effects (13, 66).

The ER-dependent pathway presumably involves the activation of the Ah receptor by the acid-catalyzed products of I3C and subsequent regulation of estrogen metabolism (17). In our studies, no effects on growth were observed within 48 h of treatment with ICZ or DIM. However, it is likely that the ER-dependent effects of these indoles require treatment periods longer than a week (9). The regulation of CDK6 expression appears to be specific for the I3C-mediated ER-independent pathways. Several studies with human breast cancer cells have shown that the ER pathway stimulates cell proliferation by targeting the expression and/or activity of G_1-acting cell cycle components (3, 52, 67). Although the immediate promoter targets of the ER are unknown, in MCF7 cells the estrogen-induced activation of CDK4 and CDK2 kinase activity was shown to be accompanied by the increase in cyclin D1 expression and decreased CDK inhibitor association with the cyclin E-CDK2 protein complex (36). No changes in CDK6 expression were reported in these studies, although in other human breast cancer cells, antiprogestin or antiestrogen treatment was shown to increase production of p21 (42).

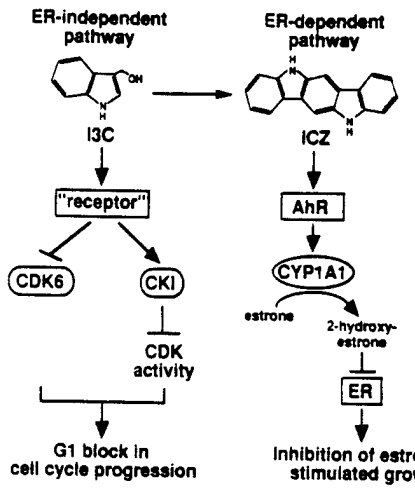

FIG. 11. **Model for the ER-independent and ER-dependent antiproliferative effects of I3C in breast cancer cells.** For the ER-independent pathway, I3C suppresses breast cancer cell growth by a rapid inhibition of CDK6 expression and activity and a later stimulation of CDK inhibitor (*CKI*) production. We propose that this effect causes an inhibition of the activity of G_1-acting CDKs, resulting in decreased retinoblastoma protein phosphorylation, and thereby induces a G_1 block in cell cycle progression. We also propose that I3C is mediating these effects through a putative cellular receptor (*"receptor"*). In contrast, the ER-dependent pathway is mediated by the I3C acid-catalyzed product ICZ, which binds to and activates the aromatic hydrocarbon receptor (*AhR*). The aromatic hydrocarbon receptor transcriptionally activates cytochrome P4501A1 (*CYP1A1*)-dependent monooxygenase, which inactivates estrone and thereby prevents the estrogen-stimulated growth of breast cancer cells.

Taken together with previous studies on the acid-catalyzed products of I3C (18, 68), our results with I3C indicate that dietary indoles are likely to work through both ER-independent and ER-dependent pathways (see Fig. 11). It is tempting to consider that I3C, or perhaps a cellular metabolite of I3C, interacts with a putative indole receptor to reduce the expression and activity of the CDK6 cell cycle component, resulting in the G_1 arrest of breast cancer cells by an ER-independent pathway. The I3C-mediated decrease in the amount of CDK6 protein may have multiple effects on the cell cycle control of breast cancer cells. The inhibited production of active CDK6 could contribute to the observed decrease in endogenous phosphorylation of Rb and thereby directly influence the cell cycle arrest. It is also possible that the decreased production of CDK6 protein could indirectly affect the stoichiometry of the other G_1-acting CDK complexes by releasing bound CDK inhibitors and cyclins. For example, the activities of CDK2 and/or CDK4 could then be affected, although the expression of these

CDKs remains constant. Furthermore, I3C treatment resulted in a 50% increased expression of the p21 and p27 CDK inhibitors after the cells reached their maximal cell cycle arrest. We are currently attempting to determine whether I3C alters the expression and/or function of other G_1-acting cell cycle components that may also contribute to the reduction in endogenous Rb phosphorylation. Another of our future goals will be to identify the putative indole receptor and to characterize the ER-independent pathway by which I3C regulates CDK6 gene expression and cell cycle control in human breast cancer cells.

Acknowledgments—We express our appreciation to Erin J. Cram, Helen L. Henry, Meredith L. Leong, and Anita C. Maiyar for critical evaluation of this manuscript and helpful experimental suggestions. We also thank other members of both the Firestone and Bjeldanes laboratories for helpful comments throughout the duration of this work. We thank Wei-Ming Kao, Peter Schow, Khanh Tong, Vinh Trinh, and Linda Yu for technical assistance. We are also grateful to Jerry Kapler for excellent photography and Anna Fung for help in the preparation of this manuscript.

REFERENCES

1. Birt, D. F., Pelling, J. C., Nair, S., and Lepley, D. (1996) *Prog. Clin. Biol. Res.* **395,** 223–234
2. Freudenheim, J. L., Marshall, J. R., Vena, J. E., Laughlin, R., Brasure, J. R., Swanson, M. K., Nemoto, T., and Graham, S. (1996) *J. Natl. Cancer Inst.* **88,** 340–348
3. Meier, C. A. (1997) *J. Recept. Signal Transduct. Res.* **17,** 319–335
4. Hamel, P. A., and Hanley, H. J. (1997) *Cancer Invest.* **15,** 143–152
5. Loub, W. D., Wattenberg, L. W., and Davis, D. W. (1975) *J. Natl. Cancer Inst.* **54,** 985–988
6. Wattenberg, L. W., and Loub, W. D. (1978) *Cancer Res.* **38,** 1410–1413
7. Sharma, S., Stutzman, J. D., Kelloff, G. J., and Steele, V. E. (1994) *Cancer Res.* **54,** 5848–5855
8. Morse, M. A., LaGreca, S. D., Amin, S. G., and Chung, F. L. (1990) *Cancer Res.* **50,** 2613–2617
9. Bradlow, H. L., Michnovicz, J., Telang, N. T., and Osborne, M. P. (1991) *Carcinogenesis* **12,** 1571–1574
10. Grubbs, C. J., Steele, V. E., Casebolt, T., Juliana, M. M., Eto, I., Whitaker, L. M., Dragnev, K. H., Kelloff, G. J., and Lubet, R. L. (1995) *Anticancer Res.* **15,** 709–716
11. Wattenberg, L. W. (1990) *Basic Life Sci.* **52,** 155–166
12. Shertzer, H. G. (1984) *Chem. Biol. Interact.* **48,** 81–90
13. Michnovicz, J. J., and Bradlow, H. L. (1990) *J. Natl. Cancer Inst.* **82,** 947–949
14. Jellinck, P. H., Forkert, P. G., Riddick, D. S., Okey, A. B., Michnovicz, J. J., and Bradlow, H. L. (1993) *Biochem. Pharmacol.* **45,** 1129–1136
15. Tiwari, R. K., Guo, L., Bradlow, H. L., Telang, N. T., and Osborne, M. P. (1994) *J. Natl. Cancer Inst.* **86,** 126–131
16. De, K. C., Marsman, J. W., Venekamp, J. C., Falke, H. E., Noordhoek, J., Blaauboer, B. J., and Wortelboer, H. M. (1991) *Chem. Biol. Interact.* **80,** 303–315
17. Bjeldanes, L. F., Kim, J. Y., Grose, K. R., Bartholomew, J. C., and Bradfield, C. A. (1991) *Proc. Natl. Acad. Sci. U. S. A.* **88,** 9543–9547
18. Grose, K. R., and Bjeldanes, L. F. (1992) *Chem. Res. Toxicol.* **5,** 188–193
19. Chen, Y.-H., Riby, J., Srivastava, P., Bartholomew, J., Denison, M., and Bjeldanes, L. (1995) *J. Biol. Chem.* **270,** 22548–22555
20. Sherr, C. J. (1996) *Science* **274,** 1672–1677
21. Stillman, B. (1996) *Science* **274,** 1659–1664
22. van den Heuvel, S., and Harlow, E. (1993) *Science* **262,** 2050–2054
23. Morgan, D. O. (1995) *Nature* **374,** 131–134
24. Leone, G., DeGregori, J., Sears, R., Jakoi, L., and Nevins, J. R. (1997) *Nature* **387,** 422–425
25. Qin, X. Q., Livingston, D. M., Ewen, M., Sellers, W. R., Arany, Z., and Kaelin, W. G., Jr. (1995) *Mol. Cell. Biol.* **15,** 742–755
26. Elledge, S. J., and Harper, J. W. (1994) *Curr. Opin. Cell Biol.* **6,** 847–852
27. Sherr, C. J., and Roberts, J. M. (1995) *Genes Dev.* **9,** 1149–1163
28. Gartel, A. L., Serfas, M. S., and Tyner, A. L. (1996) *Proc. Soc. Exp. Biol. Med.* **213,** 138–149
29. Alessandrini, A., Chiaur, D. S., and Pagano, M. (1997) *Leukemia* **11,** 342–345
30. Buckley, M. F., Sweeney, K. J., Hamilton, J. A., Sini, R. L., Manning, D. L., Nicholson, R. I., deFazio, A., Watts, C. K., Musgrove, E. A., and Sutherland, R. L. (1993) *Oncogene* **8,** 2127–2133
31. Keyomarsi, K., and Pardee, A. B. (1993) *Proc. Natl. Acad. Sci. U. S. A.* **90,** 1112–1116
32. Schuuring, E., Verhoeven, E., Mooi, W. J., and Michalides, R. J. (1992) *Oncogene* **7,** 355–361
33. Hunter, T. (1997) *Cell* **88,** 333–346
34. Norberg, T., Jansson, T., Sjogren, S., Martensson, C., Andreasson, I., Fjallskog, M. L., Lindman, H., Nordgren, H., Lindgren, A., Holmberg, L., and Bergh, J. (1996) *Acta Oncol.* **5,** 96–102
35. Hartmann, A., Blaszyk, H., Kovach, J. S., and Sommer, S. S. (1997) *Trends Genet.* **13,** 27–33
36. Prall, O. W. J., Sarcevic, B., Musgrove, E. A., Watts, C. K. W., and Sutherland, R. L. (1997) *J. Biol. Chem.* **272,** 10882–10894
37. Goya, L., Maiyar, A. C., Ge, Y., and Firestone, G. L. (1993) *Mol. Endocrinol.* **7,** 1121–1132
38. Sanchez, I., Goya, L., Vallerga, A. K., and Firestone, G. L. (1993) *Cell Growth Differ.* **4,** 215–225
39. Baker, S. J., Markowitz, S., Fearon, E. R., Willson, J. K., and Vogelstein, B. (1990) *Science* **249,** 912–915
40. Neumann, J. R., Morency, C. A., and Russian, K. O. (1987) *Biotechniques* **5,** 444–447
41. Musgrove, E. A., Hamilton, J. A., Lee, C. S., Sweeney, K. J., Watts, C. K., and Sutherland, R. L. (1993) *Mol. Cell. Biol.* **13,** 3577–3587
42. Musgrove, E. A., Lee, C. S., Cornish, A. L., Swarbrick, A., and Sutherland, R. L. (1997) *Mol. Endocrinol.* **11,** 54–66
43. Weinberg, R. A. (1995) *Cell* **81,** 323–330
44. Planas-Silva, M. D., and Weinberg, R. A. (1997) *Mol. Cell. Biol.* **17,** 4059–4069
45. Wang, Q. M., Luo, X., and Studzinski, G. P. (1997) *Cancer Res.* **57,** 2851–2855
46. Bardon, S., Vignon, F., Derocq, D., and Rochefort, H. (1984) *Mol. Cell. Endocrinol.* **35,** 89–96
47. Bergan, R., Kyle, E., Nguyen, P., Trepel, J., Ingui, C., and Neckers, L. (1996) *Clin. Exp. Metastasis* **14,** 389–398
48. Hirokawa, M., Kuroki, J., Kitabayashi, A., and Miura, A. B. (1996) *Immunol. Lett.* **50,** 95–98
49. Costello, J. F., Plass, C., Arap, W., Chapman, V. M., Held, W. A., Berger, M. S., Huang, H. J. S., and Cavenee, W. K. (1997) *Cancer Res* **57,** 1250–1254
50. Timmermann, S., Hinds, P. W., and Munger, K. (1997) *Cell Growth Differ.* **8,** 361–370
51. Russo, A. A., Jeffrey, P. D., and Pavletich, N. P. (1996) *Nat. Struct. Biol.* **3,** 696–700
52. Wilcken, N. R., Sarcevic, B., Musgrove, E. A., and Sutherland, R. L. (1996) *Cell Growth Differ.* **7,** 65–74
53. Kwon, T. K., Buchholz, M. A., Chrest, F. J., and Nordin, A. A. (1996) *Cell Growth Differ.* **7,** 1305–1313
54. Ewen, M. E., Oliver, C. J., Sluss, H. K., Miller, S. J., and Peeper, D. S. (1995) *Genes Dev.* **9,** 204–217
55. Ishida, T., Kobayashi, N., Tojo, T., Ishida, S., Yamamoto, T., and Inoue, J. (1995) *J. Immunol.* **155,** 5527–5535
56. Meyerson, M., and Harlow, E. (1994) *Mol. Cell. Biol.* **14,** 2077–2086
57. Teixeira, C., and Pratt, M. A. C. (1997) *Mol. Endocrinol.* **11,** 1191–1202
58. Pennisi, E. (1996) *Science* **273,** 1171
59. Powles, T. J. (1997) *Semin. Oncol.* **24,** Suppl. 1, S1-48–S1-54
60. Forbes, J. F. (1997) *Semin. Oncol.* **24,** Suppl. 1, S1-5–S1-19
61. Legha, S. S. (1988) *Ann. Intern. Med.* **109,** 219–228
62. Wiebe, V. J., Osborne, C. K., Fuqua, S. A., and DeGregorio, M. W. (1993) *Crit. Rev. Oncol. Hematol.* **14,** 173–188
63. Baldwin, W. S., and LeBlanc, G. A. (1992) *Chem. Biol. Interact.* **83,** 155–169
64. Bradfield, C. A., and Bjeldanes, L. F. (1984) *Food Chem. Toxicol.* **22,** 977–982
65. McDanell, R., McLean, A. E., Hanley, A. B., Heaney, R. K., and Fenwick, G. R. (1989) *Food Chem. Toxicol.* **27,** 289–293
66. Bradlow, H. L., Michnovicz, J. J., Halper, M., Miller, D. G., Wong, G. Y., and Osborne, M. P. (1994) *Cancer Epidemiol. Biomarkers Prev.* **3,** 591–595
67. Strobl, J. S., Wonderlin, W. F., and Flynn, D. C. (1995) *Gen. Pharmacol.* **26,** 1643–1649
68. Liu, H., Wormke, M., Safe, S. H., and Bjeldanes, L. F. (1994) *J. Natl. Cancer Inst.* **86,** 1758–1765

11) Personnel Employed Under This Grant

a) Bjeldanes lab—

Yu-Chen Chang – Postdoctoral researcher
Zhongdong Liu – Postdoctoral researcher
Chunling Feng – Postdoctoral researcher
Jacques Riby – Staff research associate
Richard Staub – postdoctoral researcher

b) Firestone lab –

Carolyn Cover -- Grad Student and postdoctoral researcher
Gunnel Hallden -- Postdoctoral researcher
Gary Firestone -- Summer Salary
Ross Ramos -- Staff research associate
Eric Williams -- Staff research associate
Erin Cram -- Grad Student and postdoctoral researcher
Sarah Jump -- Staff research associate
Jean Hsieh -- Staff research associate
Edward Wang -- Staff research associate
Joanne Zhang -- Postdoctoral researcher
Hanh Garcia -- Grad Student
Jenny Kung -- Lab Asst (Undergrad)
Jocelyn Hsu -- Lab Asst (Undergrad)